Acta Periodica Technologica

ACTA PERIODICA
TECHNOLOGICA

CONTENT

EDITORIAL POLICY
INSTRUCTION FOR MANUSCRIPT PREPARATION

Original scientific paper

MODELING OF DISPERSE DYE ADSORPTION ON MODIFIED POLYESTER FIBERS

Marija Kodrić[1], Dragan Đorđević[1]*, Sandra Konstantinović[1], Mirjana Kostić[2], Tatjana Šarac[1]

[1] University of Niš, Faculty of Technology, Bulevar oslobođenja 124, 16000 Leskovac, Serbia
[2] University of Belgrade, Faculty of Technology and Metallurgy, Karnegijeva 4, 11000 Belgrade, Serbia

The results of the research on the ability of adsorption of dye on polyester fibers at a temperature of 98 °C are presented in this paper. The fibers were previously modified in aqueous solutions of NaOH, KOH or Al(OH)₃. Typically, the dyeing of the fibers takes place at high temperatures and under pressure in the presence of the carrier. Previous processing before adsorption-dyeing, alkali hydrolysis, changes the surface morphology of polyester fibers. Based on dye exhaustion results, it was found that the dye adsorption on modified polyester fibers (degree of exhaustion 18.2 %, for a dye concentration of 200 mg·dm⁻³ and adsorption time of 5 min) has been bigger than adsorption to unmodified fibers (degree of exhaustion 10 %, for a dye concentration of 200 mg·dm⁻³ and adsorption time of 5 min). The five-parameter nonlinear model of Fritz-Schlunder is the most efficient in simulating isothermal adsorption of disperse dye on polyester fibers (the correlation coefficient is 0.995). Other adsorption models, Dubinin-Radushkevich, Marczewski-Jaroniec and Hill give poorer results and cannot be used to explain the adsorption of the disperse dye for polyester fibers (the correlation coefficients are 0.891, 0.922 and 0.973, respectively).

Keywords: adsorption, polyester, disperse dye, nonlinear modeling.

INTRODUCTION

The synthetic fiber sector is continually exploring new areas to diversify products and give them new properties. Thus, in recent years, great advances have been made in the development of fibers derived from polyester and, for the first time, its consumption has now surpassed the consumption of cotton, the most used natural fiber (1).

Polyethylene terephthalate (PET) fiber, which is a type of polyester (PES) fiber, is the most widely used synthetic fiber due to its good physical and chemical properties. It is also well known that PET fiber is dyed using disperse dyes at high temperatures of 120-130 °C, owing to its hydrophobic nature and highly compact molecular structure (2).

It is known that most polyester textile materials are dyed in high-temperature (HT) conditions. However, it may occasionally occur circumstances in which the use of HT conditions is undesirable, and other methods must be used. These circumstances are, for example, the presence of other fibers mixed with polyesters that are unstable in high-temperature conditions or the need to achieve a brighter color of textile. Some other factors

---

* Corresponding author: Dragan Đorđević, University of Niš, Faculty of Technology, Bulevar oslobođenja 124, 16000 Leskovac, Serbia, e-mail drag_64@yahoo.com

Original scientific paper

may also occur in response to the increasing customer demands from textile production (3).

The fact is that the polyester fiber has a very compact and crystalline structure and is extremely hydrophobic. For this reason, its aqueous dyeing is carried out at high temperature and high pressure using disperse dyes. The dyeing of the polyester can be represented by several successive processes such as dissolving and dispersing the disperse dye, transferring dissolved dye from the aqueous solution to the surface of the fibers, diffusing and adsorbing the dye on the surface of the fibers, and diffusing from the surface to the inside of the fiber. Thus, it should be added that it is very well known that additives affect the processes of dyeing. (4).

Nowadays hydrolytic modification of the surface of polyester materials is more and more used for obtaining different and better appearance. It has been shown that polyethylene terephthalate has good conditions for modification by processing with alkalis. The reaction with NaOH is saponification polyethylene terephthalate, and the products of reactions are sodium-terephthalate and ethylene-glycol. It is an irreversible reaction, which shows that in case of greater mass loss than wanted it is not possible to fix the material. It is often called the peeling of polyester because by measuring the diffraction of X-rays, it is proved that alkali hydrolysis appears only at the surface of fibers, and the inner morphological structure of fibers stays unchanged. Treatment of fabrics with alkali leads to the decrease of fiber diameter and exposure of the new surfaces and hence the fabric properties will change (5-8).

This work tends to contribute to the explanations of dye adsorption on polyester fibers through the modeling process, i.e. abilities of dye adsorption at chemically modified PES fibers in aqueous alkaline solution, at a temperature of 98 °C without a carrier. The aim is to successfully perform the dye adsorption or dyeing of alkaline hydrolyzed hydrophobic fiber in less extreme conditions. Also, if the exhaustion of dye is large enough, there will be less colored wastewater and less harm to the environment.

EXPERIMENT

Raw, undyed 100 % polyester (polyethylene terephthalate) fibers have been used which is common in practice with the following characteristics: length 90 mm, fineness 1.5 dtex, tenacity 51.7 cN·tex^{-1}, elongation at break 34.5 %.

Before dyeing 1 g of the PES fibers have been modified by water solution (50 dm^3) of NaOH, KOH and Al(OH)$_3$ for 30 min, fibers: liquor ratio has been 1:50 while the temperature of the process has been 60 °C.

Dyeing of this modified PES fibers has been performed by disperse dye C.I. Disperse Blue 81, molecular formula $C_{14}H_9BrN_2O_4$ and molar mass of 349.14 g·mol^{-1}, at 98 °C, without carriers. According to its molecular structure, the dye is classified into anthraquinones and is shown in Figure 1.
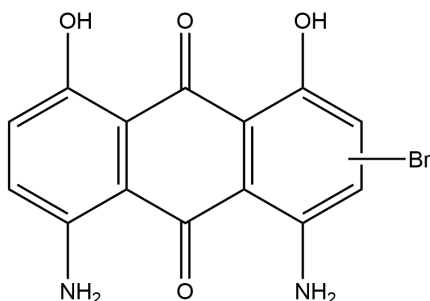
Figure 1. Structure of the applied disperse dye C.I. Disperse Blue 81
(by software ChemBioDraw Ultra 14.0)

The test of dyeing-adsorption has been performed in the way that 1 g of fibers have been dyed in the solution of a constant volume of 0.1 dm^3 on a shaker with a turn of 120 rpm; dye concentration has been 50, 100, 150 and 200 mg·dm^{-3}. The time of adsorption–dyeing has been 5, 10, 20, 40 and 60 min. Equilibrium time has been 60 min because it has been shown that with longer dyeing there are no significant changes in the level of dye exhaustion. The aqueous solution of the dye has had the dispersing agent (Dispersant SP, Achitex Minerva, Italy) 1.5 g·dm^{-3} and formic acid (pH=4.5), whereas the temperature of the dye has been 98 °C.

For determining the concentration of dye in the solution, UV–VIS spectrophotometry and apparatus Cary 100 Conc UV–VIS, Varian (absorption maximum on 630 nm) have been used.

The dye exhaustion (9) or degree of exhaustion has been calculated via equation:

$$Dye\ Exhaustion = \frac{C_0 - C_t}{C_0} \cdot 100\ (\%) \qquad [1]$$

where: C_0 and C_t (mg·dm^{-3}) are the initial and dye concentration in time t.

The amount of the adsorbed dye (9) obtained via equation:

$$q_e = \frac{C_0 - C_e}{w} \cdot V \qquad [2]$$

where: q_e (mg·g^{-1}), the mass of adsorbed dye per mass unit of fibers in equilibrium; C_e (mg·dm^{-3}), equilibrium dye concentration in the solution; w (g), the mass of fibers and V (dm^3), the volume of solution for dyeing.

The Dubinin–Radushkevich (D-R) isotherm can be applied for the estimation of apparent free energy and the characteristics of adsorption (10).

The Dubinin–Radushkevich equation defined by the following equation:

$$q_e = q_{mDR} \cdot \exp\left[-K_{DR} \cdot \left(R \cdot T \cdot \ln(1 + \frac{1}{C_e}) \right)^2 \right] \qquad [3]$$

where K_{DR} is the Dubinin–Radushkevich isotherm constant related to the adsorption energy (mol^2·kJ^{-2}), q_{mDR} is the theoretical isotherm saturation capacity (mg·g^{-1}), R is the gas constant (8.314 J·mol^{-1} K^{-1}) and T is the temperature (K).

Hill (H) has proposed an isotherm model from the non-ideal competitive adsorption model to define different adsorbate binding on a homogeneous surface of adsorbent (10).

3

This isotherm model undertakes that the adsorption is basically a cooperative manifestation, including the ligand-binding capability at one site onto the macromolecule, influencing various binding sites onto the same macromolecule.

The Hill isotherm can be represented as follows:

$$q_e = \frac{q_{mH} \cdot C_e^{n_H}}{K_H + C_e^{n_H}} \qquad [4]$$

If n_H is greater than 1, this isotherm indicates positive cooperativity in binding, n_H is equal to 1, it indicates non–cooperative or hyperbolic binding and n_H is less than 1, indicating negative cooperativity in binding.

Marczewski–Jaroniec (M–J) isotherm (10) which is as well recognized as the four-parameter general Langmuir equation is recommended based on the suppositions of local Langmuir isotherm and the adsorption energies distribution in the active sites.
Marczewski–Jaroniec isotherm is expressed as follows:

$$q_e = q_{mMJ} \cdot \left(\frac{(K_{MJ} \cdot C_e)^{n_{MJ}}}{1 + (K_{MJ} \cdot C_e)^{n_{MJ}}} \right)^{\frac{m_{MJ}}{n_{MJ}}} \qquad [5]$$

The parameter n_{MJ} and m_{MJ}, characterize the heterogeneity of surface, can vary from 0 to 1. This isotherm reduces to Langmuir isotherm for the value of both n_{MJ} and m_{MJ} equal to 1, to Langmuir-Freundlich isotherm for n_{MJ} equal to m_{MJ} connected with the symmetrical quasi-Gaussian energy distribution and to the Toth isotherm for m_{MJ} equal to 1 corresponding to asymmetrical quasi-Gaussian energy distribution. The parameter m_{MJ} describes the spreading of the distribution in the path of higher adsorption energies, while n_{MJ} describes this spreading in the path of lesser adsorption energies.

Fritz-Schlunder (F-S) have proposed a five-parameter empirical expression which can represent a broad field of equilibrium data (9):

$$q_e = \frac{q_{mFS} \cdot K_1 \cdot C_e^{m_1}}{1 + K_2 \cdot C_e^{m_2}} \quad \text{with } m_1 \text{ and } m_2 \leq 1 \qquad [6]$$

where q_e is the adsorbed amount at equilibrium (mg·g⁻¹), C_e the equilibrium concentration of the adsorbate (mg·dm⁻³), q_{mFS} the Fritz-Schlunder maximum adsorption capacity (mg·g⁻¹) and K_1, K_2, m_1, and m_2 are the Fritz-Schlunder parameters.

RESULTS AND DISCUSSION

Alkali hydrolysis leads to the greatest mass loss of PES fibers (9-11.0 %). Physical characteristics vary slightly, the tenacity falls slightly (5-10 %), and elongation at break shows a small increase (3-6 %), all compared to untreated samples of PES fibers.

The level of dye exhaustion in the dyeing of alkali hydrolyzed PES fibers has shown in Figure 2. The results are shown only for the previous treatment of fiber with potassium hydroxide since this pre-treatment showed the best results of the degree of exhaustion compared to pre-treatment with sodium or aluminum hydroxide.

These results can confirm the fact that alkali pre-treatments change surface morphology of PES fibers, increasing the porosity (during the previous process in alkali solution), decreases the size of dye particles so that more individual molecules of disperse

Original scientific paper

dye are present in water, and there are real chances that the applied alkali increased fibers permeability, which gives the possibility to a greater number of dye molecules to diffuse into PES fibers (11).

In the process of dyeing of raw PES fibers, i.e. in the disperse dye adsorption process for PES fibers, the degree of dye exhaustion ranges from 10 % (18.2 % for KOH modified PES fibers) to 60 % (69.9 % for KOH modified PES fibers) for an initial dye concentration of 200 mg·dm^{-3} at the time of dyeing 5 and 60 min.

Isotherm adsorption is of essential significance for investigation of the process of dyeing at a temperature of 98 °C. The analysis of isothermal data by their fitting via different isothermal equations is an important step towards finding the right model which can be used for controlling the process of dyeing (12).

In this investigation, nonlinear isothermal two-, three-, four- and five-parameter models, i.e. D-R, H, M-J and F–S equation have been used. For the fitting of experimental points, a "trial-and-error" non-linear regression method has used, which is implemented using Microsoft Excel software (12).
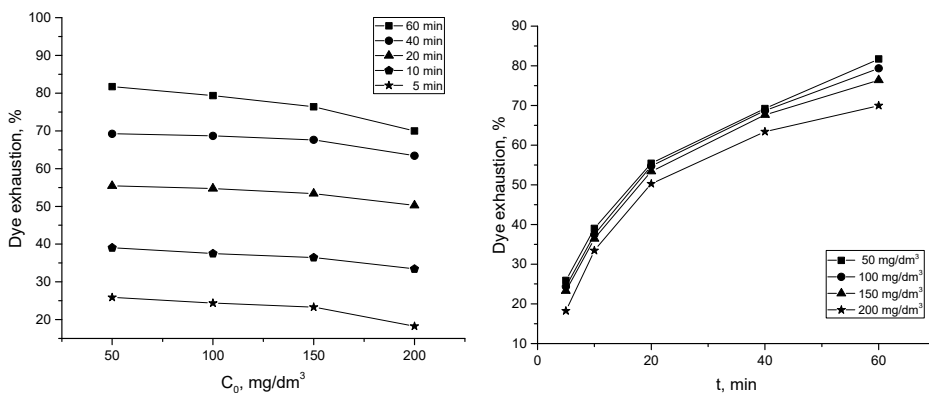
Figure 2. The level of exhaustion of dye on PES fibers during a different time and initial concentrations

This software was used to compare and optimize isotherms using optimization to minimize the residual sum of squares error (SSE) or maximize the coefficient of determination (R^2) between the experimental and the modeled values.

Figure 3 gives a comparable display of isothermal models of D-R, H, M-J and F-S through the nonlinear fitting of experimental data. Parameters of models obtained from nonlinear regression are listed in Table 1. SSE (0.26) and R^2 (0.995) in five-parameter F-S isotherm is the highest of the four models, which confirms the fact that this model is the most efficient in nonlinear simulating of isothermal adsorption of disperse dye on PES fibers, which can be noticed at a visual review of nonlinear curves in a diagram of Figure 3. Then, three-parameter H model follows, also with high SSE (1.48) and a smaller R^2 (0.973), then four-parameter M–J model which has poorer statistical parameters, SSE (4.32) and R^2 (0.922) and finally, two-parameter D-R with the worst results (SSE=6.09 and R^2=0.891). F-S, as five-parameter isotherm is dominant, according to the cover of

Original scientific paper

experimental points, even though the other nonlinear models are not far away, especially H model.
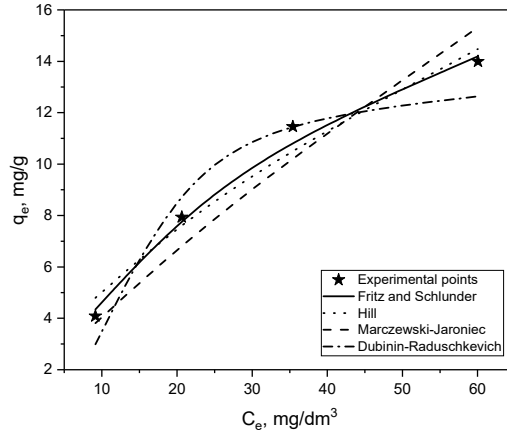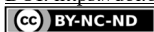
Figure 3. Nonlinear adsorption isotherms during PES fibers dyeing

Table 1. Analytic equations of nonlinear isotherms with coefficients for the system dye-PES fibers

An analytic expression of a nonlinear model	Model parameters		SSE	R²
Dubinin–Radushkevich: $q_e = 13.12 \cdot \exp\left[-1.4 \cdot 10^{-5} \cdot \left(3084.5 \cdot \ln(1+\frac{1}{C_e})\right)^2\right]$	q_{mDR}, mg/g	13.12	6.09	0.891
	K_{DR}, mol²/kJ²	$1.4 \cdot 10^{-5}$		
Hill: $q_e = \dfrac{3.3 \cdot 10^6 \cdot C_e^{0.59}}{2.5 \cdot 10^6 + C_e^{0.59}}$	q_{mH}, mg/dm³	$3.3 \cdot 10^6$	1.48	0.973
	n_H, –	0.59		
	K_H, –	$2.5 \cdot 10^6$		
Marczewski–Jaroniec: $q_e = 1.3 \cdot 10^{-6} \cdot \left(\dfrac{\left(1.3 \cdot 10^{-5} \cdot C_e\right)^{0.05}}{1+\left(1.3 \cdot 10^{-5} \cdot C_e\right)^{0.05}}\right)^{-35}$	q_{mMJ}, mg/g	$1.3 \cdot 10^{-6}$	4.32	0.922
	K_{MJ}, dm³/mg	$1.3 \cdot 10^{-5}$		
	n_{MJ}, –	0.05		
	m_{MJ}, –	-1.75		
Fritz–Schlunder: $q_e = \dfrac{0.59 \cdot C_e^{0.86}}{1+7.8 \cdot 10^{-5} \cdot C_e^{2.14}}$	q_{mFS}, mg/g	0.35	0.26	0.995
	K_1, –	1.71		
	K_2, –	$7.8 \cdot 10^{-5}$		
	m_1, –	0.86		
	m_2, –	2.14		

CONCLUSION

It is shown that dye adsorption of alkali modified fibers has increased, the dye exhaustion grows in comparison with the raw sample.

The five-parameter nonlinear model of F-S is the most efficient in simulating isothermal adsorption of disperse dye on PES fibers.

Other adsorption models, D-R, H, and M-J give poorer results and can not be used to explain the adsorption of the disperse dye for PES fibers.

The results of this work achieved by these effects indicate the possibility of a different approach in the process of dyeing the polyester by disperse dye, for the benefit of greater exhaustion, economy, and protection of the environment.

REFERENCES

1. Ovejero, R.G.; Sanchez J.R.; Ovejero, J.B.; Valldeperas J., Lis, M.J. Kinetic and Diffusional Approach to the Dyeing Behavior of the Polyester PTT, *Text. Res. J.* **2007**, *77* (10), 804.809.
2. Kima, T.-K.; Sonb, Y.-A.; Lim, Y.-J. Thermodynamic parameters of disperse dyeing on several polyester fibers having different molecular structures, *Dyes Pigments*. **2005**, *67*, 229-234.
3. Iskender, M.A., Becerir, B., Koruyucu, A. Carrier Dyeing of Different Energy Level Disperse Dyes on Polyester Fabric, *Textile Res. J.* **2005**, *75* (6) 462-465.
4. Mashaly, H.M.; Abdelghaffar, R.A.; Kamel, M.M.; Youssef, B.M. Dyeing of Polyester Fabric using Nano Disperse Dyes and Improving their Light Fastness using ZnO Nano Powder, *Indian J. Sci. Technol*. **2014**, *7* (7) 960-967.
5. Ibrahim, N.A.; Youssef, M.A.; Helal, M.H.; Shaaban, M.F. Exhaust Dyeing of Polyester-Based Textiles Using High-Temperature-Alkaline Conditions, *J. Appl. Polym. Sci.* **2003**, *89*, 3563-3573.
6. Haghighatkish M.; Youscfi, M. Alkaline Hydrolysis of Polyester Fibers-Structural Effects, *Iran. J. Polym Sci. Technol*. **1992**, *11* (2) 56-61.
7. Youssef, Y.A.; Ahmed, N.S.E.; Mousa A.A.; El-Shishtawy, R.M. Alkaline Dyeing of Polyester and Polyester/Cotton Blend Fabrics Using Sodium Edetate, *J. Appl. Polym. Sci.* **2008**, *108*, 342-350.
8. Hou, A.; Li, M.; Gao, F.; Xie, K.; Yu, X. One-step dyeing of polyethylene terephthalate fabric, combining pretreatment and dyeing using alkali-stable disperse dyes, *Color. Technol*. **2013**, *129*, 438-442.
9. Hamdaouia, O.; Naffrechoux, E. Modeling of adsorption isotherms of phenol and chlorophenols onto granular activated carbon Part II. Models with more than two parameters, J. *Hazard. Mater.* **2007**, *147*, 401-411.
10. Podder M.S.; Majumder C.B. Sequestering of As(III) and As(V) from wastewater using a novel neem leaves/$MnFe_2O_4$ composite biosorbent, Int. *J. Phytoremediation*. **2016**, *18* (12) 1237-1257.
11. Xu, W.; Yang, C. Hydrolysis and dyeing of polyester fabric using microwave irradiation, *Color. Technol*. **2002**, *118*, 211-214.
12. Amrhar, O.; Nassali, H.; Elyoubi, M.S. Application of nonlinear regression analysis to select the optimum absorption isotherm for Methylene Blue adsorption onto Natural Illitic Clay, *Bull. Soc. R. Sci. Liège*. **2015**, *84*, 116-130.

REMOVAL OF NATURAL ORGANIC MATTER AND EMERGING CONTAMINANTS FROM GROUNDWATER USING OZONATION AND GAC FILTRATION

Jelena J. Molnar Jazić, Marijana M. Kragulj Isakovski, Aleksandra M. Tubić, Tamara B. Apostolović, Malcolm A. Watson, Snežana P. Maletić, Jasmina R. Agbaba*

University of Novi Sad, Faculty of Sciences, Department of Chemistry, Biochemistry and Environmental Protection, Trg Dositeja Obradovića 3, 21000 Novi Sad, Republic of Serbia

This work presents results from a pilot-scale drinking water treatment plant used to investigate the performance of ozone oxidation and granulated activated carbon (GAC) adsorption in removing natural organic matter (NOM) and specific organic micropollutants from groundwater. The investigated groundwater has a relatively low NOM content (1.83±1.01 mg C/L total organic carbon, TOC). Using gas chromatography/mass spectrometry (GC/MS) screening analysis, a variety of different organic compounds were identified, including benzophenone, 2-phenoxyethanol, butylated hydroxytoluene and benzoic acid, all contaminants of emerging concern (CEC) identified by NORMAN. The application of the ozonation process resulted in a 4-20% NOM reduction, based on the TOC values. Estimated removal of CECs by ozone increased with increasing ozone dose (up to 1.0 g O_3/m^3) and was in the range 24-70%. Adsorption on GAC further improves total NOM and CECs removal compared to the ozonation alone. Combined use of ozone and GAC provides up to 16-33% TOC reduction as well as 70-82% CECs removal. UV absorbance values at 254 nm can serve as an indicator of aromatic carbon content in water, and were significantly reduced after ozonation and GAC filtration (by up to 50%). Among the CECs investigated, benzophenone was the most prone to oxidation/adsorption treatment. In addition to the naturally present organic matter, CECs detected can serve as indicators of anthropogenic pollution which may alter drinking water quality. Tracking their behaviour during treatment allows assessment of the efficiency of the technological line and optimization of the oxidation process in the case of groundwater pollution by infiltration.

Keywords: ozonation, GAC filtration, NOM, emerging substances

INTRODUCTION

Drinking water treatment plants face great challenges in optimizing technologies to avoid human health risks and to ensure environmental sustainability. Population growth is in direct correlation with the lower availability of water sources, as quality deteriorates due to land use and climate changes, hydrology and water quality changes (1). An important series of new contaminants are of particular concern, the emerging (or micro-) pollutants (2), with varied concentrations (ranging from ng/L to mg/L) whose transformation through drinking water treatment processes can lead to compounds which may be more

---

* Corresponding author: Jasmina Agbaba, University of Novi Sad, Faculty of Sciences, Department of Chemistry, Biochemistry and Environmental Protection, Trg Dositeja Obradovića 3, 21000 Novi Sad, Republic of Serbia, e-mail: jasmina.agbaba@dh.uns.ac.rs

toxic, persistent and less biodegradable than their predecessors. The NORMAN network was created to keep track of such contaminants and maintains a list of substances detected in European aquatic environments, but which are not currently included in routine environmental monitoring programs. The NORMAN network (2016) list now has 700 contaminants of emerging concern (CEC), their metabolites and transformation products, and these contaminants may be candidates for future legislation due to their adverse effects and/or persistency (3). CECs are categorized into more than 20 classes relating to their origin including: pharmaceuticals, pesticides, disinfection by-products, and wood preservation and industrial chemicals (4). The most important environmental effects of CECs refer to: bioaccumulation and biomagnification, persistency, toxicity, endocrine disruption potential, carcinogenic effects, and mutagenic and teratogenic effects (5).

Conventional treatment processes that include physical-chemical and biological treatments as the major steps during water treatment, are principally designed to eliminate organic matter and finally prevent outbreaks of infectious waterborne diseases by applying chlorination in the final step (6). However, previous research has shown that many organic micropollutants are not completely removed during conventional drinking water treatments (coagulation-flocculation, filtration, chlorination) (7). In addition, chlorination as a means of drinking water disinfection, although an indispensable treatment process since the early 20th century (8), may lead to reactions between free chlorine and CECs in water, resulting in the formation of disinfection by-products (DBPs) such as nitrogen-containing DBPs including haloacetonitriles, halonitromethanes and haloacetamides, carbonaceous DBPs including trihalomethanes, haloacetic acids and chloral hydrate as well as brominated and iodinated DBPs (8). The combined use of ozone and activated carbon has been developed to improve process efficacy for the treatment of water rich in natural organic matter (NOM) which can interfere and reduce the target pollutants removal (6).

The aim of this study was to investigate the possibility of NOM and selected CECs removal from groundwater using ozone oxidation with different ozone doses and GAC adsorption. The investigation was carried out using a modular drinking water pilot plant.

EXPERIMENTAL

Materials

All solvents used, dichloromethane, hexane and methanol, were purchased from J.T. Baker and were ultra resi-analysed quality. Analytical standards were purchased from Sigma-Aldrich. Potassium indigotrisulfonate and potassium iodide were purchased from Sigma-Aldrich. All other chemicals were of analytical grade and were used without further purification.

Pilot plant investigations

The water treatment was carried out using a modular drinking water pilot plant with a capacity of 2 m³/h. The groundwater investigated was drawn from the first aquifer layer from wells of a depth of around 30 m (AP Vojvodina, Republic of Serbia). It was subjected to the following treatments: aeration, sand filtration, ozonation, adsorption on

GAC. The water flow through the ozonation column was about 1300 L/h. Ozone was ge-nerated from ambient air using a General Electric ozone generator with a 10 g/h capacity.

Ozone gas was introduced into the ozonation column by injector and the applied ozone doses ranged from 0.3-1.0 g O_3/m^3, based on the ozone demand of the investigated water. *Off*-ozone was removed from the top of the column and underwent destruction via activated carbon. The pilot plant was equipped with two ozonation columns and a retention (stabilization) column. Water flowing from the retention column was fed to the GAC adsorber. The adsorbers were designed as closed vessels with a GAC layer and were operated in downflow mode. The treated water was collected in a reservoir and sampled for further analysis. This work presents the results of the influence of ozonation and GAC filtration on the total NOM and specific CECs removal.

Analytical methods

The concentration of ozone in the gas phase and in water samples was determined by iodometric procedure and the indigo colorimetric method according to the standard methods (9). Determination of pH in water samples was carried out on-site using a WTW InoLab portable pH meter, according to SRPS H.Z1.111:1987. The TOC content in the water samples was determined by Elemental LiquiTOCII according to method SRPS ISO 8245:2007. UV_{254} absorbance was measured in a 1 cm quartz cell on a CINTRA 1010, GBC Scientific Equipment spectrophotometer at a wavelength of 254 nm.

Gas chromatography/mass spectrometry (GC/MS, Agilent Technologies 7890A/ 5975C) was used for screening analysis. Chromatographic conditions were as follows: initial tempe-rature 70 °C for 2 min, then 25 °C/min to 150 °C, then 3 °C/min to 200 °C, then 8 °C/min to 280 °C, hold 10 min. Injection temperature 250 °C, injection mode splitless, injection volume 2 μl. MS source temperature 230 °C, MS Quad temperature 150 ºC, transfer line temperature 280°C. Acquisition mode Scan/SIM. Results of GC/MS analysis were evaluated using Deconvolution Reporting Software (DRS) that combines results from the Agilent MSD Productivity ChemStation, the NIST Automated Mass Spectral Deconvolution and Iden-tification Software, and the NIST 2008 Mass Spectral Search Program (NIST08). Samples for GC/MS analysis were prepared using an extraction procedure according to USEPA 3510C method guidelines.

RESULTS AND DISCUSSION

Groundwater characteristics

The groundwater was subject to defferisation and demanganisation (aeration and sand filtration: A/F). This water then underwent ozone and GAC treatments with the following characteristics: pH 7.9±0.1; electroconductivity 635±28 μS/cm; hardness 15,4±0,6 °dH; $KMnO_4$ consumption 5,1±0,4 mg/L; 1.83±1.01 mg C/L TOC and 0,025±0,01 cm^{-1} UV_{254}. The investigated groundwater has a relatively low content of total organic matter. How-ever, results of GC/MS analysis showed that different organic compounds are present in the water samples, including hydrocarbons, organic acids and esters of organic acids, al-cohols and aldehydes, phenols and organonitrogen compounds, with up to 40 compounds detected in total. Among the identified compounds benzophenone (BP), 2-phenoxyetha-

nol (2-PE), butylated hydroxytoluene (BHT) and benzoic acid (BA) were selected as contaminants of emerging concern (CEC) identified by NORMAN. CEC have been detected in the environment but are not yet included in routine monitoring programmes at the EU level. The estimated CEC concentrations were in range 35-150 ng/L. Taking into account that the fate, behaviour and (eco)toxicological effects of CEC are not well understood their fates during the water treatment processes were monitored.

BP is commonly used in many kinds of cosmetics and sunscreens and represents a typical ultraviolet-absorbing chemical. BP is commonly detected in effluents of wastewater treatment plants, lakes, surface and groundwaters and even in tap waters at concentrations between several nanograms per liter and micrograms per liter. BP has endocrine-disrupting effects *in vitro* and *in vivo* thus it needs to be removed during the water treatment preparation (10,11). Aromatic carboxylic acids including BA are used as raw materials or generated in various industries such as printing and dyeing, pharmaceuticals, food, cosmetics and paper mills and have a low biodegradability. BA is detected in the effluents of the pharmaceutical industry, in surface waters and groundwater (12). BHT is a toluene-based ingredient used as a preservative in food and personal care products. 2-PE is a bactericide often used in dermatological products, such as skin creams and sunscreens; and also, as fixative for perfumes, insecticide and topical antiseptic and has been found in surface waters at concentrations up to 14 µg/L (13) and 129 ng/L in groundwater (14). Previous investigations have shown relatively high concentrations of the studied CEC in the range up to 0.1-40 µg/L, which indicates the necessity to apply appropriate water treatments for their removal from drinking water sources.

Effects of ozone oxidation and GAC filtration on the total NOM removal

Figure 1 presents the results of the total NOM removal from water using ozonation and GAC filtration based on the TOC value (Figure 1a) and UV_{254} absorbing compounds (Figure 1b). The application of the ozonation process resulted in a 4-20% TOC reduction. Combined use of ozone and GAC provides up to 16-33% TOC reduction. UV absorbance values at 254 nm can serve as indicators of aromatic carbon content in water and were significantly reduced after ozonation and GAC filtration (by up to 50%).
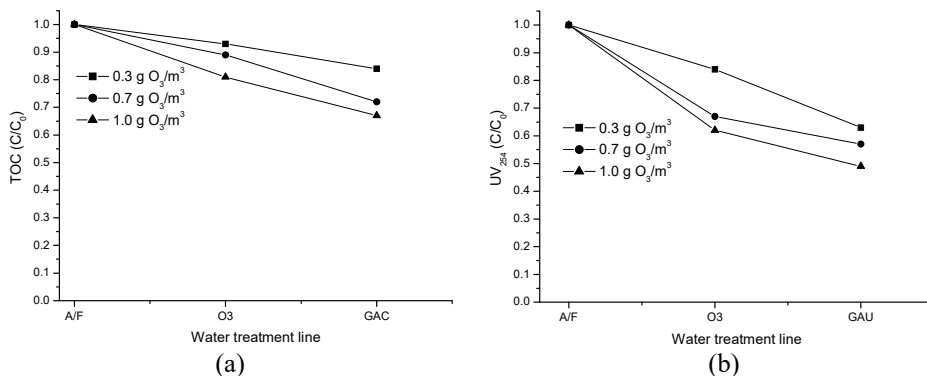
Figure 1. Effects of ozonation and GAC filtration on the (a) TOC and (b) UV_{254} reduction in water

Original scientific paper
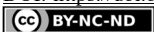
Effects of ozone oxidation and GAC filtration on the removal of certain CEC

Figure 2 presents the results of the CEC removal from water using ozonation and GAC filtration. Estimated removal of CECs by ozone increased with increasing ozone dose (up to 1.0 g O_3/m^3) and was in the range 24-70%.
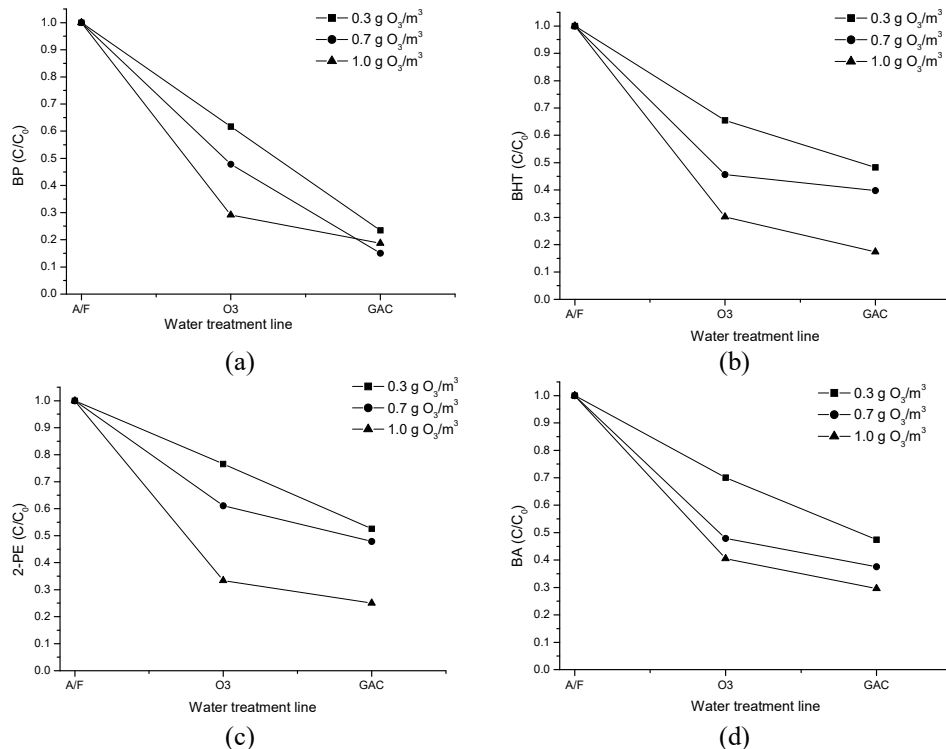
Figure 2. Effects of ozonation and GAC filtration on the (a) BP, (b) BHT, (c) 2-PE and (d) BA removal from water

The efficacy of CEC degradation by ozone alone increases with increasing ozone dose. Adsorption on GAC further improves CECs removal compared to ozonation alone, due to the affinity to adsorb not only persistent CEC but also their oxidation intermediate products (15). Combined use of ozone and GAC provides 70-83% CECs removal. The results show that of the CECs investigated, BP was the most prone to oxidation/adsorption treatment, probably due to the presence of two aromatic rings susceptible to electrophilic ozone attack. The highest degree of BHT, BA and 2-PE removal was achieved using the highest applied ozone dose of 1.0 g O_3/m^3 in combination with GAC adsorption (up to 82%, 70% and 75%, respectively), while a maximal BP removal of 82% was obtained using 0.7 g O_3/m^3 in pretreatment to the GAC filtration. Previous studies indicate that most of the investigated CEC can be degraded using ozone under laboratory conditions (10,12, 13). However, there is a lack of data related to their behaviour using a

combined treatment of ozone and GAC at a higher level such as pilot scale and in real drinking water conditions, indicating the significance of the data obtained in this study.

CONCLUSION

A pilot-scale investigation of drinking water treatment showed that ozonation combined with adsorption on GAC can reduce total NOM content as well as contaminants of emerging concern from water with high efficiency. The efficacy of total NOM and CEC removal increased with increasing ozone dose in the pretreatment before GAC. Even though CEC are not yet included in routine monitoring programmes at the EU level or in the Republic of Serbia, they are indicators of anthropogenic pollution which may alter drinking water quality so there is a need for their monitoring during water treatment.

Acknowledgements

REFERENCES

1. Teodosiu, C.; Gilca, A.F.; Barjoveanu, G.; Fiore, S. Emerging pollutants removal through advanced drinking water treatment: A review on processes and environmental performance assessment. *J. Clean. Prod.* **2018**, *197*, 1210-1221.
2. Pal, A.; He, Y.; Jekel, M.; Reinhard, M.; Gin, K.Y.H. Emerging contaminants of public health significance as water quality indicator compounds in the urban water cycle. *Environ. Int*. **2014**, *71*, 46-62.
3. Norman Network [WWW Document], 2016. Network of reference laboratories, research centres and related organisations for monitoring of emerging environmental substances, 2015, (LIST of emerging substances latest update February 2016). http://www.norman-network.net/. Access 30.09.2019.
4. Geissen, V.; Mol, M.; Klumpp, E.; Umlauf, G.; Nadal, M.; Van der Ploeg, M.; Van de Zee, S.E.A.T.M.; Ritsema, C.J. Emerging pollutants in the environment: A challenge for water resource management. *International Soil and Water Conservation Research*, **2015**, 3, 57–65.
5. Guillen, D.; Ginebreda, A.; Farre, M.; Darbra, R.M.; Petrovic, M.; Gros, M.; Barcelo, D. Prioritization of chemicals in the aquatic environment based on risk assessment: analytical, modeling and regulatory perspective. *Sci. Total Environ*. **2012**, *440*, 236-252.
6. Rozas, O.; Baeza, C.; Nunez, K.; Rossner, A.; Urruta, R.; Mansilla, H. D. Organic micropollutants (OMPs) oxidation by ozone: Effect of activated carbon on toxicity abatement. *Sci. Total Environ*. **2017**, *590-591*, 430-439.
7. Stackelberg, P.E.; Gibs, J.; Furlong, E.T.; Meyer, M.T.; Zaugg, S.D.; Lippincott, R.L. Efficiency of conventional drinking-water-treatment processes in removal of pharmaceuticals and other organic compounds. *Sci. Total Environ*. **2007**, *377*, 255-272.
8. Hu, J.; Chu, W.; Sui, M.; Xu, B.; Gao, N.; Ding, S. Comparison of drinking water treatment processes combinations for the minimization of subsequent disinfection by-products formation during chlorination and chloramination. *Chem. Eng. J.* **2018**, *335*, 352-361.

Original scientific paper

9. AWWA-APHA-WEF, Standard Methods for the Examination of Water and Wastewater, 20th edn. American Public Health Association/American Water Works Association/Water Environment Federation, Washington, DC, USA, 2012.
10. Guo, Y.; Lin, Q.; Xu, B.; Qi, F. Degradation of benzophenone-3 by the ozonation in aqueous solution: kinetics, intermediates and toxicity. *Environ. Sci. Pollut. R.* **2016**, *23*, 7962–7974.
11. Gao, Q.; Blum, K.M.; Gago-Ferrero, P.; Wiberg, K.; Ahrens, L.; Andersson, P.L. Impact of on-site wastewater infiltration systems on organic contaminants in groundwater and recipient waters. *Sci. Total Environ.* **2019**, *651*, 1670-1679.
12. Zhong, X.; Cui; C., Yu, S. Exploring the pathways of aromatic carboxylic acids in ozone solutions. *RSC Advances* **2017,** *7*, 34339- 34347.
13. Real, F.J.; Benitez, J.F.; Acero, J.L.; Casas, F. Comparison between chlorination and ozonation treatments for the elimination of the emerging contaminants amitriptyline hydrochloride, methyl salicylate and 2-phenoxyethanol in surface waters and secondary effluents. *J. Chem. Technol. Biot.* **2014**, *90*, 1400–1407.
14. Kong, L.; Kadokami, K.; Duong, H.T.; Chau, H.T.C. Screening of 1300 organic micro-pollutants in groundwater from Beijing and Tianjin, North China. *Chemosphere* **2016**, *165*, 221-230.
15. Rivera-Utrilla, J.; Sanchez-Polo, M.; Ferro-Garcia, M.A.; Prados-Joya, G.; Ocampo-Perez, R. Pharmaceuticals as emerging contaminants and their removal from water. A review. *Chemosphere* **2013**, *93*, 1268-1287.
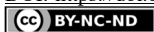
THE INCREASING EFFICIENCY OF UPFLOW CLARIFIERS AT THE DRINKING WATER PREPARATION

Stanislav Dushkin[1], Serhii Martynov[2]*, Stanislav Dushkin[3]

[1] O. M. Beketov National University of Urban Economy in Kharkiv, Kharkiv, Ukraine
[2] National University of Water and Environmental Engineering, Rivne, Ukraine
[3] National University of Civil Defence of Ukraine, Kharkiv, Ukraine

The article discusses the use of concentrated coagulant aluminum sulfate solution to increase the efficiency of upflow clarifiers for drinking water preparation. The water treatment using coagulants from roughly dispersed and colloidal contaminants is one of the most common methods. However, the reagent consumption is quite significant under adverse coagulation conditions (insufficient alkalinity, high chromaticity, and low water temperature), therefore this method requires improvement. It was established that the considered method for the increasing efficiency of upflow clarifiers of water supply systems at drinking water preparation by using the concentrated solution of aluminum sulfate coagulant can reduce the reagent consumption by an average of 15-20%, to improve the water treatment quality and to increase the treatment setups productivity. Therefore, the actual tasks are to study the features of the coagulation process and the influence of various factors for the natural water treatment quality and the scientific improvement and technological regime choice elaboration for water treatment in upflow clarifiers with the concentrated coagulant solution using.

Keywords: upflow clarifiers, drinking water quality, water treatment processes, aluminum sulfate coagulant

INTRODUCTION

Water resources are the national wealth and one of the main components of the economic development of each country (1). The water supply provides the industry stable functioning, satisfies social, hygienic, cultural, aesthetic and other population needs (2, 3). It is necessary to have a number of plants for the water collection, lifting, treatment, accumulation, transportation and distribution to provide the population and the industrial complex by water (4).

The surface water preparation often involves the colloidal and suspended solids retention, which sizes are fluctuating over a wide range (5). Single- or two-stage schemes of water reagent preparation can be used for this purpose (2). The sedimentation tanks or upflow clarifiers are used in the first stage of water treatment (6). The treatment efficiency in upflow clarifiers is higher than in the sedimentation tanks, as a result of combining the processes of water sedimentation, flocculation and filtration through the suspended sediment bed. As a result, the overload to the second stage of water preparation (to the rapid filter) decreases.

---

* Corresponding author: Serhii Martinov, National University of Water and Environmental Engineering, Rivne, Ukraine, e-mail: s.y.martynov@nuwm.edu.ua

The task of the water clarifying technological process improving at the upflow clarifiers mainly leads to creation the optimal conditions, to obtain the large flakes with a highly developed surface and to reduce the time of their formation (7, 8). The high effect of water clarification is achieved at clarifiers; at the same time, they are not without drawbacks, such as the sensitivity to the water flow rate changes through the suspended sediment bed, to the water temperature and other parameters (9). The effectiveness of upflow clarifiers depends on the suspended bed state in the working chamber. The source water quality (suspended solids presence, water chemical composition, temperature), hydraulic conditions (ascending water flow rate, its distribution between the clarification zone and the sediment separation zone), the sediment chemical composition and structure in the suspended bed (flakes size, their strength and volumetric weight), are the main factors, which are determining the intensity of suspended bed formation and the suspended solids content in it.

It is advisable to improve the efficiency of upflow clarifiers by optimizing the contact medium properties that can be achieved by implementing the studies in the following directions (10, 11):

- by increasing the suspended sediment concentration;
- by improvement the contact medium physicochemical properties (fall velocity, specific gravity, volume concentration, particles coalescence force);
- by increasing the ability of suspended sediment coagulating (changes ξ potential and adsorption capacitance);
- by optimization the compaction conditions for excess sediment in the sediment compactor;
- by searching the possibility of reducing the input coagulant doses.

The greatest difficulties during the exploitation of upflow clarifiers are occurring during the treatment of low turbid colour water when suspended sediment formation and the flakes amalgamation with a dense structure are very slow. The suspended bed concentration is insufficient and its sorption ability is small to achieve the necessary degree of water clarification at high rates of the increasing flow in clarifiers. The situation is more complicated in winter because the processes of water coagulation and clarification are slowed down significantly at a low temperature of the source water (12, 13).

It is possible to intensify the water purification processes in upflow clarifiers using the concentrated solution of the aluminum sulfate coagulant. The process of solid-phase nuclei formation, their growth and transformation into coagulation centers at water treatment with a concentrated coagulant solution occurs more intensively than using a diluted coagulant solution. It should be noted that coagulant salts in more concentrated solutions are hydrolyzed to a lesser extent in diluted ones; aluminum hydroxides formed from a less hydrolyzed salt and have a larger coagulating ability (14). Electron microscopic studies showed that the emerging aluminum hydroxide sols acquire a more branched crystalline structure when using a concentrated coagulant solution; the last one allows intensifying the processes of drinking water treatment.

The purpose of the work is to increase the efficiency of upflow clarifiers at the preparation of drinking water using a concentrated solution of aluminum sulfate coagulant.

The influence of a concentrated solution of aluminum sulfate coagulant to the change in the following basic parameters of the upflow clarifier was studied for this:

Original scientific paper

- the fall velocity of the clarifiers contact medium;
- the change in the suspended sediment concentration along with the clarifier height;
- the dependence of sediment suspension concentration on upstream water velocity.

EXPERIMENTAL

Laboratory setup is equipped by upflow clarifiers

The studies were conducted at a laboratory setup; they are shown in Fig. 1.
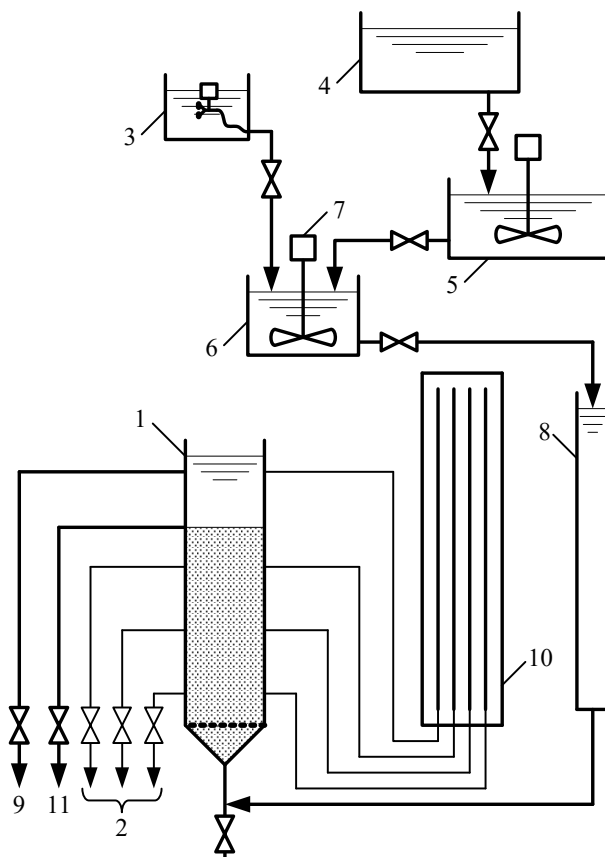
Figure 1. Scheme of the laboratory setup with clarifiers

1 – the clarifier; 2 – the sampling drainages; 3 – the coagulant batcher; 4 – the tank with the polluter; 5 – the tank with the source water; 6 – the mixing tank; 7 – the mixer; 8 – the air separator; 9 - the clarified water sampling (the outlet of treated water); 10 – the piezometric shield; 11 – the pipe of the excess sediment removal

Original scientific paper

The setup consists of a clarifier 1, made of plexiglass tube with a diameter of 100 mm and a height of 2.5 m. The clarifier transparent walls allowed us to visually observing the water treatment process. The clarifier after 200 mm height was equipped by sampling tubes 2 for sampling from different beds of the clarifier. The water with finely dispersed kaolin was fed into the tank with the source water from the tank with the polluter 4, where it was mixed by the mixer 7. The obtained water model was mixed in the mixing tank 6 using the mixer with a coagulant solution from coagulant batcher 3. A piezometric shield 10 was used to control the water pressure in clarifiers. The clarified water outlet 9 was carried out along the circular gutter from the boundary part of the clarifier. The excess sediment was removed into the sewage by pipe 11.

The filtrate quality and head losses in the suspended bed of the clarifier were fixed during our studies. The filtrate quality was evaluated by measuring the light attenuation coefficient using the photoelectric calorimeter. Head losses were determined according to the piezometer data of the piezometric shield.

Our studies were fulfilled with the water of The Seversky Donets River and with test water in the winter period and in the spring flood period, when the impurities coagulation process is the most difficult. The qualitative indicators of the studied water are given in Table 1.

The coagulant solution concentration did not exceed 25%. The coagulant doses were in the range of 45-70 mg/dm^3, counting on a marketable product.

Table 1. The qualitative characteristic of studied water

The indicator's name	The winter period	The spring flood period
Temperature, °C	2.6 - 3.1	8.8 - 10.1
The suspended substances content, mg/dm^3	28.0 - 35.0	21.5 - 23.4
Chromaticity, degrees platinum cobalt scale (PCS)	25 - 31	33 - 45
pH	7.9 - 8.1	6.9 - 7.1
Alkalinity, mmol/dm^3	2.5 - 2.8	1.7 - 2.1

The laboratory setup for study the particles fall velocity of suspended bed

The hydraulic characteristic of the clarifier contact medium determines the sedimentation rate and the degree of the suspension homogeneous. The water rate in the clarifier and its productivity depends on it. The volumetric suspended solids concentration and residual solids content in clarified water depends on the hydraulic characteristics at a given water rate in the clarifier (6, 15).

Fig. 2 shows a setup for determining the fall velocity of the coagulated suspension of upflow clarifiers contact medium. The laboratory setup consists of a glass cylinder with

conical ends and it works on the pressure principle, which allows regulating the rate of its filling over a wide range. The suspended sedimentation time is adopted following the rules of the water treatment technological analysis (16, 17). So, the sedimentation time of the suspended solids fall velocity is 0.2 mm/s, the settling time was 24 minutes, 0.4 mm/s – 9 minutes, etc (6). Samples were taken from the upper part of the device (above mark A) and the lower part of the device (below mark B) after the specified sedimentation period. The weight content of suspended solids was determined in each sample.
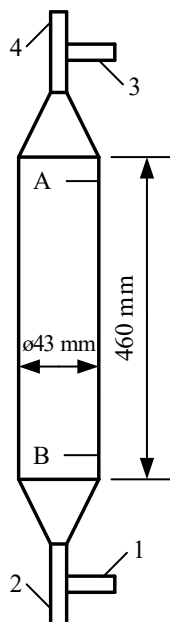
Figure 2. Setup for determination the fall velocity of suspended solids:

1, 3 – the branch pipe for connecting the rubber tubes with clamps for regulation the fluid motion mode; 2 – the branch pipe for the contact medium sample inlet from the laboratory setup into the device; 4 – the branch pipe for the air outlet.

The weight concentration of suspended solids in samples, mg/dm^3 taken from the contact medium was determined by the formula:

$$C=(g_1+g_2)/V_0 \qquad [1]$$

where g_1 is the sediment weight in a sample taken from the upper part of the device, mg; g_2 is the sediment weight in a sample taken from the lower part of the device, mg; V_0 is the part of the device volume from the end of branch pipe A to mark 2, mm3.

Then the percent of the suspended solids in each device was determined by the formula:

$$K=(C \cdot V_1 - g_1)/(C \cdot V_1) \tag{2}$$

where V_1 is the part of the device volume between marks A and B, dm³.

The corresponding sedimentation rate V of suspended solids for each of the obtained values K was determined by dividing the distance between marks A and B (mm) to the sedimentation time of the sample (seconds). These values and the rates of suspended solids sedimentation, at a given particle fall velocity, under various conditions of its formation are represented at graphs.

The sediment amount, which was sedimented into the cone of the first cylinder in 6 minutes, characterizes the percentage of the suspended solids that were sedimented from the test water at a rate of 1.2 mm/s or more according to the (6) study. The sediment amount, which was sedimented into the cone of the second cylinder in 36 minutes, characterizes the percentage of the suspended solids that were sedimented from the test water at a rate of 0.2 mm/s and more.

The results of the determination of the suspended solids sedimentation rate, %, are expressed by the formula:

$$S=A/B \tag{3}$$

where A is the amount of the suspended solid (as a percentage from the initial), which was sedimented with a sedimentation rate of 1.2 mm/s and more; B is the suspension amount (in percent of the initial) that was sedimented at a rate of 0.2 mm/s and more.

RESULTS AND DISCUSSION

The influence of concentrated solution of aluminum sulfate coagulant to the fall diameter of the clarifiers contact medium

The value of the coagulated suspended solids fall velocity is one of the main indicators of the upflow clarifiers' work. The fast and complete heterogeneous system separation (the natural water) depends on the suspended solids fall velocity that was formed during water treatment with reagents.

Some conditions must be complied with determining the hydraulic characteristics of suspended solids of the clarifiers contact medium. The suspended solids should save the same particle size and volume concentration in the samples taken for study, like in the clarifier working area. The breaking of suspended solids flakes, their sedimentation and amalgamation should not occur at sampling for this purpose.

The study results are shown in Fig. 3.

It was established that the sedimented coagulated suspension amount increases at 25% with the increasing of coagulant solution concentration.
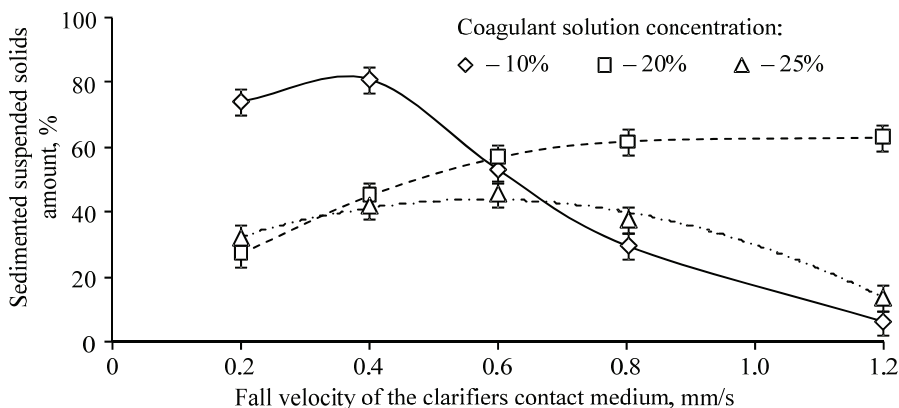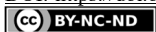
Figure 3. The influence of concentrated solution of aluminum sulfate coagulant to the fall velocity of the upflow clarifiers contact medium

The influence of the concentrated solution with aluminum sulfate coagulant to the changes of suspended sediment concentration along with the clarifier height

The suspended solids content in the clarified water, their physical properties and the coagulant dose affect to flakes specific gravity and the size of suspended sediment.

The sediment value concentration that is entered into the sediment compactor has a significant impact on the compaction process. It is compacted better and faster if the sediment concentration is higher with the same specific gravity of flakes.

The observations were carried out at a laboratory setup (Fig. 1) with the steady-state mode of the clarifiers work at the end of the cycle. The sampling was not disturbing the upper boundary position of the suspended sediment, i.e., the amount of the entering sediment into the clarifier was corresponding to the collected sediment amount.

The research results are shown in Fig. 4.

The variable weight concentration of the suspended sediment presence along the bed height was observed during observation, using conventional and concentrated coagulant solution. The heaviest particles were accumulated at the bottom as a result of hydraulic sorting.

During the patterns of change study, it was found that the suspended sediment weight concentration along the suspended bed height increases with the increasing concentration of the coagulant solution. This process occurs over the all suspended sediment bed height at water treatment with 20% of the aluminum sulfate coagulant solution, the suspended solids concentration at a depth of 140 cm is 1250 mg/dm^3 and using 10% of the coagulant solution it is 671 mg/dm^3, etc.

Original scientific paper
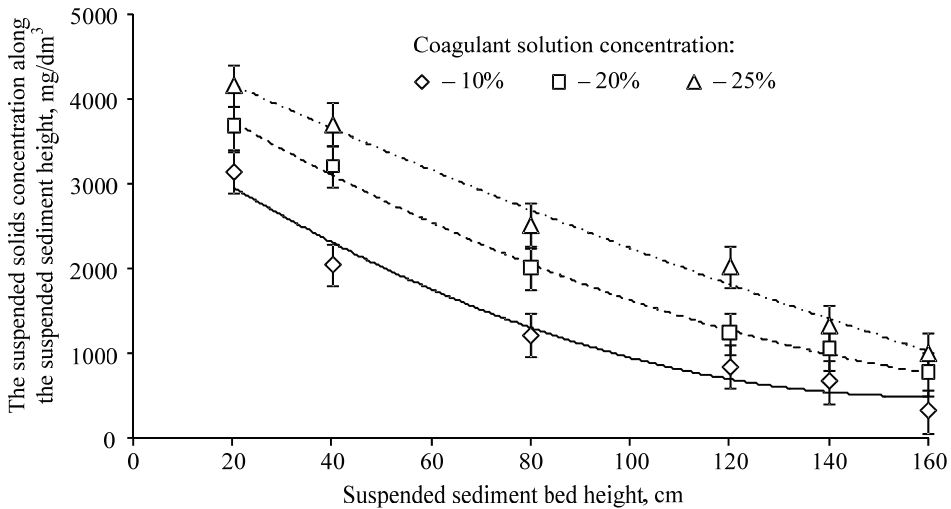
Figure 4. The suspended solids concentration changes along the bed height in the upflow clarifiers

The increasing productivity of upflow clarifiers

The intensifying effect of the concentrated coagulant to the processes of suspended sediment formation in clarifiers, water treatment in these structures, the excess sediment compaction allowed us to conclude that it is possible to reduce the coagulant estimated doses and to increase the productivity of clarifiers without the deterioration of clarified water quality.

Table 2 shows studies with different coagulant aluminum sulfate concentrations at the test water.

During studies, the ascending water flow rate in the clarifier at water treatment with a 10% of coagulant solution was 0.5–1.0 mm/s, and at the concentrated coagulant solution using it was 0.6–1.2 mm/s, which allowed to increase the throughput ability of clarifiers and to increase its productivity. The decrease of clarified water transparency has occurred when the clarifiers medium is increased during water treatment with 10% of the coagulant solution.

The studies are showing the possibility of reducing the concentrated coagulant solution doses. Reducing the coagulant dose using 10% of the coagulant solution is impractical because the increased turbidity of clarified water is observed. The concentrated coagulant solution doses can be reduced during its use on the average of 10-25%, without the deterioration of the clarified water turbidity.

Table 2. Experimental data

Temperature, °C	Initial Water Indicators			Coagulant solution concentration, %	Dose coagulant $Al_2(SO_4)_3$, mg/dm³ (by marketable product)	Upstream rate, mm/s	The clarified water indicators		
	Turbidity, mg/dm³	Transparency, cm	Chromaticity, degree PCS				Turbidity, mg/dm³	Transparency, cm	Chromaticity, degree PCS
2.6 – 3.1	25	36.7	75	10	20	0.5–1.0	3.8 – 4.0	230 – 243	21 – 23
	100	9.2			60		4.1 – 4.4	210 – 225	21 – 24
	200	4.2			85		4.8 – 5.3	175 – 193	23 – 25
2.6 – 3.1	25	36.7	75	20	17	0.7 – 1.25	3.1 – 3.3	287 – 300	19 – 20
	100	9.2			52		3.2 – 3.4	284 – 290	19 – 22
	200	4.2			71		3.8 – 4.2	220 – 243	21 – 23
8.2 – 8.9	25	36.7	75	20	12	1.0–1.5	2.9 – 3.1	>300	18 – 20
	100	9.2			42		2.9 – 3.2	290 – 300	20 – 21
	200	4.2			60		3.6 – 3.9	233 – 257	21 – 24
8.2 – 8.9	25	36.7	75	25	10	1.25–1.75	2.5 – 2.7	>300	17 – 18
	100	9.2			37		2.7 – 2.9	>300	18 – 20
	200	4.2			55		3.2 – 3.5	257 – 290	20 – 23
2.6 – 3.1	25	36.7	75	25	17	1.0 – 1.25	3.1 – 3.2	290 – 300	18 – 20
	100	9.2			48		3.1 – 3.4	283 – 300	19 – 21
	200	4.2			68		3.7 – 4.1	225 – 250	21 – 23
8.2 – 8.9	25	36.7	75	25	11	1.0 – 1.5	2.8 – 3.0	>300	18 – 19
	100	9.2			40		2.9 – 3.1	>300	19 – 22
	200	4.2			57		3.4 – 3.8	243 – 287	21 – 23

Table 3 shows the effectiveness of the concentrated coagulant solution using during the water clarification process in upflow clarifiers at various concentrations.

Table 3. The efficiency of using the concentrated coagulant solution at the water clarification process in upflow clarifiers models at various activation modes

Coagulant solution concentration, %	The upstream rate increasing, %	Coagulant dose reduction, %	Clarified water turbidity reducing (max), %	Chromaticity of the clarified water reducing, %
20	12	10 – 16	28 – 34	10 – 12
25	17	20 – 25	40 – 45	18 – 25

Original scientific paper

The analysis of our obtained data allows concluding that the greatest effect is observed at water treatment with the 25% of the aluminum sulfate coagulant solution.

It was established that the concentrated coagulant solution of aluminum sulfate use allows achieving the clarified water transparency of 290-300 cm and more at sufficiently low turbidity values of clarified water in the clarifier (up to 100 mg/dm^3).

The reduction of the clarified water turbidity in upflow clarifiers influences the operation of system treatment facilities in general, using the concentrated coagulant solution. It is known, that the fine suspended solution, which is difficult to remove (at a sedimentation rate of 0.2-0.4 mm/s or less), is sedimented to the constructions of the second treating stage (filters) with the clarified water, where one part is deposited at the film on the filters surface, another part is in the pores of the filter bed, etc. As a result, the head losses during the water passage through the filters gradually increase, and upon reaching a certain limit value the last one must be output for washing. The filters run duration (the filter duration from one washing to another) significantly affects the treatment setups operation. Moreover, the consumption for filters washing composes a large part (approximately 70%) from current expenses for the filters exploitation. Therefore, the filters run duration will be longer with the lower suspended solids content in water, which is entered into the filters. The treatment setup will operate more efficiently and vice versa the filter run duration decreases with the suspended solution amount increasing in filtered water.

CONCLUSIONS

(1) The method for increasing the efficiency of the upflow clarifiers was proposed for the clarified water treatment with the concentrated coagulant solution of aluminum sulfate that allows optimizing the contact medium properties of the clarifier.

(2) The studies of the regularity work of upflow clarifiers with the impurities coagulating by the concentrated coagulant solution of aluminum sulfate, allowed increasing the fall velocity of coagulated suspended solids by an average of 30%. The increasing of the suspended solution weight concentration along with the suspended sediment bed height, the increasing of the suspended sediment specific gravity with the invariable duration of its formation, the possibility of increasing the upflow rate without the significant reducing of the suspended sediment concentration were noted.

(3) It was established that the use of concentrated coagulant solutions at the water clarification process allows reducing its dose by an average of 15% without the deterioration of the clarified water quality, to increase the throughput ability of upflow clarifiers by 10-20%.

(4) The efficiency of water treatment with the concentrated coagulant solution is maximum at the suspended solids content up to 200 mg/dm^3.

REFERENCES

1. Moshynsky, V.; Riabova, O. Approaches to Aquatic Ecosystems Organic Energy Assessment and Modelling. *NATO Science for Peace and Security Series C: Environmental Security.* **2013**, *128*, 125–135.

2. Tuhai, A.M.; Orlov, V.O. *Vodopostachannia*; Kyiv: Znannia, 2009; p 735.
3. Moshynsky, V. Modern Water Conditions in The Northwest Part of Ukraine: An Analysis. *Water Engineering and Management*. **2001**, *148* (4), 22.
4. Vasylenko, A.A.; Hrabovskyi, P.A.; Larkyna, H.M.; Polyshchuk, A.V.; Prohulnyi V.Y. *Rekonstruktsyia i intensyfykatsyia sooruzhenyi vodosnabzhenyia i vodootvedenyia*; Kyiv: KNUBA, ONABA, 2007; p 307.
5. Jahn, S. Drinking water from Chinese rivers: challenges of clarification. *Journal of Water Supply: Research and Technology-Aqua*. **2001**, *50* (1), 15–27.
6. Kurhaev, E.F. *Osvetlytely vody*; Moscow: Akva-Terra, 2012; p 139.
7. Drahynskyi, V.L.; Alekseeva, L.P.; Hetmantsev, S.V. *Koahuliatsyia v tekhnolohyy ochystky pryrodnykh vod*; Moscov: Nauka, 2005; p 576.
8. Bello Sefiu, A.; Agunsoye Johnson, O.; Adebisi Jeleel, A.; Hassan Suleiman, B. Effect of aluminium particles on mechanical and morphological properties of epoxy nanocomposites. *Acta Periodica Technologica*. **2017**, *48*, 25–38.
9. Kulykov, N.Y.; Naimanov, A.Y.; Omelchenko, N P.; Chernyshev, V.N. *Teoretycheskye osnovy ochystky vody*; Donetsk: Noulydzh, 2009; p 298.
10. Babenkov, E.D. *Ochystka vody koahuliantamy*; Moscow: Nauka, 1977; p 356.
11. Orlov, V.O.; Shevchuk, B.Y. *Intensyfikatsyia raboty vodoochystnykh sooruzhenyi*; Kyiv: Budivelnyk, 1989; p 125.
12. Kliachko, V.A.; Apeltsyn, Y.E. *Podhotovka vody dlia promyshlennoho i horodskoho vodosnabzhenyia*; Moscow: Stroyiyzdat, 1962; p 818.
13. Rybalova, O.; Artemiev, S.; Sarapina, M.; Tsimbal, B.; Bakhareva, A.; Shestopalov, O.; Filenko, O. Development of methods for estimating the environmental risk of degradation of the surface water state. *Eastern European Journal of Enterprise Technologies*. **2018**, *2/10* (92), 4–17.
14. Kulsky L.A.; Goronovsky Y.T.; Koganovsky A.M.; Shevchenko M.A. *Spravochnik po svojstvam, metodov analiza y ochistki void*; Kyiv: Nauk. Dumka, 1980. p. 680.
15. Dushkin, S.; Martynov, S.; Dushkin, S. The contact clarifiers' work intensification at drinking water preparation. *Journal of Water and Land Development*. **2019**, *41* (IV–VI), 55–60.
16. Adgar, A.; Cox, C.; Jones, C.A. Enhancement of coagulation control using the streaming current detector. *Bioprocess and Biosystems Engineering*. **2005**, *27*, 349–357.
17. Nakorchevskaia, V.F.; Kulskyi, L.A.; Romodanova, V.A.; Zaitseva, V.M. Povyshenye effektyvnosty obrabotky vody putem prymenenyia kontsentryrovannykh rastvorov koahulianta. *Vodosnabzhenye i sanytarnaia tekhnyka*. **1974**, *1*, 22–25.

USE OF PHOTO-FENTON FOR MACROLIDE ANTIBIOTIC AZITHROMYCIN REMOVAL

Marcela Jaramillo-Baquero[1,2], Henry Zúñiga-Benítez[1,2]*, Gustavo A. Peñuela[1]

[1] Grupo GDCON, Facultad de Ingeniería, Sede de Investigación Universitaria (SIU),
Universidad de Antioquia UdeA, Calle 70 # 52 -21, Medellín, Colombia
[2] Departamento de Ingeniería Química, Facultad de Ingeniería,
Universidad de Antioquia UdeA. Calle 70 # 52-21, Medellín, Colombia

Azithromycin (AZT) is one of the most used antibiotics worldwide. This has led to its introduction into different environmental compartments, which implies that conventional technologies used in wastewater treatment are not enough to remove this kind of pollutants. Photo-Fenton is an advanced oxidation process in which ferrous ions (Fe^{2+}), under light radiation, catalyzes H_2O_2 decomposition generating hydroxyl free radicals ($HO^•$) which have the potential to oxidize different organic molecules. In this way, this study presents the main results regarding the evaluation of photo-Fenton using simulated sunlight in the removal of AZT from aqueous solutions. The effects of operational parameters such as ferrous ions and hydrogen peroxide initial concentrations were assessed. In addition, some tests were carried out in order to evaluate the extent of pollutant mineralization considering the dissolved organic carbon and the nitrate ions presence on treated samples. In general, results indicated that Fe^{2+} and H_2O_2 initial concentrations have a significant effect on pollutant removal.

Keywords: Advanced oxidation technologies; antibiotics; azithromycin; photo-Fenton; water quality

INTRODUCTION

Antibiotics are drugs used for the treatment of different diseases caused by bacteria in animals and humans. When antibiotic residues reach water bodies they can cause a selection of microorganisms and trigger the emergence of resistant bacterial strain, which could generate diseases not treatable with conventional antibiotics (1, 2).

Macrolide antibiotics, including azithromycin (AZT, $C_{38}H_{72}N_2O_{12}$), are some of the most used drugs worldwide, a fact that has led to their introduction into surface and even drinking water. This also implies that conventional technologies used in wastewater treatment are not enough to prevent the entry of this kind of pollution into water and ecosystems (3–6).

Advanced oxidation technologies have proven to be efficient in removing organic contaminants present in aqueous matrices. In particular, Fenton and photo-Fenton processes have been able to oxidize various types of organic pollutants. The reaction consists in the generation of highly reactive species such as the hydroxyl free radical ($HO^•$) from the catalytic decomposition of H_2O_2 in the presence of iron species and light radiation.

---

* Corresponding author: Henry Zúñiga-Benítez, Departamento de Ingeniería Química, Facultad de Ingeniería, Universidad de Antioquia UdeA. Calle 70 # 52-21, Oficina 18-319, Medellín, Colombia, e-mail: henry.zuniga@udea.edu.co

An important aspect of this type of methodologies is that they allow the use of radiation with a wavelength similar to that of the sun, favoring its subsequent application on a larger scale using sunlight directly (7, 8).

Having into account the above, the main objective of this study is to present the results related to the use of photo-Fenton under simulated sunlight radiation at laboratory scale in the removal of AZT from aqueous solutions considering the effect of operational variables such as H_2O_2, Fe^{2+} and antibiotic initial concentration. In addition, organic matter mineralization was evaluated considering the variation of the total organic carbon and nitrates content of the treated samples.

EXPERIMENTAL

Chemicals and solutions

Used chemicals were of analytical grade. Azithromycin dihydrate (98%) was purchased from AK Scientific. Iron (II) sulphate heptahydrate ($FeSO_4 \cdot 7H_2O$, Sigma Aldrich) was used as ferrous ions source. Hydrogen peroxide (35% w/w) and isopropyl alcohol were supplied by Merck. Control of pH was done using concentrated solutions of NaOH and HCl obtained from Alfa-Aesar. Sodium thiosulphate pentahydrate ($Na_2S_2O_3 \cdot 5H_2O$, Sigma Aldrich) was used for quenching remaining H_2O_2 during the sampling stage. All the aqueous solutions were prepared using ultra-pure water. Methanol and ammonium formate (NH_4HCOO) for chromatographic analysis were of LC/MS grade.

Photocatalytic experiments

A Suntest CPS+ (Atlas) photosimulator (wavelength: 290-800 nm and irradiance: 500 W m^{-2}) was employed to carried out all the experiments.

Borosilicate glass flasks containing 50.0 mL of 1.0 mg L^{-1} pollutant aqueous solution were used for light exposition. Solution pH was 3.0 during reaction time. Distance from the lamp to the liquid surface was ~15.0 cm, and the liquid depth inside the flasks was ~5.0 cm.

Analytical methods

Samples of 1.0 mL were withdrawn at different time intervals and analyzed after quenching remnant H_2O_2 using an Acquity UPLC system (Waters Corporation) and an Acquity UPLC BEH C18 column (1.7 mm, 50 mm, 2.1 mm, Waters). Mobile phase was a mix of water: methanol 95:5 and methanol: water 95:5. Solvents ratio was 60/40 for one min, then 40/60 for one additional min, next 10/90 for one min and finally 40/60 for two minutes. Masslynx 4.1 (Micromass) software was used to process data.

Mineralization of organic matter was evaluated considering the dissolved organic carbon (DOC) and nitrates concentration in the treated samples using the *Standard Methods for the Examination of Water and Wastewater* methods 4129D and 526D (9).
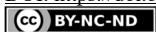
RESULTS AND DISCUSSION

According to equations 1 and 2, the main source of HO$^{\bullet}$ radicals, in Fenton treatments, is the decomposition of H_2O_2, while Fe^{2+} acts as a catalyst, undergoing changes in its oxidation state under the presence of light radiation.

$$Fe^{2+} + H_2O_2 \rightarrow Fe^{3+} + OH^- + HO^{\bullet} \qquad [1]$$

$$Fe^{3+} + H_2O_2 + hv \rightarrow Fe^{2+} + HO^{\bullet} + H^+ \qquad [2]$$
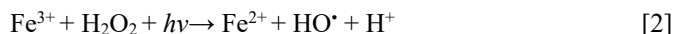
In this study, the effects of the initial concentrations of H_2O_2 and Fe^{2+} on AZT removal were evaluated in first instance performing exploratory tests considering concentrations of peroxide between 10.0 and 200.0 mg L^{-1}, and for $FeSO_4$ between 5.0 and 10.0 mg L^{-1}. Results of these preliminary experiments (data not shown) indicated that under these initial concentrations of $FeSO_4$ and H_2O_2, around 83.0 % of AZT was removed after 30 min of reaction.

Effect of Fe^{2+} initial concentration on AZT removal

Effect of ferrous ions on pollutant removal was evaluated in the range 2.5 - 7.5 mg L^{-1} $FeSO_4$. Figure 1 presents the results about AZT elimination after 30 min of photo-treatment.
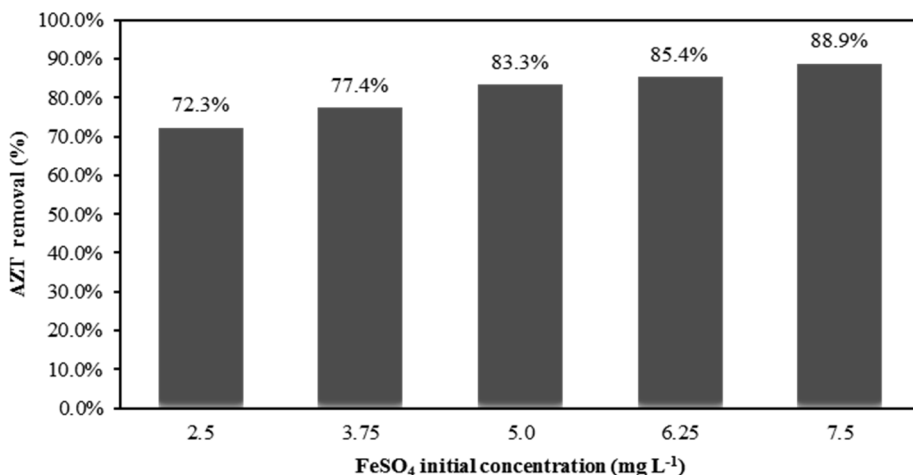
Figure 1. Effect of Fe^{2+} initial concentration on AZT removal using photo-Fenton (pollutant initial concentration 1.0 mg L^{-1}, pH 3.0, H_2O_2 initial concentration 20.0 mg L^{-1}, irradiance 500.0 W m^{-2}, reaction time 30 min).

From this figure, it is evident that increases in the concentration of ferrous ions promote a higher contaminant removal because of a probable higher HO$^{\bullet}$ radicals generation.

In this particular case, it was decided not to increase the Fe^{2+} concentration considering that the achieved antibiotic removal percentage was ~90.0% in just 30 min of reaction, and excess of Fe^{2+} could have inhibitory effects on pollutant removal as a result of $HO^{\bullet}$ scavenging (10).

Effect of H_2O_2 initial concentration on AZT removal

Effect of H_2O_2 initial concentration was evaluated in the range 5.0 - 35.0 mg L^{-1}. In this sense, Figure 2 indicates that increasing peroxide concentration between 5.0 and 27.5 mg L^{-1} favors a higher removal of AZT due, probably, to a greater generation of $HO^{\bullet}$ free radicals from H_2O_2 decomposition (equation 1). However, an excess of peroxide could react with radicals promoting the formation of species with less potential to oxidize organic pollutants, for example, the hydroperoxyl radical ($HO_2^{\bullet}$) (equation 3). $HO_2^{\bullet}$ can also react with $HO^{\bullet}$ (equation 4), which would reduce the possibility of removing the organic matter present in the solution via oxidation by $HO^{\bullet}$ (11).

$$HO^{\bullet} + H_2O_2 \rightarrow HO_2^{\bullet} + H_2 \qquad [3]$$

$$HO^{\bullet} + HO_2^{\bullet} \rightarrow H_2O + O_2 \qquad [4]$$

Considering the above, the conditions that would favor a higher AZT removal using photo-Fenton with simulated sunlight are $FeSO_4$ and H_2O_2 initial concentrations of 7.5 and 27.5 mg L^{-1} respectively.
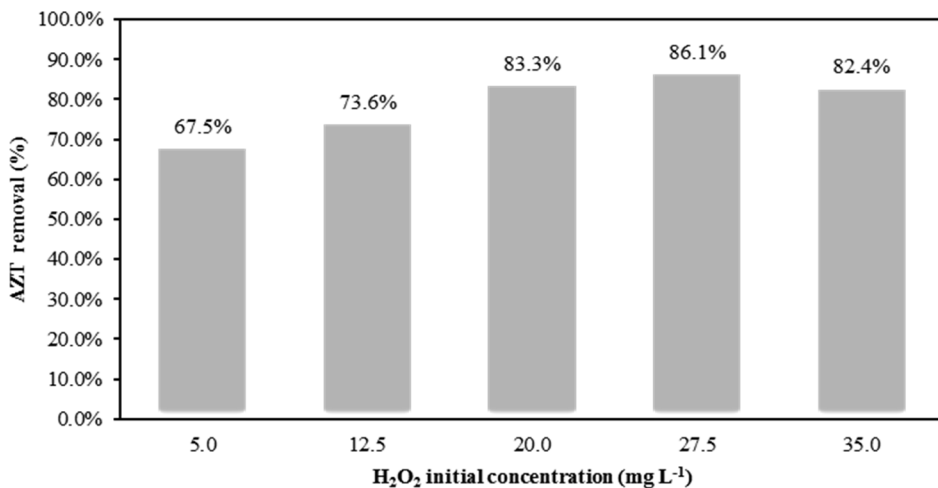
Figure 2. Effect of H_2O_2 initial concentration on AZT removal using photo-Fenton (pollutant initial concentration 1.0 mg L^{-1}, pH 3.0, $FeSO_4$ initial concentration 5.0 mg L^{-1}, irradiance 500.0 W m^{-2}, reaction time 30 min).
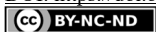
AZT removal under different experimental conditions

In order to clarify the reaction mechanism, tests were carried out considering the combination, under the evaluated experimental range, that lead to a higher extent of antibiotic removal using photo-Fenton technology. In addition, some experiments that allowed to determine the individual performance of the different agents in the reaction, and their synergistic effects were evaluated. Figure 3 indicates that photo-Fenton process resulted in an antibiotic removal higher than 90.0% after 30 min of reaction. Likewise, the role of $HO^{\bullet}$ free radicals was evaluated by performing tests under the presence of isopropanol (radicals scavenger agent), which led to a significant inhibition in AZT elimination, suggesting that $HO^{\bullet}$ would be the main responsible specie for substrate oxidation.
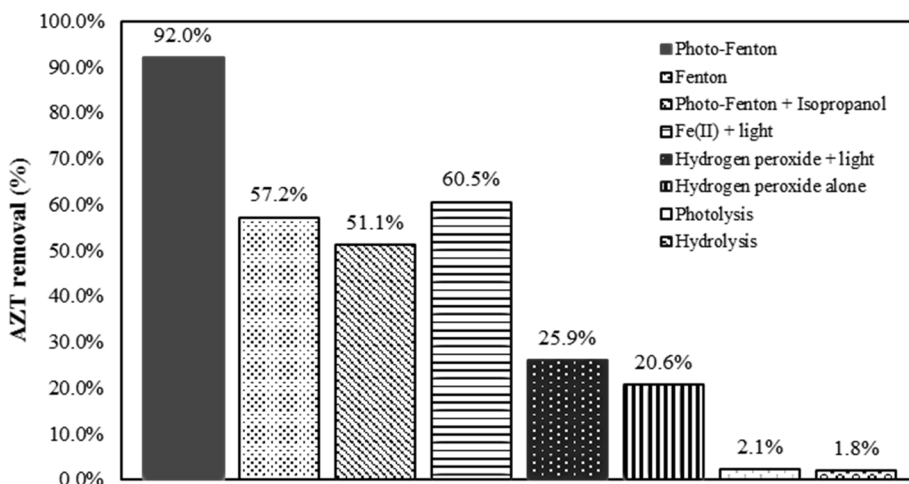
Figure 3. AZT removal under different reaction systems (pollutant initial concentration 1.0 mg L^{-1}, pH 3.0, FeSO$_4$ initial concentration 7.5 mg L^{-1}, H$_2$O$_2$ initial concentration 27.5 mg L^{-1}, irradiance 500.0 W m^{-2}, reaction time 30 min).

Another aspect that should be highlighted is the fact that the application of photo-Fenton technology conducts to a high pollutant removal, while the conventional Fenton reaction only allowed a 57.2% reduction in analyte concentration, ratifying, that the incorporation of simulated sunlight improves the efficiency of the process because of a higher regeneration of Fe^{2+} ions in the solution (equation 2).

On the other hand, it can be seen that combination of Fe^{2+} ions and sunlight led to an antibiotic removal ~ 60.0% in 30 min possibly as a result of an eventual formation of H$_2$O$_2$ after Fe^{2+} photo-transformation (equations 5 and 6) (12). The H$_2$O$_2$ could react with the Fe^{2+} ions present in the solution and generate $HO^{\bullet}$ radicals (Fenton reaction).

$$Fe^{2+} + O_2 + h\nu \rightarrow Fe^{3+} + O_2^{-\bullet} \qquad [5]$$

$$Fe^{2+} + O_2^{-\bullet} + 2H^+ \rightarrow Fe^{3+} + H_2O \qquad [6]$$

                                                            Original scientific paper
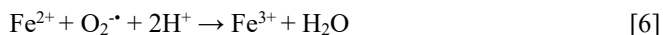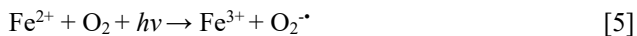
Additional tests including the presence of H_2O_2 indicated that the H_2O_2/light combination allows to achieve ~ 26.0% of AZT elimination, which could be a result of a breakdown of the peroxide molecule and radicals generation (mechanism of the UV/H_2O_2 advanced oxidation process) (13). Besides, the individual action of H_2O_2 only allowed ~20.0% of AZT removal.

Finally, it was confirmed that the individual action of sunlight and hydrolysis at optimal pH on AZT removal is negligible (removal percentages less than 3.0%).

Effect of pollutant initial concentration on AZT removal

The effect of the initial concentration of AZT was evaluated in the range 1.0 - 3.0 mg L^{-1}. Figure 4 indicates that a higher antibiotic removal is obtained under an initial concentration of 1.0 mg L^{-1}, and it decreases as the substrate concentration in the solution increases. This could be due to the fact that the amount of $HO^{\bullet}$ radicals generated during the process is constant, which would represent a limitation in the degradation of the pollutant as result of a competition between it and the generated by-products to react with the free radicals, a situation that also has been reported by other authors in the treatment of organic pollutants using photo-Fenton (14).
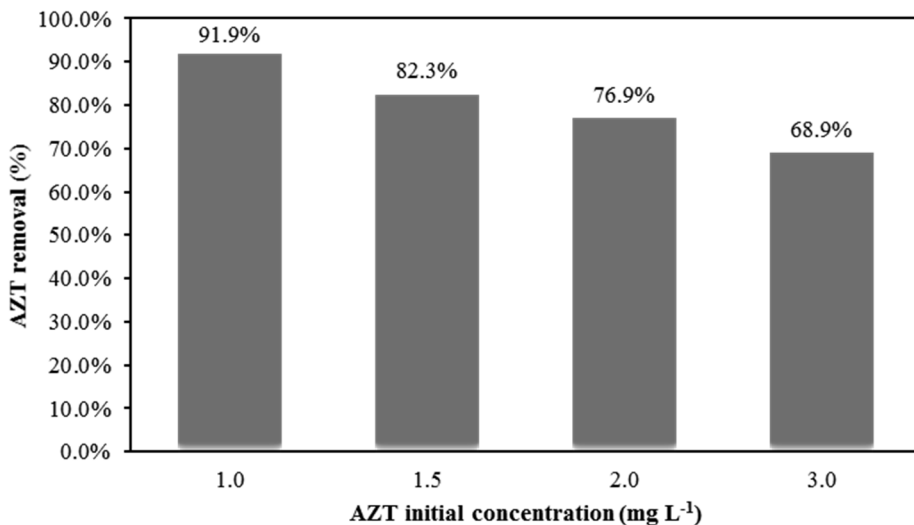
Figure 4. Effect of pollutant initial concentration on AZT removal using photo-Fenton (pH 3.0, $FeSO_4$ initial concentration 7.5 mg L^{-1}, H_2O_2 initial concentration 27.5 mg L^{-1}, irradiance 500.0 W m^{-2}, reaction time 30 min).

In addition, different authors have reported that reactions involving Fenton and photo-Fenton processes satisfy a pseudo-first order reaction kinetics (8, 14, 15). Figure 5 presents the relationship between -Ln (C/C_0) and time, indicating that the experimental data fit the proposed model appropriately (correlation coefficients > 0.85).
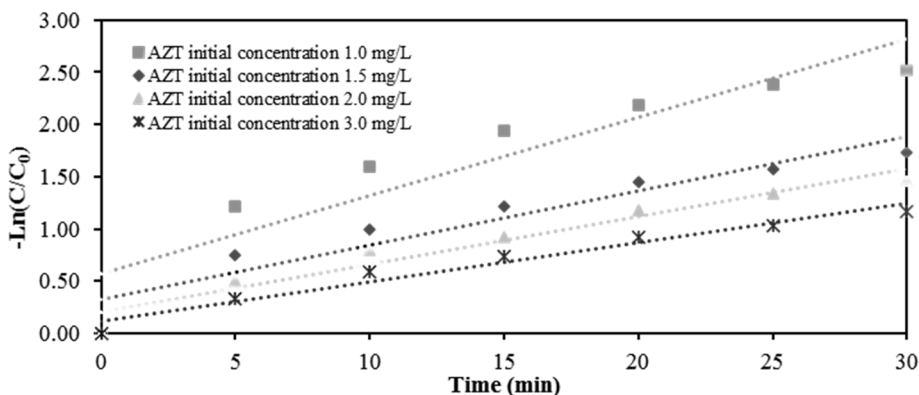
Figure 5. Pseudo-first order reaction kinetics model for AZT removal using photo-Fenton (pH 3.0, $FeSO_4$ initial concentration 7.5 mg L^{-1}, H_2O_2 initial concentration 27.5 mg L^{-1}, irradiance 500.0 W m^{-2}, reaction time 30 min).

Mineralization studies

Total mineralization of AZT would conduct to the formation of CO_2, H_2O and NO_3^{-1}. In this way, in order to assess the extent of organic matter oxidation, variation on DOC and NO_3^{-1} content in the treated samples was analyzed. In this sense, Figure 6 indicates that after 120 min of reaction, decrease in organic matter was ~67.0%, which suggests that part of the contaminant is being transformed into CO_2 and H_2O. In addition, the increase of the NO_3^{-1} presence indicates that nitrogen content on AZT molecule is also being oxidized.
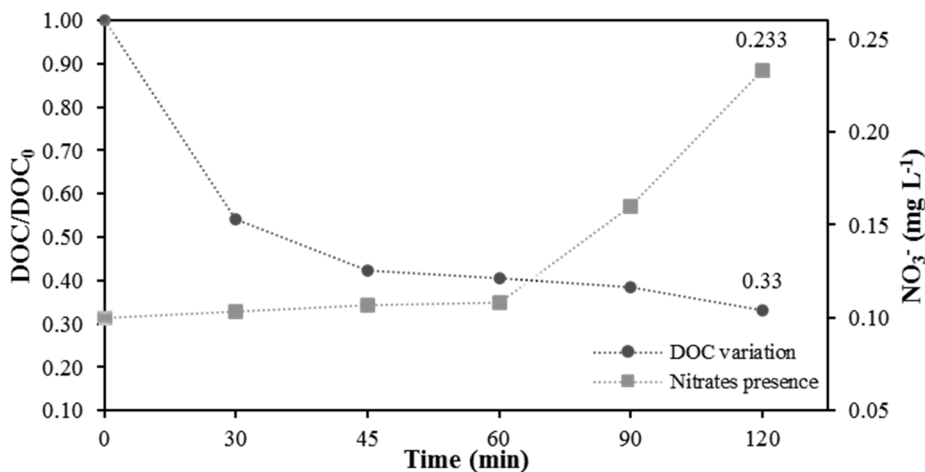
Figure 6. DOC and NO_3^{-1} variation during AZT removal using photo-Fenton (pH 3.0, $FeSO_4$ initial concentration 7.5 mg L^{-1}, H_2O_2 initial concentration 27.5 mg L^{-1}, irradiance 500.0 W m^{-2}).

CONCLUSIONS

Photo-Fenton under simulated sunlight is able to remove macrolide antibiotic azithromycin in deionized water solutions. Initial concentrations of ferrous ions and hydrogen peroxide have a significant effect on pollutant removal. However, excess of H_2O_2 inhibit the reaction.

Removal of azithromycin, under the evaluated conditions, is mainly due to the action of hydroxyl free radicals, and satisfies a pseudo-first order reaction kinetics model.

Under the studied conditions, it is possible to reach more than 60.0% of contaminant mineralization, indicating that AZT is being transformed into CO_2, H_2O and HNO_3.

Acknowledgements

REFERENCES

1. Babić, S.; Ćurković, L.; Ljubas, D., Čizmić, M. TiO_2 assisted photocatalytic degradation of macrolide antibiotics. *Curr. Opin. Green Sustain. Chem.* **2017,** *6*, 34-41.
2. Du, J.; Zhao, H.; Liu, S.; Xie, H.; Wang, Y.; Chen, J. Antibiotics in the coastal water of the South Yellow Sea in China: Occurrence, distribution and ecological risks. *Sci. Total Environ.* **2017,** *595*, 521-527.
3. Huang, B.; Wang, H.; Cui, D.; Zhang, B.; Chen, Z.; Wang, A. Treatment of pharmaceutical wastewater containing β-lactams antibiotics by a pilot-scale anaerobic membrane bioreactor (AnMBR). *Chem. Eng. J.* **2018,** *341*, 238-247.
4. Mirzaei, R.; Yunesian, M.; Nasseri, S; Gholami, M.; Jalilzadeh, E.; Shoeibi, S.; Mesdaghinia, A. Occurrence and fate of most prescribed antibiotics in different water environments of Tehran, Iran. *Sci. Total Environ.* **2018,** *(619-620)*, 446-459.
5. Saitoh, T.; Shibata, K.; Fujimori, K.; Ohtani, Y. Rapid removal of tetracycline antibiotics from water by coagulation-flotation of sodium dodecyl sulfate and poly(allylamine hydrochloride) in the presence of Al(III) ions. *Sep. Purif. Technol.* **2017,** *187*, 76-83.
6. Xiong, W.; Zeng, G.; Yang, Z.; Zhou, Y.; Zhang, C.; Cheng, M.; Liu, Y.; Hu, L.; Wan, J.; Zhou, C.; Xu, R.; Li, X. Adsorption of tetracycline antibiotics from aqueous solutions on nanocomposite multi-walled carbon nanotube functionalized MIL-53(Fe) as new adsorbent. *Sci. Total Environ.* **2018,** *627*, 235-244.
7. Cheng, M.; Zeng, G.; Huang, D.; Lai, C.; Xu, P.; Zhang, C.; Liu, Y. Hydroxyl radicals based advanced oxidation processes (AOPs) for remediation of soils contaminated with organic compounds: a review. *Chem. Eng. J.* **2016,** *284*, 582-598.
8. Alalm, M.G.; Tawfik, A.; Ookawara, S. Degradation of four pharmaceuticals by solar photo-Fenton process: Kinetics and costs estimation. *J. Environ. Chem. Eng.* **2015,** *3* (1), 46-51.
9. Standard Methods for the Examination of Water and Wastewater, 22rd ed., American Public Health Association, Washington, DC. **2017**.

10. Funai, D.H.; Didier, F.; Giménez, J.; Esplugas, S.; Marco, P.; Machulek, A. Photo-Fenton treatment of valproate under UVC, UVA and simulated solar radiation. *J. Hazard. Mater.* **2017,** *323*, 537-549.

11. Rahim Pouram, S.; Abdul Aziz, A.R.; Wan Daud, W.M.A. Review on the main advances in photo-Fenton oxidation system for recalcitrant wastewaters. *J. Ind. Eng. Chem.* **2015,** *21*, 53-69.

12. Liu, N.; Sijak, S.; Zheng, M.; Tang, L.; Xu, G.; Wu, M. Aquatic photolysis of florfenicol and thiamphenicol under direct UV irradiation, UV/H_2O_2 and UV/Fe(II) processes. *Chem. Eng. J.* **2015,** *260*, 826-834.

13. Shokri, R.; Jalilzadeh Yengejeh, R.; Babei, A.A.; Derikvand, E.; Almasi, A. UV activation of hydrogen peroxide for removal of azithromycin antibiotic from aqueous solution: determination of optimum conditions by response surface methodology. *Toxin Rev.* **2019,** *In press.*

14. Ammar, H.B.; Ben Brahim, M.; Abdelhédi, R.; Samet, Y. Enhanced degradation of metronidazole by sunlight via photo-Fenton process under gradual addition of hydrogen peroxide. *J. Mol. Catal. A Chem.* **2016,** *420*, 222-227.

15. Tamimi, M.; Qourzal, S.; Barka, N.; Assabbane, A.; Aitichou, Y. Methomyl degradation in aqueous solutions by Fenton's reagent and the photo-Fenton system. *Sep. Purif. Technol.* **2008,** *61* (1), 103-108.

CHEMICAL COMPOSITION AND CONSUMER ACCEPTABILITY OF COOKIES FLAVOURED WITH VANILLA - *AIDAN (Tetrapleura tetraptera)* BLENDS

Kazeem K. Olatoye[1]*, Adetunji I. Lawal[2], Idowu A. Olamilekan[1]

[1] Department of Food Science and Technology, College of Agriculture, Kwara State University, Malete, Nigeria
[2] Department of Food Technology, Faculty of Technology, University of Ibadan, Ibadan, Oyo State, Nigeria

Aidan is an underutilised spice with characteristic fragrant and pungent aromatic odour, similar to vanilla flavour. Chemical composition and consumer acceptability of cookies flavoured with vanilla-Aidan blends were investigated. Aidan pulp was milled and substituted for vanilla powder (25-100%) in cookies formulation. Cookies were characterised for chemical contents and sensory properties using standard methods and panellists test. Data were analysed using ANOVA at $\alpha_{0.05}$. The study revealed that chemical contents, (except carbohydrate and metabolizable energy) and sensory properties of cookies significantly improved with increase in addition of Aidan. Moisture content of the cookies ranged between (1.83-3.77%), crude protein (9.83-12.86%), ash (0.55-0.71%), fat (0.98-1.29%), fibre (0.35-0.46%), carbohydrate (81.35-86.45%) and metabolizable energy (380.60-393.94 kcal). Mineral content was significantly influenced, with phosphorus content ranging between (64.00-142.67mg/100g), iron (2.62-6.53 mg/100g) and zinc (3.80 mg/100g- 4.47 mg/100g). The ranges of tannin, phytate, flavonoid and phenolic compounds in mg/100g were 0.07-0.08, 0.17-0.23, 0.53-0.82 and 0.76-1.53 respectively. Mean scores for cookies appearance, taste, aroma, crispness and over all acceptability ranged between 7.23-8.17, 7.30-7.87, 7.33-8.07, 7.20-7.80 and 7.72-8.31, respectively. Panellists accepted sample with 3 g (75%) of Aidan and 1 g (25%) of vanilla the most. Acceptable cookies with good nutritional composition can be produced, using vanilla-Aidan blends as a flavouring agent.

Keywords: *Tetrapleura tetraptera*, cookies, spices, consumer acceptability, functional food

INTRODUCTION

In Nigeria, like many other developing countries, the increasing phenomenon of urbanisation coupled with the growing number of working mothers, have contributed greatly to the popularity and increased consumption of snack foods such as cookies and biscuits (1). Snack food industry is expanding rapidly all over the world, nonetheless, the 21st century saw the revolution of snack foods towards functional snacks (2-3). Snack making from suitable blends of appropriate food materials with incorporation of nutrients (vitamin, minerals, protein, low fat, high fibre, fat replacers, gluten free ingredients) and/or phytochemicals (anthocyanin, phenolics or flavonoids) constitutes better vehicles of nutrients conveyor and health promoters (3-5). They are regarded as functional snacks

---

* Corresponding author: Kazeem Koledoye Olatoye, Department of Food Science and Technology, College of Agriculture, Kwara State University, Malete, Nigeria, e-mail: luckykaykay@yahoo.com

known to possess additional health benefit, apart from basic nutrient. Similarly, replacement of synthetic components of the snack ingredients with more natural ones constitutes another avenue of producing less expensive functional food with bioactive substances (6-7). Thus, there is the need to explore natural flavourings and spices with noteworthy impact on organoleptic and functional properties of snacks. Such edible products with flavouring characteristics include fruits, seeds, leaves, flowers, nuts, pulp and oils from naturally occurring plants with pungent or aromatic characteristics, which have been previously used to season foods. Reportedly, an underutilised spice with characteristic fragrant and pungent aromatic odour in Nigeria is *Aidan*, according to (6). It is botanically known as *Tetrapleura tetraptera* and belongs to the family Fabaceae (formerly Leguminosae: Mimosoideae). It is commonly known as "Aidan" among the Yoruba ethnic group of south western Nigeria, "Agbolo" among the Igala people of North central Nigeria, and "dawo" among the Hausa people of Northern Nigeria. It is used as a popular seasoning spice in these areas. Compared with other commonly used spices, it is a rich source of phytochemicals which contribute to its documented biological and pharmacological activities, including cardiovascular, anti-inflammatory, hypoglycaemic, anti-hypertensive, anti-ulcerative, anti-microbial, and emulsifying properties (8-10). Currently, the use the oil extracted from *Tetrapleura tetraptera* to flavour popcorn was documented (6). However, use of *Aidan* power in contrast with extracted flavour could be free of impurities from extraction solvents. Literature report on the use of *Aidan* powder in frequently consumed snacks like cookies as flavourings is rare. Substitution of *Aidan* powder, a natural flavouring spice for synthetic and imported flavours may bring about production of less expensive, nutritive and healthy cookies. Therefore, chemical and sensory characteristics of cookies flavoured with vanilla- *Aidan* blends in cookies production was investigated.

EXPERIMENTAL

Dried pulp of *Tetrapleura tetraptera* was obtained from Forestry Research Institute of Nigeria (FRIN), Jericho, Ibadan, Nigeria. Wheat flour, sugar, salt and egg were purchased from Malete market, Ilorin and brought to Food processing Laboratory, Department of Food Science and Technology, Kwara State University, Nigeria. The chemicals and reagents used were of analytical grade and were obtained from Bumlab Nigeria Limited, Ring Road, Ibadan, Nigeria. The *Tetrapleura tetraptera* pulp was pounded using mortar and pestle to promote its surface area. It was then milled using an electric blender, sieved with a 250 µm mesh and bottled in a sterile plastic container prior to use. The cookie was formulated using the modified method of Eneche (11). The formulation was done in a way that all ingredients were kept constant, except *Aidan* and vanilla power. Vanilla powder was substituted by *Aidan* powder (25%-100%) in the formulation. The baking butter (125 g) and sugar (120 g) were mixed together manually for 5 min to get a fluffy mixture of butter and sugar. The flour (250 g), salt (2.5 g), egg (60 g) and baking powder (9 g) were mixed together and then mixed with the butter-sugar mixture to get a dough. The measured amount of water (20 ml) was gradually added into the bowl and continuous mixed until good textured, firm dough was obtained. The dough was kneaded on a clean

flat surface for 4 min and transferred to a cutting table with which a shape maker was pressed over the dough to give desired shapes. The cut dough pieces were then transferred into fluid-fat- greased baking trays and baked at 180 °C for 45 min, cooled and packaged. Cookie samples were coded as C_0, C_{25}, C_{50}, C_{75} and C_{100} for Cookie containing 0% Aidan, 25% Aidan, 50% Aidan, 75% Aidan and 100% Aidan respectively. Methods described by AOAC (12) was used to determine the proximate composition, including crude protein, fat, moisture content, crude fibre, ash and carbohydrate content of the ground cookie samples. Five grams of each sample was oven dried at 105 °C until constant weight is obtained. Moisture content was calculated as percentage of weight loss to the original weight. The micro kjeldahl method was used to determine crude Protein. One-gram sample was weighed into the digestion tubes and 15ml of conc. sulphuric acid was added followed by mixing and then addition of two tablets of kjeldahl selenium catalyst to the flask. The mixture was digested at 420 °C until the solution turned colourless and fuming ceased. 75 ml of distilled water was quickly added to the mixture to avoid caking. The digest was distilled with 50 ml of 40% sodium Hydroxide solution. The distillate (100 ml) was the collected into 25 ml boric acid mixture prepared by mixing 250 ml of 4% (w/v) boric acid, 14 ml and 20 ml of 0.02 g methyl red and 0.02 bromocresol green, respectively and made up to one liter with deionised water. The ammonium borate produced was titrated with standard 0.1N hydrochloric acid solution until green colour just disappeared. Blank were prepared and treated in a similar way. Percentage Nitrogen was calculated using the equation below:

$$\%N = \frac{1.401 \times (ml\ HCL\ sample - ml HCL\ titre\ of\ blank) \times NHCL}{Sample\ weight} \qquad \text{Eq. 1}$$

$$\% \text{ crude protein} = \% N \text{ x conversion factor (6.25)} \qquad \text{Eq. 2}$$

The soxhlet fat extraction methods was used to determine crude fat content. A 250 ml boiling flask was cleaned and dried in the oven at 105 °C for 30 min. The flask was moved into a desiccator and then allowed to cool. The flask was labeled, weighed and then filled with 300 ml petroleum ether. 2 grams of the sample was accurately weighed into a correspondingly labeled thimble. The extraction thimble was tightly plugged with cotton wool. The soxhlet apparatus was assembled and allowed to reflux for ether was collected on the top of the container in the set up and drained into another container for re-use. The flask was removed and dried at 103 °C before being transferred from oven into a desiccator for cooling and re-weighing. The percentage fat was calculated as follows:

$$\% \text{ Fat} = \text{Weight of defatted sample x100 / Weight of sample} \qquad \text{Eq. 3}$$

For ash content, three grams of dried samples from moisture determination was charred on a heater until it carbonized then incinerated in a muffle furnace at 550 °C for 6 hours the residue was weighed and aseptically kept. For crude fibre content, 100 ml TCA (Trichloroacetic acid) digestion reagent made up of 500 ml acetic acid, 450 ml distilled water, 50 ml conc. HNO_3 and 20 g TCA was added to 1 g of defatted sample. The suspension was boiled under reflux for exactly 40 min. The solution was filtered through a

                                                            Original scientific paper

whatman no. 4 filter paper of known weight. Residue was washed six times with hot water and once with industrial spirit. The filter paper and content were transferred into a known weight of porcelain dish and dried overnight at 100 °C. The porcelain dish was transferred into desiccators to cool, weighed and charred in a muffle furnace at 600 °C for 5hour. This was allowed to cool and then reweighed. The carbohydrate content was determined by difference using the formula.

% Carbohydrate = 100-(% moisture + % ash + % protein + % fat + % fibre)   Eq. 4

The energy value of the cookie was calculated from percentages of major nutrients in kilojoules per 100 g and the values were converted to kcal by dividing them by the conversion factor (4.184), according to (13) as shown in equation 1.

$$EV \ (kcal) = (Carb. \ x \ 17+ Prot. \ x \ 17+ Fat \ x \ 37)/ \ 4.184)$$ Eq. 5

Where *EV* - Energy value and *Carb*, *Prot.* and *Fat* are the percentages of carbohydrates, proteins and fats.

The content of phosphorus (P), iron (Fe) and zinc (Zn) minerals in each cookie sample was determined by digesting 2.0 g of the flour sample using the Atomic Absorption Spectrophotometric method as outlined in the Association of Official Analytical Chemists' Approved method 968.08 AOAC (14). The Folin-Denis colorimetric method described by (15) was used to determined tannin content. Five grams of the sample flour was dispersed in 50 ml of distilled water and shaken. The mixture was allowed to stand for 30min at 28 °C before it was filtered through Whatman No. 42 grade of filter paper. Preparation of a standard tannic acid solution was carried out. From the standard solution, 2 ml and equal volume of distilled water was dispersed into a separate 50 ml volumetric flask. This serve as standard and reagent blank respectively. Then, 2 ml each of the sample extracts were put in their respective labelled flask. The contents of each flask were then mixed with 35 ml distilled water and 1 ml of the Folin-Denis reagent was added to each. This was followed by addition of 2.5 ml saturated Na_2CO_3 solution. The content of each flask was made up to 50 ml with distilled water and allowed to incubate at 28 °C for 90 min. Their respective absorbance was measured in a spectrophotometer (Jenway 6305 UV) at 760 nm using the reagent blank to calibrate the instrument at zero. Calculation of tannin content was as show below:

$$\% \ tannin = \frac{100}{W} x \frac{au}{as} x \ c \ x \frac{vt}{va}$$ Eq. 6

Where *W* - weight of sample; *au* - absorbance of test sample; *as* - absorbance of the standard tannin solution. *c* - concentration of standard tannin solution; *vt* - total volume of extract; *va* - volume of extract analysed. Phytate content was determined according to the method of Young and Greaves (16). About four grams (4 g) of the sample flour were soaked in 100 ml of 2% HCl for 3 hours and then filtered. Thereafter, 25 ml of the filtrate was placed in the conical flask. A 5 ml of 0.3 % ammonium thiocyanate solution was added as an indicator and 53.3 ml of distilled water was also introduced to attain the

Original scientific paper

desired acidity. This was titrated with standard $FeCl_3$ solution until a brownish yellow colour was appeared persisting for 5 min.

$$Phytate\ in\ mg/100\ g = titre\ value\ x\ 564.11 \qquad Eq.\ 7$$

The gravimetric method was used (17) to determine the total flavonoid content, following ethyl lactate precipitation. Five-gram (5.0 g) sample was measured and mixed with 100 ml of 2% HCl solution and boiled for 30 minutes. It was allowed to cool and then filtered through Whatman No. 42 filter paper. The filtrate was treated with dropwise addition of ethyl lactate until full precipitation was obtained. The filtrate was recovered using a weighed filter paper and dried in the oven at 100 °C for 30 minutes. Cooling was done in a desiccator and reweighed. The weight of flavonoid was obtained by difference and expressed as percentage of the sample weight analysed. The formula below was used to calculate the flavonoid content.

$$\%\ Flavonoid = (100\ (W2-W1))/(Wt.\ of\ sample) \qquad Eq.\ 8$$

$W1$ - wt. of empty filter paper
$W2$ - wt. of paper + Flavonoid precipitate

Determination of total phenolic content of the sample was determined using Folin-Ciocalteu spectrophotometric method. Two grams (0.2 g) of the sample was extracted with 10 ml of pure methanol. One millilitre of the filtrate (extract) was mixed with equal volume of Folin-Ciocalteu reagent in a test tube. Also, 1 ml of standard phenol solution was treated the same way. One millilitre of saturated sodium bicarbonate solution was added to each tube and their respective content was calculated using the formula below:

$$\%\ Total\ Phenolics = \frac{100}{w} \times \frac{AU}{AS} \times \frac{c}{100} \times \frac{Vt}{Va}\ X\ D \qquad Eq.9$$

W - weight of sample
Au - Absorbance of test sample
As - Absorbance of standard tannin solution
V_t - total volume of extract
C - concentration of the standard tannin solution
V_a - Volume of extract analysed
D - Dilution factor where necessary

Sensory evaluation was conducted on cookie samples for appearance, taste, aroma, crispness and overall acceptability using multiple comparison analysis. The samples were presented to thirty-man, untrained panellists mainly, undergraduate students who are familiar with cookies, to evaluate and score them on a 9-point Hedonic scale. On the scale, 9 represented = like extremely and 1 = dislike extremely (18). All obtained data in, replicated were statistically analysed using a one-way analysis of variance (ANOVA) and means were separated by Duncan's Multiple Range Test (DMRT) using the Statistical

package for social science (SPSS) IBM VERSION 21.0 package (Armonk, New York). Significance was accepted at 0.05 probability level.

RESULTS AND DISCUSSION

Proximate composition and metabolizable energy of cookies flavoured with *Aidan* as substitute for vanilla

The moisture content of the cookies ranged between 1.83% and 3.77% and were lower than (6.20-13.41%) reported by (7) in similar study involving substitution of vanilla by African nutmeg in cookies production (Table 1). The low moisture content suggested their microbial stability (19). The crude protein, fat, ash and fibre contents of the cookies ranged between (9.83-12.86%), (0.98-1.29%), (0.55-0.71%) and (0.35-0.46%) respectively. The carbohydrates (81.35-86.45) and metabolizable energy (380.60-393.94 kcal) however decreased with substitution of vanilla by *T. tetrapleura.* The protein content was close to the value reported by (6-7) in similar studies. The increased protein can contribute significantly to the recommended daily intake of proteins for adults (34-56 g day^{-1}) and children (13-19 g day^{-1}) (20). For long, protein has been well regarded as essential nutrient in the human diet as it helps to repair worn-out tissues (21). Low fat content of the cookies (0.98-1.29%) is desirable, being a ready-to-eat snacks. Usually, the amount of fat in a food product plays a major role in its shelf life. High fat content can promote rancidity, leading to development of unpleasant sensory properties (22). Hence, the low fat was an advantage with respect to the keeping quality of this cookie. Ash content (0.55- 0.71%) was in accordance with reported values by Eke *et al.* (23), and was an indication of adequate mineral status of the cookie (21). Fibre is regarded as essential nutrient in human diet as it absorbs water and provides roughage for the bowels, assisting intestinal transit (24). The crude fibre content was low, which is however helpful to the digestive process (24). Substitution of T. *tetraptera* for vanilla resulted in reduced carbohydrate and energy contents of the cookie. This may help in the prevention of overweight and obesity. Accurate information on energy value of foods is paramount, when it comes to the challenges of normal nutrition, undernutrition and obesity.

Table 1. Proximate composition and metabolizable energy of cookies flavoured with *Aidan* as substitute for vanilla

Sample	Crude Moisture (%)	Crude Protein (%)	Crude Fat (%)	Crude Ash (%)	Crude fibre (%)	Carbohydrate (%)	M. E. (kcal)
C$_0$	1.83^d ±0.29	9.83^c±0.30	0.98$^{\pm0}$,03	0.55^c±0.02	0.35^c±0.01	86.45^a±0.40	393.94
C$_{25}$	2.67^c±0.58	11.69±0.17	1.17±0.01	0.65^b±0.01	0.42^b±0.01	83.40^b±0.56	391.02
C$_{50}$	3.00^{bc}±0.01	12.22^{ab}±0.59	1.22^{ab}±0.06	0.68^{ab}±0.03	0.44^{ab}±0.02	82.44^c±0.70	380.60
C$_{75}$	3.33^{ab}±0.29	12.86^a±0.17	1.29^b±0.02	0.71^a±0.01	0.46^a±0.01	81.35^d±1.92	388.47
C$_{100}$	3.77^a±0.25	12.06^b±0.48	1.21^b±0.05	0.67^b±0.03	0.43^b±0.02	81.87^{cd}±0.40	386.42

Means with the same superscript in the same column are not significantly different (P≤0.05) Key: M. E. – metabolizable energy.

Original scientific paper

Mineral content of cookies flavoured with Aidan as substitute for vanilla

Mineral contents varied significantly (p≤0.05) among the samples of cookies flavoured with *Aidan* as a substitute for vanilla (Table 2). Phosphorus ranged between (64.00-142.67 mg/100 g), iron (2.62-6.53 mg/100 g) and zinc (3.80-4.47 mg/100 g). Minerals are essential for health and as such are part of all aspects of cellular function and they are involved in different structural components of human beings. Some mineral elements form an integral part of enzyme or protein structure. They are vital for normal growth, maintenance, effective immune system and prevention of cell damage (25). Phosphorus makes up to 1% of a person's total weight, it plays an important role in how the body uses carbohydrates and fats. it is normally required for bone growth, kidney function and cell growth (26). Iron is known to be an essential constituent of haemoglobin found in blood and contributes to the combat of anaemia (27). Deficiency of zinc in humans is widely recognized as important malnutrition problem, especially in areas of high cereal and low animal food consumption. Indicators of zinc deficiency include low blood plasma/serum zinc concentration, and stunting prevalence (25).

Table 2. Mineral composition (mg/100 g) of cookies flavoured with *Aidan* as substitute for vanilla flavour

Sample	Phosphorous (mg/100 g)	Iron (mg/100 g)	Zinc (mg/100 g)
C_0	$64.00^c \pm 10.58$	$2.62^b \pm 1.49$	$3.80^c \pm 0.14$
C_{25}	$105.60^b \pm 0.25$	$3.44^b \pm 0.75$	$3.99^b \pm 0.09$
C_{50}	$109.33^b \pm 2.31$	$4.05^b \pm 2.18$	$4.08^b \pm 0.03$
C_{75}	$140.00^a \pm 4.00$	$5.02^{ab} \pm 0.31$	$4.05^b \pm 0.09$
C_{100}	$142.67^b \pm 33.5$	$6.53^a \pm 0.64$	$4.47^a \pm 0.06$

Means with the same superscript in the same column are not significantly different(P≤0.05)

Phytochemical profile of cookies with Aidan as substitute for vanilla flavour

Phytochemical contents of cookies flavoured with *Aidan* as substitute for vanilla flavour varied significantly (p≤0.05) among the samples (Table 3). The ranges of tannin, phytate, flavonoid and phenolic compounds in mg/100 g were 0.07-0.08, 0.17-0.23) 0.53-0.82 and 0.76-1.53, respectively. However, some phytochemicals become antinutrients when ingested in high quantities. They interfere with digestive enzyme, for example, tannins have been reported to form complexes with proteins, reducing their digestibility and palatability (28). Tannins also inhibit the absorption of minerals like iron and zinc, but their concentrations in foods are known to decline during cooking (29-31). Similarly, phytates are known to adversely affect mineral bioavailability (31). However, the levels of these phytochemicals in this product were within the ranges earlier considered safe in humans (32). Besides, health benefits of some of these phytochemicals are documented (32). These include reductions of pathogenesis of cancer development and damage to intestinal tract (31-33). The low tannin content in the cookie samples corresponded to the

Original scientific paper

values reported by (34, 35). Inhibition of the activities of digestive and hydrolytic enzymes such as amylase, trypsin, chymotrypsin and lipase by phenolic compounds have been reported (36). They also possess anticarcinogenic, antiviral, antimicrobial, anti-inflammatory, hypotensive and antioxidant activities (36). According to Agbaire et al. (37), flavonoids are known to be potent water-soluble antioxidants and free radical scavengers which prevent oxidative cell damage. They also have strong anticancer and antiulcer activity. Flavonoids might, in addition, offer protection against the different levels of carcinogenesis. Therefore, since functional snacks usually possess additional health benefit apart from basic nutrient, cookies flavoured with *Aidan* as substitute for vanilla flavour may be considered as one.

Table 3. Phytochemical content (mg/100 g) of cookies flavoured with *Aidan* as substitute for vanilla flavour

Sample	Tannin (mg/100 g)	Phytate (mg/100 g)	Flavonoid (mg/100 g)	Total phenolics (mg/100 g)
C_0	$0.07^b \pm 0.00$	$0.17^c \pm 0.01$	$0.53^c \pm 0.02$	$0.76^b \pm 0.04$
C_{25}	$0.07^{ab} \pm 0.00$	$0.18^c \pm 0.01$	$0.67^b \pm 0.07$	$0.91^b \pm 0.06$
C_{50}	$0.08^{ab} \pm 0.01$	$0.21^b \pm 0.02$	$0.68^b \pm 0.04$	$0.95^b \pm 0.20$
C_{75}	$0.08^a \pm 0.01$	$0.23^a \pm 0.01$	$0.77^{ab} \pm 0.07$	$1.00^b \pm 0.17$
C_{100}	$0.08^{ab} \pm 0.00$	$0.23^a \pm 0.11$	$0.82^a \pm 0.07$	$1.53^a \pm 0.02$

Means with the same superscript in the same column are not significantly different($P \le 0.05$)

Sensory properties of cookies with Aidan as substitute for vanilla flavour

Table 4. shows the results for the sensory evaluation of the cookies. There was no significant difference ($p < 0.05$) between the mean sensory scores for most attributes of cookie samples and control, especially taste and crispness. Mean scores for cookies appearance, taste, aroma, crispness and over all acceptability ranged between 7.23 - 8.17, 7.30 - 7.87, 7.33 - 8.07, 7.20 - 7.80 and 7.72 - 8.31, respectively. The intensity of brown colour increased in cookie samples with increase in substitution levels of *aidan* for vanilla. It may be due to the colour of the *aidan* powder. Panellists accepted sample with 75% of *Aidan* and 25% of vanilla the most, though it was observed that all samples were generally accepted by panellists. The overall acceptability of the samples was based on the judgement of the panellists as perceived by their sensory organs based on the appearance, taste, aroma and crispness. Iwe (18), considered a product with overall acceptability score of 7.0 as being accepted by consumer. The sensory attributes of foods, which are detectable by human senses are often used as food quality indices and may also serve as references during food selections (38).

Table 4. Sensory attributes of cookies flavoured with *aidan* as substitute for vanilla flavour

Sample	Appearance	Taste	Aroma	Crispness	Overall acceptability
C_0	$7.93^{ab}\pm0.87$	$7.87^{a}\pm0.82$	$7.60^{ab}\pm1.07$`	$7.80^{a}\pm1.06$	$7.83^{ab}\pm0.97$
C_{25}	$7.23^{c}\pm1.10$	$7.77^{a}\pm0.99$	$7.57^{ab}\pm0.94$	$7.63^{a}\pm1.03$	$7.76^{b}\pm0.79$
C_{50}	$7.33^{bc}\pm1.32$	$7.30^{a}\pm1.29$	$7.33^{b}\pm1.15$	$7.20^{a}\pm1.19$	$7.72^{b}\pm0.99$
C_{75}	$8.17^{a}\pm1.15$	$7.60^{a}\pm14.65$	$8.07^{a}\pm1.14$	$7.93^{a}\pm16.66$	$8.31^{a}\pm0.97$
C_{100}	$7.73^{abc}\pm1.11$	$7.67^{a}\pm0.66$	$7.40^{b}\pm0.93$	$7.53^{a}\pm1.38$	$7.86^{ab}\pm0.74$

Means with the same superscript in the same column are not significantly different($P\leq0.05$)

CONCLUSIONS

Substitution of vanilla powder by *Tetrapleura tetraptera* powder as a flavouring agent during cookies production yielded acceptable cookies with adequate nutritional composition. The cookie samples had adequate proximate composition, metabolizable energy, mineral (phosphorus, zinc and iron) and phytochemical (phenolics and flavonoids) contents which are essential for human health. However, low contents of antinutrient (tannin and phytate) which could reduce the digestibility and palatability of cookies when ingested were observed, but fell within tolerable limits. *Tetrapleura tetraptera* powder can be utilized as substitute for vanilla powder to obtain nutritious and acceptable cookies or similar snacks. Further study on antioxidant properties of such product is recommended.

REFERENCES

1. Gabriel, I.O.; Faith, C.U. Production and evaluation of cold extruded and baked ready-to-eat snacks from blends of breadfruit (*Treculia africana*), Cashewnut (*Anacardium occidentale*) and coconut (*Cocos nucifera*); *Food Science and Quality Management,* **2014**, *23*, 65-77.
2. Olatoye, K.K.; Lawal, A.I.: Storability of "Dodo Ikire" (Over -ripe plantain-based snack) at ambient temperature (28±2ºC); *Agric Eng Int: CIGR Journal,* **2016**, *18*(1), 263-268.
3. Sumargo, F. Improving the utilization of dry edible beans in a ready-to-eat snack. Product by extrusion cooking. M.S. Thesis, University of Nebraska, 2016. http://digitalcommons.unl.edu/cgi/viewcontent.cgi?article=1067&context=foodscidiss (access date-feb.3, 2019)
4. Aluko, O.; Brai, M.R.; Adelore, O. Evaluation of Sensory Attributes of Snack from Maize-Moringa Seed Flour Blends. *World Academy of Science, Engineering and Technology,* **2013**, *7*(10), 944-946
5. Joanna Kolniak-Ostek. Content of bioactive compounds and antioxidant capacity in skin tissues of pear. *Journal of functional foods,* **2016**, *23*,40-51
6. Enwereuzoh, R. O.; Okafor,D. C.; Uzoukwu, A. E.; Ukanwoke, M. O.; Nwakaudu, A.A. and Uyanwa, C. N. Flavour extraction from *Monodora myristica* and *tetrapleura tetraptera* and production of flavoured popcorn from the extract. *European Journal of Food Science and Technology.* **2015**, *3*(2), 1-17.

Original scientific paper

7. Olatoye, K. K.; Fapojuwo, O. O.; Olorunshola, J. A.; Ayorinde, J. O. Potentials of African Nutmeg (*Monodora myristica*) as a Flavourant in Cookie Production; *International Journal of Food Studies*. **2019**, *8*(2), 1-12.

8. Ojewole J.A.; Adesina S.K. Mechanism of the hypotensive effect of scopoletin isolated from the fruit of *Tetrapleura tetraptera*. *Planta Med.* **1983**, *49*(1),46–50.

9. Akin-Idowu, P.E.; Ibitoye, D.O.; Ademoyegun, O.T.; Adeniyi, O.T. Chemical Composition of the Dry Fruit of *Tetrapleura tetraptera* and its Potential Impact on Human Health. *J Herbs Spices Med Plants.* **2011,** *17*, 52–61.

10. Okokon, J.E.; Udokpoh, A.E.; Antia B.S. Antimalaria activity of ethanolic extract of *Tetrapleura tetraptera* fruit. *J. Ethnopharmacol.* **2007**, *111*, 537–40.

11. Eneche, E.H. Biscuit making potential of millet /pigeon pea flour blends. *Plant foods for Human nutrition,* **1999,** *54*, 21-27.

12. A.O.A.C, **1995**. Official methods of Analysis, 15th edition, Vol.2.Association of official Chemists. Arlington, Virginia.

13. Maclean, W., Harnly, J., Chen, J., Chevassus-Agnes, S., Gilani, G., Livesey, G., & Warwick, P. (**2003**, February). Food energy–Methods of analysis and conversion factors. In *Food and agriculture organization of the united nations technical workshop report* (Vol. 77, pp. 8-9). https://www.ars.usda.gov/research/publications/publication/?seqNo115=172524 (access date - June .13, 2019)

14. AOAC, **1990** Official Methods of Analysis; Association of Official Analytical Chemists 15th ed., Washington D.C.USA

15. Kirk, H.; Sawyer, R. Frait Pearson Chemical Analysis of Food. 8th ed. Longman Scientific and Technical. Edinburgh. **1998**; 211-212.

16. Young, S.M.; Greaves, J.S. Influence of variety and treatment on phytic acid of Wheat. *Food Research* **1990**, *5*, 1-61.

17. Harborne, J.B. Phytochemical Methods. Chapman and Hall Ltd., London, **1973**, pp. 49-188.

18. Iwe, M.O. Handbook of sensory analysis and methods. projoint communications services Ltd.,Enugu. **2002**, pp 70-72.

19. Aruah, B.C.; Uguru, M.I.; Oyiga, B.C. Genetic Variability and interrelationship among some Nigerian pumpkin accessions (*Cucurbita spp.*). *Plant Breeding. International Journal*. **2012**, *6*, 34-41.

20. Food and Nutrition Board. Dietary reference intake for energy, carbohydrate, fiber, fatty acids, cholesterol, protein and amino acids. *Food and Nutrition Board, Institute of Medicine. National Academy Press.* (KH)*Washington, DC,* **2002**, pp. 422-541

21. Baah, F.D. Characterisation of water yam (*Dioscorea alata*) for existing and potential foods products. Faculty of Biosciences College of sciences Kwame Nkrumah University of Science and Technology, Kumasi Ghana. **2009**, PhD Thesis

22. Ihekoronye, A.I.; Ngoddy, C.P.O. Integrated Food Science and technology or tropics. Macmillian publisher. London, **1985**, pp. 257-264.

23. Eke, J.; Achinewhu, S.C.; Sani. L. Nutritional and sensory qualities of some Nigerian cakes. *Niger. Food J.* **2008,** *26*(2), 12-17.

24. Alaise, C.; Linden, G. Food Biochemistry. Chapman and Hall, Food Science Book. Aspen Publishers Inc. Maryland. **1999**. pp. 15-121.

25. Nazanin, R.; Richard. H.; Roya, K.; Rainer, S. Zinc and its importance for human health: An integrative review *Journal of research in medical sciences*, **2013**, *18*(2), 144-157.

26. Fallon, S.; Enig, M.G. Nourishing traditional. The cookbook that challenges policitally correct nutrition and the diet dictocrats. Revised 2nd Edn., **2001**, 40-45.

27. De Villota, D.; Ruiz, E. D.; Carmona, M. T.; Rubio J. J.; de Andrés, S. Equality of the in-vivo and in-vitro oxygen-binding capacity of haemoglobin in patients with severe respiratory disease. *British Journal of Anaesthesics,* **1981**, *53*(12), 1325–1328.

28. Ekpeyong, T.E. Chemical composition and amino acid content of African breadfruit (*Treuclia africana* Decne). *Food Chemistry,* **1985**, *17*, 59–64.

29. Lewu, M.N.; Adebola, P.O.; Afolayan, A.J. Effect of cooking on the mineral contents and anti-nutritional factors in seven accessions of *Colocasia esculenta(L.)* Schott growing in South Africa. *Journal of Food Composition and Analysis,* **2010,** *23*, 389-393.

30. Achy, Y.J.; Koffi, B.K.P.; Ekissi, E.S.G.; Konan, K.H.; Kouame, P.L. Assessment of physicochemical Properties and anti-nutritional factors of flour from yam (*Dioscorea bulbifera*) bulbils in southeast Côte d'Ivoire. *International Journal of Advanced Research*, **2016,***4* (12),871-887.

31. Bhandari, M. R.; Kasai, T.; Kawabata, J. Nutritional evaluation of wild yam (*Dioscorea spp.*) tubers of Nepal. *Food Chemistry,* **2005**, *82*, 619-623.

32. Ugwu, F. M.; Oranye, N. A. Effects of some processing methods on the toxic components of African breadfruit (Treculia africana). *African Journal of Biotechnology* **2006**, *5*(22), 2329-2333.

33. Makkar, H.P.S.; Becker, K. Nutritional value and antinutritional components of whole and ethanol extracted Moringa oleifera leaves. *Animal Feed Science and Technology,* **1996**, *63,* 211-228.

34. Uhegbu, F.; Iweala, E.; Kanu, I. Studies on the chemical and antinutritional content of some Nigerian spices. *International Journal of Nutrition and Metabolism,* **2011**, *3*(6), 72-76

35. Ndulaka, J. C.; Ekaiko, M. U.; Ogbonna C. R.; Asiegbu, E. I. A comparatives study on the nutritional and anti-nutritional values of the seeds of *Piper guineense*, *Monodora myristica* and *Ocimum gratissimum* as popular spices used in south eastern Nigeria. *European Journal of Advanced Research in Biological and Life Sciences,* **2016**. 4(1). 22-27.

36. Shetty, K. Biotechnology to harness the benefits of dietary phenolics focus on Lamiaceae. *Asia Pacific Journal of Clinical Nutrition.* **1997**, *6*, 162-171.

37. Agbaire, P.O.; Emoyan, O.O. Nutritional and Anti-nutritional levels of some local vegetables from Delta state, Nigeria. *African Journal of Food Science*. **2011**, *6*(1) 8-11.

38. Ganhão, R.; Estévez, M.; Armenteros, M.; Morcuende, D. Mediterranean berries as inhibitors of lipid oxidation in porcine burger patties subjected to cooking and chilled storage. *Journal Integr. Agriculture* **2013**, *12*(11), 1982 - 1992.

THE COMPARISON OF FIVE NEUTRON SOURCES VIA ^{7}LI(P,N) REACTION FOR THE DESIGN OF A FACILITY BASED ON PROMPT GAMMA RAY NEUTRON ACTIVATION ANALYSIS (PGNAA) IN VIVO DETECTIONS OF BORON

J. G. Fantidis[1]*, G. E. Nicolaou[2]

[1] Department of Electrical Engineering-Physics, International Hellenic University, Kavala, Greece;
[2] Laboratory of Nuclear Technology, School of Engineering, 'Democritus' University of Thrace, Xanthi, Greece

Prompt Gamma Ray Neutron Activation Analysis (PGNAA) is a useful nondestructive method with numerous applications. In this study neutron yield from ^{7}Li(p,n) reaction with proton energies of 2.5, 3, 4, 4.5 and 5 MeV was used in order to provide the necessary thermal beam to the investigated sample. The facility was designed and simulated using the MCNPX Monte Carlo code. The primary goal was the enhancement of the signal to noise ratio and the improvement of the detection limit of the system. An extensive series of simulations were performed for each source in order to examine the consequence of the solid angle which formed between the neutron beam and the collimator detector. Boron was used as an element which emits the prompt gamma rays and according to the simulations, 2.5 and 3 MeV protons beams offer the best performance, while for proton beam with energy in the range between 4-5 MeV the results indicate slightly poorer performance. Simulations are presented for the in-vivo PGNAA in the human liver.

Keywords: PGNAA, ^{7}Li(p,n) reaction, Lithium target, Boron, MCNPX

INTRODUCTION

Prompt Gamma Neutron Activation Analysis is a useful nondestructive testing radio-analytical method for the fast detection of elemental and isotopic compositions in various fields of activity. The object is irradiated by a low energy neutron beam and the identification based on the detection of the gamma radiation which is emitted after neutron capture (n,γ) reaction. This technique has been widely used for measurement of many low Z elements such as H, B, C, N, Si, P, S, Cl and some others elements with high neutron capture cross-sections e.g. Hg, Cd, Sm and Gd. The hydrogen and boron measurements are really important owing to the lack of other reliable analytical methods. Especially the ^{10}B concentration in human during the boron neutron capture therapy can be detected easily and accurately, as a result of high neutron capture cross section of ^{10}B(3837 b), via 478 keV prompt gamma ray (1-4).

The aim of this work is to study the performance of a Prompt Gamma Neutron Activation Analysis (PGNAA) facility which is based on neutrons production via ^{7}Li(p,n) reaction, using proton beams with energies of 2.5, 3, 4, 4.5 and 5 MeV. The presented

---

* Corresponding author: Jacob G. Fantidis, Department of Electrical Engineering-Physics, International Hellenic University, Kavala, Greece, e-mail: fantidis@teiemt.gr

unit has been designed and simulated using the MCNPX 2.5 Monte Carlo code (5). For each proton beam the primary purpose is to enhance the signal to noise ratio of the emitted gamma-rays, through the ^{10}B(n, a)^{7}Li reaction. Boron was selected as the investigated material for in vivo calculations because has a useful interest both for the in vivo PGNAA in the human liver during the BNCT and in its determination in water samples.

MATERIAL AND METHODS

The choice of the ^{7}Li(p,n) reaction is based on the fact that this is one of the most promising neutron sources, because it provides a low energy, high intensity spectrum. However, the lithium metal has a relatively low melting point temperature (182°C) and for this reason usually requires a heat removal system. According to the experimental works by Bayanov et al. a simple cooling system, which is based on water, can be used for proton beam current up to 10 mA (6-7). Several researcher have been calculated the neutron spectra from the ^{7}Li(p,n) reaction for a wide range of the proton energies, but some discrepancies are noted (8-9). The produced neutron yield can be described by the equation (10-12):

$$\frac{d^2N}{d\Omega dE_n} = igD \left(\frac{d\sigma_{pn}}{d\Omega}\right)_{CMS} \frac{d\Omega_{CMS}}{d\Omega} \frac{dE_p}{dE_n} S^{-1}(E_p) \qquad [1]$$

where i and g express the proton beam current and the number of protons per μA respectively, D indicates the atomic density of ^{7}Li, $\left(\frac{d\sigma_{pn}}{d\Omega}\right)_{CMS}$ denotes the differential cross-section of the ^{7}Li(p,n) reaction, E_p is the proton energy, E_n is the energy of the emitted neutrons in the solid angle Ω and finally $S^{-1}(E_p)$ is the inverse stopping power in lithium. The relevant neutron spectra (that used in the simulations) corresponding to 2.5, 3, 4, 4.5 and 5 MeV protons were derived from previous work by Bakshi et al. [9] and by Bleuel et al. [13] and are depicted in Figure 1. The estimated total neutron yields per μA are equal to 8.83×10^8, 1.56×10^9, 3.62×10^9, 4.96×10^9 and 6.48×10^9 ncm^{-2}s^{-1} for proton energy beams of 2.5, 3, 4, 4.5 and 5 MeV, respectively. The number of photons with energy E_{ijk} corresponding to the presence of the element i is given by the equation (4):

$$C(E_{ijk}) = \frac{m_i I_{ij} N_A}{M_i} \sigma_{ij} G\varphi \Gamma_{ij}(E_{ijk}) S(E_k)\varepsilon(E_k)T_c \qquad [2]$$

where: i, j, k indicate the element, the isotope and the gamma energy respectively, m_i express the mass of the element i in the sample, I_{ij} is the isotopic abundance of the emitting isotope, N_A is the Avogadro number, M_i is the molar mass of the element, σ_{ij} is the mean activation cross-section of the jth isotope, G is the neutron self-shielding factor, φ is the total neutron flux, Γ_{ij} is the prompt gamma yield per capture, $S(E_k)$ express the gamma self-shielding in the sample, $\varepsilon(E_k)$ is the total efficiency of counting, T_c is the counting time.

c paper
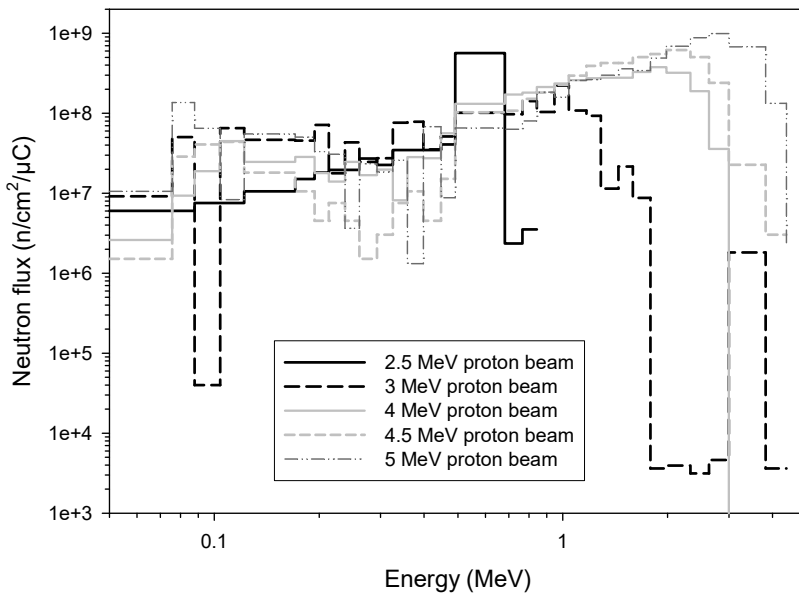
Figure 1. Neutron spectra for the protons beam with energy 2.5, 3, 4, 4.5 and 5 MeV

The mean cross-section σ_{ij} can be calculated by the equation:

$$\sigma_{ij} = \frac{\int_0^\infty \sigma_{ij}(E)\varphi_0(E)dE}{\varphi_0} \qquad [3]$$

where φ_0 is the total neutron flux at the surface of the sample. For the ^{7}Li(p,n) reaction, the photon yield of the (p, γ) reaction can be estimated by the formula (14):

$$Y_{p-\gamma} = D \int_0^{E_{P0}} \frac{\sigma_{p-\gamma}(E_p)}{-S(E_p)} dE_p \qquad [4]$$

where E_{p0} is the incident proton energy and $\sigma_{p-y}(E_p)$ denotes the total cross section, as a function of proton energy E_p. The minimum detectable concentration (MDC) of boron in water samples is easily calculated by the equation (15):

$$MDC = 4.653 \times \frac{C}{P} \times \sqrt{B} \qquad [5]$$

where C is the concentration of boron, B is the background counts and P is the net count of the characteristic gamma-ray peak. The error in MDC is given by the formula:

$$\sigma_{MDC} = \frac{C}{P} \times \sqrt{2 \times B} \qquad [6]$$

One of the main problems of most PGNAA facilities is the low signal to noise ratio because of the inherently relatively large background, which reduce this ratio. The presence of the collimated detectors is necessary in order to stop the undesired stray gamma rays to reach the detector however, simultaneously this means than the detector is able to "see" just a small part of the investigated sample. Previous works (16-17) illustrate that the field of view between of the detectors and the neutron beam create a volume of intersection. The solid angle and the thermal neutron flux within this volume determine the detectors response. According to previous work, the solid angle (Ω_D) can be measured with the help of a Monte Carlo method, which make use of a total variance reduction and is expressed by formula:

$$\Omega_D = \frac{1}{N}\sum_{i=1}^{N} W_i \qquad\qquad [7]$$

where W_i is a weighting factor correlated with the location within the volume V, that emit induced gamma-rays and subtend a non-zero solid angle with the detector, while N is the number of these positions.

Figure 2 illustrates the side view of the simulated geometrical configuration. This arrangement includes (1) a polyethylene cube with side 20 cm, (2) lead layers with 3 cm thicknesses that cover the polyethylene box, in order to stop the gamma ray, while borated polyethylene sheets with thicknesses 1cm shield the rest of the neutrons (3). A cylindrical void (4), with length of 24 cm and diameter of 2 cm, permits the neutrons from the lithium disk source (5) to reach the irradiated object (6), which is a cubic phantom with a sidelength of 16 cm. The distance of the phantom from the borated poly-ethylene sheets is 5 cm, while the distance between phantom and source is 15cm. Based on the fact that the typical quantities of the boron in a healthy and in a sick liver are about 8 and 50 ppm, respectively [18], the theoretical phantom contains water with 50 ppm of ^{10}B homogeneously distributed (the selection of the suitable boron compound escapes the purposes of the present work). A cylindrical aperture (7), with 5 cm height and 4 cm diameter, permits the produced gamma rays to arrive at the detector (8), which has both a diameter and a height of 5 cm. A lead straight bore collimator (9) with height and dia-meter 10 and 12 cm respectively, was used to minimize the background.
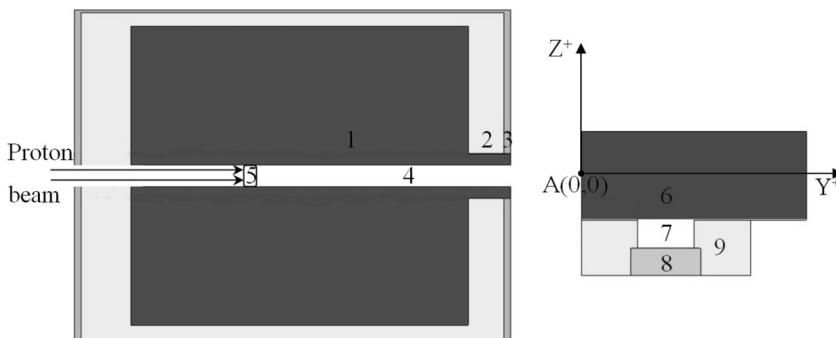
Figure 2. Geometric configuration of the simulated experimental facility

RESULTS AND DISCUSSION

In order to enhance the gamma-ray detection sensitivity for a 0.478 MeV photons, a number of simulations for different positions, both for the collimator detector and for the lithium target were carried out, for every proton beam. The F8:P pulse height tally that calculates the energy distribution of pulses created in the detector cell per starting neutron, was selected as an optimization index. The detector and its collimator were moved along the Z and the Y directions. Tables 1-5 show the normalized results for every neutron source. According to results from the Table 1 the best detection sensitivity has been achieved at y = -4 cm and z =-5 while ±1 cm from this position the boron detection sensitivity is very high (with normalised values among 0.94-0.98). The comparison between the "best" and the initial "symmetric" position indicates that the symmetric position provides 60% lower boron peak area.

For the 3 MeV proton beam the "best" positions occur at y = -3 cm and z =-3. According to the results a small shift for this position reduces more the boron peak (with normalised values among 0.78-0.96) in comparison with the 2.5 MeV proton beam. The "symmetric" position gives 40% lower gamma peak area (Table 2).

Table 1. The normalized signal peak area for the different positions of the proton beams with energy 2.5 MeV and collimator detector relative to the object

Detector position (Y axis)	Neutron source position (Z axis)						
	2	1	0	-1	-2	-3	-4
0	0.31	0.39	0.51	0.64	0.76	0.81	0.83
-1	0.31	0.41	0.53	0.67	0.79	0.87	0.88
-2	0.36	0.43	0.58	0.71	0.88	0.96	0.96
-3	0.35	0.46	0.58	0.70	0.84	0.96	0.99
-4	0.38	0.46	0.58	0.75	0.91	0.97	0.98
-5	0.33	0.42	0.54	0.70	0.83	0.95	1.00
-6	0.34	0.39	0.50	0.68	0.84	0.94	0.97

Table 2. The normalized signal peak area for the different positions of the proton beams with energy 3 MeV and collimator detector relative to the object

Detector position (Y axis)	Neutron source position (Z axis)						
	2	1	0	-1	-2	-3	-4
0	0.45	0.55	0.62	0.71	0.77	0.82	0.82
-1	0.43	0.49	0.60	0.69	0.75	0.89	0.87
-2	0.41	0.50	0.60	0.75	0.78	0.93	0.88
-3	0.40	0.46	0.64	0.75	0.85	1.00	0.94
-4	0.40	0.48	0.62	0.76	0.85	0.96	0.93
-5	0.41	0.48	0.58	0.72	0.84	0.95	0.91
-6	0.38	0.43	0.49	0.67	0.76	0.89	0.88

The result is similar for the 4 MeV proton beam but the "best" position records at y = -3 cm and z = -4 (Table 3). The neutron source based on 4.5 MeV proton beam, offers the maximum boron peak area at y = -3 cm and z = -5 (Table 4). Table 5 illustrates the relevant results for the 5 MeV proton beam with the maximum value at y = -3 cm and z = -3.

Table 3. The normalized signal peak area for the different positions of the proton beams with energy 4 MeV and collimator detector relative to the object

Detector position (Y axis)	Neutron source position (Z axis)						
	2	1	0	-1	-2	-3	-4
0	0.48	0.58	0.61	0.71	0.76	0.85	0.90
-1	0.44	0.52	0.60	0.66	0.76	0.87	0.88
-2	0.45	0.57	0.66	0.81	0.85	0.90	0.86
-3	0.38	0.49	0.64	0.80	0.84	0.95	0.86
-4	0.46	0.54	0.64	0.74	0.90	1.00	0.98
-5	0.45	0.54	0.64	0.78	0.91	0.94	0.92
-6	0.37	0.45	0.56	0.72	0.89	0.95	0.92

Table 4. The normalized signal peak area for the different positions of the proton beams with energy 4.5 MeV and collimator detector relative to the object

Detector position (Y axis)	Neutron source position (Z axis)						
	2	1	0	-1	-2	-3	-4
0	0.44	0.53	0.62	0.71	0.78	0.93	0.86
-1	0.47	0.53	0.59	0.75	0.83	0.87	0.85
-2	0.48	0.57	0.70	0.82	0.88	0.92	0.90
-3	0.50	0.62	0.74	0.85	0.97	1.00	0.96
-4	0.54	0.61	0.73	0.81	0.88	0.98	0.97
-5	0.48	0.60	0.66	0.76	0.89	1.00	0.98
-6	0.49	0.58	0.67	0.78	0.81	0.90	0.86

With these criteria both the signal to noise ratio ($S/\sqrt{B}$) and the corresponding relative error $\left(r_s = \sqrt{S + 2B}/S\right)$, "best" position and "symmetrical" position were compared for each of the five considered neutron source. The results are listed in Table 6 for neutron flux equal to 3×10^9 n/s and irradiation time of 100 s. For the 2.5 MeV protons beam ($S/\sqrt{B}$) and r_s have increased by factors of 1.35 and 1.41, respectively. In the case of 3 MeV protons beam ($S/\sqrt{B}$) and r_s have improved by factors of 1.10 and 1.32 respectively. As regards the 4 MeV protons beam ($S/\sqrt{B}$) and r_s have increased by factors of 1.11 and 1.22, respectively. Similar is the amelioration in the case of the 4.5 MeV protons beam with enhancement for ($S/\sqrt{B}$) and r_s by 1.13 and 1.20 respectively. Finally, for the 5 MeV proton beam both ($S/\sqrt{B}$) and r_s increased by factors of 1.13 and 1.21 correspondingly. Based on the results of the Table 6 the facility which incorporates the 2.5 MeV proton

beam has the better performance while the 3 MeV proton beam provides to the unit the second better results. Proton beams with energy 4, 4.5 and 5 MeV have similar perfor-mance and comparatively slightly worse from the facility which uses the 3 MeV proton beam.

Table 5. The normalized signal peak area for the different positions of the proton beams with energy 5 MeV and collimator detector relative to the object

Detector position(Y axis)	Neutron source position (Z axis)						
	2	1	0	-1	-2	-3	-4
0	0.34	0.47	0.57	0.73	0.84	0.91	0.89
-1	0.35	0.44	0.59	0.77	0.88	0.91	0.91
-2	0.34	0.43	0.63	0.79	0.92	0.98	0.94
-3	0.40	0.51	0.63	0.75	0.90	1.00	0.98
-4	0.36	0.45	0.60	0.77	0.92	1.00	0.99
-5	0.38	0.45	0.55	0.72	0.88	0.99	0.98
-6	0.34	0.45	0.55	0.70	0.85	0.92	0.91

Table 6. The comparison of the 5 neutron beams with flux 3×10^9 n/s and irradiation counting time 100 s

	2.5 MeV protons beam	3 MeV protons beam	4 MeV protons beam	4.5 MeV protons beam	5 MeV protons beam
Signal to noise ratio					
Symmetric	5.62E+1	6.81E+1	6.40E+1	6.05E+1	5.39E+1
Best	7.58E+1	7.51E+1	7.10E+1	6.81E+1	6.08E+1
Relative error					
Symmetric	5.23E-2	5.16E-2	4.84E-2	4.91E-2	5.05E-2
Best	3.70E-2	3.90E-2	3.96E-2	4.08E-2	4.17E-2

With the help of the F8:P tally the MDC of boron is calculated for each protons beam. According to the results the MDC and the σ_{MDC} for the protons beams with energy 2.5, 3, 4, 4.5 and 5 MeV is 3.7±1.1, 3.7±1.1, 3.9±1.2, 4.1±1.3 and 4.9±1.5 ppm respectively. Figure 3 shows simulated values for the boron concentration versus the 0.478 MeV peak area for the 2.5 MeV protons beam. The enlarged MCNPX calculated gamma ray spectra for 4 different boron concentrations of aqueous sample are illustrated in Fig. 4.

Original scientific paper
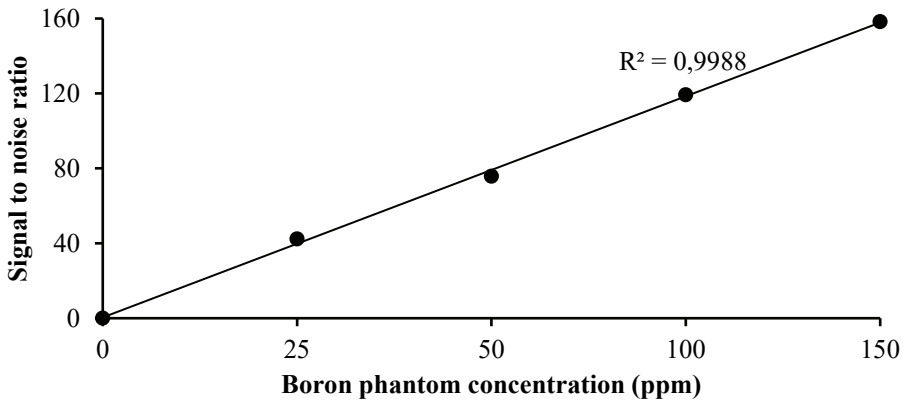
Figure 3. Relationship between the Signal to Noise ratio and the Boron concentration

The dose equivalent rate (DER) in the phantom both from neutrons and photons was also calculated for each neutron source. The neutron flux was considered equal to 3×10^9 n/s and irradiation counting time 100 s for the "best" position of each source. The DER was calculated with the combination of the F4 tally and DE, DF cards. Tally calculates the flux in the phantom cell while the DE, DF cards convert the flux into the dose equivalent. Table 7 shows the results of the simulations, the DER varied between 0.56 and 2.43mSv while based on the fact that tissue weighting factor of liver is 0.05 the effective dose varied between 28.21 and 121.67μSv. The 2.5 MeV proton beam provides the lower DER while
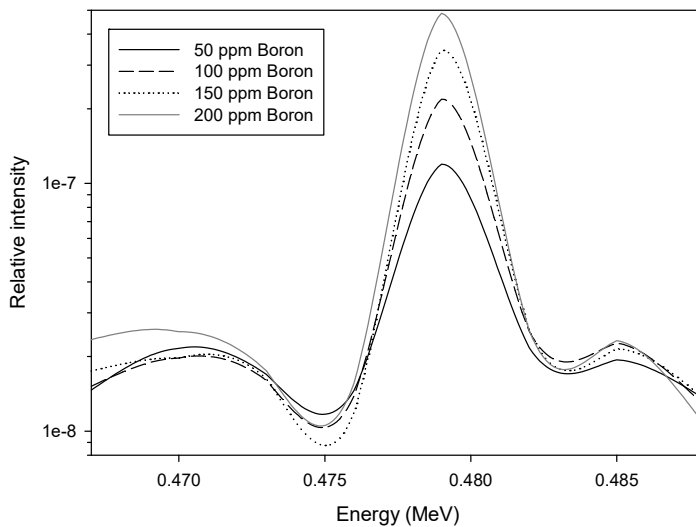
Figure 4. Enlarged gamma ray spectra (containing 50–200 ppm boron) over 0.465–0.49 MeV energy
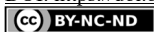
Table 7. The calculated maximum DER

Proton beam	2.5 MeV	3 MeV	4 MeV	4.5 MeV	5 MeV
Dose equivalent rate (µSv)	28.21	34.83	100.42	102.92	121.67

CONCLUSIONS

In the present work five neutrons sources via the ^{7}Li(p,n) reaction using protons beams with energy in the range from 2.5 to 5 MeV was evaluated with the help of MCNPX Monte Carlo code for the design of a PGNAA facility. The comparison based on the finding of the position which offer the best signal to noise ratio and hence improve the detection sensitivity of the system. By virtue of the importance of the boron in the human body this element used as example element although the same procedure will be also applied for a number of elements such as Gd (0.182 MeV), Hg (0.368 MeV), Sm (0.334 & 0.44 MeV) and Cd (0.559 MeV). According to the results both 2.5 and 3 MeV protons beam provide in the facility the best performance while the facilities which based on proton beam in the energy range between 4-5 MeV have a slightly poorer performance. The effective dose in the human liver for in vivo quantification for neutron flux 3×10^9 n/s and irradiation time 100 s varies from 28.21 up to 121.67 µSv.

REFERENCES
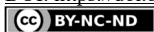
1. Atanackovic, J.; Grinyer, J.; Chettle, D. R.; Byun, S. H. The comparison of two MCNP models used for prompt gamma in vivo detection of cadmium and mercury. *Nucl. Instrum. Methods Phys.* Res. *B*. **2007**, *263* (1), 169-174.
2. Gräfe, J. L.; Chettle, D. R.; McNeill, F. E. In vivo detection of samarium by prompt gamma neutron activation analysis: a comparison between experiment and Monte-Carlo simulation. *J. Anal. At. Spectrom.* **2015**, *30* (12), 2441-2448.
3. Fantidis, J. G.; Nicolaou, G. Optimization of beam shaping assembly design for boron neutron capture therapy based on a transportable proton accelerator. *Alexandria engin. jour.* **2018**, *57*(4), 2333-2342.
4. Radia, I. A. E. A.; Rep, Y. Neutron Generators for Analytical Purposes. IAEA radiation technology reports series, **2012**, ISSN 2225-8833.
5. Hendricks, J. S. MCNPX version 2.5.c (LA-UR-03-2202). Los Alamos National Laboratory 2003.
6. Bayanov, B.; Belov, V.; Kindyuk, V.; Oparin, E.; Taskaev, S. Lithium neutron producing target for BINP accelerator-based neutron source. *Appl. Radiat. Isotopes* **2004**, *61* (5), 817-821.
7. Bayanov, B.; Kashaeva, E.; Makarov, A.; Malyshkin G.; Samarin S.; Taskaev, S. A neutron producing target for BINP accelerator-based neutron source. *Appl. Radiat. Isotopes*, **2009**, *67* (7-8), S282-S284.
8. Atanackovic, J.; Matysiak, W.; Witharana, S.; Dubeau, J.; Waker, A. J. Measurements of neutron energy spectra from ^{7}Li(p, n)^{7}Be reaction with Bonner sphere spectrometer, Nested Neutron Spectrometer and ROSPEC. *Radiat. protec. dosim.* **2014**, *161* (1-4), 221-224.
9. Bakshi, A. K.; Dawn, S.; Suryanarayana, S. V.; Datta, D. Spectrometry and dosimetry of neutron beams produced by 7Li (p, n) reactions in the proton energy range of 3–5 MeV. *Nucl. Instrum. Methods Phys. Res.* **2020**, *A949*, 162926.

10. Allen, D. A.; Beynon, T. D. A design study for an accelerator-based epithermal neutron beam for BNCT. *Phys. Medic & Biology*, **1995**, *40* (5), 807.

11. Matysiak, W.; Prestwich, W. V.; Byun, S. H. Precise measurements of the thick target neutron yields of the ^{7}Li (p, n) reaction. *Nucl. Instrum. Methods Phys. Res. A*, **2011**, *643* (1), 47-52.

12. Atanackovic, J.; Matysiak, W.; Dubeau, J.; Witharana, S.; Waker, A. Measurement of neutron energy spectra and neutron dose rates from ^{7}Li(p, n)^{7}Be reaction induced on thin LiF target. *Nucl. Instrum. Methods Phys. Res. A*, **2015**, *774*, 6-16.

13. Bleuel, D. L.; Donahue, R. J.; Ludewigt, B. A.; Vujic, J. Designing accelerator-based epithermal neutron beams for boron neutron capture therapy. *Medical physics,* **1998**, *25* (9), 1725-1734.

14. Lee, C. L.; Zhou, X. L.; Kudchadker, R. J.; Harmon, F.; Harker, Y. D. A Monte Carlo dosimetry based evaluation of the reaction near threshold for accelerator boron neutron capture therapy. *Medical physics,* **2000**, *27* (1), 192-202.

15. Naqvi, A. A.; Al-Anezi, M. S.; Kalakada, Z.; Al Matouq, F. A.; Maslehuddin, M.; Gondal, M.A.; Isab, A.A., Khateeb-ur-Rehman, Dastageer, M. Response tests of a LaCl3: Ce scintillation detector with low energy prompt gamma rays from boron and cadmium. *Applied Radiation and Isotopes*, **2012**, *70* (5), 882-887.

16. Nicolaou, G. Absolute measurement of activity of a volumetric object by collimated detectors: Solid angle issues. *Radiation measurements*, **2006**, *41* (2), 213-216.

17. Fantidis, J.G.; Nicolaou, G.E.; Tsagas F.N. Localisation and distribution of radioactivity in soil: solid angle issue. International conference on environmental radioactivity, Vienna 22–27 April 2007, Austria.

18. Koivunoro, H.; Bleuel, D. L.; Nastasi, U.; Lou, T.P.; Reijonen, J., Leung, K-N. BNCT dose distribution in liver with epithermal D–D and D–T fusion-based neutron beams. *Applied Radiation and Isotopes,* **2004**, *61* (5), 853-859.

STABILITY OF ENCAPSULATED *Lactobacillus rhamnosus* GG IN COCOA (*Theobroma cacao* L.) JUICE

Olufunke O. Ezekiel[1], Oloruntobiloba F. Ojuola[1], Olajide E. Adedeji[2]*

[1] Department of Food Technology, University of Ibadan, Ibadan, Nigeria
[2] Department of Food Science and Technology, Federal University Wukari, PMB 1020, Wukari, Nigeria

This study investigated the stability of Lactobacillus rhamnosus GG (LGG) in cocoa juice. Lactobacillus rhamnosus GG was encapsulated separately with sodium alginate and sodium alginate+gum Arabic, and incorporated into cocoa pulp juice. Un-encapsulated LGG (free cell) served as a control. The viability of free and encapsulated LGG in cocoa juice and simulated gastrointestinal conditions was evaluated. The juice was stored at 4 °C for 28 days and its chemical composition was determined weekly. Colour attributes and sensory properties of the freshly prepared juice were also determined. The percentage yield of LGG encapsulated with sodium alginate and sodium alginate+gum Arabic was 80.8 and 89.9%, respectively. Sodium alginate+gum Arabic encapsulated LGG showed higher viability in cocoa juice and simulated gastrointestinal conditions than free cell and LGG encapsulated with sodium alginate only. There was no significant (p>0.05) difference in the pH of cocoa juice that contained sodium alginate only (CJSA) and the one that contained sodium alginate+gum Arabic (CJAG). Titratable acidity of CJAG was significantly (p<0.05) higher than CJSA throughout the storage. Significantly higher pH, total soluble solids, and sugar were recorded for cocoa juice that contained the free cell (CJFC) compared to CJSA and CJAG. There was no significant (p>0.05) difference between CJSA and CJAG in terms of the degree of lightness, however, the samples differed significantly (p<0.05) in terms of chroma, and colour intensity. There was no significant (p>0.05) difference between CJFC and CJAG in terms of colour, appearance, aroma, taste, and consistency. This study showed that the encapsulation of LGG with sodium alginate and gum Arabic improved its stability in cocoa juice.

Keywords: Cocoa juice, encapsulation, gastrointestinal condition, *Lactobacillus rhamnosus* GG, viability.

INTRODUCTION

Probiotics are defined as living organisms that provide health benefits to the host when ingested in sufficient quantities, usually 10^7 CFU/mL at consumption time (1). Lactic acid bacteria (LAB) are the commonest probiotic microorganisms due to their beneficial effects on the gastrointestinal tract (1). Lactic acid bacteria can withstand extreme acidic pH in the gastrointestinal tract and remain active (2). Species that belong to genera *Lactobacillus*, which include *Lactobacillus plantarum*, *Lactobacillus johnsonii*, *Lactobacillus acidophilus*, *Lactobacillus sakei*, *Lactobacillus bulgaricus*, *Lactobacillus salivarius, and Lactobacillus rhamnosus* have been used as probiotics in food systems,

especially, milk products (3). *Lactobacillus rhamnosus* is one of the most extensively studied probiotic lactic acid bacteria due to its remarkable growth pattern (4). *Lactobacillus rhamnosus* is a facultative, rod-shaped, non-sporulating mesophilic anaerobe (4). Recent studies have shown its effectiveness in combating gastrointestinal diseases such as infant diarrhea and lactose intolerance (2). Its effective antagonistic prowess on common pathogens such as *Escherichia coli*, *Streptococci*, *Clostridium* spp., *Salmonella* spp., and *Clostridium difficile* has also been established (5). *Lactobacillus rhamnosus* acts by adhering to the mucosa of the intestine and colonizes the gastrointestinal tract and produces antimicrobial substances, which have high antagonistic activity against pathogens (2).

In recent times, there has been an increased interest in the improvement of the viability of probiotic organisms in the gastrointestinal tract. This is needful to ensure that the organisms tolerate and survive harsh conditions of the stomach and intestines until they reach the upper intestinal tract where they are required to proliferate (6). Encapsulation is an efficient technology for improving the viability of probiotics in the gastrointestinal tract (7). Several authors have reported improvement in the viability of LAB such as *Lactobacillus paracasei* NFBC 338 (8) and *Lactobacillus rhamnosus* GR1 (2), consequent to their encapsulation before use. Alginate is the commonest biopolymer used for the encapsulation of probiotics due to its ease of handling, non-toxic nature, low cost, availability, and good gelling properties (9). In practice, encapsulating materials are combined with prebiotics to further improve the viability of probiotics in the gastrointestinal tract (10). Prebiotics function by modifying the condition of the gastrointestinal tract to promote the continuous proliferation of probiotics (2). The use of alginate beads, either singly or in combination with prebiotics, for the immobilization or encapsulation of probiotics, has proven to be very effective for probiotics such as *Lactobacillus rhamnosus, Lactobacillus plantarum, Lactobacillus acidophilus*, and *Bifidiobacterium lactis* (11, 12). Gum Arabic is an edible exudate from *Acacia senegal,* which has a good prebiotic property (13). The combination of alginate and gum Arabic for improved viability of probiotics in food systems and gastrointestinal tract is well documented (14, 15).

Traditionally, dairy products are considered as media for administering probiotics, however, increased interest in the development of functional foods in recent times has shifted attention to non-dairy products (16, 17). White and Hekmat (2) reported the development of probiotic apple juice using *Lactobacillus rhamnosus* GR1. Similar studies have been conducted using aloe vera (11), mango juice (1), tomato, and carrot juices (18). Moreover, more studies are required to evaluate the stability of encapsulated probiotics in other non-dairy food products, such as cocoa juice, which have high nutritional benefits. Cocoa (*Theobroma cacao* L.**)** is an important crop in many West African countries such as Nigeria, Ghana, and Cote d'Ivoire (19). The pulp is a component of cocoa fruit, which plays important role during fermentation operation for the recovery of cocoa beans (20). The quantity of the pulp is one of the factors that determine the overall quality of the beans (19). In many cases, the pulp is more than what is required, thus, the excess serves as an important raw material for the production of juice, wine, jam, kefir, and jelly (21).

This is because, the cocoa pulp is a rich source of sugars (15%), organic acids (5%), and pectin (1.5%), which contribute to the nutritional, aesthetic, and refreshing properties of the products (20). Other nutrients that are present in considerable quantity include ascorbic acid, pyridoxine, niacin, K, Mg, and Ca (22). Cocoa juice is the most popular

product of cocoa pulp due to its ease of production, reduced nutrient loss during processing, and high organoleptic attributes (23). Therefore, cocoa juice has the potential to serve as a carrier of probiotics. The objective of this study was to evaluate the effect of encapsulation, using sodium alginate and gum Arabic, on the viability of *Lactobacillus rhamnosus* GG in cocoa juice.

MATERIALS AND METHODS

Lyophilized *Lactobacillus rhamnosus* was obtained from GG Valio Ltd., Helsinki, Finland. Cocoa (*Theobroma cacao* L.) pods were obtained from the Cocoa Research Institute of Nigeria, Ibadan, Nigeria. Sodium alginate (Foodchem, Shanghai, China) and gum Arabic (Zeenab, Abuja, Nigeria) were procured from Bristol Plc., Lagos, Nigeria. All reagents used were of analytical grade.

Preparation of *Lactobacillus rhamnosus* GG Culture

Lactobacillus rhamnosus GG (LGG) culture was prepared based on the procedure outlined by Chaikham et al. (24) with slight modification in cultivation time. Five grams of lyophilized pellets of LGG were rehydrated in 50 mL of Man Rogosa Sharpe (MRS) broth at room temperature (28±2 °C) for 15 min. The broth was incubated at 37 °C under an anaerobic condition in an Anaerocult (Merck, Germany) for 16 h with continuous shaking (110 rpm). Thereafter, the MRS-broth culture was cultivated on MRS broth at 37 °C for 48 h to multiply the organism. Subsequently, stock cultures were prepared by mixing MRS-broth culture and sterile glycerol (Oxoid, Germany) (4:1, v/v) in sterile cryogenic vials and stored at -80 °C until required. To prepare probiotic culture for immediate use, a vial of each culture was thawed at room temperature (28±2 °C) and inoculated on MRS broth at 37 °C in an AnaeroGen system (Wesel, Germany). Thereafter, the recovered cell was multiplied by incubating anaerobically on MRS broth at 37 °C for 24 h. The cell was washed twice with peptone water (Oxoid, Germany) and separated in a centrifuge (K24IR, Centurion Scientific, UK) at 3,000 × g for 25 min. The cells were diluted with peptone water to a concentration of 10^9 CFU/mL.

Preparation of beads and encapsulation of *Lactobacillus rhamnosus* GG

Alginate beads containing LGG were prepared using the method described by Mohamed et al. (25). A 75 mL aliquot of 3% sodium alginate solution was autoclaved (121°C, 15 psi) for 15 min, cooled to room temperature (28±2 °C), and mixed with 25 mL of 10^9 CFU/mL LGG. The solution was gently agitated for the even distribution of the organism in the mixture. Subsequently, the mixture was dispensed into 100 mL of 0.1 M $CaCl_2$ and allowed to stand for 30 min to harden the beads. The beads were washed with sterile peptone water and stored at 4 °C for further use. Combined sodium alginate and gum Arabic (sodium alginate+gum Arabic) beads were prepared according to the method of Krishnan et al. (26). Three grams of gum Arabic was dissolved in 100 mL of de-ionized water at 4 °C for 12 h and the mixture was sheared in a homogenizer (Huanghua Faithful, China) until a uniform medium was formed. The mixture was sterilized (121 °C, 15 psi) for 15 min and cooled to room temperature (28±2 °C). A 0.1M $CaCl_2$ solution was added to the

gum arabic medium, allowed to dissolve, and 10 mL/L Tween 80 (Sigma, Germany) was added. Sodium alginate-probiotic cell solution (as earlier discussed) was dispensed into the gum Arabic/$CaCl_2$ medium and allowed to stand for 30 min to harden the beads. The beads were washed with sterile peptone water and stored at 4 °C for further use.

Incorporation of *Lactobacillus rhamnosus* GG into *cocoa juice*

The ripe cocoa pods were washed, opened with a sharp knife, and the pulp was extracted with the aid of a de-pulping machine (CP-12M, Wuhan Acme Agro Tech., China). The pulp was filtered using a 75 μm sieve and cocoa juice was obtained. The juice was pasteurized (80 °C, 15 min) and cooled to room temperature (28±2 °C). One gram each of encapsulated LGG and un-encapsulated LGG (free cell) was inoculated separately per 100 mL of the juice. The mixture was mixed gently for the optimum distribution of the cells. The mixture was incubated at 37 °C for 48 h. Each of the juice samples was divided into two halves. For the first half, LGG was recovered from the juice and its viability was determined. The viability of the recovered LGG in simulated gastric and intestinal conditions was also evaluated. For the second half, the juice (containing LGG) was subjected to refrigerated (4 °C) storage for 28 days and its chemical composition was determined every week. Colour attributes and sensory properties of the freshly prepared probiotic juice were also determined.

Viability of encapsulated *Lactobacillus rhamnosus* GG in simulated gastrointestinal conditions

Viability of free and encapsulated LGG was evaluated in simulated gastric and intestinal juices following the methods described by Chaikam et al. (24). Simulated gastric juice was prepared by adding 0.3% pepsin to 5 mL of an electrolyte solution. The electrolyte solution was prepared by mixing 6.2 g/L NaCl, 2.2 g/L KCl, 0.22 g/L $CaCl_2$, 1.2 g/L $NaHCO_3$ and lysozyme, and pH was adjusted to 2.5 with 1 M HCl. The mixture was sterilized (121°C, 15 psi) for 15 min. Twenty milligrams each of free and encapsulated LGG was incubated in 5 mL simulated gastric juice for 60 min in an incubator (CLN 115, Pol Eko Aparatura, Poland) at 37 °C. Thereafter, the capsules were removed and rinsed in sterile water. The viability of LGG was determined at 30 min interval. Simulated intestinal juice was prepared by adding 10 mL of 0.45% bile salt and 0.1% pancreatin (v/w) to 5 mL of the electrolyte solution. The pH was adjusted to 8 using 0.5 M NaOH, and the solution was sterilized. Fifteen milligrams each of free and encapsulated LGG was incubated in 5 mL of simulated intestinal juice for 120 min at 37 °C in an incubator (CLN 115, Pol Eko Aparatura, Poland). The viability of LGG was determined at 30 min interval.

Analyses

Determination of particle size and yield of encapsulated *Lactobacillus rhamnosus* GG. The particle size of beads was determined based on the procedure described by Ivanovska et al. (27). A 20 mg bead was suspended in 5 mL acetate and phosphate buffers of pH 1.5 and 7.4, respectively. The mixture was agitated at a temperature and speed of 37 °C and 300 rpm, respectively. Beads were removed at a time interval from the swelling
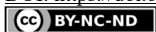
medium and particle size assay was done with the aid of Master sizer (Hydro 2000, Malvern Ltd., UK). Particle size was obtained using Equation 1.

$$\text{Particle size} = \frac{Dt\text{-}Do}{Do} \times 100 \qquad [1]$$

where Dt and Do were mean volume diameters of micro-particle at a time, t, and in a dry state, respectively.

The percentage yield of encapsulated LGG was determined based on the procedure described by Chavari et al. (28). *Lactobacillus rhamnosus* GG was released by homogenizing 1g of bead in 99 mL of sterile 0.1 M citrate buffer (pH 6.0). The homogenized fluids were diluted serially to appropriate concentrations and pour plated in MRS agar. The plates were anaerobically incubated at 37 °C for 48 h and thereafter enumerated as log CFU/mL. The encapsulation yield (EY), which is a combined measurement of the efficacy of entrapment and the survival of viable cells during the microencapsulation procedure was obtained using Equation 2.

$$EY = \frac{N}{No} \times 100 \qquad [2]$$

where: *N* is the number of viable entrapped LGG released from the beads, and *No* is the number of free cells added to the biopolymer mix during the production of the beads.

Determination of the chemical composition of cocoa juice. Titratable acidity (TTA) and pH of cocoa juice were determined using the AOAC (29) methods. A refractometer (ATR-W2 plus 2009/230, United Kingdom) was used to determine total soluble solids while the phenol-sulphuric method (30) was used to determine total sugars.

Determination of colour attributes of cocoa juice. Colour attributes, L* (a measure of lightness), a* (a measure of redness and greenness), and b* (a measure of yellowness and blueness) were measured with the aid of a colour meter (Chromameter CR-400/410, Japan). From the data obtained, hue angle, chroma, and colour intensity were obtained using Equations 3, 4, and 5, respectively.

$$\text{Hue angle} = \text{Tan}^{-1} \, b/a \qquad [3]$$
$$\text{Chroma} = \sqrt{\Delta a^2 + \Delta b^2} \qquad [4]$$
$$\text{Colour intensity} = \sqrt{\Delta L^2 + \Delta a^2 + \Delta b^2} \qquad [5]$$

Sensory evaluation of cocoa juice. Sensory evaluation of cocoa juice samples was done using a nine-point Hedonic scale, which had two extremities i.e. 1 = dislike extremely and 9 = like extremely (2). Fifty panellists that consisted of Postgraduate students of Faculty of Technology, University of Ibadan, Nigeria, were asked to assess the samples for colour, appearance, aroma, taste, consistency, and overall acceptability. The samples were served to the panellists at 8 °C in individual booths under fluorescent light. Potable water was provided in between samples for palate cleansing.

Statistical analysis. Raw data were analyzed statistically using the Statistical Package for Social Scientist 23.0 (Stat-Ease Inc., Minneapolis, USA). The means and standard deviation of means were obtained using two-way analysis of variance (ANOVA) while

Original scientific paper

Duncan's multiple range test was used to separate the means. The tests were carried out at $\alpha_{0.05}$.

RESULTS AND DISCUSSION

Particle size and yield of *Lactobacillus rhamnosus* GG

The average particle size and yield of LGG encapsulated with sodium alginate were 2.28 mm and 80.8% respectively, and 2.42 mm and 89.9% for sodium alginate+gum Arabic encapsulated LGG (Figure 1).
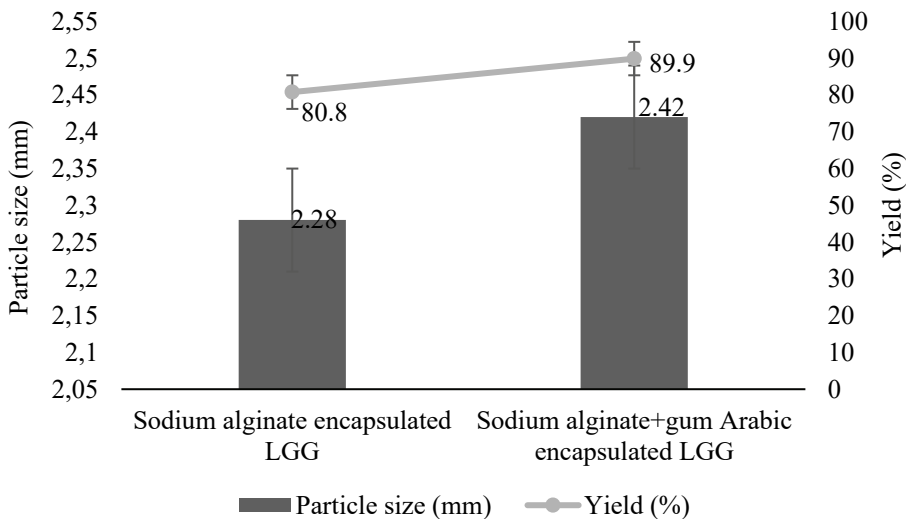
Figure 1. Particle size and yield of encapsulated *Lactobacillus rhamnosus* GG
LGG-*Lactobacillus rhamnosus* GG

The average particle size obtained in this study was similar to 0.5-3.0 mm reported by Etchepare et al. (9). According to Ivanovska et al. (27), beads of particle sizes <3 mm are suitable for easy incorporation into food systems. They are stable and colonize easily in the gastrointestinal tract. There was no significant (p>0.05) difference between *Lactobacillus rhamnosus* GG encapsulated with sodium alginate and sodium alginate + gum Arabic in terms of size. However, significantly (p<0.05) higher yield (89.9%) was recorded for LGG encapsulated with sodium alginate + gum Arabic. This indicated higher protection of LGG's viability as a result of the combined use of sodium alginate and gum Arabic. This could be due to increased encapsulation efficiency owing to high prebiotic potential of gum Arabic (31).

Stability of *Lactobacillus rhamnosus* GG in cocoa juice

The viability of free and encapsulated LGG in cocoa juice is presented in Figure 2.

Original scientific paper
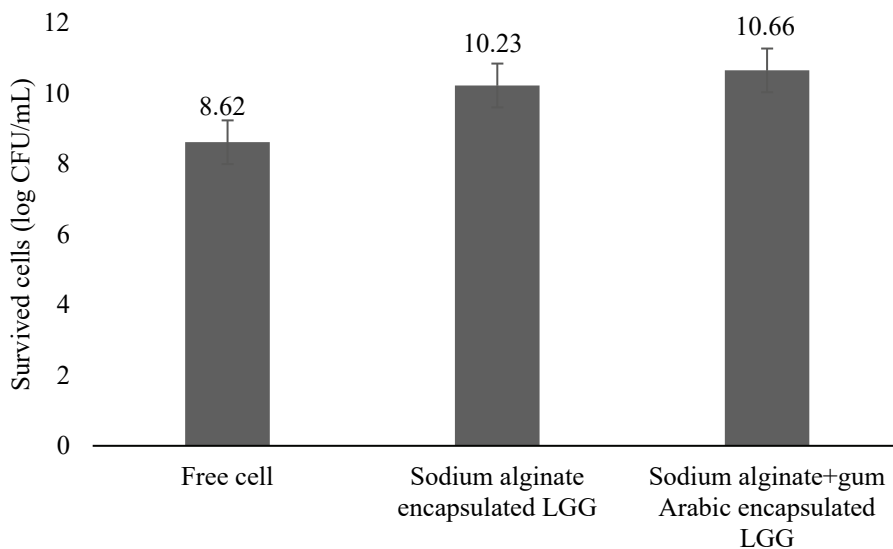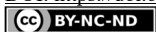
Figure 2. Stability of *Lactobacillus rhamnosus* GG in cocoa juice
LGG- *Lactobacillus rhamnosus* GG, Free cell- unencapsulated LGG

Encapsulation of LGG significantly ($p < 0.05$) preserved its viability in cocoa juice. Significantly ($p < 0.05$) lower viability (8.62 log CFU/mL) was recorded for the free cell compared to the encapsulated LGG. This could be due to the predisposition of the free cell to the harsh acidic condition of the juice. According to Prakash et al. (7), the main objective of encapsulating probiotics is to protect them against harsh conditions in the gastrointestinal tract, as well as in food matrices. Previous studies had reported improvement in the viability of LAB, such as *Lactobacillus paracasei* NFBC 338 (8) and *Lactobacillus rhamnosus* GR1 (2), consequent to their encapsulation before use. Significantly ($p < 0.05$) higher viability (10.66 log CFU/mL) was recorded for LGG encapsulated with sodium alginate+gum Arabic compared to LGG encapsulated with sodium alginate only (10.23 log CFU/mL). This implied better stability of LGG as a result of improved protection offered by a double-layered matrix created by the combination of sodium alginate and gum Arabic. This result aligned with the findings of Wang et al. (30) who reported improved stability of a double-layered encapsulated *Bifidiobacterium adolescentis* in pineapple and grape juices.

Survival of *Lactobacillus rhamnosus* GG in simulated gastrointestinal conditions

The viability of free and encapsulated *Lactobacillus rhamnosus* GG in simulated gastric condition is presented in Figure 3.

Original scientific paper
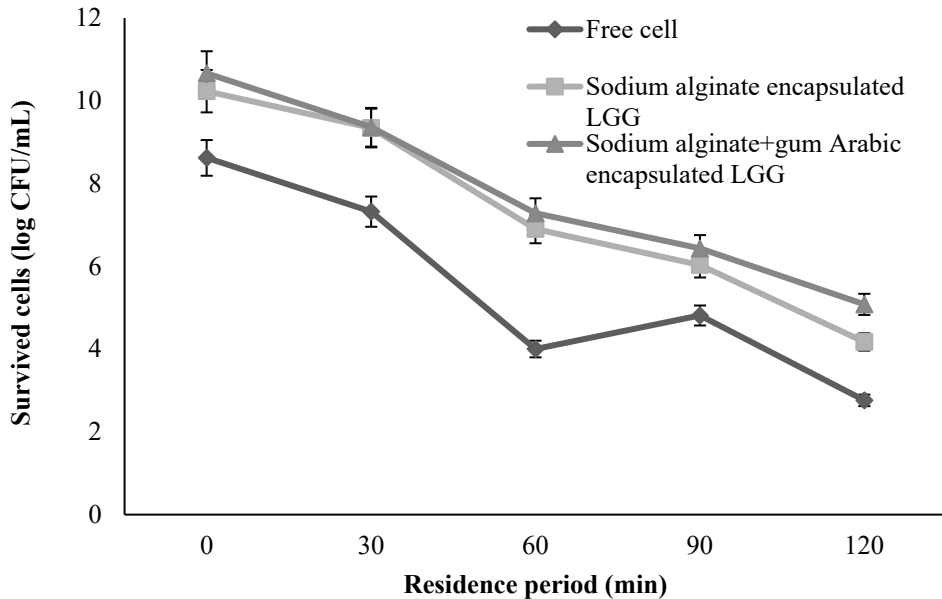
Figure 3. Stability of *Lactobacillus rhamnosus* GG in simulated gastric juice
LGG- *Lactobacillus rhamnosus* GG, Free cell- unencapsulated LGG

Irrespective of encapsulating materials used, the survival of LGG decreased as the residence period increased. During the first 30 min of incubation, the free cell was <7 log CFU/mL, while the population of the encapsulated samples was >9 log CFU/mL. Many studies (7, 30, 32) had shown that encapsulation could increase the survival of probiotics by inhibiting the diffusion of calcium ions outside the capsules. Mokkarram et al. (33) showed that *Lactobacillus acidophilus* and *Lactobacillus rhamnosus* exposed to simulated gastric condition had higher viability when encapsulated in calcium alginate. The free cell further decreased to 2.76 log CFU/mL after 120 min. This indicated an approximate 73% reduction in viability. The result indicated that the free cell would be sensitive to the acidic environment of the stomach, which might affect its survival. Kim et al. (34) also reported that at pH 1.2, un-encapsulated *Lactobacillus acidophilus* was destroyed after 1 h of incubation. After 60 min of incubation, higher viability was recorded for LGG encapsulated with sodium alginate + gum Arabic compared to the LGG encapsulated with sodium alginate. This could be due to the formation of a double layer membrane by sodium alginate and gum Arabic, which probably led to the reduced interaction between LGG and gastric juice. Ivanovska et al. (27) also reported high viability of *Lactobacillus casei* consequent to its encapsulation with chitosan and calcium alginate. According to Sivudu et al. (18), the combined use of alginate and prebiotics, such as gum Arabic and chitosan, confers a high level of inertness against many enzymes of the intestinal tract.

The viability of free and encapsulated LGG in the simulated intestinal condition is presented in Figure 4.

Original scientific paper
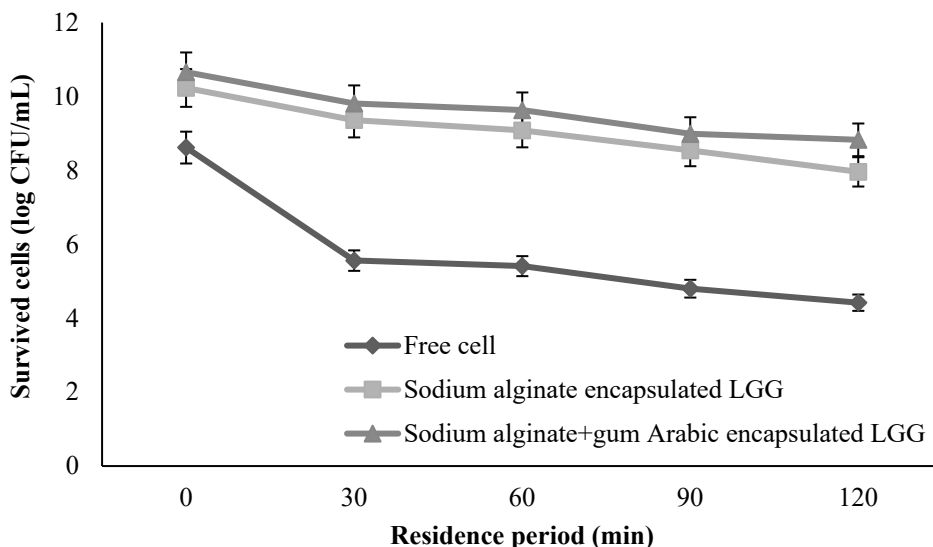
Figure 4. Stability of *Lactobacillus rhamnosus* GG in simulated intestinal juice
LGG - *Lactobacillus rhamnosus* GG, Free cell - unencapsulated LGG.

Generally, there was a significant reduction in viability of the free cell after exposure to simulated intestinal condition. The viability of the free cell reduced from 10.60 to 4.41 log CFU/mL, and this indicated a 58.4% loss of viability. This could be due to the unfavourable pH of the intestine. Mokkarram et al. (33) also reported a reduction in the viability of *Lactobacillus rhamnosus* when subjected to intestinal juice. During the early stages of incubation, LGG encapsulated with sodium alginate and sodium alginate + gum Arabic was stable. However, after 120 min of incubation, higher viability was recorded for LGG encapsulated with sodium alginate + gum Arabic. Viability of LGG encapsulated with sodium alginate and sodium alginate + gum Arabic was 8.0 and 8.83 log CFU/mL, respectively. This corresponded to 23.8 and 16.3% reduction, respectively. Higher stability recorded for LGG that was encapsulated with sodium alginate + gum Arabic could be due to the synergistic effect of sodium alginate and gum Arabic in protecting the organism against the harsh conditions of the intestine. Wang et al. (30) also reported higher survival efficiency of *Lactobacillus casei* encapsulated with sodium alginate and vegetable protein.

Chemical composition of cocoa juice during storage

Changes in pH, titratable acidity, total soluble solids, and total sugar of probiotic cocoa juice as influenced by encapsulation of LGG are presented in Table 1. After 7 days of storage, there was a general reduction of the pH of cocoa juice as storage progressed. The reduction in pH could be attributed to the elaboration of organic acid as storage progressed (32). Prakash et al. (7) also reported decreasing pH of litchi juice during storage. Also, after seven days of storage, there was no significant ($p>0.05$) difference in

the pH of cocoa juice samples that contained the free cell (CJFC), encapsulated LGG, and the freshly prepared cocoa juice. However, after 21 days of storage, significantly ($p<0.05$) lower pH was recorded in cocoa juice samples that contained encapsulated LGG compared to CJFC. This implied that the encapsulation of LGG caused a significant ($p<0.05$) reduction in the pH of the juice. This could be due to the increased utilization of cocoa juice sugars, especially sucrose, by the encapsulated LGG, which probably led to the increased elaboration of organic acids (11).

Table 1. Chemical composition of cocoa juice as influenced by encapsulated *Lactobacillus rhamnosus* GG

Storage period (day)	Encapsulation material	pH	Titratable acidity (%)	Total soluble solids (°Brix)	Total sugar (mg/100 mL)
0	Freshly prepared juice	$4.06^a\pm0.01$	$1.61^a\pm0.02$	$9.87^a\pm0.02$	$25.10^a\pm0.04$
7	Free cell	$4.05^a\pm0.01$	$1.58^a\pm0.01$	$9.53^b\pm0.06$	$16.14^b\pm0.24$
	Sodium alginate	$4.06^a\pm0.01$	$1.57^a\pm0.01$	$8.20^g\pm0.01$	$9.48^e\pm0.00$
	Sodium alginate + gum Arabic	$4.06^a\pm0.11$	$1.59^a\pm0.01$	$8.97^{de}\pm0.06$	$7.56^i\pm0.40$
14	Free cell	$4.05^{ab}\pm0.01$	$1.35^c\pm0.01$	$9.53^b\pm0.06$	$11.57^{bc}\pm0.06$
	Sodium alginate	$3.53^d\pm0.06$	$1.41^{bc}\pm0.01$	$8.90^f\pm0.00$	$10.89^c\pm0.02$
	Sodium alginate + gum Arabic	$3.50^d\pm0.00$	$1.46^b\pm0.01$	$9.00^d\pm0.00$	$8.82^f\pm0.02$
21	Free cell	$4.03^b\pm0.01$	$1.25^f\pm0.05$	$9.47^c\pm0.06$	$10.97^c\pm0.15$
	Sodium alginate	$3.80^c\pm0.00$	$1.38^e\pm0.02$	$8.90^{de}\pm0.00$	$10.99^c\pm0.01$
	Sodium alginate + gum Arabic	$3.83^c\pm0.06$	$1.43^d\pm0.02$	$8.97^{de}\pm0.06$	$10.01^e\pm0.05$
28	Free cell	$4.02^b\pm0.01$	$1.06^f\pm0.01$	$9.47^c\pm0.06$	$10.77^d\pm0.19$
	Sodium alginate	$3.70^{cd}\pm0.00$	$1.35^e\pm0.02$	$8.83^e\pm0.06$	$8.33^g\pm0.05$
	Sodium alginate + gum Arabic	$3.70^{cd}\pm0.00$	$1.41^d\pm0.01$	$8.83^e\pm0.06$	$8.08^h\pm0.00$

Values are means±standard deviations of triplicate scores. Means with different superscripts in column were significantly ($p<0.05$) different.

This is advantageous because the low pH of juice that contained encapsulated LGG would result in increased pH stability of the juice. Teanpaisan et al. (11) also reported the stability of the pH of orange juice containing encapsulated *Lactobacillus paracasei* SD1. Throughout the storage, results also showed that there was no significant ($p>0.05$) differrence in the pH of cocoa juice that contained sodium alginate only (CJSA) and the one that contained sodium alginate+gum Arabic (CJAG). Irrespective of the nature of LGG, there was no significant ($p>0.05$) difference in titratable acidity of the samples during the first 7 days of storage. However, after 14 days of storage, there was a significant ($p<0.05$) difference in titratable acidity of the samples. Significantly ($p<0.05$) higher titratable

acidity was recorded for CJAG compared to CJSA. This could be attributed to the accumulation of higher organic acids in the juice owing to the high metabolic activity of sodium alginate+gum Arabic encapsulated LGG (24). This further validated the effectiveness of combined use of alginate and gum Arabic for the encapsulation of LGG. Wang et al. (30) also reported a similar trend in pineapple and grape juices that contained double-layered encapsulated *Bifidiobacterium adolescentis.*

Significantly (p<0.05) higher total soluble solids and sugar were recorded in CJFC compared to CJSA and CJAG. Lower soluble solids and sugar recorded for CJSA and CJAG could be due to increased proliferation of LGG, which probably resulted in a higher rate of sugar catabolism (35). This finding contradicted that of Prakash et al. (7) who reported insignificant (p>0.05) change in total soluble solids of litchi juice as a result of the microencapsulation of *Lactobacillus casei* 359 with sodium alginate and gum acacia. Throughout the storage, significantly (p<0.05) higher total soluble solids and sugars were recorded for CJSA compared to CJAG. This could be due to the increased rate of sugar degradation of LGG encapsulated with sodium alginate and gum Arabic.

Colour attributes of cocoa juice as influenced by encapsulated *Lactobacillus rhamnosus* GG

The colour attributes of cocoa juice samples are presented in Table 2. The samples differed significantly (p<0.05) in terms of L*. Significantly (p<0.05) higher L* was recorded for CJFC compared to CJSA and CJAG. This implied a reduction in L* of cocoa juice as a result of the encapsulation of LGG with sodium alginate and gum Arabic.

Table 2. Colour attributes of cocoa juice as influenced by encapsulated *Lactobacillus rhamnosus* GG

Encapsulation material	L*	a*	b*	Hue angle	Chroma	Colour intensity
Free cell	66.95[a]±0.42	0.41[c]±0.01	2.03[c]±0.17	85.78[a]±0.03	1.77[c]±0.09	19.68[c]±0.38
Sodium alginate	51.09[b]±0.03	0.44[b]±0.01	5.87[b]±0.06	85.97[a]±0.07	5.52[b]±0.04	34.85[b]±1.16
Sodium alginate + gum Arabic	50.41[b]±0.36	0.48[a]±0.02	6.57[a]±0.01	85.79[a]±0.17	6.28[a]±0.07	36.50[a]±0.12

Values are means±standard deviations of triplicate scores. Means with different superscripts in column were significantly (p<0.05) different. L* (a measure of lightness), a* (a measure of redness and greenness), b* (a measure of blueness and yellowness)

This could be due to the effect of the encapsulating materials, which caused the contraction of colour. Teanpaisan et al. (11) had attributed a reduction in clarity or lightness of fruit juice containing encapsulated cells to the contrasting colour of juice and beads. Significantly (p<0.05) lower a*, b*, chroma, and colour intensity were recorded for CJFC compared to CJSA and CJAG. Significantly (p<0.05) higher a* and b* in CJSA and CJAG could be due to the impartation of colour by sodium alginate and gum Arabic, which culminated in increased redness and yellowness. There was no significant (p>0.05) difference between CJSA and CJAG in terms of L*, however, the samples differed

Original scientific paper

significantly (p<0.05) in terms of a*, b*, chroma, and colour intensity. In all the listed parameters, significantly (p<0.05) higher values were recorded for CJAG. This result indicated that the incorporation of sodium alginate + gum Arabic encapsulated LGG into cocoa juice caused an improvement in the colour attributes of the juice. This is advantageous because it could result in increased acceptability of the juice. High chroma and colour intensity of CJAG could imply high colour purity of the juice (36). The hue angle of the samples was 85.78-85.97, and the parameter did not significantly (p>0.05) differ among them. The hue angle obtained in this study showed a deviation between 0 and 90°, and this implied deviation from red to yellow. This was evident by the creamy white colouration of the juice samples.

Sensory properties of cocoa juice as influenced by encapsulated *Lactobacillus rhamnosus* GG

The effect of encapsulation of LGG on the sensory properties of cocoa juice is presented in Table 3. There was no significant (p<0.05) difference among the samples in terms of colour and appearance. This showed that the encapsulation of LGG did not alter the acceptable colour of the juice. This could be due to the stability of the creamy colour of the juice. Cocoa juice that contained sodium alginate+gum Arabic encapsulated LGG compared significantly (p<0.05) with CJFC in terms of taste and consistency. This contradicted the findings of Sivudu et al. (18) who reported that the presence of encapsulated beads in tomato and carrot juices negatively affected their swallowability (consistency). Higher preference was given to CJAG in terms of aroma, while CJFC performed better in terms of overall acceptability.

Table 3. Sensory properties of cocoa juice as influenced by encapsulated
Lactobacillus rhamnosus GG

Encapsulation material	Colour	Appearance	Aroma	Taste	Consistency	Overall acceptability
Free cell	7.46[a] ± 1.23	7.02[a]±1.24	6.42[ab] ± 1.84	6.46[a] ± 1.53	6.56[a] ± 1.01	7.41[a] ± 1.12
Sodium alginate	6.93[b] ± 1.16	7.03[a]±1.03	6.12[c] ± 1.81	6.11[b] ± 1.51	6.20[b] ± 1.64	6.07[c]± 1.28
Sodium alginate + gum Arabic	7.41[a] ± 1.64	7.04[a] ± 1.51	6.67[a] ± 1.68	6.52[a] ± 1.28	6.51[a] ± 0.43	7.27[b] ± 1.36

Values are means±standard deviations of fifty scores. Means with different superscripts in column were significantly (p<0.05) different.

Both CJFC and CJAG showed better preference than CJSA in all the parameters. High preference for CJAG could be due to improved purity and particle size of the juice as a result of enhanced activity of sodium alginate + gum Arabic encapsulated LGG. This result did not align with the findings of Teanpaisan et al. (11) who reported reduced consumer preference of juice that contained double-layered beads. High aroma preference for CJAG could be due to the bio-availability of aroma compounds owing to the increased activity of sodium alginate + gum Arabic encapsulated LGG. According to Pereira and Rodrigues (32), lactic acid bacteria are associated with the development of aroma compounds that are preserved by microencapsulation.

CONCLUSIONS

This study showed that the encapsulation of LGG with sodium alginate and gum Arabic stabilized the organism in cocoa juice. The combination of sodium alginate and gum Arabic for the encapsulation of LGG resulted in a higher yield compared to the use of sodium alginate alone. Higher stability was obtained for the encapsulated LGG in cocoa juice compared to the un-encapsulated LGG. The viability of the organism in simulated gastro-intestinal conditions also followed a similar trend. Incorporation of LGG into cocoa juice caused a significant ($p < 0.05$) reduction of its titratable acidity, total solids, and sugars during storage. Higher titratable acidity, total solids, sugars, chroma, and colour intensity were recorded for CJSA and CJAG compared to CJFC. Overall, CJAG performed better in the listed parameters than CJSA. Also, CJAG compared favourably with CJFC in terms of colour, appearance, aroma, taste, and consistency. The valorization of cocoa pulp into value-added products will reduce wastage. Besides, the incorporation of a probiotic organism and prebiotic in cocoa juice will improve its health-promoting potential, especially in the prevention against gastro-intestinal diseases such as infant diarrhea, lactose intolerance, and colon cancer.

CONFLICT OF INTEREST

Researchers hereby declare that there is no conflict of interest whatsoever in this research.

REFERENCES

1. Gheisari, H.R.; Davar, M.; Shekarforoush, S. S. Stability of microencapsulated *Lactobacillus casei* in mango fruit juice and its survival at simulated human gastro-intestinal condition. *Int. J. Pharm. Res. Allied Sci.* **2018**, *7*, 64-71.
2. White, J.; Hekmat, S. Development of probiotic fruit juices using *Lactobacillus rhamnosus* GR-1 fortified with short chain and long chain inulin fiber. *Ferment*. **2018**, *27*, 1-12.
3. Fijan, S. Microorganisms with claimed probiotic properties: an overview of recent literature. *Int. J. Environ. Resour. Public Health.* **2014**, *11*, 4745–4767.
4. Boonma, P.; Jennifer, K.; Xiang, Q.; Jittaprasatsin, C.; Muzny, D.M.; Doddapaneni, H.; Gibbs, R.; Petrosino, J.; Tumwasorn, S.; Versalovic, J. Draft genome sequences and description of *Lactobacillus rhamnosus* strains L31, L34, and L35. *Stand. Genom. Sci.* **2014**, *9*,744-754.
5. Baharav, E.; Mor, F.; Halpern, M.; Weinberger, A. *Lactobacillus* GG bacteria ameliorate arthritis in Lewis rats. *J. Nutr.* **2004**, *134*, 1964-1969.
6. Tripathi, M.K.; Giri, S.K. Probiotic functional foods: Survival of probiotics during processing and storage. *J. Funct. Foods.* **2014**, *9*, 225–241.
7. Prakash, K.S.; Bashir, K.; Mishra, V. Development of synbiotic litchi juice drink and its physiochemical, viability and sensory analysis. *J. Food Process. Technol.* **2017**, *8*, 12-18.
8. Desmond, C.; Ross, R.P.; O'Callaghan, E.; Fitzgerald, G.; Stanton, C. Improved survival of *Lactobacillus paracasei* NFBC 338 in spray dried powders containing gum acacia. *J. Appl. Microbiol.* **2002**, *93*, 1003-1011.
9. Etchepare, M.A.; Barin, L.S.; Cichoski, A.J.; Jacob-Lopes, E.; Wagner, R.; Fries, L. Microencapsulation of probiotics using sodium alginate. *Ciencia Rural.* **2015**, *45*, 1-7.
10. Malmo, C.; La Storia, A.; Mauriello, G. Microencapsulation of *Lactobacillus reuteri* DSM 17938 cells coated in alginate beads with chitosan by spray drying to use as a probiotic cell in a chocolate soufflé. *Food Bioprocess Technol*. **2013**, *6*, 795–805.

11. Teanpaisan, R.; Chooruk, A.; Kampoo, T. Survival of free and microencapsulated human-derived oral probiotic *Lactobacillus paracasei* SD1 in orange and aloe vera juices. *Songklanakarin J. Sci. Technol.* **2015**, *37*, 265-270.

12. Chen, H.; Ma, D.; Li, Y.; Liu, Y.; Wang, Y. Effect of microencapsulation on survival and stability of *Bifidobacterium bifidum* BB01 exposed to simulated gastrointestinal conditions and in different food matrices. Acta Univ. *Cibiniensis Series E: Food Technol.* **2017**, *21*, 1-7.

13. Ahallil, H.; Abdullah, A.; Maskat, M.Y.; Sarbini, S.R. Fermentation of Gum Arabic by Gut Microbiota using *in vitro* colon model. AIP Conference Proceedings **2019**, 2111, 050004.

14. Dikit, P.; H-Kittikun, A.; Maneerat, S. Survival of encapsulated potentially probiotic *Lactobacillus plantarum* D6SM3 with bioemulsifier derived from spent yeast in simulated gastrointestinal conditions. *Songklanakarin J. Sci. Technol.* **2015,** *37* (4), 425-432.

15. Nami, Y.; Haghshenas, B.; Khosroushahi, A.Y. Effect of psyllium and gum Arabic biopolymers on the survival rate and storage stability in yogurt of *Enterococcus durans* IW3 encapsulated in alginate. *Food Sci. Nutr.* **2016**, *5*, 554–563.

16. Martins, E.M.F.; Ramos, A.M.; Vanzela, E.S.L.; Stringheta, P.C.; de Oliveira Pinto, C.L.; Martins, J.M. Products of vegetable origin: A new alternative for the consumption of probiotic bacteria. *Food Res. Int.* **2013**, 5*1*, 764–770.

17. Horáčková, S.; Rokytová, K.; Bialasová, K.; Klojdová, I.; Sluková M. Fruit juices with probiotics – new type of functional foods. *Czech J. Food Sci.* **2018**, *36*, 00-5.

18. Sivudu, S.N.; Ramesh, B.; Umamahesh, K.; Reddy, O.V.S. Probiotication of tomato and carrot juices for shelf-life enhancement using micro-encapsulation. *J. Food Biosci. Technol.* **2016**, *6*, 13-22.

19. Afoakwa, E.O; Kongor, J.E.; Takrama, J. F.; Budu, A.S. Changes in acidification, sugars and mineral composition of cocoa pulp during fermentation of pulp pre-conditioned cocoa (*Theobroma cacao*) beans. *Int. Food Res. J.* **2013** *20*(3), 1215-1222.

20. Puerari, C.; Magalhães, K.T.; Schwan, R.F. New cocoa pulp-based kefir beverages: Microbiological, chemical composition and sensory analysis. *Food Res. Int.* **2012**, *48*, 634-640.

21. Duarte, W. F.; Dias, D. R.; Oliveira, J. M.; Teixeira, J. A.; de Almeida e Silva, J. B.; Schwan, R. F. Characterization of different fruit wines made from cacao, cupuassu, gabiroba, jaboticaba and umbu. *LWT - Food Sci.Technol.* **2010**, *43*(10), 1564–1572.

22. Endraiyani, V. Total phenolics and antioxidant capacity of cocoa pulp: processing and storage study. A Masters thesis, Graduate School-New Brunswick Rutgers, The State University of New Jersey, **2011**, pp 2.

23. Anvoh, K.Y.B.; Zoro, B.I.; Gnakri, D. Production and characterization of juice from mucilage of cocoa beans and its transformation into marmalade. *Pakistan J. Nutr.* **2009**, *8*, 129-133.

24. Chaikham, P.; Apichartsrangkoon, A.; Worametrachanon, S.; Supraditareporn, W.; Chokiatiroted, E.; Wielee, TV. Activities of free and encapsulated *Lactobacillus acidophilus* LA5 or *Lactobacillus casei* 01 in processed longan juices on exposure to simulated gastrointestinal tract. *J. Sci. Food Agric.* **2013**, *93* (9), 2229-2238.

25. Mohamed, H.N., Shuhaimi, M., Anwar, F, & Yazid, A.M. (2017). Development of alginate – gum arabic beads for targeted delivery of protein. *Journal of Biomolecular Research and Therapeutics,* 6, 1-6.

26. Krishnan, S.; Kshirsagar, A.C.; Singhal, R.S. The use of gum arabic and modified starch in the microencapsulation of a food flavoring agent. *Carbohydr. Polym*. **2005**, *62*, 309-315.

27. Ivanovska, T.P.; Petrushevska-Tozi, L.; Grozgdanov, A.; Petkvska, R.; Hadjieva, J.; Popovski, E.; Stafilov, T.; Mladenovska, K. From optimization of symbiotic microparticles prepared by spray-drying to development of new functional carrot juice. *Chem. Ind. Chem Eng. Q.* **2014**, *20*, 549−564.

28. Chavarri, M.; Maranon, I.; Ares, R.; Ibanez, F.; Marzo, F.; Villaran M. Microencapsulation of a probiotic and prebiotic in alginate-chitosan capsules improves survival in simulated gastro-intestinal conditions. *Int. J. Food Microbiol.* **2010**, *12*, 185-189.

29. AOAC. Official Method of Analysis of AOAC Intl. 19th ed. Method 991.43. Association of Official Analytical Chemists, Arlington, VA, USA. **2010**.

30. Wang, J.; Korber, D.R.; Low, N.H.; Nickerson, M.H. Encapsulation of *Bifidobacterium adolescentis* cells with legume proteins and survival under stimulated gastric conditions and during storage in commercial fruit juices. *Food Sci. Biotechnol.* **2015**, *24*, 383-391.

31. Calame, W.; Weseler, A.R.; Viebke, C.; Flynn, C.; Siemensma, D. Gum arabic establishes prebiotic functionality in healthy human volunteers in a dose-dependent manner. *Braz. J. Nutr.* **2008**, *100*, 1269–1275.

32. Pereira, A.L.F.; Rodrigues, S. Turning fruit juice into probiotic beverages. In: Fruit Juices Extraction, Composition, Quality and Analysis. Rajauria G, Tiwari B. (eds). Academic Press, USA. **2018**, pp 279-287.

33. Mokkarram, R.R.; Mortazavi, S.A.; Najafi, M.B.H.; Shahidi F. The influence of multi-stage alginate coating on survivability of potential probiotic bacteria in simulated gastric and intestinal juice. *Food Res. Int.* **2009**, *42*, 1040-1045.

34. Kim, S.; Cho, S.Y.; Kim, S.H.; Song, O.; Shind, S.; Cha, D. Effect of microencapsulation on viability and other characteristics in *Lactobacillus acidophilus* ATCC 43121. *LWT – Food Sci. Technol.* **2008**, *41*, 493–500.

35. Kumar, A.; Kumar, D. Development of antioxidant rich fruit fortified probiotic buttermilk (lassi) using *Lactobacillus rhamnosus* culture. *Int. J. Biol., Pharm. Allied Sci.* **2016**, *5*, 1855-1868.

36. Correia, P.M.R.; Soares, A.M.; Brites, C. Quality characteristics of maize flour and breads. *Int. J. Food Eng.* **2016**, *2* (2), 113-118.

INACTIVATION KINETICS AND THERMODYNAMIC PROPERTIES OF POLYGALACTURONASE PRODUCED BY *Aspergillus awamori* CICC 2040 ON PRETREATED ORANGE AND PLANTAIN PEELS

Olajide E. Adedeji[1]*, Olufunke O. Ezekiel[2]

[1] Department of Food Science and Technology, Federal University Wukari, PMB 1020, Wukari, Nigeria
[2] Department of Food Technology, University of Ibadan, Ibadan, Nigeria

This study investigated the effect of pretreatment of orange and plantain peels on the inactivation kinetics and thermodynamic properties of polygalacturonase (PG) produced by Aspergillus awamori CICC 2040. Orange and plantain peel powders were subjected to microwave-assisted NaOH pretreatment and used as substrates for PG production. Un-treated peels served as controls. The PG was purified using acetone precipitation and column chromatography, and the inactivation kinetics, temperature dependency, and thermodynamic properties of the crude and purified PGs were determined. Higher inactivation rate constant was obtained for crude PG produced using pretreated orange peel (CPOF) and plantain peel (CPPF) compared to PG produced using untreated orange peel (Uo) and plantain peel (Up). At all the temperatures considered, higher half-life and decimal reduction time were recorded for CPOF and CPPF compared to Uo and Up. The highest half-life (45.60 min) and decimal reduction time (151.49 min) were recorded for CPOF at 60 °C. Lower half-life and decimal reduction time were obtained for purified PGs compared to the crude PG. Polygalacturonase produced from pretreated peels had lower activation energy than those produced from untreated ones. The higher activation energy was recorded for the PG produced using orange peel compared to the one from plantain peels. The enthalpy of CPOF and CPPF was slightly lower than Uo and Up. The pretreatment of the peels resulted in a reduction of Gibbs free energy (ΔG) and entropy (ΔS) of crude and purified PG. Higher ΔG and ΔS were recorded for the purified PG compared to the crude PG. Negative entropy and enthalpy were recorded for all the PGs. The findings from this study showed that the kinetic and thermodynamic properties of PG, produced by Aspergillus awamori CICC 2040, were enhanced by the pretreatment of orange and plantain peels.

Keywords: *Aspergillus awamori* CICC 2040, thermostability, polygalacturonase, pretreatment, purification

INTRODUCTION

Pectinases are enzymes that are involved in the breaking down of pectin-rich materials that are the main constituents of plant tissues (1). They modify cell wall structures through tissue maceration and cell lysis, which results in tissue degradation (2). Pectinases are important enzymes in the food industry, particularly in fruit and vegetable processing, and represent 10% of estimated commercialized enzymes (3). Fungi, especially members of the *Aspergillus niger* group, are good producers of pectinases (3). Pectinases

---

* Corresponding author: Olajide E. Adedeji, Department of Food Science and Technology, Federal University Wukari, PMB 1020, Wukari, Nigeria, e-mail: adedeji@fuwukari.edu.ng

are produced through solid-state and submerged fermentation processes (1, 4). Based on substrate preference, three classes of pectinases are known. They are esterase, lyase, and polygalacturonase (PG) (1). Among these pectinases, PG finds higher industrial applications due to its stability at various pH values and temperatures (5). Polygalacturonase (E.C. 3.2.1.15) is a hydrolytic pectinase that has an affinity for glycosidic bonds in galacturonic acid (6). Production of PG and its applications in fruit and vegetable processing are well documented (2, 5, 7).

In recent times, the use of agricultural residues as feedstock for the production of microbial products is becoming increasingly popular due to the high cost of traditional feedstock (8). Orange (*Citrus sinensis* L.) and plantain (*Musa paradisiaca* L.) peels are suitable substrates for the production of PG due to their wide availability (9, 10). However, the high lignocellulosic content of these peels limits their bio-conversion (11). Consequently, pretreatment of these peels for the improved proliferation of microorganisms and increased activity and/or yield of bio-products is imperative (12, 13).

Pretreatment of residues enhances the proliferation of microorganisms, thereby increasing the bioconversion rate of agricultural residues; consequently, it improves the yield and activity of products (9). Besides, pretreatment disrupts the highly organized lignin-carbohydrate composite of agricultural residues (9, 14). This results in lignin removal with an attendant increase in surface area of carbohydrate amenable to hydrolysis (15). In recent times, pretreatment of residues involving two or more methods is becoming popular due to the synergistic effect of each of the methods (16). In particular, microwave-assisted alkaline pretreatment of residues is considered highly efficient due to the high degradation of lignin fibres by microwave radiation in the presence of alkali (17, 18). Also, pretreatment that involves a combination of microwave radiation and alkali is attributed to high solids recovery (18). Properties of enzymes, e.g. cellulase, pectinase, and xylanase, produced from pretreated agricultural residues are well documented (9, 19, 20). These studies demonstrated an increase in the activity of microbial enzymes as a result of the pretreatment of agricultural feedstocks. However, information on the properties of these enzymes as influenced by the pretreatment of residues is sparsely reported. In our previous study (21), it was observed that pretreatment of orange and plantain peels enhanced the activity, stability, chemical composition, and physical properties of PG produced by *Aspergillus awamori* CICC 2040. However, further studies are required to evaluate the correlation between residue pretreatment, inactivation kinetics, and thermodynamic properties of microbial enzymes.

Inactivation and thermodynamic studies determine the thermo-stability and economic viability of enzymes in food and non-food systems (22). According to de Oliveira et al. (23), the thermodynamic properties of enzymes are related to parameters such as half-life, decimal reduction time, activation energy, enthalpy (ΔH), entropy (ΔS) and Gibbs free energy (ΔG). Abdel Wahab et al. (24) reported that these concepts are the cornerstones for understanding various biological processes such as enzyme reaction, protein folding, and interaction. Information on thermodynamic properties of three-phase partitioned exo-PG and immobilized PG from *Aspergillus* spp. are well documented (22, 25, 26). This study was designed to evaluate the effect of microwave-assisted alkaline pretreatment of orange and plantain peels on the inactivation kinetics and thermodynamic properties of PG produced by *Aspergillus awamori* CICC 2040.

MATERIALS AND METHODS

Materials

Peels of orange (*Citrus sinensis* L. Osbeck) and plantain (*Musa paradisiaca* Linn.) were obtained from small-scale food processing factories in Ibadan, Nigeria. Fungal strain, *Aspergillus awamori* CICC (China Centre of Industrial Culture Collection) 2040, was obtained from China National Research Institute of Food and Fermentation, Beijing, China. Polygalacturonic acid (Oxoid, England) was procured from Bristol Scientific Company Ltd., Lagos, Nigeria. All reagents used were of analytical grade.

Methods

Production of orange and plantain peel powders

Orange and plantain peels were blanched (80 °C for 3 min), rinsed, and dried in a hot air oven (NL9023A, Genlab Ltd., England) at 60 °C for 48 h. The dried peels were milled into powders with the aid of a blender (BLX750RD, Kenwood, UK) and sieved with the aid of 0.8025 mm sieve (United States Pharmacopoeia Standard Sieve, Metallurgy Corp., Canada). The powders were packaged in polyethylene containers (ZipLock, Yantai Bagmont Co., China) and stored at -20 °C in a freezer (Fc 260, Hisense, China) for subsequent analyses.

Pretreatment of orange and plantain peel powders

Microwave-assisted NaOH pretreatment of orange peel powder (OPP) and plantain peel powder (PPP) was done following the procedure outlined by Peng et al. (27). Peel powder (5 g) was soaked in 500 mL 0.1 M NaOH for 12 h. Subsequently, the mixture was treated in a laboratory microwave oven (NX-802, with 25 L capacity, 800 W power output, and frequency of 2450 MHz, Nexus, China) at 720 W for 10 min. The residue was recovered and washed several times with distilled water to remove adhering NaOH. Pretreated peels were oven-dried at 60 °C to constant moisture content and stored (-20 °C) in a freezer (Fc 260, Hisense, China). Untreated OPP and PPP served as controls.

Culturing of microorganism

Fungal strain *Aspergillus awamori* CICC 2040 was maintained on malt extract agar (MEA) (ACROS Organics, USA) at 28 °C for 6 days. Inoculums for the experiments were prepared from heavily sporulated MEA slants (21).

Polygalacturonase production

Polygalacturonase was produced from *Aspergillus awamori* CICC 2040 under solid-state fermentation based on the procedure outlined by Dey et al. (7). Five grammes of pretreated and untreated peel powders were mixed with 10 mL Czapek-dox medium (2.5 g/L NaNO$_3$, 1 g/L KH$_2$PO$_4$, 0.5 g/L KCl and 0.5 g/L MgSO$_4$.2H$_2$O) at pH 4.0 in a 250 mL Erlenmeyer flask. The mixture was autoclaved (121°C, 15 psi) for 15 min and cooled

to room temperature (28±2 °C). Thereafter, 10^6 spores/mL of *Aspergillus awamori* was inoculated and this was incubated at 28 °C for 5 days in an incubator (CLN115, Pol Eko Aparatura, Poland). After fermentation, a 50 g/L suspension of the mass was made using distilled water and kept in an incubator (CLN115, Pol Eko Aparatura, Poland) at 30 °C for 1 h. The suspension was centrifuged at 2200 × g for 10 min in a centrifuge (K24IR, Centurion Scientific Ltd., UK) and the supernatant was removed with the aid of What-man No. 1 filter. Crude PG extract was stored at -20 °C until required.

Purification of polygalacturonase

The crude PG extract was purified using acetone precipitation and column chromato-graphy as described by Anand et al. (2). Crude PG extract (5 mL) was mixed with 15 mL of 99% cold acetone and kept at 4 °C with continuous stirring for 12 h. The solution was centrifuged at 8000 × g for 20 min and the resulting pellet was separated from the supernatant. The pellet was dissolved in 0.1 M citrate buffer (1:10, w/v) at pH 5.0, filte-red with the aid of 0.45 μ filter, and loaded on a chromatographic column (Sephadex G-100 Column, MP Biomedicals, USA). The column was maintained at 12.0 mL/h flow rate and protein fractions were collected.

Analyses

Determination of inactivation and thermodynamic properties

The inactivation kinetics of PG was determined by incubating the enzyme in a water bath (NL9023A, Genlab Ltd., England) at temperatures 60, 70, 80, and 90 °C in the absence of substrate. Aliquots were taken, every 20 min for 2 h, and cooled in an ice bath and assayed for PG activity. Percentage residual activity was calculated as the ratio of enzyme activity at a given time to the initial activity (28). The inactivation rate constant (kd) was obtained from a semi-log graph of residual activity and time. Half-life ($t_{1/2}$) and decimal reduction time (D) were calculated as the ratio of ln 2 and kd, and ln 10 and kd, respectively (25).

Arrhenius equation (Eq. 1) was used to evaluate the temperature dependency of PG.

$$\ln kd = \ln (ko) - \left(\frac{Ea}{R}\right)\left(\frac{1}{T}\right) \tag{1}$$

where *Ea* is the activation energy (J/mol), *ko* is the Arrhenius equation constant, *R* is the ideal gas constant = 8.314 J/molK, and *T* is the temperature (K).

Eyring equation (Eq. 2) was used for the estimation of thermodynamic data

$$kd = \left(\frac{K_B}{h}T\right)e^{\left(\frac{\Delta H}{RT}\right)}e^{\left(\frac{\Delta S}{R}\right)} \tag{2}$$

where k_B is Boltzman's constant, 1.38×10^{-23} J/K; h is Plank's constant, 6.63×10^{-34} Js.

The enthalpy of activation ΔH, J/mol; free energy of activation ΔG, J/mol, and entropy ΔS, J/molK were obtained from Eqs. 3, 4, and 5, respectively.

Original scientific paper

$$\Delta H = E_a - RT \qquad [3]$$

$$\Delta G = -RT \ln \frac{k_d}{K_B T} h \qquad [4]$$

$$\Delta S = \frac{\Delta H - \Delta G}{T} \qquad [5]$$

RESULTS AND DISCUSSION

Inactivation kinetics and thermodynamic properties of polygalacturonase

Inactivation kinetics of crude and purified PGs are presented in Table 1. The inactivation rate constant (kd) of all the PGs investigated in this study increased with increasing temperature. This suggested a reduction in PG thermo-stability as temperature increased. The increase in kd as temperature increased could be due to the denaturation of protein consequent to the breakdown of primary, secondary, tertiary, and quaternary structures of proteins without disruption of covalent bonds (25, 29). This followed earlier trends described for PG (24), glucoamylase (28), protease (30), and β-fructofurasinosidase (23). At every temperature considered, kd differed depending on the source of the substrate used for PG production. Higher kd was obtained for crude PG produced using pretreated OPP (CPOF) and PPP (CPPF) compared to PG produced using untreated orange peel (Uo) and plantain peel (Up). This implied higher thermo-stability of crude PG produced using pretreated OPP and PPP. This could be due to the modification of nutrients, e.g. increase in the concentration of inducer substrates (pectin and sugars), and structures of the peels following their pretreatment. According to Norouzian et al. (31), variation in carbon and nitrogen sources, and their ratio could have a crucial influence on enzyme's properties such as activity and thermo-stability. Han et al. (32) had reported differences in kd of glucoamylase produced from *Aspergillus awamori* on different wastes, such as cake, pastry, and bread, due to their different chemical constituents. Half-life and decimal reduction time of PG decreased with increasing temperature. This was consistent with an increase in kd as temperature increased. Han et al. (32) also reported decreasing half-life of glucoamylase with increasing temperature. Decimal reduction time of peroxidase also reduced with increasing temperature (33). The highest half-life (36.10-45.60 min) and decimal reduction time (119.93-151.49 min) were obtained at 60 °C. At all the temperatures considered, higher half-life and decimal reduction time were recorded for CPOF and CPPF compared to Uo and Up. The variation in half-life and decimal reduction time of PGs obtained from this study suggested differences in their thermodynamic properties. Therefore, CPOF, which had the highest half-life (45.60 min) and decimal reduction time (151.49 min) could be said to be most thermo-stable at 60 °C. According to Melikoglu et al. (28), half-life and decimal reduction time are good indicators of enzyme thermo-stability, therefore, Up, which had the lowest half-life and decimal reduction time at all the temperatures considered could be said to be the least thermo-stable PG. The purification of PG resulted in an increase in kd at all the temperatures considered. However, lower half-life and decimal reduction were obtained for purified PGs compared to the crude PGs. This could be due to an increase in the sensitivity factor (Z value) resulting from the purification operation (22). High R^2 (0.905-0.994) recorded for all the PGs at different temperatures suggested good fitness of experimental data.
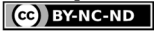
Table 1. Inactivation kinetics of crude and purified polygalacturonase

Temperature (°C)	Parameter	Crude polygalacturonase				Purified polygalacturonase			
		Uo	CPOF	Up	CPPF	PUo	PCPOF	PUp	PCPPF
60	kd (min⁻¹)	0.0151	0.0152	0.0142	0.0154	0.0326	0.0380	0.0336	0.0496
	R²	0.961	0.973	0.907	0.905	0.911	0.949	0.955	0.961
	t½ (min)	43.90	45.60	36.10	45.01	13.26	18.24	20.63	23.97
	D (min)	145.49	151.49	119.93	149.52	70.63	80.59	68.53	76.42
70	kd (min⁻¹)	0.0202	0.0232	0.0214	0.0222	0.0371	0.0636	0.0441	0.0552
	R²	0.970	0.977	0.900	0.905	0.924	0.932	0.962	0.978
	t½ (min)	31.31	34.31	24.41	31.22	18.68	22.90	15.72	17.56
	D (min)	113.99	119.99	81.08	103.72	52.06	66.20	52.21	61.71
80	kd (min⁻¹)	0.0315	0.0335	0.0346	0.0394	0.0571	0.0703	0.0481	0.0648
	R²	0.980	0.994	0.949	0.914	0.974	0.994	0.987	0.994
	t½ (min)	20.00	22.00	20.03	23.58	7.14	9.86	8.41	10.70
	D (min)	73.10	78.10	66.55	78.32	40.33	32.75	47.87	53.53
90	kd (min⁻¹)	0.0387	0.0425	0.0608	0.0681	0.0671	0.0852	0.0707	0.0770
	R²	0.945	0.937	0.927	0.943	0.933	0.970	0.987	0.996
	t½ (min)	17.91	21.33	11.40	14.41	7.33	8.14	8.80	9.00
	D (min)	59.50	70.85	37.87	47.87	23.32	27.03	32.57	37.90

kd-inactivation rate constant; t½-half-life; D- decimal reduction time; Uo- Crude PG produced from un-treated orange peel; CPOF- Crude PG produced from pre-treated orange peel; Up- Crude PG produced from un-treated plantain peel; CPPF- Crude PG produced from pre-treated plantain peel; PUo- Purified PG produced from un-treated orange peel; PCPOF- Purified PG produced from pre-treated orange peel; PUp- Purified PG produced from un-treated plantain peel; PCPPF- Purified PG produced from pre-treated plantain peel.

Temperature dependency of polygalacturonase inactivation

Temperature dependency of crude and purified PG as described in terms of activation energy of denaturation is presented in Table 2. Positive activation energy was obtained for all the PGs. This indicated a catalytic reaction of enzyme deactivation (28). Dogan and Tari (25) also reported positive activation energy for PG produced by *Aspergillus sojae*. The activation energy was 2.26-3.07 kJ/mol for crude PG and 1.23-2.15 kJ/mol for purified PG. This implied a higher reaction rate of purified PG owing to the reduction of the energy barrier, consequent to an increased motion and collision frequency of purified PG and substrate (24). The impurities in the crude PG might have resulted in a reduction in the rate of collision of the enzyme and substrate. Polygalacturonase produced from pretreated OPP and PPP had lower activation energy than those produced from untreated ones. Also, the activation energy of PG from OPP was higher than those from PPF.

According to Lam et al. (34), activation energy connotes the energy required to form activation complex for protein hydrolysis, therefore, the low activation energy of PG produced from pretreated PPF implied that it required lesser energy to form the complex, and this will improve the economy of the operation. Arrhenius model used for the temperature dependency of inactivation rate constant showed linear conformations with high R^2

that ranged from 0.891 to 0.989. This suggested a single conformation up to the transition temperature (28).

Table 2. Temperature dependency of crude and purified polygalacturonase

Parameter	Crude polygalacturonase				Purified polygalacturonase			
	Uo	CPOF	Up	CPPF	PUo	PCPOF	PUp	PCPPF
ko (min^{-1})	0.011	0.010	0.013	0.012	0.024	0.033	0.027	0.042
Ea (J/mol)	3.71	3.07	3.03	2.26	2.15	2.1	1.92	1.23
R^2	0.982	0.987	0.966	0.919	0.953	0. 891	0.947	0.989

ko- Arrhenius constant; Ea- activation energy; Uo- Crude PG produced from un-treated orange peel; CPOF- Crude PG produced from pre-treated orange peel; Up- Crude PG produced from un-treated plantain peel; CPPF- Crude PG produced from pre-treated plantain peel; PUo- Purified PG produced from un-treated orange peel; PCPOF- Purified PG produced from pre-treated orange peel; PUp- PG produced from un-treated plantain peel; PCPPF- PG produced from pre-treated plantain peel.

Thermodynamic properties of polygalacturonase

Thermodynamic properties of crude and purified PGs as described by enthalpy, free energy, and entropy at different temperatures (60 to 90°C) are presented in Table 3.

Table 3. Thermodynamic properties for thermal inactivation of crude and purified polygalacturonase

Temperature (ºC)	Parameter	Crude polygalacturonase				Purified polygalacturonase			
		Uo	CPOF	Up	CPPF	PUo	PCPOF	PUp	PCPPF
60	ΔH (J/mol)	-2764.85	-2765.49	-2765.53	-2766.30	-2766.41	-2766.46	-2766.64	-2767.33
	ΔG (J/mol)	93466.98	93448.70	93637.11	93412.51	91336.25	90911.90	91252.60	90174.34
	ΔS (J/molK)	-288.984	-288.932	-289.497	-288.825	-282.591	-281.316	-282.34	-279.104
70	ΔH (J/mol)	-2847.99	-2848.63	-2848.67	-2849.44	-2849.55	-2849.60	-2849.78	-2850.47
	ΔG (J/mol)	95528.36	95133.49	95363.79	95259.13	93794.71	92257.66	93301.82	92661.60
	ΔS (J/molK)	-286.812	-285.662	-286.334	-286.031	-281.762	-277.281	-280.325	-278.461
80	ΔH (J/mol)	-2931.13	-2931.77	-2931.81	-2932.58	-2932.69	-2932.74	-2932.92	-2933.61
	ΔG (J/mol)	97093.82	96913.16	96818.34	96437.07	95348.13	94737.77	95851.52	94976.87
	ΔS (J/molK)	-283.357	-282.847	-282.578	-281.500	-278.416	-276.687	-279.843	-277.367
90	ΔH (J/mol)	-3014.27	-3014.91	-3014.95	-3015.72	-3015.83	-3015.88	-3016.06	-3016.75
	ΔG (J/mol)	99307.40	99024.72	97944.03	97601.83	97646.47	96925.73	97488.75	97231.13
	ΔS (J/molK)	-281.878	-281.101	-278.124	-277.183	-277.307	-275.321	-276.873	-276.165

ΔH- Enthalpy; ΔG- Gibbs free energy; ΔS- Entropy; Uo- Crude PG produced from un-treated orange peel; CPOF- Crude PG produced from pre-treated orange peel; Up- Crude PG produced from un-treated plantain peel; CPPF- Crude PG produced from pre-treated plantain peel; PUo- Purified PG produced from un-treated orange peel; PCPOF- Purified PG produced from pre-treated orange peel; PUp- Purified PG produced from un-treated plantain peel; PCPPF- Purified PG produced from pre-treated plantain peel.

The ΔH of CPOF and CPPF was slightly lower than Uo and Up. This could be due to the increased mobilization of pectin in the peels, following their pretreatment, which increased the stability of the PG. The lower ΔH recorded for CPOF and CPOF could be advantageous because low ΔH is an indication of increased mobility, collision, and inte-

raction of enzyme and substrate molecules (28). Besides, purification caused an increase in the ΔH of the PGs probably due to the disruption of non-covalent linkages of proteins in the enzyme (29). Irrespective of substrate pretreatment and enzyme purification, ΔG increased with increasing temperature. This suggested a reduction in the energy barrier of inactivation and an increasing degree of spontaneity as temperature increased (33).

The pretreatment of the peels resulted in a reduction of ΔG of crude and purified PGs. This could be due to an increase in the rate of collision between the enzyme and substrate, hence, an improvement in the efficiency of the enzyme. This result suggested that the pretreatment of the peels enhanced the thermal unfolding of the enzyme (24), and thus, improved its stability. The variation in ΔH and ΔG of the PGs could be due to differences in pectin and sugar contents of the peels as a result of the pretreatment operation (21). Han et al. (32) also reported variation in the thermodynamic properties of bread wastes due to differences in their chemical composition. Negative entropy (ΔS) was obtained for all the PGs at all temperatures, and this, according to Riaz et al. (35), could be attributed to the orderliness of the PG-substrate structure in the reacting system. A lower ΔS was recorded for the crude and purified PGs produced using pretreated peels compared to those from untreated peels. This could be due to the modification of the pectin of the peels, following their pretreatment, which probably caused an increase in covalent binding between PG and substrate (22). Since ΔS is correlated with the order of rigidity of enzyme-substrate complex, the low value obtained for PG from pretreated peels implied high orderliness of the structure of the PG during its transition stage (26). Negative ΔS was recorded for all the PGs in this study and this implied that the structure of the PG-substrate complex at the transition stage was more ordered in the reacting system (25). Also, negative ΔS and ΔH recorded for the PGs depicted spontaneity of the inactivation process (28). A similar result was also reported for glucoamylase (32). Lower ΔG and ΔS were recorded for purified PGs compared to the crude PGs and this implied increased enzyme-substrate interaction and orderliness of structure (26). This could be attributed to the reduction of interfering compounds, such as phenolic and colour compounds, which would have otherwise reduced the degree of interaction between the enzyme and the substrate (21).

CONCLUSIONS

The findings from this study showed that the pretreatment of orange and plantain peels enhanced the kinetic and thermodynamic properties of PG. Polygalacturonase produced from pretreated peels had higher inactivation rate, thermo-stability, and reaction rate than PG produced from un-treated peels. The pretreatment of the peels resulted in PG with higher efficiency in terms of spontaneity and the order of enzyme-substrate structure. Investigation on the kinetic and thermodynamic properties of PG would assist in determining the thermo-stability and economic viability of the enzyme in food and non-food systems.

REFERENCES

1. Garg G, Singh A, Kaur A, Singh R, Kaur J and Mahajan R. Microbial pectinases: an eco-friendly tool of nature for industries. *3 Biotech.* **2016**, *6*, 47-59.

Original scientific paper

2. Anand G, Yadav S and Yadav D. Purification and characterization of polygalacturonase from *Aspergillus fumigatus* MTCC 2584 and elucidating its application in retting of *Crotalaria juncea* fiber. *3 Biotech*. **2016**, *6*, 201-207.

3. Anuradha K, Padma PN, Venkateshwar S and Reddy G. Selection of nutrients for polygalacturonase production by Aspergillus awamori MTCC 9166 using Placket-Burman design. *Indian J. Biotechnol*. **2014**, *13*, 502-507.

4. Reynolds AG, Knox A and DiProfio F. Evaluation of macerating pectinase enzyme activity under various temperature, pH and ethanol regimes. *Beverages*. **2018**, *4*, 10-23.

5. Anuradha K, Padma PN,Venkateshwar S and Reddy G. Mango juice clarification with polygalacturonase produced by *Aspergillus awamori* MTCC 9166 - Optimization of conditions. *Int. Food Res. J.* **2016**, *23* (1), 147-151.

6. Heerd D, Yegin S, Tari C and Fernandez-Lahore M. Pectinase enzyme complex production by *Aspergillus spp*. in solid-state fermentation: a comparative study. *Food Bioprod Process*. **2012**, *90*, 102-110.

7. Dey TB, Adak S, Bhattacharya P and Banerjee R. Purification of polygalacturonase from *Aspergillus awamori* Nakazawa MTCC 6652 and its application in apple juice clarification. *LWT - Food Sci. Technol.* **2014**, *59*, 591-595.

8. Wadhwa M, Bakshi MPS and Makkar HPS. Wastes to worth: value added products from fruit and vegetable wastes. *CAB Rev*. **2015**, *10*, 43-68.

9. Li P, Xia J, Shan Y, Nie Z and Wang F. Effect of surfactant and microwave-assisted pretreatment on orange peel on extracellular enzymes production by *Aspergillus japonicas* PJ10. *Appl. Biochem. Biotechnol.* **2015**, *176*, 758-771.

10. Castillo-Israel KAT, Baguio SF, Diasanta MDB, Lizardo RCM, Dizon EI and Mejico MIF. Extraction and characterization of pectin from Saba banana [Musa 'saba'(*Musa acuminata* x *Musa balbisiana*)] peel wastes: A preliminary study. *Int. Food Res. J.* **2015**, *22* (1), 190-195.

11. Lai C, Tang S, Yang B, Gao Z, Li X and Yong Q. Enhanced enzymatic saccharification of corn stover by in-situ modification of lignin with poly (ethylene glycol) ether during low temperature alkali pretreatment. *Bioresour. Technol*. **2017**, *244*, 92-99.

12. Jonsson LJ and Martin C. Pretreatment of lignocelluloses: Formation of inhibitory by products and strategies for minimizing their effects. *Bioresour. Technol.* **2016**, *199*, 103-112.

13. Agu OS, Tabil LG and Dumonceaux T. Microwave-assisted alkali pre-treatment, densification and enzymatic saccharification of canola straw and oat hull. Bioeng. **2017**, *4*, 25-32.

14. Wang S, Lia F, Zhang P, Jin S, Tao X, Tanga X and Wang H. Ultrasound assisted alkaline pretreatment to enhance enzymatic saccharification of grass clipping. *Energy Convers. Manag*. **2017**, *149*, 409–415.

15. Rahnama N, Mamat S, Shah UK, Ling FH, Abdulrahman NA and Ariff AB. Effect of alkali pretreatment of rice straw on cellulose and xylanase production by local *Trichoderma harzianum* SNRS under solid state fermentation. *Bioresour.* **2013**, *8* (2), 2881-2896.

16. Dutra ED, Santos FA, Alencar BRA, Reis ALS, Souza RFR, Aquino KAS, Morais MA and Menezes RSC. Alkaline hydrogen peroxide pretreatment of lignocellulosic biomass: status and perspectives. *Biomass Convers. Biorefin,* **2017**, doi: 10.1007/s13399-017- 0277-3.

17. Starr T, Harper DP and Rials TG. The effects of electron beam irradiation dose on the mechanical performance of red maple (*Acer rubrum*). *Bioresour.* **2015**, *10*, 956–969.

18. Inan H, Turkay O and Akkiris C. Microwave and microwave-chemical pretreatment application for agricultural waste. *Desalination Water Treat*. **2016**, *57* (6), 2590-2596.

19. Salihu A, Abbas O, Sallau AB and Alam Z. Agricultural residues for cellulolytic enzyme production by *Aspergillus niger*: effect of pretreatment. *3 Biotech* **2015**, *5*, 1101-1106.

20. El-Shishtawy RM, Mohamed SA, Asiri AM, Gomaa AM, Ibrahim IH and Al-Talhi HA. Saccharification and hydrolytic enzyme production of alkali pretreated wheat bran by *Trichoderma virens* under solid state fermentation. *BMC Biotechnol*. **2015**, *15*, 37-50.

Original scientific paper

21. Adedeji OE and Ezekiel OO. Pretreatment of selected peels for polygalacturonase production by *Aspergillus awamori* CICC 2040: Purification and application in mango juice extraction. *Bioresour. Technol. Rep.* **2019**, *7*, 100306.

22. Silva J, de Franc PRL, Converti A and Porto T.S. Kinetic and thermodynamic characterization of a novel *Aspergillusaculeatus* URM4953 polygalacturonase. Comparison of free and calcium alginate-immobilized enzyme, *Process Biochem*. **2019**, https://doi.org/10.1016/j.procbio.2018.07.010.

23. de Oliveira RL, Silva MF, Converti A and Porto TS. Biochemical characterization and kinetic/thermodynamic study of *Aspergillus tamarii* URM4634 β-fructofuranosidase with transfructosylating activity. *Biotechnol. Prog.* **2018**, https://doi.org/10.1002/btpr.2879.

24. Abdel Wahab WA, Karam EA, Hassan ME, Kansoh AL, Esawya MA and Awad GEA. Optimization of pectinase immobilization on grafted alginate-agar gel beads by 24 full factorial CCD and thermodynamic profiling for evaluating of operational covalent immobilization. *Int. J. Biol. Macromol.* **2018**, *113*, 159–170.

25. Dogan N and Tari C. Characterization of three-phase partitioned exopolygalacturonase from *Aspergillus sojae* with unique properties. *Biochem Eng*. J. **2008**, *39*, 43-50.

26. Silva J, de França PRL,Converti A and Souza Porto T. Pectin hydrolysis in cashew apple juice by *Aspergillus aculeatus* URM4953 polygalacturonase covalently-immobilized on calcium alginate beads: A kinetic and thermodynamic study. *Int J Biol Macromol,* **2018**, https://doi.org/10.1016/j.ijbiomac.2018.12.236

27. Peng H, Chen H, Qu Y, Li H and Xu J. Bioconversion of different sizes of microcrystalline cellulose pretreated by microwave irradiation with/without NaOH. *Appl. Energy* **2014**, *117*, 142-148.

28. Melikoglu M, Lin CSK and Webb C. Kinetic studies on the multi-enzyme solution produced via solid state fermentation of waste bread by *Aspergillus awamori. Biochem. Eng. J.* **2013**, *80*, 76– 82.

29. Kant S, Vohra A and Gupta R. Purification and physicochemical properties of polygalacturonase from *Aspergillus niger* MTCC 3323. *Protein Expr. Purif.* **2013**, *87* (1), 11-16.

30. Ortiz GE, Noseda DG, PonceMora MC, Recupero MN, Blasco M and Albertó E. A comparative study of new *Aspergillus* strains for proteolytic enzymes production by solid state fermentation. *Enzym. Res.* **2016**, doi: http://dx.doi.org/10.1155/2016/3016149

31. Norouzian D, Akbarzadeh A Scharer JM and Young MM. Fungal glucoamylases. *Biotechnol. Adv.* **2006**, *24*, 80−85.

32. Han W, Lam WC, Melikoglu M, Wong MT, Leung HT, Ng CL, Yan P, Yeung SY and Lin CSK. Kinetic analysis of a crude enzyme extract produced via solid State fermentation of bakery waste. *Sustain Chem. Eng.* **2015**, *3*, 2043−2048.

33. Deylami MZ, Rahman RA, Tan CP, Bakar J and Lasekan O. Thermodynamics and kinetics of thermal inactivation of peroxidase from mangosteen (*Garcinia mangostana*) pericarp. *J. Eng. Sci. Technol.* **2014**, *9* (3), 374-383.

34. Lam WC, Pleissner D and Lin SKC. Production of fungal glucoamylase for glucose production from food waste. *Biomol* **2013**, *3*, 651−661.

35. Riaz M, Perveen R Javed MR, Nadeem H and Rashid MH. Kinetic and thermodynamic properties of novel glucoamylase from *Humicola* spp. *Enzym. Microbiol. Technol.* **2007**, *41*, 558–564.

EVALUATION OF SOME BIOLOGICAL ACTIVITIES OF PHENOLIC COMPOUNDS OBTAINED FROM TWO ALGERIAN MEDICINAL PLANTS: *Mentha rotundifolia* AND *Satureja calamintha*

Benfares Redhouane[1]*, Boudjema Khaled[2,3], Behlali Hadjira[2], Imedjdouben Imene[2],
Kennas Abderrezak[4], Fazouane Fethia[2,3], Jaroslava Švarc-Gajić[5]

[1] *National Center for Research and Development of Fisheries and Aquaculture (CNRDPA) 11, Bd Amirouche, PO Box 67, Bou Ismaïl 42415 Tipaza, Algeria*
[2] *Research Laboratory in Food Technology, University of M'Hamed, Bougara, Boumerdes, 35000, Boumerdes, Algeria*
[3] *Laboratory of Applied Biochemistry, Department of Biology, University of M'Hamed, Bougara, Boumerdes, 35000, Boumerdes, Algeria*
[4] *Laboratory of Soft Technology, Valorization, Physical-chemistry of Biological Materials and Biodiversity, Faculty of Sciences, University M'hamed Bougara of Boumerdes, 35000, Boumerdes, Algeria*
[5] *Faculty of Technology, University of Novi Sad, Bulevar cara Lazara 1, 21 000 Novi Sad, Serbia*

In this work phytochemical characterization of two medicinal plants from Lamiaceae family, Mentha rotundifolia and Satureja calamintha, has been carried out. Extracts obtained with different solvents were screened for different plant secondary metabolites and were biologically characterized by defining their antiradical and antibacterial activities. Phytochemical screening of M. rotundifolia and S. calamintha confirmed their richness in different secondary metabolites. The determination of phenolic compounds revealed high polyphenols contents in water: methanol (30:70) extracts with concentrations of 20.64±1.74 mg EAG/g DW and 13.45±0.91 mg EAG/g DW for M. rotundifolia and S. calamintha, respectively. These extracts were also characterized by high concentrations of flavonoids (Mentha rotundifolia 12.33±1.58 mg EQ/g DW, Satureja calamintha 7.11±0.02 mg EQ/g DW). Furthermore, the water:methanol (30:70) extract of M. rotundifolia was the most effective in inhibiting free radicals. Recorded inhibition diameters for both plant samples and tested microbial strains ranged from 6.66 mm to 13.66 mm. Presented results confirmed that tested indigenous Algerian plants are favorable sources of polyphenols with antioxidant and antimicrobial properties.

Keywords: *Mentha retundifolia*, *Satureja calamintha*, phytochemical screening, extraction, phenolic compounds, antioxidant activity, antibacterial activity.

INTRODUCTION

Medicinal plants have been used since ancient times in folk medicine to prevent or treat different diseases. In fact, their therapeutic properties are due to the presence of hundreds or even thousands of natural bioactive compounds, most often plant secondary metabolites (1). Algeria has an important plant heritage characterised by its richness and diversity. In coastal areas, mountain ranges, high plateaus, steppes and Saharian oases,

---

* Corresponding author: Benfares Redhouane, National Center for Research and Development of Fisheries and Aquaculture (CNRDPA) 11, Bd Amirouche, PO Box 67, Bou Ismaïl 42415 Tipaza, Algeria, e-mail: benfaresredhouane@yahoo.fr

more than 3000 plant species have been identified. Among these natural resources, aromatic and medicinal plants, such as *Mentha rotundifolia and Satureja calamentha,* occupy large space (2).

Mentha rotundifolia or mint, has a special place in herbal medicine owing to its tonic, aromatic and digestive properties used to relieve colic, nausea, diarrhea and Crohn's disease (3). Bioactive compounds from mint demonstrate also hypotensive and vasodilating activities, as well as effects on sympathetic nerve centers (relaxing, stimulating, depressing). It`s antibacterial, antifungal and antimalarial properties, have also been reported (4).

The genus *Satureja,* belonging to the Lamiaceae family, comprises about 30 species distributed in Tropical Africa, Europe and North America (5). *Satureja calamintha* subsp. *nepeta* (L.) Briq enjoys great popularity in Algeria as a traditional cure for coughs, impaired digestion and mild respiratory infections. In addition to acting as expectorant, stomachic and tonic, the plant has antiseptic, antispasmodic and carminative properties (6). Satureja species are also used as potent disinfectants and odoriferous agents in perfumes (7).

In this work, two plants used in traditional Algerian medicine, namely *Mentha rotundifolia* and *Satureja calamintha* were studied. Their secondary metabolites were extracted using different solvents (methanol, water:methanol (30:70) and water). Total polyphenols, flavonoids and tannins were quantified and their contents were related to antioxidant and antibacterial activities of the extracts. Antioxidant properties of extracts were characterised by DPPH and ABTS radical scavenging tests. Antibacterial activity was screened for different bacterial strains. The extracts were also subjected to phytochemical screening to reveal major plant constituents responsible for the reported activities.

EXPERIMENTAL

Samples

In this work aerial parts of *S. calanintha* and *M. rotundifolia* were studied. *M. rotundifolia* was harvested in Jijel and Bejaia regions (North East of Algeria) during the period from February to April 2018, while *S. calamintha* was harvested in the Jijel area during the same period. The stems and leaves of the samples were air dried at room temperature during 15 days and were powdered and stored at 4 °C for further analysis.

Chemicals and reagents

Gallic acid, butylhydroxytoluene (BHT), Folin-Ciocalteu, quercetin, 2,2-diphenyl-1-picrylhydrazyl (DPPH) were purchased from Sigma-Aldrich (USA). Methanol, acetic and hydrochloric acids, ammonia, ferric trichloride, dimethyl sulfoxide (DMSO) were obtainned from Merck (Germany), Rectapur, Cheminova (France) and Fluka. Mueller-Hinton agar and broth were obtained from Pasteur Institute (Algeria).

Original scientific paper

Phytochemical screening

Phytochemical screening was performed to detect different chemical classes in decoctions and infusions of the samples, using the method as described by Bruneton (8). In general, the method relies on specific chemical reaction between specific chemical class and reagents.

Polyphenols

Free flavonoids

A few drops of concentrated HCl and a few milligrams of magnesium were added to 1 ml of the infusion. The reaction gives an orange-red coloration in the presence of flavonoids.

Anthocyanins

The identification of anthocyanins was done by adding 10 drops of ammonia to 5 ml of the plant infusionl. The reaction gives a greenish-blue coloration.

Leuco-anthocyanins

Powdered plant material (2 g) was introduced into 20 ml of a propanol/chloric acid (v/v) mixture. The solution thus obtained was then placed in a water bath (100°C) for a few minutes. In the presence of leucoanthocyanins a red coloration develops.

Tannins

Total tannins

A few drops of ferric chloride solution (5%) were added to 5 ml of the infusion. The positive reaction gives a black or greenish blue coloration in the presence of tannins.

Gallic tannins

Sample infusion (5 ml) was introduced into a vial using a graduated pipette and then supplemented with 2 g of sodium acetate and few drops of ferric chloride solution (1%). After stirring, a dark blue coloration appears in the presence of gallic tannins.

Condensed tannins

Five milliliters of the sample infusion were added to 2 g of ammonium acetate and three drops of ferric chloride solution (1%) after what the mixture was shaken. The appearance of a blue-black coloration indicated the presence of catechetical tannins.

Free quinones

Powder plant material (2 g) was moistened with 2 ml of hydrochloric acid (1 M) which was in contact with 20 ml of chloroform during three hours. The mixture was filtered and then stirred with 5 ml of ammonia.The appearance of red coloration indicated the presence of free quinones.

Reducing sugars (Fehling's test)

Twenty drops of the Fehling reagent were added to 1 ml of infusion and 2 ml of distilled water. A positive reaction was characterized by the appearance of a brick red precipitate.

Cardiac glycosides

Two milliliters of the infusion were mixed with 2 ml of chloroform and concentrated sulfuric acid was carefully added. The formation of a dark reddish brown layer at the interface indicated the presence of cardiac glycosides.

Alkaloids

A mixture of 5 ml of infusion, 2 ml of HCl and 1 ml of Dragendroff reagent gives a red or orange precipitate in the presence of alkaloids.

Coumarins

The presence of coumarin was revealed after mixing 5 ml of the infusion and 0.5 ml of ammonia (25%). An observation of the fluorescence under an ultra violet lamp at 365 nm indicated the presence of coumarin.

Saponosides

Hydrochloric acid (5 ml, 0.1 M) and 5 ml of NaOH (0.1 M) were introduced separately into two test tubes. The tubes were shaken after addition of few drops of the infusion. Foam formation indicated the presence of saponosides.

Heteroglycosides

O-heterosides

Distilled water (5 ml) and 0.5 ml of HCl were mixed with powdered plant material previously put in contact with $CHCl_3$. Then, the mixture was heated for 15 minutes. After cooling and filtration, 2.5 ml of $CHCl_3$ were added and the organic phase thus formed was separated. The appearance of a brown color after addition of 0.5 ml of diluted ammonia indicated the presence of O-heterosides.

C-heterosides

Distilled water (10 ml) and 1 ml of ferric chloride solution (10%) were added to the aqueous phase previously obtained for O-heterosides. The mixture was heated for 30 minutes in a water bath and then cooled. The organic phase was separated after mixing with 5 ml of diluted NH_4OH (50%). The appearance of, more or less intense red coloration, indicated the presence of C-heterosides.

Sterols and triterpenes

Five milliliters of the infusion were added to 5 ml of acetate anhydride. After that 1 ml of H_2SO_4 was added to the bottom of the tube without stirring. The formation of a brownish red ring at the contact area of the two liquids and a purple coloration of the supernatant layer indicated the presence of sterols and triterpenes.

Extraction of phenolic compounds

Twenty grams of powdered stems and leaves of the samples were macerated separately with 250 ml of different solvents (pure methanol, water-methanol (30/70) and water) for 24 h. The obtained extracts were filtered through Wattman paper and solvents were evaporated under reduced pressure at 40° C using rotary vacuum evaporator (RV 8 IKA, Belgium). After evaporation, the residues were dissolved in small volume of the adequate solvent and kept in sterile vials at 4°C until use.

Determination of total polyphenols

Sample (100 µl) was dissolved in 500 µl of Folin-Ciocalteu reagent (diluted 1/10) and 1 ml of distilled water was added. The solution was mixed and incubated at room temperature for 1 min. After that 1500 µl of 20% sodium carbonate solution was added. The mixture was shaken and incubated for 2 hours in the dark at room temperature. The absorbance of the samples was measured at 760 nm using spectrophotometer (Varian 50 Tablet, USA) and the results were expressed in milligrams of gallic acid equivalent (GAE) per gram of dry plant matter. A calibration curve was defined using gallic acid as a standard (9).

Determination of flavonoids

Total flavonoids were determined by mixing 500 µl of the extract with 2 ml of distilled water and 0.15 ml of sodium nitrite solution (15% w/v). After 6 minutes at room temperature, 0.15 ml of aluminum chloride solution (10% w/v) was added. After 6 minutes of incubation at room temperature, 2 ml of sodium hydroxide solution (4 % w/v) were added to the mixture adjusting the volume to 5 ml with distilled water. The mixture was agitated and incubated for 15 min and the absorbance was measured at 510 nm (10). The results were expressed in milligrams of quercetin equivalent (EQ) per gram of dry plant matter.

Determination of condensed tannins

Condensed tannins were determined using the vanillin method in an acidic medium. A crude extract (50 µl) was added to 1500 µl of the vanillin/methanol solution (4%, m/v) and then mixed using a vortex. Then, 750 µl of the concentrated hydrochloric acid were added and allowed to react at room temperature for 20 minutes. Absorbance at 550 nm was measured against a blank (11). The concentration of tannins was expressed in milligram of catechin equivalents per gram (g) of dry matter (mg EC/g MS) from the calibration curve defined by catechin.

Biological activity

Antioxidant activity

DPPH assay

The antioxidant activity of the extracts was defined *in vitro* by DPPH radical scavenging and ABTS assays. The results were compared against a positive control containing butylated hydroxytoluene (BHT). The DPPH (1,1-diphenyl-2-picrylhydrazyl ($C_{18}H_{12}N_5O_6$) is a stable free radical, which gives a dark violet color in solution. When it is reduced, the color becomes pale yellow. The DPPH assay was performed following method as described by Sanchez-moreno et *al.* (12). Different concentrations of the extracts (500 µL) were added to 375 µl of absolute methanol and 125 µl of DPPH methanolic solution (60 mM) used as a free radical source. The obtained mixture was covered with parafilm and incubated in dark for one hour. The absorbance was measured at 517 nm using a spectrophotometer (T70 UV–visible) and compared to BHT calibration curve. DPPH solution was used as a blank. The antioxidant activity was expressed as percentage of inhibition of DPPH free radicals (A%) and calculated using the following formula:

$$A\% = [(A_0 - A_s)/A_0]\ 100$$

where A_0 is the absorbance of the blank and A the absorbance of the sample.

Moreover, the concentration for 50% inhibition (IC_{50}) was calculated by linear regression equation of the corresponding scavenging effect vs. concentration dependence.

ABTS assay

The 2,2′-azino-bis (3-ethylbenzothiazoline-6-sulfonic acid) (ABTS•+) radical scavenging activity was measured according to the method of Re et *al* (13) with small modifications. First, ABTS and potassium persulfate were dissolved in distilled water to obtain final concentrations of 7 mM and 2.45 mM, respectively. The obtained solutions were allowed to stand in the dark at room temperature (25 °C) for 12 to 16 h before use in order to generate ABTS radical. Finally, The ABTS•+ solution was diluted with ethanol, to adjust the absorbance to 0.70±0.02 at 734 nm. Trolox (2.5 mM) solution was prepared in methanol for use as a stock standard.
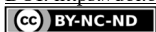
The scavenging ability of the sample was expressed on percentage using the following equation:

$$I_{ABTS} \% = [(A_{blank} - A_{sample})/A_{blank}] \times 100$$

where:

A $_{blank}$ is the absorbance of the blank containing only ABTS$^{\bullet+}$ solution,

A $_{sample}$ is the absorbance of the ABTS$^{\bullet+}$ solution after the addition of the sample.

Antibacterial activity

The antibacterial activity of the extracts was determined by the disc-diffusion method that used impregnated discs. Nutrient agar medium was prepared by pouring 15 ml of Muller Hinton agar into Petri dishes. After cooling and solidification, 100 µl of bacterial suspension was spread on the surface of agar medium using a Pasteur pipet. Then, with sterile forceps, filter paper discs 6 mm in diameter impregnated with 15 µl of the tested extract were placed on the agar (14, 15). Each assay was done in three replicates. The Petri dishes were closed with parafilm and stored at 4°C for 2 hours, after what they were turned and incubated at 37°C for 18-24 hours. Chloramphenicol antibiotic (1 mg/ml) was used as a standard. The antibiotic disc was deposited on the surface of the agar medium, previously seeded with a culture of the studied strain. The sensitivity of bacteria to antibiotic was assessed according to the same protocol as with paper discs impregnated with the extract.

Statistical analysis

All experiments were performed in triplicates and the results were presented as mean ± standard deviation. Analysis of variance was conducted using ANOVA with two factors in the software STATISTICA 5.5 and differences were considered to be significant at probability less than 0.05 ($P < 0.05$).

RESULT AND DISCUSSION

Phytochemical screening

Phytochemical screening was conducted to detect different chemical classes in infusions and decoctions of *M. rotundifolia* and *S. calamintha*. The results are presented in Table 1.
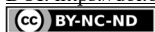
Table 1. Identified chemical classes in *M. rotundifolia* and *S. calamintha* extracts

Metabolites	Sample		
	M. rotundifolia (Jijel)	*M. rotundifolia* (Bejaia)	*S. calamintha*
Flavonoids	+++	+++	++
Anthocyanes	+++	+++	+
Leucoanthocyanes	-	-	-
Total tanins	+++	+++	+++
Glycosides anthraquinones	-	-	-
Cardiac glycosides	-	-	-
Quinones	-	-	-
Reducing sugars	++	+++	+++
Alcaloids	++	+++	+++
Coumarins	+++	++	+
Saponines	+++	+++	+++
O-heterosides	+++	++	+++
C-heterosides	+++	++	+
Sterols and triterpenes	++	+++	++

(-): Absence, (+): Presence in low concentrations, (++): Presence in average concentrations, (+++): Presence in high concentrations.

In both studied plants same classes of compounds were identified. Six classes of compounds were indentified in the extracts of *M. rotundifolia* in high concentrations, more specifically flavonoids, anthocyanins, total tannins, gallic tannins, reducing compounds and saponins. The concentrations of reducing sugars, alkaloids, coumarins, O-heterosides, C-heterosides, sterols and triterpenes showed moderate concentration variation in *M. rotundifolia* species depending on the geographical region.

Leucoanthocyanins, anthraquinone, cardiac glycosides and quinines were not detected in either of the studied plan extracts. Presented results were in agreement with the results obtained by Seladji (16) who reported numerous secondary metabolites in *M. rotundofilia.* In addition, here obtained results concerning both gallic and catechetical tannins were also in concordance with those found by Bounihi (17). Concerning the *S. calamintha*, the results of phytochemical screening revealed also the presence of numerous secondary metabolites. The plant showed to be high in total and gallic tannins, reducing compounds, alkaloids, saponins and heterosides. Reported results were in agreement with numerous other studies that dealt with chemical characterisation of the plant (18, 19, 20).

Extraction yield

The extraction yields for three different solvents (pure methanol, methanol:water (70:30) and water) was compared (Figure 1).
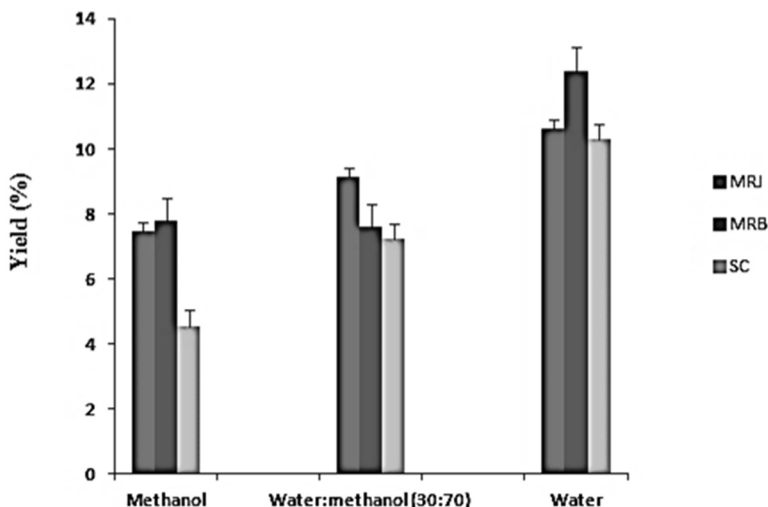
Figure 1. Extraction yield for three different solvents (%)
MRJ: *Mentha rotudifolia* harvested in the Jijel region; MRB: *Mentha rotundifolia* harvested in the Bejaia region, SC: *Satureja calamintha*.

The highest extraction yields for all studied samples was seen for the aqueous extracts, being in agreement with the results reported by Majhenic et *al* (21), Seladji (16) and Bougendoura (22). This can be explained by simple fact that water is a polar solvent, solvating wide range of molecules including significant amount of non-phenolic compounds such as carbohydrates and proteins, which in plants, are present in higher concentrations than secondary plan metabolites (23).

Total polyphenols content

Phenolic compounds are secondary plant metabolites synthesized by many plants. Numerous biological activities have been reported for these chemical classes (24). The total polyphenols were determined in all extracts and were expressed in milligrams of gallic acid equivalents per gram of dry matter (mg EAG/g DW). The results obtained are presented in Table 2.

Table 2. The content of total polyphenols in extracts

Sample	Total polyphenols (mg EAG/g DW)		
	Methanol	Water : methanol (30:70)	Water
MRJ	16.02±2.63	20.52±5.34	7.06±0.45
MRB	13.16±1.34	20.64±1.74	9.74±1.25
SC	9.31±1.18	13.45±0.91	12.83±1.83

The highest content of total poplyphenols was determined in water: methanol extract of *Mentha rotundifolia* collected from Béjaia region (20.64 mg EAG/g DW) whereas the water extracts of the three studied plants had the lowest total polyphenols content varying from 7.06 to 12.83 mg EAG/g DW. Less polar phenolic substances, mostly phenolic acids, were not quantitatively extracted with pure water leading to lower recoveries and explaining the lowest contents of total phenols when using pure water, in comparison to other two solvents (25). According to Lapornic et *al* (26), the use of water in combination with organic solvent contributes to the creation of a moderately polar medium which ensures the extraction of different classes of phenolic compounds.

The results on total polyphenols contents in methanolic extracts were in agreement with the results of Seladji (2015) who analysed methanolic extract of *Mentha rotun-difolia*. Contents determined in this work, however, were superior to those reported by Benabdallah et *al* (27) who analysed water:methanol (20:80) extracts of *Mentha rotundifolia* (15.10±0.60 mg EAG /g MS) collected in the East of Algeria. Here determined contents of total polyphenols in methanolic extracts of *Satureja calamentha* were ~3 fold greater of those reported by Bougendoura (22). It should be, however, taken into consideration that the content of plants metabolites is dependent on numerous factors, such as geographical region, climate, soil composition, stress etc.

Flavonoids content

Determined flavonoid contents for all analysed extracts are presented in Table 3.

Table 3. Flavonoids contents in extracts

Sample	Flavonoids content (mg EAG/g DW)		
	Methanol	**Water : methanol (30 :70)**	**Water**
MRJ	12.01±0.50	13.55±2.53	6.49±0.76
MRB	11.47±0.80	12.33±1.58	11.28±0.73
SC	6.88±1.04	7.11±0.02	5.61±0.82

Similarly as for total phenols contents, the highest flavonoids contents were obtained in water:methanol extracts, but didn`t differ substantially from the contents seen in methanolic extracts. For three tested solvents the contents of flavonoids ranged from 5.61 to 13.55 (mg EQ/g DW), with water extracts presenting the lowest concentrations. The contents of flavonoids in *M. rotundifolia* extracts determined in this work were substantially higher of those reported by Seladji (16) who reported flavonoids contents of 2.19±0.08 mg EC/g DW and 1.97±0.04 mg EC/g DW for methanolic and aqueous extracts, respectively.

Original scientific paper

The content of condensed tannins

The contents of condensed tannins in analysed samples are illustrated in table 4.

Table 4. The contents of condensed tannins

Plant	Condensed tannins content (mg EAG /g DW)		
	Methanol	**Water:methanol (30 :70)**	**Water**
MRJ	4.50±2,59	0.52±0.05	3.64±0.03
MRB	3.01±0.13	0.75±0.05	3.76±1.19
SC	3.00±0.85	0.57±0.14	4.45±0.20

On oppose to other phenols classes, the contents of condensed tannins were the lowest in water:methanol extracts, whereas methanolic and aqueous extracts presented comparable contents. In methanolic extracts the contents varied from 3 to 4.5 mg EAG /g DW, whereas in aqueous extracts the contents ranged 3.64-4.45 mg EAG /g DW. Here obtainned results were comparable with those reported by Seladji (22) who determined the concentration of tannins in *M. rotundifolia* between 0.6 and 1.2 mg EAG /g DW for aqueous extract, and between 1.1 and 1.5 EAG /g DW for methanolic extracts.
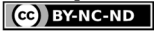
Biological activity

Antioxidant activity

Free radicals are known to be a major factor in biological damages. The DPPH radical scavenging and the ABTS assay are commonly used to evaluate the ability of plant extracts to scavenge free radicals. (13). The results of antioxidant activity of the extracts obtained are shown in table 5.

Table 5. DPPH scavenging activity of the extracts

Sample	Pure methanol			Water-methanol (30:70)			Water		
	MRJ	**MRB**	**SC**	**MRJ**	**MRB**	**SC**	**MRJ**	**MRB**	**SC**
Concentration (mg/ml)	0.56±0.20	0.97±0.15	0.93±0.01	0.90±0.23	0.94±0.13	1.14±0.07	ND	ND	ND
% of inhibition of DPPH	76.80	59.81	68.33	80.13	78.90	78.46	ND	ND	ND

ND: Not determined

Table 5 indicates that water-methanol and methanolic extracts had a good ability to scavenge DPPH radicals, while aqueous extracts were inactive, which was in collision with the previously determined contents of polyphenols in aqueous extracts. Namely, previous results confirmed the presence of total polyphenols, flavonoids and condensed tannins in the aqueous extracts of all three plant samples. The content of these natural antioxidants was lower in comparison to methanol extracts, however owing to well-known DPPH-scavenging activity of these chemical classes, it was reasonable to expect

Original scientific paper

radical-scavenging activity. Water-methanol and methanolic extracts of *M. rotundifolia* (Jijel) at concentrations of 0.90 mg/ml and 0.56 mg/ml inhibited around 80.13% and 76.80% of DPPH radicals, respectively. Water-methanol and methanolic extracts of the *S. calamintha* plant inhibited around 78.46% and 68.33% of DPPH radical, respectively, corresponding to concentrations of 1.14 and 0.93 mg/ml respectively. Furthermore, at a concentration of 0.9 mg/ml, the water-methanol and methanol extracts of *M. rotundifolia* (Bejaïa) presented the inhibition percentages of 78.93% and 59.81%. High antioxidant activity could be related to high polyphenols in the samples.

Since water:methanol extracts showed to be the most efficient in inhibiting DPPH radicals, their IC_{50} values were calculated and compared to standard antioxidants BHT (buthylhydroxytoluen). Calculated IC_{50} were low, reflecting significant antiradical activity (Table 6).

Table 6. Calculated IC_{50} values for water: methanol extracts

Extract	IC_{50} (mg/ml)	IC_{50} (mM Eq Trolox/g DW)
MRJ	1.41	17.91
MRB	1.27	18.85
SC	1.51	31.06
BHT	0.53	-
Trolox	-	1.27

Calculated IC_{50} values for *M rotundifolia* (Jijel and Bejaia) and *S calamintha* were 1.41, 1.27 and 1.51 mg/ml, respectively, being around 2.4-2.8 higher in comparison to the standard. Benabdallah et al (27) reported better DPPH scavenging activity for *M. rotundifolia* and the same solvent, whereas for *S. calamintha.* the authors found lesser activity.

Examined extracts demonstrated weaker inhibition effect for ABTS radicals in comparison to DPPH radicals, which could be attributed to different redox potentials, reaction stoichiometry or/and steric effects of the two radicals (28). Calculated IC_{50} values for *M. rotundifolia* from the two regions Jijel and Bejaia) were very close corresponding to 17.91 and 18.85 mM Eq Trolox/g DW, respectively and much lower in comparison to. *S. calamintha* (31.06 mM Eq Trolox/g DW). Here presented results were in concordance with those cited by Nickavar et *al.* (28) who calculated IC_{50} (DPPH$^\bullet$) = 21.71 µg/ml and IC_{50}(ABTS$^{\bullet+}$) = 158.90 µg/ml for *M. rotundifolia* collected in Teheran, Iran.

The Fig 2 represents the spider diagram which is used to better visualize the relationship between total polyphenols, flavonoids, tannin and antioxydant activity of the most active water : methanol extracts. Water : methanol extract of *Mentha rotundufolia* from Bejaia had the highest content of total polyphenols and demonstrated the most pronounced antioxidant activity, followed by *Mentha rotundufolia* from Jijel.
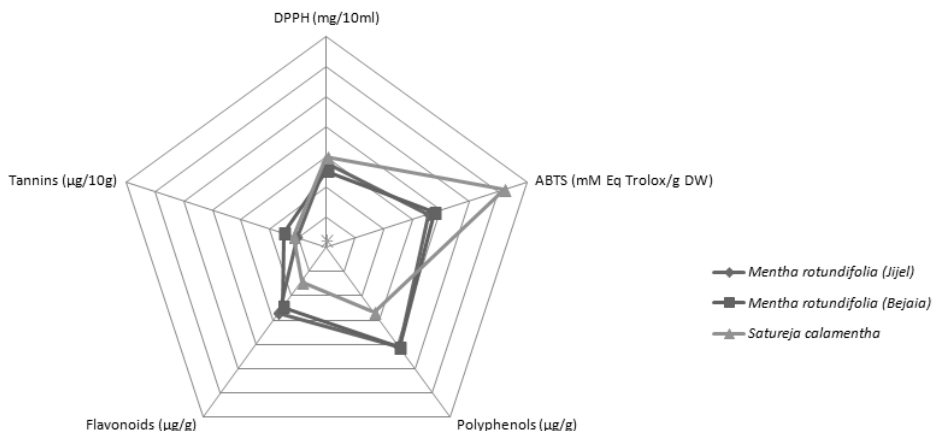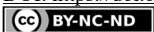
Figure 2. Antioxidant activities and total polyphenols content of the tested plants

Antibacterial activity

The antimicrobial activity of water-methanol extracts of the studied plants was performed using the disk diffusion method (Table 7).

Table 7. Antibacterial activity of water-methanol extracts

Bacteria strains	Inhibition zone (mm)			
	MRJ	**MRB**	**SC**	**Chloramphénicol**
Enterococcus faecalis	10.66±0.94	10.33±0,94	7.00±0.81**	10±00
Staphylococcus aureus	8.66±1.88*	10.33±2.49	11.33±2.86	14±00
SARM	10.33±0.47*	13.66±0.94	11.66±0.94	18.33±0.5
Escherichia coli	7.33±0.94	10.66±0.94***	8.66±0.47***	30±00
Pseudomonas aeruginosa	8.66±1.24	10.66±0.47***	7.00±0.47***	22.50±0.50
Micrococcus luteus	7.66±0.47*	9.33±0.47*	6.66±0.94*	17.50±2.50

It could be noted that antibacterial activity of *M. rotundifolia* was close to standard antibiotic chloramphenicol for *Enterococcus faecalis*, *Micrococcus luteus*, *Pseudomonas aeruginosa*, *Escherichia coli* and *SARM*. The inhibition zone of the extracts of both plants was inferior in comparison to chloramphenicol.

The inhibitory effect of the *M. rotundifolia* (Bejaïa) extract against six bacterial strains could be described by inhibition zone ranging from 9.33 to 13.66 mm. This extract demonstrated statistically significant results against *Escherichia coli*, *Pseudomonas aeruginosa* and *Micrococcus luteus*. The extract of the same plant *M. rotundifolia* but col-

Original scientific paper

lected from different region (Jijel) had lower antibacterial activity against all tested strains. Inhibition zones for this extract ranged from 7.33 to 10.66 mm. These results were statistically significant for *Staphylococcus aureus*, *SARM* and *Micrococcus luteus*. Statistically significant results for methanolic extract (70%) of *S. calamintha* were noted for *Escherichia coli*, *Pseudomonas aeruginosa* and *Micrococcus luteus*. Similar results were reported by Seladji (16) who studied antibacterial activity of the methanolic extract of the *M. rotundifolia* harvested in West of Algeria against three common strains (*Escherichia coli*, *Staphylococcus aureus* and *Pseudomonas aeruginosa*). Labiod, (19) reported the absence of antibacterial activity against *Escherichia coli, Staphylococcus aureus and Enterococcus faecalis* for the methanolic extract of *S. calamintha* harvested growing in East of Algeria. On the other hand, a very effective inhibitory effect on bacterial growth of this plant extract was reported by Benkhedimallah and Kismoun (18) who determined inhibition diameters ranging from 15.75 to 25.50 mm.

CONCLUSION

The results of the phytochemical screening of *M. rotundifolia* and *S. calamintha* revealed the presence of different secondary metabolites, namely flavonoids, tannins, reducing compounds, alkaloids and saponins. The determination of phenolic compounds revealed high polyphenols contents in water : methanol (30:70) extracts with the concentrations range of 20.64±1.74 mg EAG/g DW and 13.45±0.91 mg EAG/g DW for *M. rotundifolia* and *S. calamintha,* respectively. The extracts were also characterized by high concentrations of flavonoids, more specifically for the two plants the contents were 13.55±2.53 mg EQ/g DW and 7.11±0.02 mg EQ/g DW, respectivelly. The evaluation of antioxidant activity by the DPPH test showed that the water : methanol (30:70) extract of *M. rotundifolia* was the most effective in inhibiting radicals. Furthermore, the study of antibacterial activity revealed that the water : methanol (30:70) extracts obtained from the three plants had significant inhibitory activity against different pathogenic strains of bacteria, in some cases superior to standard antibiotic chloramphenicol. These findings suggest that these extracts could be used as potential natural antimicrobial agents.

Acknowledgements

REFERENCES

1. Boudjouref, M. Study of antioxidant and antimicrobial activities of extracts obtained from *Artemisia campestris* L. Thesis of magister, University of Setif, Alegria, 2011.
2. Duraffourd, C.; Lapraz, J.C.; Chemli, R. La plante médicinale de la tradition à la science. 1er congrès Intercontinental. Tunis. Ed.Granche. Paris,1997.
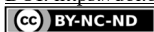
3. Laghouiter, O.K.; Gherbi, A.; Laghoutter, H.Etude de l'activité antioxydante des huiles essentielles de certaines cultivées dans la région Ghardaia. *Rev. ElWahat pour les recherches et les études.* **2015**, *8*(1),84-93.

4. Tripathi, P.; Dubey, N.K.; Banerji, R.; Chansouria, J.P.N. Evaluation of some essential oils as botanical fungitoxicants in management of post-harvest rotting of citrus fruits. *World J. Microb. Biot.* **2004**, *20*, 317-321.

5. Bensouici, C.; Benmerache, A.; Chibani, S.; Kabouche, A.; Abuhamdah, S.; Semra, Z.; Kabouche, Z. Antibacterial activity and chemical composition of the essential oil of *Satureja calamintha ssp. sylvatica* from Jijel, Algeria. *Pharm. Lett.* **2013**, *5*(2), 224-227.

6. Baba Aissa, F. Encyclopedie des plantes utiles. Flore d'Algérie et du Maghreb, substances végétales d'Afrique d'Orient et d'Occident. Ed Librairie moderne-Rouiba, 2000.

7. Chiej, R. Macdonald encyclopedia of medicinal plants. Ed Macdonald. London.1984.

8. Bruneton, J. Pharmacognosie, Phytochimie plantes médicinales. 3ème édition, Tec & Doc, Paris, 1999.

9. Lister, E.; Wilson, P. Measurement of total phenolics and ABTS assay for antioxidant activity (personal communication). Crop Research Institute, Lincoln, New Zealand, 2001.

10. Tefiani, I. Contribution to the phytochemical study and the antioxidant effect of green algae extracts: Ulva linza. M.S thesis, University of Tlemcen, Algeria, 2015.

11. Julkunen-Titto, R. Phenolic constituents in the leaves of northem wiliows methods for the analysis of certain phenolics. *J. Agric. Food Chem.* **1985**, *33*, 213-217.

12. Sanchez-Moreno, C.; Larrauri, J.A.; Saura-Calixto, F.A procedure to measure the antiradical efficiency of polyphenols. *J. Sci. Food Agric.* **1998**, *8*(2), 270-276.

13. Re, R.; Pellegrini, N.; Proteggente, A.; Pannala, A.; Yang, M.; Rice-Evans, C. Antioxidant activity applying an improved ABTS radical cation decolorization assay. *Free Radic. Biol. Med.* **1999**, *26*, 1231-1237.

14. Joffin, J.N.; Leryral, G. Microbiologie. Dictionnaire des Techniques, 3éme ED., Collection biologie Technique . CRDP d'aquitaine, Bordeaux, 2001.

15. Boudjema, K.; Mouhouche, A.; Guerdouba, A.; Hali, L, Composition, physicochemical analysis, antimicrobial and anti- inflammatory activities of essential oils obtained from *Ruta chalepensis. L* growing wild in north of Algeria, *J. Chem. Soc. Pakistan.* **2018**(a), *40*(6) ,1054-1062.

16. Seladji, M. Phytochemical study, antioxidant and antimicrobial activities of extracts from five medicinal plants and analysis of their essential oils. Ph.D. Thesis, University of Tlemcen, Algeria, 2014.

17. Bounihi, A. Phytochemical screening, toxicological study and pharmacological valorization of *Melissa officinalis* et *Mentha rotundifolia* (Lamiacées). Ph.D. Thesis, University of Mohammed V, Rabat, Morocco, 2016.

18. Benkhedimallah, R.; Kismoun, S. Phytochimical and biological of the plant *Satureja calamintha*, M.S. thesis, Université of Constantine, Algeria, 2014.

19. Labiod, R. Enhancement of essential oils and extracts of *Satureja calamintha nepeta*: antibacterial, antioxidant and fungicidal activities. Ph.D. Thesis, University of Annaba, Algeria, 2016.

20. Boudjema, K.; Bouanane, A.; Gamgani, S.; Djeziri, M.; Abou Mustapha, M.; Fazouane, F. Phytochemical profile and antimicrobial properties of volatile compounds of *Satureja calamintha* (L.) Scheel. from northern Algeria. *Trop. J. Pharm. Res.* **2018**(b), *17*(5), 857-864.

21. Majhenic, L.; Skerget, M.; Knez, Z. Antioxidant and antimicrobial activity of guarana seed extract. *Food Chem.* **2007**, *10*, 1258-1268.

22. Bougandoura, N. Antioxidant and antimicrobial powers of plant species extracts *Satureja calamintha sspnepta* (nabta) and *Ajugaiva* L. (chendgoura) from western Algeria, Thesis of Magister, University of Tlemcen, Algeria, 2014.

23. Bonnaillie, B.; Salacs, M.; Vassiliova, E.; Saykova, I. Etude de l'extraction de composés phé-noliques à partir de pellicules d'arachide, *Arachis hypogaea* L. *Revue de génie industriel*, **2012**, *7*, 35-45.

24. Ghasemzadeh, A; Ghasemzadeh, N. Flavonoids and phenolic acids: Role and biochemical activity in plants and human. *J. Med. Plant Res.* **2011**, *5*(31):6697-6703.

25. Cazes, J. Encyclopedia of chromatograph. Second Edition. Edition Taylor & Francis, 2005.

26. Lapornic, B.; Prosek, M.; Wondra, A.G. Comparison of extracts prepared from plant by-products using different solvents and extraction time. *J. Food Eng.* **2005**, *71*, 214-222.

27. Benabdallah, A.; Rahmoune, C.; Boumendjel, M.; Aissi, O.; Messaoud, C**.** Total phenolic content and antioxidant activity of six wild Mentha species (Lamiaceae) from northeast of Algeria. *Asian Pac. J. Trop. Biomed.* **2016**, *6*(9), 760-766.

28. Nickavar, B.; Alinaghi, A.; Kamalinejad, M. Evaluation of the antioxidant properties of five Mentha species. *Iran. J. Pharm. Res.* **2008**, *7*(3), 203-209.
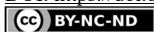
STUDY OF WHEAT STRAW DELIGNIFICATION IN A ROTARY-PULSATION APPARATUS

Larysa A. Sablii[1], Oleksandr M. Obodovych[2]*, Vitalii V. Sydorenko[2], Tamila,V. Sheyko[3]

[1] National Technical University of Ukraine "Igor Sikorsky Kyiv Polytechnic Institute", 37, Peremohy Ave., 03056 Kyiv, Ukraine
[2] Institute of Engineering Thermophysics of National Academy of Sciences of Ukraine, 2A Marii Kapnist Str., 03057 Kyiv, Ukraine
[3] Institute of Food Resources of NAAS, 4a , Sverstyuka str., 02002 Kyiv, Ukraine

This paper presents the results of studies of isolation lignin and hemicelluloses efficiency during the pre-treatment of wheat straw for hydrolysis in a rotary-pulsation apparatus. The pre-treatment of lignocellulosic raw materials for hydrolysis is a necessary step in the second-generation bioethanol production technology. The lignocellulose complex is destroyed during this process, and this allows hydrolytic enzymes access to the surface of cellulose fibers. The pre-treatment is the most energy-consuming stage in bioethanol production technology, since it usually occurs at high temperature and pressure for a significant time. One of the ways to improve the efficiency of this process is the use of energy-efficient equipment that allows intensifying heat and mass transfer. An example of such equipment is a rotary-pulsation apparatus, which are effective devices in stirring, homogenization, dispersion technologies, etc.

The treatment of wheat straw in a rotary-pulsation apparatus was carried out under atmospheric pressure without external heat supply at solid/water ratios of 1:10 and 1:5 in the presence of alkali. It was determined that the treatment of the water dispersion of straw at ratio of 1:10 due to the energy dissipation during 70 minutes leads to the release of 42 % of lignin and 25.76 % of easily hydrolyzed polysaccharides. Changing the solid / water ratio from 1:10 to 1:5 leads to an increase in the yield of lignin and easily hydrolyzed polysaccharides to 58 and 33.38 %, respectively.

Keywords: wheat straw, delignification, pretreatment, rotor-pulsating apparatus

INTRODUCTION

The production of bioethanol from lignocellulosic raw materials (second-generation bioethanol) has both a number of advantages and disadvantages in comparison with traditional raw materials containing starch. The main advantage is the availability and low cost of raw materials, which is usually agriculture and forestry wastes. The main disadvantage of this production is the high cost of bioethanol, because of the peculiarities of the technology for converting cellulose into fermentable sugars. The bioethanol production process can be divided into four stages.

The first stage is raw material grinding. Usually, this is a process of mechanical action on raw materials. Straw choppers, disintegrators, ball mills, etc. are used as equipment.

---
* Corresponding author: Oleksandr M. Obodovych, Institute of Engineering Thermophysics of National Academy of Sciences of Ukraine, 2A Marii Kapnist Str., 03057 Kyiv, Ukraine, e-mail: tdsittf@ukr.net

Original scientific paper

The final parameters of the first stage are the type of raw material and its particle size. Studies of many authors have confirmed the dependence of the release of reducing sugars isolation in the hydrolyzate on the degree of dispersion of raw material (1-3).

The second stage of the process is the hydrolysis, which consists of raw materials pre-treatment for hydrolysis and hydrolysis itself (acidic or enzymatic). The pre-treatment is a necessary step, especially for enzymatic hydrolysis, since the presence of lignin and hemicelluloses in the raw material prevents the access of hydrolytic enzymes to the surface of cellulose fibers. The stage of hydrolysis refers to physicochemical processes since it is carried out at high temperatures and pressures (hydrolysis with dilute acids).

The result of the second stage is a hydrolysate with the required concentration of reducing sugars. The pre-treatment is the subject of extensive research because it is the most energy-consuming process in the production of bioethanol (4,5).

The alcoholic fermentation stage is the third stage of bioethanol production. This stage concerns biotechnology and is a type of fermentation in which carbohydrates, mainly glucose, are converted into ethanol molecules and carbon dioxide. This stage consists of the hydrolysate fermentation phase, which is carried out by yeast, and the alcohol distillation phase. The fermentation stage provides optimal temperature and additional nutrition conditions for obtaining yeast biomass. The final parameter of the third stage is 96% ethyl alcohol.

The fourth stage is the of ethanol dehydration to a concentration of 99.5% ethyl alcohol. Currently, the process is purely physical in nature and is based on the ability of zeolites to absorb water molecules from an azeotropic water-alcohol mixture due to the characteristics of the crystal lattice.

The hydrolysis production experience shows that the processing of organic biomass profitability can only be achieved by its deep complex treatment to obtain products, which cost exceeds the cost of the initial lignocellulosic raw material as fuel.

One of the stages of complex processing of lignocellulose is the process of isolation lignin and hemicelluloses from the lignocellulose complex to further obtaining valuable chemical products or fuel from it. This stage is an integral part of the preliminary preparation of raw materials for hydrolysis.

The alkaline method is considered as one of the most promising pre-treatment methods among the many methods that are used to prepare lignocellulosic raw materials for hydrolysis, because of the high efficiency of delignification and high final total sugar yield (6).

The improvement of alkali-based pre-treatment technology has been the subject of many scientific studies in recent years. The authors of the patent (7) proposed a method for producing cellulose by lignin isolation. The method provides, in particular, pulping cellulose-containing material in an alkaline solution in combination with thermo-mechanical-chemical activation of cellulose-containing materials using rollers, knife crushers, hummer crushers, disk mills and their combinations. Pulping of one-year-old plant materials was carried out in an alkali solution with a concentration of 0.7 wt% of straw/water ratio 1:15 with the addition of hydrogen peroxide 0.25 wt% and SAS with a concentration of 0.1 wt%. The temperature of the pulping solution was 100 °C and the pulping time was 35 minutes. The highest lignin yield 46.6% was obtained when processing alfalfa straw using a series connection of two hammer crushers.

The effect of sodium hydroxide concentration on the yield of lignin and hemicelluloses during the pre-treatment of wheat straw for hydrolysis by hydrolytic bacteria isolated from termites was determined in (8). The pre-treatment process took place at a temperature of 80 °C for 4 hours without additional stirring. At 1% concentration of sodium hydroxide and the ratio of solid/water, the yield of lignin was 23.23%, hemicelluloses - 18.6%. An increase in the concentration of sodium hydroxide to 10% led to an increase in the yield of lignin to 69.5% and hemicelluloses to 55.55%.

The temperature and time dependence of the wheat straw processing in the autoclave in a 2.5% sodium hydroxide solution was studied by Asghar U, Irfan M, Iram M, et al. (9). The results showed that the period of 90 minutes at a temperature of 121 °C strongly affects the substrate, reaching a maximum cellulose content of 83%, delignification of 81%, and hemicelluloses content of 10.5%.

The use of an extruder for the pre-treatment of wheat straw in an alkaline solution followed by extraction was studied in [10]. It was determined that the pre-treatment of wheat straw in a single-screw extruder at the temperature of 155 °C for 3 minutes and a sodium hydroxide concentration of 1% leads to the isolation of 6.1% of lignin. An increase in the concentration of sodium hydroxide to 6% leads to the release of 8.7% of lignin. Further extraction of wheat straw in 0.86% sodium hydroxide solution at the temperature of 80 °C for 180 min led to the release of 70% lignin.

One of the ways to increase the efficiency of the complex processing of lignocellulosic raw materials is the implementation of energy-efficient equipment that makes it possible to increase the degree of conversion of raw materials into main and by-products. An example of equipment that significantly intensifies heat and mass transfer in liquid multicomponent media are rotary-pulsation apparatus, which are effective devices for mixing, homogenization, dispersion and the like technologies.

The purpose of the work was to determine the efficiency of lignin and hemicelluloses extraction during the pre-treatment of wheat straw for hydrolysis in a rotary-pulsation apparatus (hereinafter RPA).

EXPERIMENTAL

The raw material for the research was wheat straw, pre-grinded in the disintegrator to an average particle size of 100 microns.

Rotary-pulsating apparatus

The study was carried out on setup, the main hydraulic diagram of which is shown in Fig. 1.
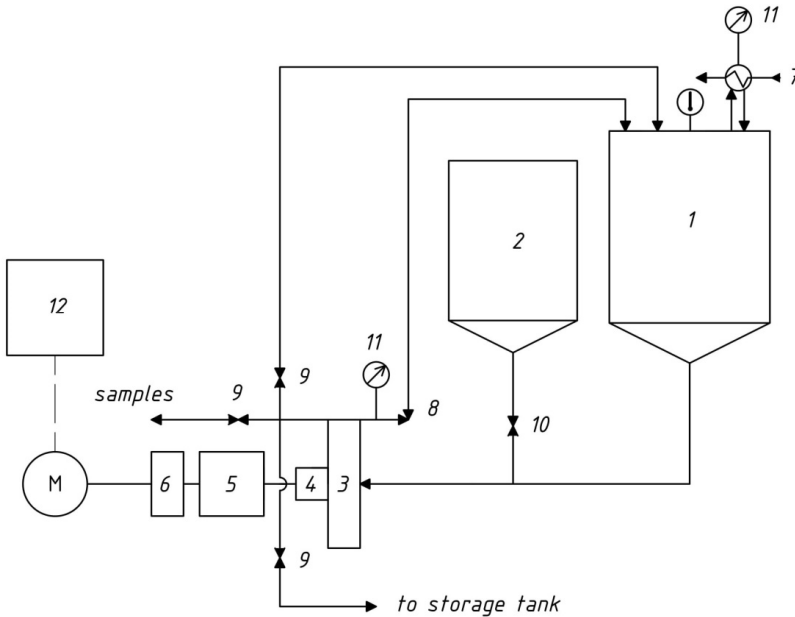
Figure 1. Schematic hydraulic diagram of the experimental setup
1-receiving tank; 2- raw materials tank; 3 – RPA; 4 - stuffing unit; 5 - bearing unit; 6- coupling; 7 - reflux
condenser; 8 - corner ball valve; 9 - ball valve ½ "; 10 - ball valve 1 "; 11 - pressure gauge; 12 - control unit.

Receiving tank 1 with a volume of 50 liters is designed for a mixture of raw materials
and an alkaline solution during processing. Tank 1 is connected to RPA through the inlet
pipe. Tank 2 for raw materials is used for loading wheat straw. The supply of raw
materials is controlled by a ball valve 10. The tank for raw materials is connected to the
RPA through the inlet pipe. RPA 3 is used for pre-treatment of a mixture of wheat straw
and alkaline solution. The RPA consists of housing, stator (inner radius 85.85 mm; outer
radius 97.85 mm, width 44.5 mm, 24 holes with a diameter of 14.3 mm) and rotor (inner
radius 67.5 mm; outer radius 85.25 mm, width 44 mm). The gap width between the stator
and the rotor is 0.6 mm. The outlet pipe of RPA is connected to the upper part of the tank
1 by two pipelines through the angle ball valve 8 and the ball valve 9. The pressure gauge
11 is connected to the outlet pipe of RPA.

The rotary motion from the motor shaft through the coupling 6 is transmitted to the
RPA shaft located on the console together with the bearing unit 5. The stuffing unit 4 is
designed to ensure the tightness of the RPA during operation. The reflux condenser 7 is
designed to prevent changes in the ratio of the components of the alkaline solution during
processing. Control unit 12 is a separate stationary unit for remote control of the setup.
The unit is equipped with an input automatic device, a frequency converter, an ammeter,
and an electricity meter. The minimum volume of fluid for treatment in the installation is
10 liters.

Determination of lignin content

The isolation of lignin was carried out the following way. The weighed experimental amount of straw was soaked in two liters of water. The rest of the water was mixed with sodium hydroxide, in the amount of 1 wt %. The resulting solution was filled in the receiving tank and RPA. The required rotor speed was set. The parameter of variation was the ratio of straw to water.

The temperature of the mixture was measured at regular intervals with different solid/water ratios after starting the engine at the frequency determined by the experimental conditions. The mixture treatment lasted about 70 minutes. The temperature of the mixture at the end of the treatment was 95 °C. The lignin content was determined by separating it from the filtrate followed by weighing.

Determination of the content of reducing substances

The concentration of reducing substances in the hydrolysate obtained after treatment was determined parameter. The amount of reducing substances was first defined in the untreated raw material. Then the residue remaining on the first filter was washed with water until neutral, dried to constant weight, and polysaccharides were determined. The difference was used to define the amount of reducing substances that were released during processing in RPA.

The concentration of reducing substances was determined by the DNSA method. DNSA method is a colorimetric technique that consists of a redox reaction between 3,5-Dinitrosalicylic acid and reducing sugars present in the sample. The reducing power of these sugars depends on their carbonyl group, which can be oxidized to the carboxyl group by mild oxidants, while DNS (yellow) is reduced to 3-Amino-5-nitrosalicylic acid (red-brown), which can be quantified by spectrophotometry at 540 nm, the wavelength of maximum absorption (11).

RESULTS AND DISCUSSION

The processes associated with chemical transformations usually require a high temperature maintaining in the reaction zone. An external supply of heat distributed throughout the reaction zone leads to significant energy costs. The localization of the sufficient energy supply to carry out the necessary chemical transformations into the reaction zone is the principle of the method of Discrete Pulse Energy Input (12).

It is known that the fluid flow is heated by passing through the working zone of the RPA (13), especially the flow of multicomponent mixtures. The temperature increase, due to the dissipation of the flow of mechanical energy, is one of the mechanisms that allow the delignification process to be carried out without external heat supply. The dynamics of temperature change in the installation with a rotation speed of 47.75 rps at different solid/water ratio over time is shown in Fig. 2.
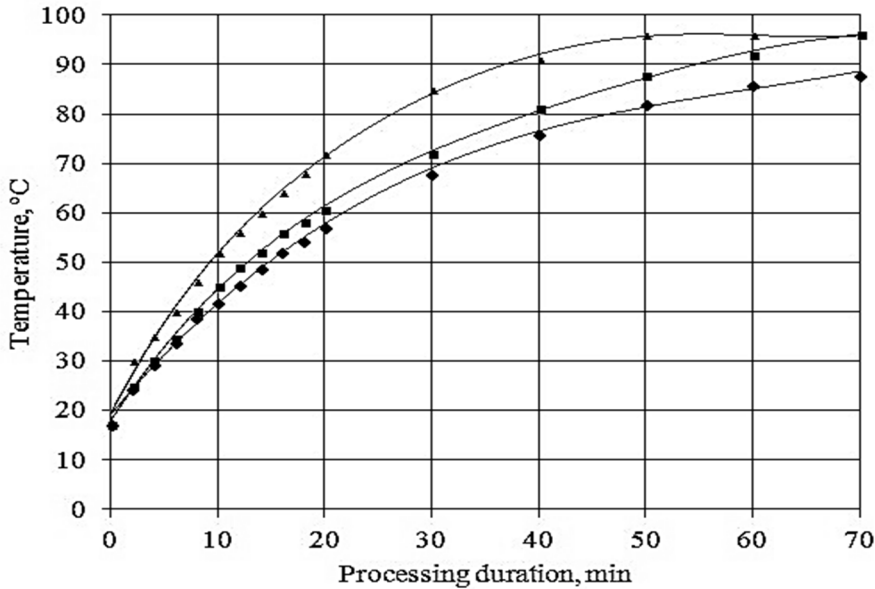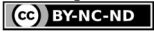
Figure 2. Dynamics of temperature change of water dispersion of straw at different solid/water ratio over time: ■ - 1:10; ▲ - 1: 5; ♦ - water.

Samples were taken every 10 minutes. The data about the amount of extracted lignin are given in the Table 1.

Table 1. Dependence of the lignin extraction on the duration of treatment at rotation speed of 47.75 rps

solid/water ratio 1:10							
sample	1	2	3	4	5	6	7
processing duration, min	10	20	30	40	50	60	70
% of the total lignin	10	18	25	32	38	41	42
solid/water ratio 1:5							
% of the total lignin	18	29	36	45	50	55	58

From the data in Table 1 we can conclude that the treatment of water suspension of straw in RPA allows isolating up to 42 % of lignin for 70 minutes under atmospheric pressure without external thermal energy supply. Changing the solid/water ratio of the water dispersion of straw from 1:10 to 1:5 leads to an increase in the amount of lignin release, since the temperature of the mixture increases more intensively.

Further increasing of straw content in the water dispersion of straw leads to significant energy consumption and unstable processing for the selected RPA design.

The histogram of the content of reducing substances in the residue on the filter depending on the treatment duration at straw/water ratio of 1:10 and 1:5 respectively is presented in Fig. 3. The initial indicator in the histogram is the content of reducing substances in the raw material at complete hydrolysis.
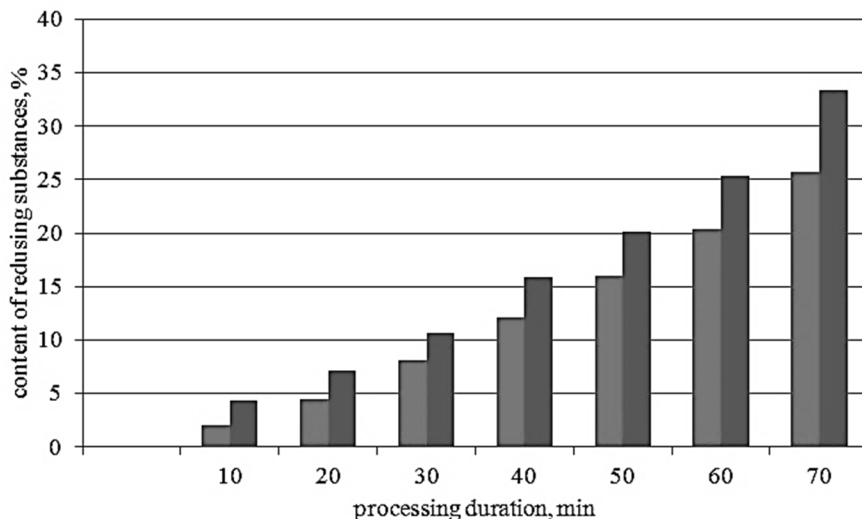

Figure 3. Histogram of the content of easily hydrolysable reducing substances in residue on the filter depending on the duration of treatment at the solid/water ratio of 1:10 (blue) and 1:5 (red).

The obtained data indicate that the cellulose content does not change during processing, but the hemicelluloses content in the hydrolysate increases during processing. A significant (up to 25.76%) amount of hemicelluloses gets into the solution at the solid/water ratio of 1:10 under experimental conditions. The increase of the solid/water ratio to 1:5 leads to an increase in the percentage of the polysaccharides (up to 33.38%).

CONCLUSIONS

A change in the solid / water ratio from 1:10 to 1: 5 leads to an increase in the yield of lignin and easily hydrolyzable polysaccharides, both in percentage terms and by weight, but a further decrease in the solid / water ratio requires a change in the design parameters of the apparatus**.**

REFERENCES

1. Nurtdinov, R.M.; Valeeva, R.T.; Mukhachev, S.G.; Kharina, M.V. Predvaritelnaia obrabotka rastitelnogo syria i otkhodov selskokhoziaistvennogo proizvodstva s tseliu povysheniia vykhoda redutsiruiushchikh veshchestv. *Vestnik Kazanskogo tekhnologicheskogo universiteta.* **2011**, 9, 264-267.

2. Barakat, A.; Mayer-Laigle C., Solhy, A.; Arancon, R.A.D.; de Vries, H.; Luque, R. Mechanical pretreatments of lignocellulosic biomass: towards facile and environmentally sound technologies for biofuels production. *RSC Advances*. **2014**, 4(89), 48109–48127 DOI: 10.1039/C4RA07568D

3. Hendriks, A.T.W.M.; Zeeman, G. Pretreatments to enhance the digestibility of lignocellulosic biomass. *Bioresour Technol*. **2009**, 100(1), 10–18.

4. Tsegaye, B.; Balomajumder, C.; & Roy, P. Alkali pretreatment of wheat straw followed by microbial hydrolysis for bioethanol production. *Environmental Technology*. **2017**, 1–9, 1203-1211 doi:10.1080/09593330.2017.1418911

5. Zheng, Q.; Zhou, T.; Wang, Y. et al. Pretreatment of wheat straw leads to structural changes and improved enzymatic hydrolysis. *Scientific Reports*, **2018**, 8(1). doi:10.1038/s41598-018-19517-5

6. Xu, H., Li, B., & Mu, X. Review of Alkali-Based Pretreatment To Enhance Enzymatic Saccharification for Lignocellulosic Biomass Conversion. *Industrial & Engineering Chemistry Research*, **2016**. 55(32), 8691–8705. doi:10.1021/acs.iecr.6b01907

7. Deberdeev, T.R., Garaeva, M.R., Fadeeva, K.S., Yakovlev, I.D., Deberdeev, R.Ya. Method of producing cellulose. RU.2677063,2019

8. Bahiru Tsegaye, Chandrajit Balomajumder & Partha Roy Alkali pretreatment of wheat straw followed by microbial hydrolysis for bioethanol production. *Environmental Technology*, **2019**, 40:9, 1203-1211. DOI: 10.1080/09593330.2017.1418911

9. Asghar, U., Irfan, M., Iram, M., et al. Effect of alkaline pretreatment on delignification of wheat straw. *Nat Prod Res*. **2015**. 9(2), 125-131. doi:10.1080/14786419.2014.964712

10. Stankovska, M., Fiserova, M., JURAJ Gigac, Yu., and ANDREJ Pazitny, A. Effect of alkaline extrusion pretreatment of wheat straw on filtrate composition and enzymatic hydrolysis. *Cellulose Chem. Technol.*, **2018**, 52 (9-10), 815-822

11. Miller, G. L. Use of dinitrosalicylic acid reagent for the determination of reducing sugar. *Analytical Chemistry*, **1959**, 31(3), 426-428.

12. A.A. Dolinskij, A.A.; Ivanickij, G.K. Teplomassoobmen i gidrodinamika v parozhidkostnyh dispersnyh sredah. Teplofizicheskie osnovy diskretno-impulsnogo vvoda energii; Naukova Dumka: Kyiv, 2008; p. 381.

13. Basok, B.I.; Davydenko, B.V.; Obodovich, A.N.; Pirozhenko, I.A. Dissipaciya energii v aktivnoj zone rotorno-pulsacionnogo apparata. *Dopovidi NAN Ukrainy*. **2006**, 12, 81 – 87.

Original scientific paper

UNMODIFIED GLASSY CARBON ELECTRODE AS A RELIABLE SENSOR FOR SENSITIVE VOLTAMMETRIC QUANTIFICATION OF VITAMIN D₃

Ana D. Đurović[1]*, Zorica S. Stojanović[1], Snežana Ž. Kravić[1], Tanja Ž. Brezo-Borjan[1], Jovana J. Kos[2]

[1] University of Novi Sad, Faculty of Technology Novi Sad, Bulevar cara Lazara 1, 21000 Novi Sad, Serbia
[2] University of Novi Sad, Institute of Food Technology in Novi Sad, Bulevar cara Lazara 1, 21000 Novi Sad, Serbia

In this paper a sensitive voltammetric method was developed for determination of vitamin D₃ in commercial dietetic supplements using unmodified glassy carbon electrode as a working electrode. Following the optimization of the square-wave voltammetric method, the linear relationship between the peak current and vitamin D₃ concentration was perceived in the concentration range of 1.25-105 μmol/L. The calculated values of detection limit and quantification limit were 0.24 and 0.73 μmol/L, respectively. In addition, the developed analytical procedure revealed exceptional precision with RSD values for intra- and inter-day (n=7) lower than 3%. Finally, developed voltammetric method was successfully applied for the determination of vitamin D₃ in dietetic supplements using standard addition method.

Keywords: vitamin D₃, voltammetry, glassy carbon electrode, dietetic supplements

INTRODUCTION

Vitamin D₃ (cholecalciferol, IUPAC 9,10-seco(5Z,7E)-5,7,10(19)-cholestatriene-3b-ol, Figure 1) is a prohormone obtained by conversion of its precursor 7-dehydrocholesterol upon ultraviolet radiation in the epidermis (1). Even though the main functions of vitamin D₃ are related to calcium and phosphorus homeostasis which are required for a wide range of biological processes (1), in recent studies significantly wider health implications of vitamin D₃ deficiency are reported. In fact, deficiency of this valuable vitamin is associated with cardiovascular diseases, metabolic disorders, cancer, neuropsychiatric disease and deregulation of the immune system (2-5). Regarding to the important functions in the human body, attention should be paid to the necessary daily dose of this vitamin. Under conditions distinctive for modern lifestyle, such as reduced sunlight exposure, blocking of UV light by air pollution, clothing and sunscreens, as well as various geographical and seasonal factors, vitamin D₃ becomes an important nutritional factor, and must be supplied via diet (1). However, it should be aware of the fact that rich sources of this vitamin are very limited, consequently adequate supplementation is advisable, especially in winter months.

---

* Corresponding author: Ana Đurović, University of Novi Sad, Faculty of Technology Novi Sad, Bulevar cara Lazara 1, 21000 Novi Sad, Serbia, e-mail: djurovic.ana@tf.uns.ac.rs
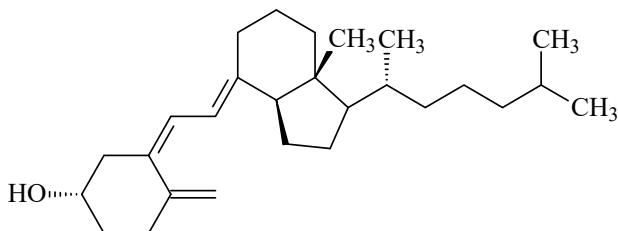
Figure 1. Structural formula of vitamin D_3

Considering the importance of this vitamin on the human health, a number of methods that are focused on the quantification of vitamin D_3 have been published in the literature, and were summarized in a recent study (6). A majority of these methods are based on the chromatography, but also capillary electrophoresis, and immunoassays have been reported as well (6). Although chromatography is established as a standard method for cholecalciferol determination, complicated sample preparation procedures, long analysis time, high cost of instrumentation, and a long-term training period of the laboratory staff are disadvantages associated with its practical use. To overcome these drawbacks, the development of the simple analytical methods, using green solvents and non-toxic materials, while improving sensitivity, as well as the reproducibility with reduced duration of the analysis is emphasized. In the light of these demands, voltammetric methods can meet these rigorous requirements, and can serve as an alternative method for cholecalciferol determination. Despite numerous advantages provided by voltammetric techniques, so far a small number of papers enabling the quantification of vitamin D_3 in real samples have been published (7-13). The use of glassy carbon electrode (GCE) as a working electrode for quantification purposes of this vitamin has already been apperceived in the literature (9, 13). Glassy carbon as a carbon-based material has attracted serious attention in electroanalysis, primarily because of its multiple advantages such as: broad potential window, low background current, rich surface chemistry, low cost, chemical inertness, non-toxicity (14), and its use has not been unattended in the analysis of various organic substances even nowadays (15).

The objective of the present study was to develop a simple, fast and reliable voltammetric procedure for cholecalciferol determination using unmodified GCE. In comparison to the existing methods that imply the same working electrode material (9, 13), the developed procedure can be characterized with improved sensitivity. Following optimization and validation, the developed voltammetric procedure has been successfully applied for quantification of cholecalciferol in commercially available dietetic supplements.

EXPERIMENTAL

Chemicals and solutions

Cholecalciferol (purity ≥ 98%) was purchased from Sigma-Aldrich (St. Louis, Missouri, USA). Standard solution of cholecalciferol (10 mmol/L) was prepared by dissolving of the appropriate amount of the substance in the ethanol (Fisher Scientific, Hamp-

ton, New Hampshire, USA). All other chemical used were of analytical reagent grade and were used as received. Double distilled water was used for preparing all the solutions.

Instrumentations

Voltammetric measurements were performed using a three-electrode system comprised GCE (total surface area of 7.07 mm^2) as the working electrode, Ag/AgCl (3.5 mol/L, KCl) and platinum wire as the reference and auxiliary electrode, respectively. Electrodes were connected to potentiostat PalmSens 4 (GA Houten, Netherlands), which was controlled by PSTrace 5.4 software. All potentials were referred to the above mentioned reference electrode. An ultrasonic bath Iskra (Kranj, Slovenia) with working frequency of 30 Hz, and power of 500 W was used at the end of the polishing procedure of GCE, and to support dissolution of the dietetic supplements, as well. The surface of the GCE was polished with water suspension of Al$_2$O$_3$ particle size 1 μm Merck (Darmstadt, Germany) on the special polishing pad until a mirror-like surface was obtained, followed by sonication in ethanol and water mixture (1/1, v/v) for 5 min. After subsequent rinsing with double distilled water and drying, the working electrode was ready for measurements.

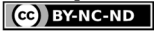## Measurement procedure for voltammetric analysis

For performing voltammetric measurements, the supporting electrolyte (15 mL) and a three-electrode system were placed in the glass cell. After 5 s of stirring, and the same period of quiescence time, square-wave voltammograms were recorded in the potential range from +0.7 V to +1.4 V. For performing square-wave voltammetry (SWV) experiments, the following optimal parameters were selected: amplitude of 75 mV, step potential of 5 mV, frequency 25 Hz with equilibrium time of 10 s.

A comparative chromatographic analysis using HPLC

For HPLC analysis, a liquid chromatograph Agilent 1200 (Agilent Technologies Inc., USA) equipped with diode array detector, Chemstation Software, binary pump, vacuum degasser, auto sampler and Agilent column (Eclipse XDB-C18, 1.8 μm, 4.6 × 50 mm) were used. Detection wavelength was set to 260 nm. Pure methanol was used as the mobile phase with isocratic conditions. Furthermore, the following HPLC conditions were chosen: flow rate of 0.4 mL/min, and the column temperature of 30 °C.

Real samples analysis

Dietetic supplements of cholecalciferol in the form of film tablets were crushed in a mortar and accurately transferred into the glass with the supporting electrolyte. The content was sonicated for 10 min and filtered using Whatman filter paper No. 1 (Whatman International, Maidstone, UK) in the calibrated flask. For the analysis 10 mL of the prepared sample was transferred to the glass cell, and SWV was performed by following the optimal parameters of the analysis using standard addition method with three replicate experiments for quantification. For HPLC analysis, after sonication the samples were fil-

tered through a 0.45 μm membrane syringe filter Chromafil®Xtra PET45/25, (Macherey-Nagel, Düren, Germany), a volume of 15 μL was injected into HPLC system, analysed in triplicates, and quantified by means of calibration curve.

RESULTS AND DISCUSSION

In order to find optimal experimental conditions for voltammetric determination of cholecalciferol using GCE as a working electrode, extensive SWV studies were performed in the anodic potential range from +0.7 V to +1.4 V, in various supporting electrolytes. Due to poor solubility of cholecalciferol in water, the supporting electrolytes were prepared in 50% of ethanol (v/v). 0.1 mol/L acetate and citrate buffers, 0.04 mol/L Britton-Robinson buffer, 0.05 mol/L solutions of HNO_3, H_2SO_4 and HCl were tested as the supporting electrolytes. In all studied supporting electrolytes one well-defined oxidation peak was observed. However, 0.05 mol/L solution of H_2SO_4 was selected as the optimal supporting electrolyte, as it showed the best characteristics in terms of sensitivity, linearity and peak definition. Square-wave voltammograms recorded in the 0.05 mol/L H_2SO_4 solution containing 50% of ethanol without and with 50 μmol/L of cholecalciferol is shown in Figure 2.
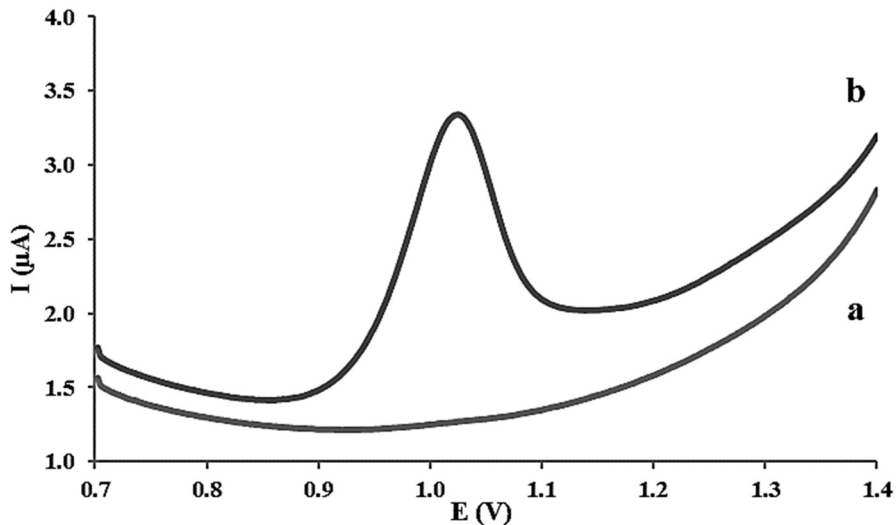
Figure 2. Square-wave voltammograms recorded at GCE for (a) blank, and (b) in the solution containing 50 μmol/L of cholecalciferol. Supporting electrolyte 0.05 mol/L H_2SO_4 containing 50% of ethanol, t_{eq} = 10 s, ΔE = 5 mV, E_{amp} = 75 mV, f = 25 Hz.

Aiming to develop a sensitive method for determination of cholecalciferol content in the supplements, various parameters of the SWV, such as pulse amplitude (E_{amp}), frequency (f), step potential (ΔE) and equilibrium time (t_{eq}) in 0.05 mol/L H_2SO_4 in 50%

ethanol with respect to the peak current (I_p) were studied and optimized. During experiments each parameter was changed, while others were kept at constant level in the solution containing 50 µmol/L of cholelaciferol. In the optimization study next parameters proved to be optimal: E_{amp} = 75 mV, f = 25 Hz, ΔE = 5 mV and t_{eq} = 10 s.

Calibration curves were constructed by adding aliquots of vitamin D_3 standard solution in the glass cell with the supporting electrolyte under the optimized condition of the SWV analysis. A linear response was observed in the concentration range of 1.25-105 µmol/L of cholecalciferol, and it can be described by the equation I_p (µA) = 0.0475·c (µmol/L) – 0.2007 (r = 0.9959) (Figure 3).
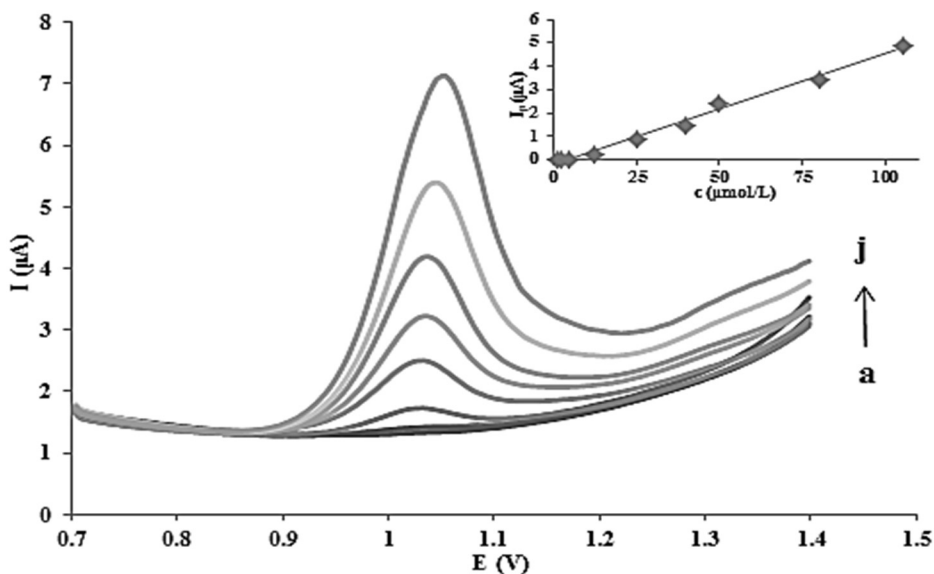

Figure 3. Square-wave voltammograms of cholecalciferol with corresponding calibration curve (inset): a) blank, b) 1.25, c) 2.5, d) 5, e) 12.5, f) 25, g) 40, h) 50, i) 80, and j) 105 µmol/L. Equilibrium time 10 s, potential step 5 mV, amplitude 75 mV, frequency 25 Hz.

For the purpose of determination limit of detection (LOD) and limit of quantification (LOQ) values, the linearity range of lower concentrations was used (1.25-40 µmol/L), and LOD and LOQ values were calculated as follows: LOD = 3.3 S_a/b, and LOQ = 10 S_a/b (16), where S_a stands for standard deviations of the intercept, while b represents the slope of the calibration curve (n = 3). Calculated LOD and LOQ values were 0.24 and 0.73 µmol/L, respectively. The results presented in this study have shown favourable LOD value and wide linear range for determination of cholecalciferol, which are better in comparison to those obtained by the use of GCE (9, 13), or some modified GCE materials (8, 10, 11). It should be emphasized that herein presented procedure does not require modification, which usually involves complicated and prolonged procedures (11, 12).

The precision of the presented procedure was evaluated under the optimized conditions of the SWV analysis at two different cholecalciferol concentrations (25 µmol/L and 50 µmol/L) by seven replications during the same day (intra-day), and during seven con-

secutive days (inter-day). Obtained values of relative standard deviations (RSD) were lower than 3% indicating satisfactory precision of the proposed method.

In order to examine the applicability of the presented method in the analysis of real samples, two dietetic supplements of vitamin D_3 were analysed. Based on the obtained results presented in Table 1, the determined contents of vitamin D_3 were close to values declared by the manufacturer. Additional confirmation of the accuracy of the developed method was performed by HPLC analysis (Table 1).

Table 1. Assay of vitamin D_3 in dietetic supplements using the presented square-wave voltammetric procedure and HPLC as a comparative analysis

Sample	Labeled content (µg/tablet)	Proposed voltammetric method (µg/tablet)[a]	HPLC (µg/tablet)[a]
1	50	47.08 ± 0.66 (94.16)	46.63 ± 0.09 (93.26)
2	25	24.51 ± 0.45 (98.04)	24.65 ± 0.15 (98.60)

[a] Mean value ± SD, Recovery (%), n=3.
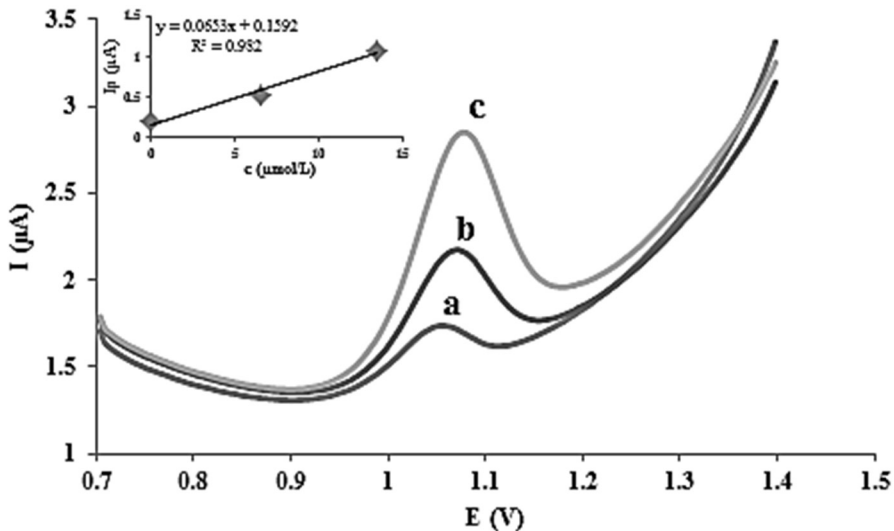
Figure 4. Square-wave voltammograms for determination of vitamin D_3 in the sample of dietetic supplement using the standard addition method with two successive additions with corresponding analytical curve (inset): (a) Sample 1, spiked sample with cholecalciferol: (b) + 6.50 µmol/L, (c) + 13.52 µmol/L. t_{eq} = 10 s, ΔE = 5 mV, E_{amp} = 75 mV, f = 25 Hz.

Moreover, RSD values obtained for the samples were less than 1.9%, indicating on the high precision of the developed voltammetric procedure. Statistical comparison of the results obtained by voltammetric procedure with chromatographic HPLC method using

                                                              Original scientific paper

the paired t-test showed no statistically significant difference between the two methods at 95% confidence level. Finally, square-wave voltammograms recorded during the analysis of the sample (Figure 4) revealed that the peak of vitamin D_3 was not interfered by any of the matrix compounds of the formulations additives such as: cellulose, talc, magnesium stearate and starch, confirming thus the selectivity of the herein presented voltammetric procedure.

CONCLUSION

In this work a new electroanalytical method for determination of vitamin D_3 has been described. The method is based on the oxidation of the analyte on the surface of the unmodified glassy carbon electrode as a working electrode, and subsequent determination using square-wave voltammetry. In comparison to the previously reported papers dealing with voltammetric determination of this vitamin by using unmodified or modified GCE, better analytical performances were achieved, regarding favourable LOD value and wider linear range, and most of all, without complicated working electrode preparation or modification procedures. The practical utility was successfully demonstrated in the analysis of the dietetic supplements containing vitamin D_3, with satisfying recovery values and low RSD values indicating on high accuracy and precision of the developed method. Based on these facts, herein presented voltammetric procedure could be considered as a significant contribution in the field of applied analytical chemistry in determination of cholecalciferol content in different samples.

Acknowledgement

REFERENCES

1. Norman, A. W.; Henry, H. L. Vitamin D. In Handbook of Vitamins; Zempleni, J., Rucker, R. B., McCormick, D. B., Suttie, J. W., Eds.; 4th Ed., CRC Press; Taylor & Francis Group: Boca Raton, Florida, **2007**; pp 41-111.
2. Kheiri, B.; Abdalla, A.; Osman, M.; Ahmed, S.; Hassan, M.; Bachuwa, G. Vitamin D deficiency and risk of cardiovascular diseases: A narrative review. *Clin. Hypertens.* **2018**, *24*, 1-9.
3. Eyles, D. W.; Burne, T. H.; McGrath, J. J. Vitamin D, effects on brain development, adult brain function and the links between low levels of vitamin D and neuropsychiatric disease. *Front. Neuroendocrinol.* **2013**, *34* (1), 47-64.
4. Aranow, C. Vitamin D and the immune system. *J. Investig. Med.* **2011**, *59* (6), 881-886.
5. Krishnan, A. V.; Trump, D. L.; Johnson, C. S.; Feldman, D. The role of vitamin D in cancer prevention and treatment. *Endocrinol. Metab. Clin. North. Am.* **2010**, *39* (2), 401-18.
6. Yin, S.; Yang, Y.; Wu, L.; Li, Y.; Sun, C. Recent advances in sample preparation and analysis methods for vitamin D and its analogues in different matrices. *TrAC, Trends Anal. Chem.* **2019**, *110*, 204-220.

7. Đurović, A.; Stojanović, Z.; Kravić, S.; Kos, J.; Richtera, L. Electrochemical determination of vitamin D$_3$ in pharmaceutical products by using boron doped diamond electrode. *Electroanalysis* **2020**, *32*, 741-748.

8. Kahya, Ş.; Cittan, M.; Çelik, A. Electrochemical behaviour of cholecalciferol on a multiwalled carbon nanotube modified glassy carbon electrode. *Cumhuriyet Sci. J.* **2018**, *39* (4), 1081-1088.

9. Nallbani, A.; Holubová, J.; Sýs, M.; Arbneshi, T.; Vytřas, K. Voltammetric determination of cholecalciferol at glassy carbon electrode performed in water-ethanol mixture. *Potr. S. J. F. Sci.* **2018**, *12* (1), 166-172.

10. Men, K.; Chen, Y.; Liu, J.; Wei, D. Electrochemical detection of vitamin D$_2$ and D$_3$ based on a Au-Pd modified glassy carbon electrode. *Int. J. Electrochem. Sci.* **2017**, *12* (10), 9555-9564.

11. Raymundo-Pereira, P. A.; Lima, A. R. F.; Machado, S. A. S. A nanostructured label-free platform based on an ultrathin film for ultrasensitive detection of a secosteroid hormone. *RSC Adv.* **2016**, *6* (41), 34458-34467.

12. Canevari, T. C.; Cincotto, F. H.; Landers, R.; Machado, S. A. S. Synthesis and characterization of α-nickel (II) hydroxide particles on organic-inorganic matrix and its application in a sensitive electrochemical sensor for vitamin D determination. *Electrochim. Acta* **2014**, *147*, 688-695.

13. Méndez, J. H.; Pérez, A. S.; Zamarreño, M. D.; Garcia, M. L. H. Voltammetric determination of vitamin D$_3$ with a rotating glassy carbon electrode. *J. Pharm. Biomed. Anal.* **1988**, *6* (6-8), 737-741.

14. Wang, J. Analytical Electrochemistry; 3rd Ed., Wiley-VCH: Hoboken, New Jersey, **2006**; pp 131.

15. Pinto, G. F.; Rocha, D. P.; Richter, E. M.; Muñoz, A. A.; Silva, S. G. Indirect determination of formaldehyde by square-wave voltammetry based on the electrochemical oxidation of 3,5–diacetyl–1,4–dihydrolutidine using an unmodified glassy-carbon electrode. *Talanta* **2019**, *198*, 237-241.

16. ICH, International Conference on Harmonisation. Validation of Analytical Procedures: Text and Methodology. 1996. https://www.ich.org/fileadmin/Public_Web_Site/ICH_Products/ Guidelines/ Efficacy/E6/E6_R1_Guideline.pdf (accessed 1 June 2020).

MATHEMATICAL MODELLING OF THIN LAYER DRYING KINETICS OF CASHEW APPLE POMACE IN HOT AIR OVEN DRYER

Bobby Luka Shekarau[1,2]*, Riyang Zakka[2], Tswenma Tsokwa[3], Taitiya Kenneth Yuguda[4], Paul Udom Okon[5]

[1] Department of Agricultural Engineering, Federal University Wukari, Taraba State, Nigeria
[2] Department of Food Science and Technology, Federal University Wukari, Taraba State, Nigeria
[3] Department of Chemical Engineering, Federal University Wukari, Taraba State, Nigeria
[4] Department of Environmental Engineering, College of Environment, Hohai University, P. R. China.
[5] Department of Mechanical/Production Engineering, Federal University of Agriculture Makurdi, Benue State, Nigeria

Due to renewed interest in fruit residue application, cashew apple pomace and other fruit pomace are receiving unparallel attention as substitute for food ingredient or food enrichment options. This necessitates this study to investigate drying as vital approach in preserving and conditioning cashew apple pomace. In this study, cashew apple fruits were blended in fruit blender and filtered through 150 microns filter; the filtrate was further tightened in a fabric material and pressed with manual hydraulic press to further express the juice in it. The pomace was stored in a refrigerator at 3 °C for 18 h to homogenise the moisture. The pomace was divided into nine equal weights, a portion was fed into hot air oven dryer at 60 °C and constant circulating air velocity of 2.2 m/s, the changes in mass was measured using digital mass balance after every 10 minutes. The procedure was repeated at 70 and 80 °C and in triplicate; in each case the mass of the samples was measured. It was found that cashew pomace dry under a single falling rate period, effective moisture diffusivity increased with increasing drying temperature and ranges from 9.02015×10⁻⁹ to 2.12177×10⁻⁸, activation energy was estimated as 41.880 kJ/K, specific drying energy consumption decreased with increasing drying temperature and ranges from 24.1 to 45.3 MJ/kg. Our proposed drying model was found to adequately simulate the drying kinetics of cashew apple pomace.

Keywords: activation energy, cashew apple pomace, drying modelling, effective moisture diffusivity; specific energy consumption

INTRODUCTION

Cashew pomace is a byproduct of cashew apple fruit juice extraction. It has high moisture content (1) therefore it must be dried as soon as possible to prevent microbial growth and inhibit biochemical reactions and consequent deterioration. Cashew apple pomace is rich in dietary fibre, protein, fat, carbohydrate, calcium, phosphorus and iron (1). In the past, cashew apple pomace are used mainly as animal feeds, recently it has received renewed interest for many applications to supplement food ingredients for the

---

purpose of food enrichment with vitamins and minerals or bioactive compounds, such application are reported in cakes, muffin and biscuits, it is also used for fat and wheat substitution in baked foods and sugar replacement in many food products (1, 2, 3, 4).

When developing empirical models that predict food drying kinetics, fruits, vegetables and their associated by-products are mostly dried in thin layer to allow the drying material extract reasonably high quantity of heat from heated air, maintaining high air/feed ratio in the dryer (5, 6). Moisture migration in biomaterials during drying occur in either falling rate period or constant rate period, for fruits and vegetables, due to high interplaying effect of diffusion process, they are mostly dried in falling rate period (7).

Studying drying characteristics will assist in identifying appropriate drying methods, control drying processes, optimize dried product quality and in designing dryers (8). Drying is sometimes expensive and time consuming to conduct an in-depth study to determine the suitable control conditions, thus, drying characteristics is used to express the moisture removal process due to couple effect of heat and mass transfer and its link to the process variables (8), hence; an excellent understanding of the drying rate has since become an important factor in developing drying models.

Thin layer drying models exist for different moisture ratio curves (9); however, the goal of every drying model is to satisfactorily predict the drying kinetics of the dried sample with zero noise and zero residual, thus drying models are continually developed to obtain a robust model with excellent performance functions.

Studies carried out on drying fruit pomace are documented in Sharma et al. (10) and Kumar et al. (11) for dried apple pomace, Andréia et al. (12) for dried Caja pomace, and De Menezes et al. (13) for dried Yellow passion fruit pomace. Studies on drying kinetics of fruit pomace are limited, for cashew apple pomace, to the best of our knowledge, no research evidence was reported on its drying modelling and drying kinetics, hence, the formulation of a new and robust drying model with the underlying objective of predicting moisture ratio during drying and estimation of effective moisture diffusivity, activation energy and drying energy consumption of cashew apple pomace forms the basis of this study.

MATERIALS AND METHOD

Experimental method

Firm-ripped cashew apple fruits were plugged from cashew tree and washed with distil water and kept under ambient condition. The fruit were fed into fruit blender and blended at 200 rpm for 2 minutes. The paste was filtered through a 150 micron filter to separate the pomace from the juice; the pomace was further tight in a mesh fabric and pressed between two plates of hydraulic press for 5 minutes. The pomace were mixed together and placed in a refrigerator in an air tight polythene bag at 3 °C for 18 hours to homogenize the moisture in the pomace matrix. The cashew apple pomace was divided into nine samples each weighing 21.2 g. In each case, prior to drying, a pomace sample was stacked in a 130×120×100 mm stack placed on a mesh wire.

The drying oven was switched-on and allowed to build up to a set temperature of 60 °C; the sample was then fed into the drying chamber of the circulating hot air oven dryer (Presto-Mercury) operating at constant circulating air velocity of 2.2 m/s. After 10 minutes, the sample was removed from the drying chamber and weighed using digital weight balance (KERRO BL3002) until no further change in weight was recorded and in each case, the oven was allowed to build up to the selected drying temperature of 60 °C.

The procedure was repeated for drying temperatures of 70 and 80 °C. The experiment was carried out in triplicate and in each case the instantaneous moisture content was calculated in dry basis (db) using equation 1 for all drying temperatures and their average was computed.

$$M_{t+dt} = \frac{M_i - M_d}{M_d} \times 100 \qquad [1]$$

M_i is the mass of cashew pomace prior to drying; M_d is the mass of dried cashew apple pomace.

To obtain moisture the ratio profile and effectively formulate drying model, cashew pomace moisture ratio (MR) was estimated using equation 2.

$$MR = \frac{M_t - M_e}{M_0 - M_e} \qquad [2]$$

While the drying rate was estimated using equation 3.

$$\frac{dR}{dt} = \frac{(M_{t+dt} - M_t)}{dt} \qquad [3]$$

Mt is the moisture content of cashew pomace at an instant (%); M_e is the equilibrium moisture content (%) of cashew pomace; M_0 is the initial moisture content of cashew pomace (%); dt is the drying time interval; M_{t+dt} is the instantaneous moisture content.

Estimation of effective moisture diffusivity

Experimental method has become the most widely adopted approach in estimating effective moisture diffusivity of biomaterials; this is done with the help of drying curves base on Fick's second law of diffusion. For infinite slab and assuming a constant diffusion coefficient, uniform moisture distribution at the beginning, negligible drying temperature changes and shrinkage, the analytical solution of Fick's one-dimensional diffusion equation is expressed in equation 4 (14);

$$MR = \frac{8}{\pi^2} \sum_{n=0}^{\infty} \frac{1}{(2n-1)^2} \exp\left[\frac{-(2n+1)^2}{4L^2} \pi^2 D_{eff} t\right] \qquad [4]$$

n is the term of the experiment, D_{eff} is the effective moisture diffusivity (m²/s), t is the drying time (s) and L is half the thickness of slab (m).

The expansion term for equation 4 is

$$MR = \frac{8}{\pi^2}\left(e^{-\left(\frac{\pi}{2}\right)^2 N_{Fi}} + \frac{1}{9}e^{-9\left(\frac{\pi}{2}\right)^2 N_{Fi}} + \frac{1}{25}e^{-9\left(\frac{\pi}{2}\right)^2 N_{Fi}}\right); \qquad [5]$$

$$MR = 0.692e^{-5.78 N_{Fi}} + 0.131e^{-30.5 N_{Fi}} + 0.0534e^{-74.9 N_{Fi}} \qquad [6]$$

N_{Fi} $\left(\frac{D_{efft}}{L^2}\right)$ is the Fick number, L is half the characteristic thickness of cashew apple pomace slab.

However, for longer drying time where N_{Fi} $\left(\frac{D_{efft}}{L^2}\right) > 0.1$ and MR<0.6, the first term of the series prevails and the equation can be simplified to a linear form in equation 7.

$$\ln MR = \ln \acute{c} - st \qquad [7]$$

Where s, is the gradient and represents the drying constant (t^{-1}) which is also equal to ($\acute{c}\frac{D_{eff}}{L^2}$), $\acute{c}$ is the constant taken from the first series. For slap, $\acute{c}$ =2.47; natural-log plot of moisture ratio against drying time gives a straight line graph above Fick's number of 0.1. Effective diffusivity was estimated from the slope of straight line graph using the equation 8.

$$D_{eff} = \frac{-s(L^2)}{\acute{c}} \qquad [8]$$

Estimation of activation energy

The relationship between effective moisture diffusivity and temperature is expressed by the famous Arrhenius equation (15) expressed in equation 9.

$$D_{eff} = D_o \exp\left[-\frac{E_a}{RT}\right] \qquad [9]$$

It can be simplified to a linear equation expressed in equation 10.

$$\ln D_{eff} = \ln D_o - \frac{E_a}{RT} \qquad [10]$$

The plot of ln D_{eff} against $\frac{1}{T}$ gives a straight line plot with $-\frac{E_a}{R}$ equated to the slope and $\ln D_o$ as the intercept of the graph. The activation energy was computed using equation 11.

$$E_a = slope \times R \qquad [11]$$

E_a is the activation energy, kJ/mol., T is the absolute drying temperature, D_o is the pre-exponential Arrhenius constant m^2/s and R is the universal gas constant, kJ/mol. K.

Original scientific paper

Estimation of drying specific energy requirement

The energy consumed in drying a unit charge of cashew apple pomace in the dryer was estimated using equation 12 (16).

$$Et = \left(Av\rho_a (C_a + RhC_v)(T - T_a)t \right)$$ [12]

The density of air was estimated at different drying temperature using equation 13 (17).

$$\rho_a = \frac{353.05}{T}$$ [13]

A is the surface area of drying rack, m^2; v is the drying air velocity, m/s^2; ρ_a is air density, kg/m^3; Rh is the relative humidity of drying air, T is the drying temperature, K; T_a is the ambient air temperature, K; t is the total time taken to completely dry cashew apple pomace to equilibrium moisture, s; C_a is the specific heat capacity of air (1008.3 J/kg K); C_v is the specific heat capacity of water vapor (1828.8 J/kg K).

The energy required to dehydrate 1kg of wet cashew apple pomace, was estimated using equation 14;

$$E_{kg} = \frac{E_t}{W_w}, \text{MJ/kg}$$ [14]

W_w is the mass of water evaporated from cashew apple pomace.

Experimental uncertainty analysis

The weight of cashew apple pomace was weighed in triplicate experimental runs, like wise effective moisture diffusivity, activation energy and specific energy consumption were also computed in triplicate. The mean was computed using equation 15;

$$\text{Mean Value } (\overline{X}) = \frac{1}{n} \sum_{i=1}^{n} X_i \qquad i = 1, 2, 3 \ldots n$$ [15]

Where X_i is the measured parameter value.

To calculate the expanded uncertainty, Guassian for bell shape probability density function at 95 % uncertainty range was employed as adopted by Luka et al. (18) using equations 16-19.

Since the smallest unit of the weight balance is 0.1 g, calibration uncertainty (Δd) would be twice smaller, that is equal to 0.05 g.

To compute B-type uncertainty, equation 16 was used.

$$u(d) = \frac{\Delta d}{\sqrt{3}}$$ [16]

The result distribution was observed in A-type, thus standard uncertainty was calculated using equation 17:

Original scientific paper

$$u(d)=\sqrt{s_{\bar{x}}^2}=\left[\frac{1}{n(n-1)}\sum_{i=1}^{n}(X_i-\overline{X})^2\right]^{1/2} \qquad n=1, 2, 3…n_{th} \qquad [17]$$

n is the number of measurements.

Also, since the size of A-type and B-type uncertainties is the same, combine uncertainty was computed using equation 18.

$$u(d)=\sqrt{s_{\bar{x}}^2+\frac{\Delta d}{\sqrt{3}}} \qquad [18]$$

To compute expanded uncertainty at 95 % confidence level, k=1.96, equation 19 was used.

$$U(d)= k \times u(d) \qquad [19]$$

Mathematical modelling of moisture ratio

MATLAB 2014b was used to fit drying models listed in Table 1 to moisture ratio profile of cashew apple pomace dried at different temperatures as obtained in Khanali et al. (16) along with proposed empirical model dubbed Luka et al (equation 20).

$$MR = a\exp(-kt^n)+kt(b-a)+(1-a) \qquad [20]$$

Where a and b are model constants, k is the drying constant, t is the drying time (m) and n is the power term.

Levenberg-marquardt algorithm was used for the iteration using nonlinear least square method to estimate the coefficients of the model, coefficient of determination (R^2), mean square error (MSE) and corrected Akaike information criteria (AICc) were used as optimal performance functions of the models' fitness. AICc was used as indicator of the models performance due to low data size relative to the model parameters, that is n/K<40, in this case, a second-order bias correction factor is added to Akaike information criteria (AIC) to give a refined AIC called AICc expressed in equation 21 (19)

$$AICc= n\ln(\sigma^2) + 2K + \frac{2K(K+1)}{n-K-1} \qquad [21]$$

σ^2= MSE; K= Number of parameters estimated in the model.

$$n\ln(\sigma^2) + 2K = AIC \qquad [22]$$

$\frac{2K(K+1)}{n-K-1}$ is the correction factor

Table 1. Drying models and proposed drying model

No	Models	Equation
1	Demir et al.	$MR = a\exp(-kt^n)+b$
2	Diffusion approach	$MR = a\exp(-kt)+(1-a)\exp(-kbt)$
3	Henderson and Pabis	$MR = a\exp(-kt)$
4	Lewis	$MR = \exp(-kt)$
5	Logarithmic	$MR = a\exp(-kt)+c$
6	Midilli et al.	$MR = a\exp(-kt^n)+bt$
7	Modified Henderson and Pabis	$MR = a\exp(-kt)+b\exp(-gt)+c\exp(-ht)$
8	Page	$MR = \exp(-kt^n)$
9	Simplified Fick's diffusion equation	$MR = a\exp(-k(t/L^2))$
10	Two-term exponential	$MR = a\exp(-kt)+(1-a)\exp(-kat)$
11	Verma et al.	$MR = a\exp(-kt)+(1-a)\exp(-gt)$
12	Wangh and Singh	$MR = 1+at+bt^2$
13	Weibull	$MR = \exp(-(t/a)^b)$
14	*Luka et al.(Proposed model)*	$MR = a\exp(-kt^n)+kt(b-a)+(1-a)$

RESULTS AND DISCUSSION

Drying curves

Drying temperature obviously affects moisture removal rate from cashew apple po-mace matrix (Fig. 2), characterized by steeper drying rate gradient from highest to lowest drying temperature (Fig. 3) that is, higher drying rate at higher oven dryer temperature and lower drying rate at lower drying temperature. The drying time at 60 °C drying tem-perature is 32.29 % greater than at 70 °C, and at 70 °C is 18.18 % higher than at 80 °C, such uneven variation could be imputed to exponential relationship that exists between vapor pressure and relative humidity with increasing drying temperature, a few degree rise in temperature has an increasingly large impact on saturation point, this makes drying rate gradient more steeper as drying temperature is increased (20, 21), Moisture migration was more pronounced at the beginning of the drying at all drying temperatures and less at later stage, this could be owing to abundant free water molecules on the surface of the pomace at the beginning of the drying process (16), also since cashew apple pomace con-tains pectin (22), as moisture content reduced under heat, it become more esterified and form thick gel (23, 24) this pectin under gelling and crusting effect could form packed pectin molecules around cashew apple pomace matrix lumps causing lesser vapor per-meability and consequently reduces moisture migration from the core with pronounced effect at later stage of the drying process.
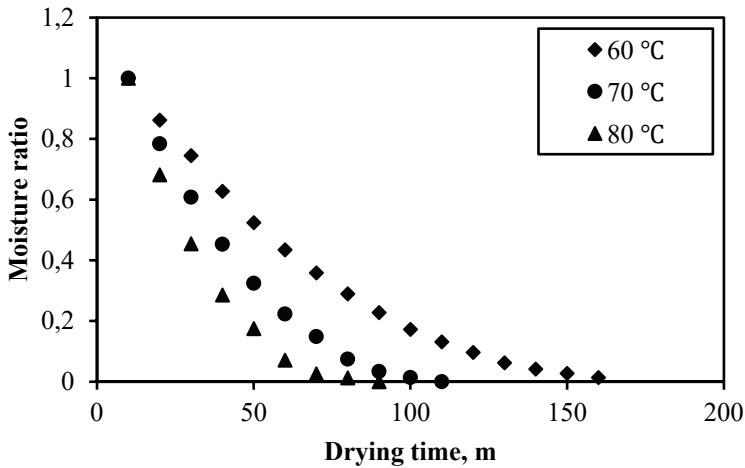
Figure 1. Moisture ratio profile of cashew apple pomace

The drying curve (Fig. 2) shows that cashew apple pomace dried only in single falling rate period and no constant rate, this infer a diffusion controlled drying process, similar drying rate curve was reported in dried apple pomace by Sharma et al. (10). Falling drying rate period is peculiar to agricultural and food products because moisture is either bounded or free) (25) in the case of cashew apple pomace, such drying period could be due to majority of the water chemically bounded to its matrix due to viscous pectin (26, 24).

Figure 2. Variation of drying rate at different drying temperature

Original scientific paper

Effective moisture diffusivity

Despite pitfalls and over simplification in models utilizing effective moisture diffusivity, it has become the most dominantly used equation for modeling drying (27).

Fig. 3 shows the plot of estimated natural-log of moisture ratio against drying time base on their corresponding fitted linear equation and coefficient of determination (R^2) for each drying temperature.
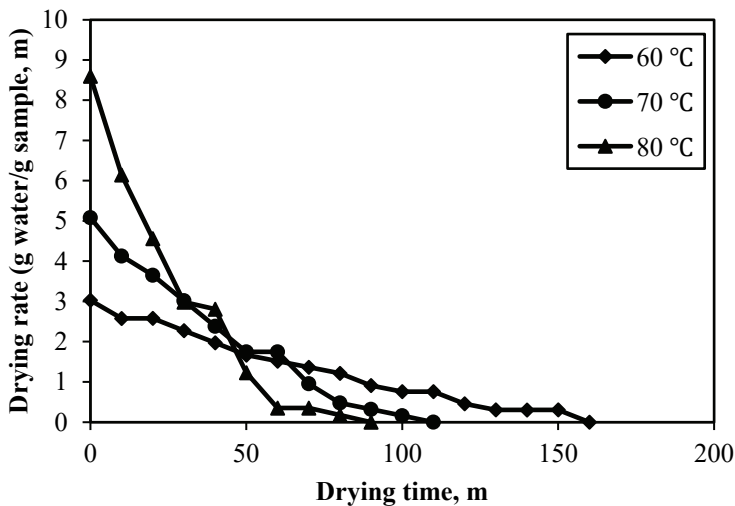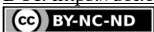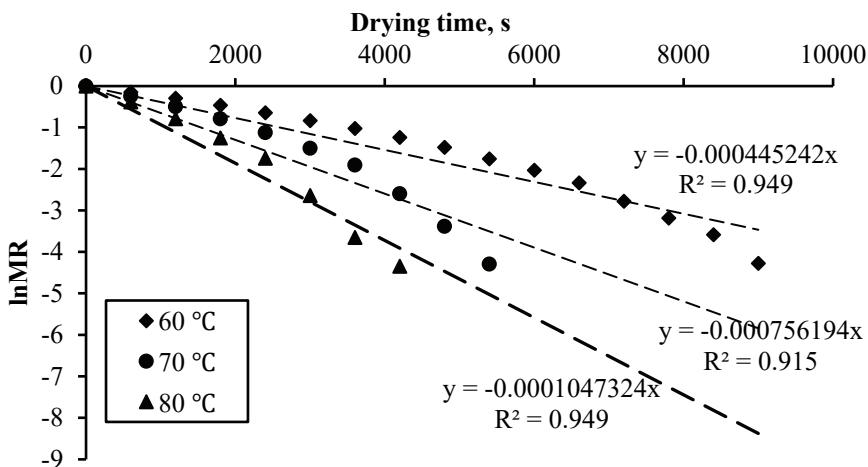

Figure 3. Variation in semi-log of moisture ratio with drying time

The estimated effective moisture diffusivities are presented in Table 2.

Table 2. Effective moisture diffusivity of cashew apple pomace

No.	Drying temperature (°C)	(D_{eff}) Effective moisture diffusivity (m²/s)
1	60	9.02015×10^{-9}
2	70	1.53000×10^{-8}
3	80	2.12177×10^{-8}

Effective moisture diffusivity of cashew apple pomace increases with increasing drying temperature, this was corroborated by the steepness of drying rate against drying time for different drying temperatures (Fig. 2) since diffusivity controls rate of moisture migration during drying. The values of effective moisture diffusivity of cashew apple pomace fall within the bracket of 10^{-12} to 10^{-8} for biological materials (28). Temperature dependent effective moisture diffusivity of cashew apple pomace at constant air velocity can be expressed in equation 23 base on Arrhenius equation;

$$D_{eff} = 3.45 \times 10^{-2} \exp\left[-\frac{5037.29}{T+273.15}\right] \qquad [23]$$

T is the drying temperature (°C).

Activation energy

The fitted linear equation used in estimating the activation energy is displayed on Fig. 4, The minimum energy required to initiate moisture migration from the surface of cashew apple pomace was estimated to be 41.880 kJ/ K this falls within the bracket of 12.7-110 kJ/K for biomaterials (29) and the estimated pre-exponential Arrhenius factor of 3.45×10^{-2} m^2/s was obtained base on the fitness line equation. The higher activation energy could be due to predominantly chemically bounded water molecules in cashew apple pomace and gel forming effect of pectin as drying progresses which inhibit rapid moisture diffusion.
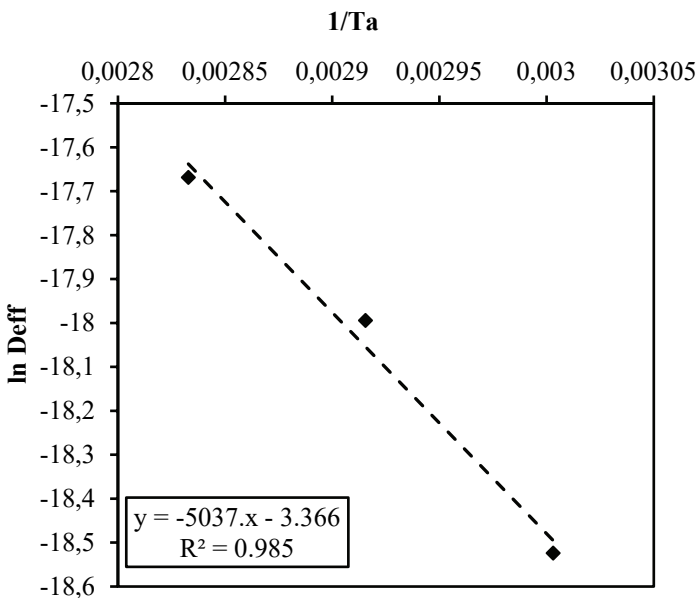
Figure 4. Fitted regression line for estimating activation energy

Energy requirement

The profile of specific energy consumption in drying a unit kilogram of cashew apple pomace is presented in Fig. 5, the specific energy consumption at 60, 70 and 80 °C are 45.3, 29.4 and 24.1 MJ/kg respectively. The highest energy requirement was obtained at 60 °C drying temperature and minimum at 80 °C drying temperature, this could be explained in terms of pronounced difference in drying time at different drying temperature; longer drying time negates the influence of increasing energy consumption obtainable from increasing dryer heater temperature and consequently results in higher specific energy consumption at drying temperature of 60 °C (28, 16), this can also be substantiated by larger coefficient of drying time against drying temperature in equation 24.
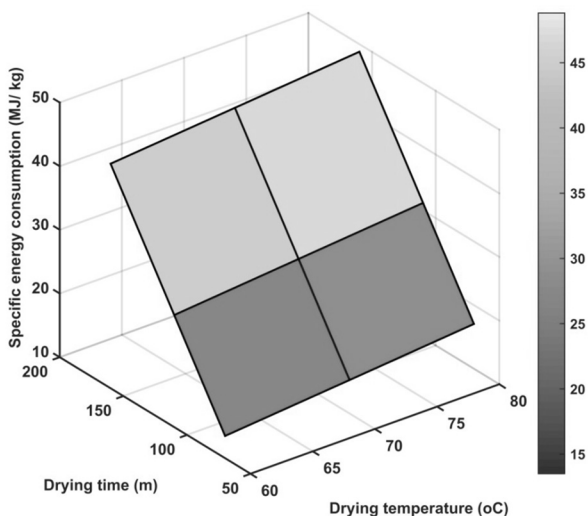
Figure 5. Variation in specific energy consumption with drying temperature and drying temperature

Regression analysis was carried out using MATLAB 2014b, to ascertain the influence of drying temperature and drying time on specific energy consumption of oven dryer when drying cashew apple pomace, the regression equation that simulates their relation is presented in equation 24 and the plot in Fig .5

$$E_{kg} = 0.177T+0.353t-21.833, \; R^2=0.9999 \qquad [24]$$

T is the drying temperature (°C) and t is the drying time (m).

Uncertainty analysis

Result of combine uncertainty error analysis presented in Table 3 shows that all the errors fall below the standard threshold of 5 %, this infer that error in measurement are within the acceptable bracket.

Table 3. Experimental combine uncertainty error

	Parameters		Combine uncertainty error		
			60 °C	70 °C	80 °C
1	Effective moisture diffusivity		$\pm1.6310^{-10}$	$\pm1.9211^{-10}$	$\pm1.7010^{-10}$
2	Specific energy consumption		±0.8565	±0.3591	±0.1944
3	Activation energy	±0.6710			

Modelling of moisture ratio of cashew apple pomace

Among the fourteen drying models fitted to each of the three drying moisture ratio data, our proposed model (Luka et al.) performed better than all of them with highest R^2 value of 0.9999, 0.9999 and 0.9997 and lowest RMSE of 0.002789, 0.004539 and 0.008063 at 60, 70 and 80 °C drying temperatures respectively. Also, our proposed model gave the lowest AICc value of -90.5 followed by Demir et al. model with AICc value of -75.2 and AICc value of -38.0 followed by Wang and Singh model with AICc value of -34.1 at 60 °C and 70 °C drying temperatures respectively, however, at 80 °C drying temperature, our proposed model has an AICc value of -5.70 compared to Lewis model which has the lowest AICc value of -20.5, this is possible owing to smaller data size and higher number of estimated model coefficients in our model (19), overall, the model proves adequate and superior at 60 °C and 70 °C drying temperature. The fitted profile of *Luka et al. model* for the three drying temperatures are presented in Figs. 6-8 and the summary of all the fitted model coefficients and performance functions are presented in Tables 4-6.
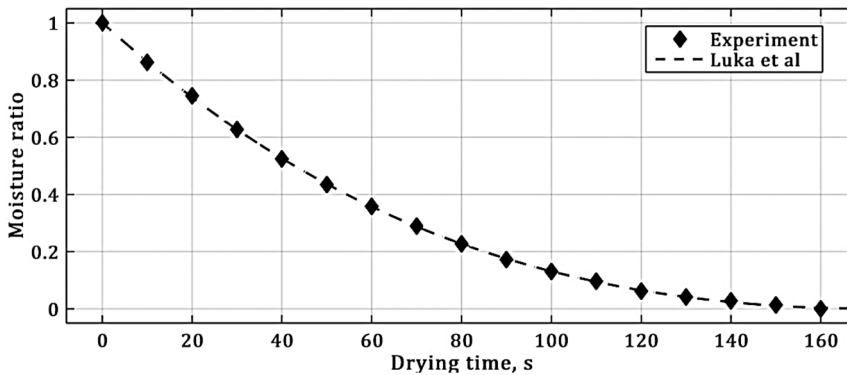
Figure 6. Model and experimental fitted line at 60 °C drying temperature
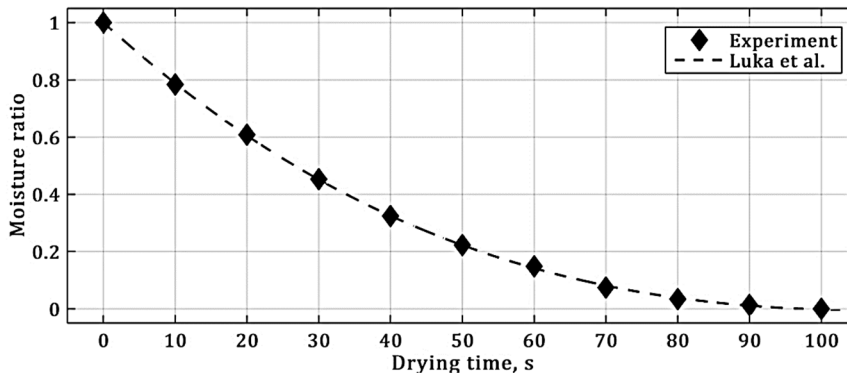
Figure 7. Model and experimental fitted line at 70 °C drying temperature
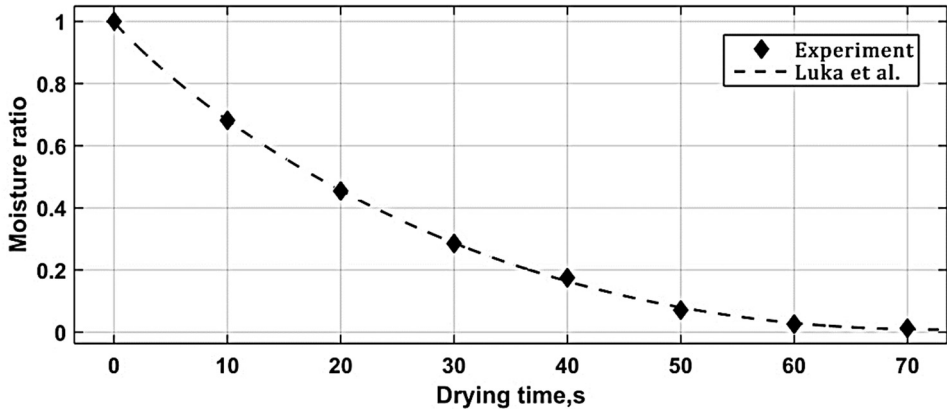
Figure 8. Model and experimental fitted line at 80 °C drying temperature

Table 4. Fitted model coefficients of cashew apple pomace at 60 °C drying temperature

No.	Model	a	b	c	g	h	L	k	n	RMSE	R^2	AICc
1	Demir et al.	1.012	-0.05197					0.00626	1.217	0.004972	0.9998	-75.2
2	Diffusion approach	0.3569	0.001107					10.92		0.1347	0.8218	-26.1
3	Henderson and Pabis	1.052						0.01924		0.0365	0.9869	-50.0
4	Lewis							0.01832		0.03978	0.9845	-45.3
5	Logarithmic		1.15	-0.1347				0.01421		0.01104	0.9990	-62.1
6	Midilli et al.		0.9563	-0.000255				0.00587	1.243	0.005549	0.9998	-67.5
7	Modified Henderson and Pabis	3.898	-3.279	0.3815	0.04229	0.09611		0.031		0.01379	0.9987	-55.2
8	Page							0.006562	1.245	0.01746	0.9972	-57.8
9	Simplified Fick's diffusion equation	1.067					1.209	0.02847		0.04179	0.985	-44.8
10	Two-term exponential	1.775						0.02517		0.01958	0.9965	-56.0
11	Verma et al.	9.123			0.0328			0.03036		0.01691	0.9972	-57.2
12	Wangh and Singh	-0.01343	4.6×10^5							0.0103	0.9990	-67.2
13	Weibull	56.59	1.245							0.01746	0.9972	-55.8
14	*Luka et al. (proposed model)*	*2.291*	*2.874*					*0.007744*	*1.022*	*0.002789*	*0.9999*	*-90.5*

Original scientific paper

Table 5. Fitted model coefficients of cashew apple pomace at 70 °C drying temperature

No.	Model	a	b	c	g	h	k	L	n	RMSE	R^2	AICc
1	Demir et al.	1.073	-0.07761				0.01525		1.132	0.01063	0.9993	-29.4
2	Diffusion approach	4.559	0.8239				0.01518			0.01253	0.9989	-33.8
3	Henderson and Pabis	1.046					0.03098			0.04661	0.9830	-24.9
4	Lewis						0.02973			0.04671	0.9811	-28.1
5	Logarithmic	1.159		-0.1475			0.02242			0.01645	0.9981	-31.1
6	Midilli et al.	0.9949	-0.000593				0.01502		1.155	0.01164	0.9992	-28.5
7	Modified Henderson and Pabis	0.207	4.928	-4.135	0.05206	0.06543	0.7368			0.02102	0.9962	1.377
8	Page						0.01082		1.272	0.0224	0.9961	-32.3
9	Simplified Fick's diffusion equation	1.057					0.05364	1.309		0.05232	0.9810	-19.1
10	Two-term exponential		1.796				0.04115			0.02497	0.9951	-31.2
11	Verma et al.	0.6416			0.02979		0.02979			0.05387	0.9799	-19.2
12	Wangh and Singh	-0.02136	0.0001152							0.01193	0.9989	-34.1
13	Weibull	35.12	1.272							0.0224	0.9961	-32.3
14	*Luka et al. (proposed model)*	*3.198*	*4.27*				*0.01047*		*1.009*	*0.004539*	*0.9999*	*-38.0*

Original scientific paper

Table 6. Fitted model coefficients of cashew apple pomace at 80 °C drying temperature

No.	Model	a	b	c	g	h	k	L	n	RMSE	R^2	AICc
1	Demir et al.	1.069	-0.07004						1.066	0.01119	0.9993	-3.45
2	Diffusion approach	3.834	0.8248				0.02495			0.01445	0.9990	-15.7
3	Henderson and Pabis	1.024					0.04416			0.0392	0.9894	-15.7
4	Lewis						0.04321			0.03583	0.9897	-20.5
5	Logarithmic	1.139		-0.1389			0.03272			0.01138	0.9993	-17.3
6	Midilli et al.		0.9983	-0.0007336			0.02955		1.087	0.01521	0.9989	-1.30
7	Modified Henderson and Pabis	3.622	0.4183	-3.04	0.2864	0.09915	0.07076			0.02306	0.9988	∞
8	Page						0.02247		1.195	0.0211	0.9964	20.0
9	Simplified Fick's diffusion equation	1.029					0.07896	1.335		0.04634	0.9877	7.50
10	Two-term exponential	1.71					0.05717			0.02288	0.9964	19.4
11	Verma et al.	9.072			0.07274		0.06796			0.02038	0.9976	13.2
12	Wangh and Singh	-0.03107	0.0002456							0.02189	0.9967	12.7
13	Weibull	23.94	1.195							0.0211	0.9969	20.0
14	*Luka et al. (proposed model)*	*3.465*	*4.466*				*0.01648*		*0.9582*	*0.008063*	*0.9997*	*5.70*

CONCLUSION

Drying kinetics of cashew apple pomace has been investigated and modelled; it was found that cashew apple pomace dry under falling rate period. Diffusion coefficient is strongly influenced by drying temperature and ranges between 9.02015×10^{-9} and 2.12177×10^{-8} for drying temperature of 60-80 °C. The activation energy required to initiate drying in cashew apple pomace was found to be 41.880 kJ/ K while the specific energy consumption ranges from 24.1 to 45.3MJ/kg with minimum required drying energy obtained at 80 °C drying temperature. Our proposed drying model (Luka et al. model) was found to perform better than all tested models and consequently proofs more adequate in simulating the drying kinetics of cashew apple pomace. Drying parameters are essential to food industries in optimizing dried food quality and dryers' performance and design.

REFERENCES

1   Akubor, P. Chemical composition, functional and pasting properties of cashew pomace and wheat flours. *International Journal of Agricultural and Veterinary Sciences*. **2016**, 28-37.

2. Quiles, A.; Grant, M.; Struck, S.; Rohm, H.; Hernando, I. Fibre from fruit pomace: a review of applications in cereal-based products. *Food Reviews International*. **2016**, doi: http://dx.doi.org/10.1080/87559129.2016.126299.

3. Akubor, P. I.; Egbekun, M. K.; Obiegbuna, J. E. Quality assessment of cakes supplemented with cashew pomace and soybean flour. *Discovery*. **2014**, *9*(20), 8-13.

4. Sagar, N., A.; Pareek, S.; Sharma, S.; Yahia, E., M.; Lobo, M. G. Fruit and vegetable waste: bioactive compounds, their extraction, and possible utilization, comprehensive. *Reviews in Food Science and Food Safety*. **2018**, 1-20. doi: http://dx.doi.org /10.1111/1541-4337.12330

5. Carl, J. B., Greeme, Q.; Floyd, L. H. *Harvesting and postharvest management*. **2019**, 132.

6. Luka, B. S.; Japhet, J. A.; Dauda, P. A. Single layer drying characteristics of hospital too far leaves (jathropher tanjorensis) under open sun and in solar dryer. *Acta technica corviniensis – Bulletin of Engineering*, **2018**, *4*, 83-88.

7. Erbay, Z.; Icer, F. A review of thin layer drying of foods: theory, modeling, and experimental results. *Critical Reviews in Food Science and Nutrition*. **2010**, *50*, 441-464.

8. Gupta, S. V.; Patil, N. Convective drying of osmo-dehydrated sapota slice. International *Journal of Agricultural and Food Science*. **2014**, *5*, 219-226.

9. Kenneth, P. B.; David, R. A. Understanding AIC and BIC in research. *Sociological Methods and Research*. **2004**, *33*(2), 261-30.

10. Sharma, A.; Singh, G.; Singh, B.; Chauhan, N.; Kumar, V.; Yadav, M. K. *Study the drying characteristics of apple pomace*. **2017**. https://www.semanticscholar.org/paper/Study-the-drying-characteristics-of-apple-pomace-Sharma-s. Accessed 14 March 2020.

11. Kumar, N.; Sarkar, B. C.; Sharma, H. K. Mathematical modeling of thin layer hot air drying of carrot pomace, *J. Food Sci. Technol.* **2012,** doi: http://dx.doi.org /10.1007/s13197-011-0266-7.6.

12. Andréia, S. D.; Edson, L. D.; Everaldo, S. D.; Jackson, A. D. Characterization and drying of caja bagasse (spondias mombin l.) in a tray dryer using a factorial planning. *Rev. Bras. Frutic. Jaboticabal.* **2012**, *34*(1), 239-247.

13. De Menezes, M. L.; Kunz, C. C.; Perine, P.; Pereira, N. C.; Dos Santos, O. A. A.; De Barros, S. T. D. Analysis of convective drying kinetics of yellow passion fruit bagasse. *Acta Scientiaru*. **2013**, *35*(2), 291-298, doi: http://dx.doi.org /10.4025/actascitechnol.v35i2.10286.

14. Skriatden, J. Moisture transfer in solid food materials: A review of mechanism, models, and measurements. *International Journal of Food Properties*. **2007**, *10*, 737-777, doi: http://dx.doi.org /10.1080/10942910601161672.

15. Akpinar, E.; Midilli, A.; Bicer, Y. Single layer drying behavior of potato slices in a convective cyclone and mathematical modeling. *Energy Conversion and Management*. **2003**, *44*, 1689-1707.

16. Khanali, M.; Banisharif, A.; Rafiee, S. Modeling of moisture diffusivity, activation energy and energy consumption in fluidized bed drying of rough rice, *Heat Mass Transfer*. **2016**, doi: http://dx.doi.org /10.1007/s00231-016-1763-z.

17. Perry, H.S. Chemical engineer's handbook. **1984**, McGraw Hill, New York.

18. Luka, B. S.; Ejilah, R. I; Owhor, S. C.; Japhet, J. A.; Ibrahim, T. K..; Udom, P. O. (In press). Effect of diesel fuel blend on flame and emission characteristics of used engine oil as heating fuel using swirl waste oil burner. Environmental and Climate Technologies.

19. Ertekin, C.; Firat, M. Comprehensive review of thin layer drying models used in agricultural products.Critical Reviews in Food Science and Nutrition. **2015**. doi: http://dx.doi.org/10.1080/10408398.2014.910493.

20. Fuch, J. Drying- the effect of temperature on relative humidity. http://techblog.ctgclean.com/ 2013/05/drying-the-effect-of-temperature-on-relative humidity/. (Accessed 12 February 2020).

21. Shi, Q.; Zheng Y.; Zhao, Y. Mathematical modeling of thin–layer pump drying of Yacon (*Smallanthuss onchifolius*) slices. *Energy Convers Manage*. **2013**, *71*, 208-216.

22. Yapo, B. M.; Koffi, K. L. Extraction and characterization of highly gelling low methoxy pectin from cashew apple pomace. Foods. **2014**, 3, 1-12, doi: http://dx.doi.org/10.3390/ foods3010001.

23. Woo, K. K.; Chong, Y. Y.; Li Hiong, S. K.; Tang P. Y. Pectin extraction and characterization from red dragon fruit (*Hylorereus polyrhizus*): A preliminary study. *Journal of Biological Science*. **2010**, *10*, 631-636.

24. Schroder, R.; Clark, C. J.; Sharrock, K.; Hallet, I. C.; Macrae, E. A. Pectin from the albedo of immature lemon fruitlets have high water binding capacity. *J. Plant Physiol*. **2004**, *161*(4), 371-379. doi: http://dx.doi.org /10.1078/0176-1617-01275.

25. Amiri, C. R.; Amiri, P. J.; Esna-Ashari, M. Modeling of moisture diffusivity, activation energy and specific energy consumption of high moisture corn in fixed and fluidised bed convective dryer. *Span J Agric Res*. **2011**, *9*, 11.28-40.

26. Karl, F. T. Wafer and waffle, processing and manufacturing. **2017**, pp. 405-486. Elsevier. http://doi.org/10.1016/B978-0-12-809438-9-9.00006-5.

27. Saravacos, G. D.; Maroulis, Z. B. Transport properties of foods. Mercel Dekker: New York, **2001**.

28. Zogzas, N. P.; Maroulis, Z. B.; Marinos-Kouris, D. Moisture diffusivity data compilation in foodstuffs. *Drying Technology*. **1996**, 14, 2225-2253.

29. Motevali, A.; Minaei, S.; Khoshtagaza, M. H. Evaluation of energy consumption in different drying methods. *Enegy Convers. Manag*. **2011**, *52*, 1192-1199.
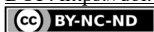
PHYTOCHEMICAL SCREENING, ANTIOXIDANT AND ANTIMICROBIAL ACTIVITIES OF GRAPE (*Vitis vinifera* L.) SEED EXTRACTS FROM *Red globe* AND *Valenci* ALGERIAN VARIETIES

Khadidja Labri[1,4]*, Houria Moghrani[1], Affaf Kord[2], Ahmed Baghdad Doukara[3], Abdelkrim Gueffai[3], Aboun Assia[5]

[1] University of Sciences and Technology Houari Boumediene (USTHB), Faculty of mechanical engineering and process engineering, BP 32 El-Alia Bab-Ezzouar 16111, Algiers, Algeria
[2] University of Sciences and Technology Houari Boumediene (USTHB), Faculty of chemistry, BP 32 El-Alia Bab-Ezzouar 16111, Algiers, Algeria
[3] Department of process engineering, Faculty of Sciences and Technology, University of Mascara - BP 305, Mamounia Mascara Road, Mascara, Algeria
[4] Department of process engineering, institution of sciences, Tipaza University Center, Morsli Abdellah, Oued Merzouk city, Tipaza, Algeria
[5] Laboratory of Veterinary Bacteriology, Pasteur Institute, Annex El Hamma, 01. Street of Dr Laveran - El Hamma – Algiers - Algeria

Until now, there is no documentation concerning the composition, biological and pharmaceutical activities of Algerian grape (Vitis vinifera L.) seeds. The present study aims to evaluate the phytochemical analysis, antioxidant and antimicrobial activities of grape seed extracts (GSEs) from the Algerian Red globe and Valenci varieties. The total polyphenols content (TPC) in the GSEs was evaluated by spectrophotometry, it was 398.01 ± 18.12 mg GAE/g GSEs and 335.11 ± 11.44 mg GAE/g GSEs for the Red globe and Valenci varieties respectively. The antioxidant activity of GSEs was also evaluated by spectrophotometry on stable free radicals of DPPH. The IC$_{50}$ for the Red globe variety was 4 ± 0.2 μg/ml, while for the Valenci variety it was 4.6 ± 0.36 μg/ml. The antimicrobial activity was determined using the disk diffusion method. Both extracts showed antimicrobial activity against the eight studied strains: Escherichia coli, Pseudomonas aeruginosa, Pasteurella sp., Salmonella sp., Staphylococcus aureus, Streptococcus faecalis, Clostridium sp., and Candida albicans. The extracts produced a clear inhibition zone for all the tested strains. Inhibition diameters greater than 19 mm were registered. The obtained results in this study indicate the differences between the Red globe and Valenci varieties, in terms of polyphenol content, antioxidant and antimicrobial activities in Algerian GSEs.

Keywords: grape seed extract, antioxidant activity, antimicrobial, Algerian *Vitis vinifera* L., phytochemical screening, DPPH radical scavenging, *Red globe*, *Valenci*, total phenolics

INTRODUCTION

One of the most important fruit crops in the world is grapes (*Vitis vinifera* L.) (1, 2) and its seeds are considered as an excellent source of polyphenolic compounds especi-

---

* Corresponding author: Khadidja Labri, University of Sciences and Technology Houari Boumediene (USTHB), Faculty of mechanical engineering and process engineering, BP 32 El-Alia Bab-Ezzouar 16111, Algiers, Algeria, e-mail: labrikhadidaja@yahoo.com

Original scientific paper
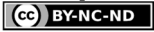
ally, catechins, epicatechins, monomeric gallic acids, polymeric, and oligomeric procya-nidins (2, 3). Grape seeds are an important part of the pomace, corresponding to 38-52% of dry matter (4). So, grape seeds are often considered as an important agricultural and industrial waste (5). In fact, Algeria is one of the richest countries in grape varieties. Worldwide, the composition, biological and pharmaceutical activities of GSEs from different varieties are very well documented, unlike the seeds of Algerian grape varieties. In this context, finding solutions to treat these wastes and developing new products would be an excellent opportunity. GSEs may be a good option, as there may be many health benefits related to their composition, especially concerning polyphenolics compounds. Thus, the possibility of reusing grape seeds is of considerable importance (5). On the other hand, in 2012 some studies have indicated that GSEs may have antibacterial and antioxidant activities (2). Also, due to its rich contents of polyphenols like proanthocyani-dins, GSEs have been proved to have the significant antioxidant ability (6-8). Besides, GSE has attracted considerable attention because of its interesting antimicrobial properties (6, 9, and 10). Recent studies have found the ability of GSEs to inactivate *Listeria monocytegenes, Bacillus cereus*, *Staphylococcus aureus*, *Bacillus subtilis*, *Lactobacillus fermentum*, *Escherichia coli*, *Streptococcus thermophilus*, *Pseudomonas aeruginosa*, and *Lactobacillus vaginalis* (6, 11). The objectives of this work were to screen the phytochemical composition, to study the antioxidant and antimicrobial activities of *grape seed extracts from Red globe and Valenci Algerian varieties*. GSEs of these two varieties were examined against eight microbial strains: *Escherichia coli* ATCC *25922, Pseudomonas aeruginosa* ATCC 27853*, Pasteurella* sp*., Salmonella sp*., *Staphylococcus aureus ATCC 25923, Streptococcus faecalis* ATCC 29212*, Clostridium* sp., and *Candida albicans.*

EXPERIMENTAL

Plant material

The samples of *Vitis vinifera L.* (*Red globe* and *Valenci*) were collected at maturity from the north-western province of Algeria at Mascara, in November 2017, exactly at 35°23'47.9" N and 0°8'25" E. Uninfected and germ-free fruit was washed with water to remove pesticide residues. The grape seeds were manually freed of pulp and skin, and dried at room temperature in the shad.

Extraction procedure

The dried grape seeds were ground into powder using a blender (Molinex®). The obtained powder was macerated in the dark with 80% methanol-water hydroalcoholic solution for 24 hours, and then the resulting flotation liquid was decanted. The remaining powdered sediment was washed with 80% methanol three more times, and the combined supernatants were vacuum filtered through a double layer of Whatman filter paper. The extracts (GSEs) were concentrated in a rotary evaporator and were kept in airtight containers at 4 °C until further use (20).
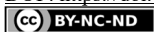
Qualitative Phytochemical Screening

Specific standard methods were used for the qualitative phytochemical screening of medicinal plant parts.

Coumarins test. 20 ml of diethyl ether was added to 0.5 g of vegetable powder. The mixture was macerated for 24 hours. After filtration and evaporation of the ether using a water bath, the dry residue obtained was mixed with 0.5 ml of 25% NH_4 OH. The observation of intense fluorescence under UV light at 366 nm in the tube indicates the presence of coumarins (12).

Test for anthracene derivatives. In a test tube, 1 g of vegetable powder was added to 10 ml of $CHCl_3$. After heating in a water bath for 15 minutes, the volume of the filtrate was filled to 10 ml with chloroform. Then, a 10% aqueous solution of KOH was added to the chloroform extract. After stirring, the presence of anthraquinones was confirmed by turning the aqueous phase to the red color (12).

Alkaloids test. 1 g of the plant material was mixed with 5 ml of a 10% $H_2 SO_4$ solution. The resulting mixture was stirred for 24 hours at room temperature. This mixture was then filtered and the volume was completed with 5 ml of distilled water, and then 1 ml of the mixture was taken separately in two test tubes (12). Few drops of Dragendorf's reagent (potassium iodide-bismuth nitrate) were added in the tube and the appearance of orange-red precipitate was taken as positive. Few drops of Mayer's reagent (composed of mercuric chloride and potassium iodide dissolved in distilled water) were added to the second tube and the appearance of buff-colored precipitate designates the existence of alkaloids (13).

Flavonoids test. 5 ml of ethanol was added to 500 mg of dry powder; the mixture was heated slightly and then filtered. The liquid filtrate was then added to a few pieces of magnesium shavings. A few drops of concentrated HCl were then introduced into the mixture. The presence of a pink, orange, or red to purple coloration indicates the existence of flavonoids (13).

Cardenolide test. 1 g of powdered grape seeds was added to 10 ml of 80% alcohol and stirred vigorously. The mixture was filtered and then lead acetate, water, and chloroform were added and allowed to evaporate to dryness. Ferric chloride and concentrated sulphuric acid were then added according to the method of Trease and Evans (14). The presence of cardenolide was confirmed by the formation of brown rings (15).

Saponins test. According to the French pharmacopeia's operating method. The extract was subjected to a foaming test for the identification of saponins. One gram of the powdered grape seeds was placed in 100 ml of distilled water, boiled for 30 minutes, then filtered and adjusted to 100 ml after cooling. In a series of 10 test tubes of 20 cm high and 10 mm in diameter. 1, 2, 3, ... 10 ml of extract was introduced successively and the volume of each tube was adjusted to 10 ml with distilled water. Each tube was shaken for 15 seconds (two shakes per second). The tubes were allowed to stand for 15 min and the foam height in each tube was measured. The foam index (If) was calculated according to the formula If = 1000/N, where N represents the number of tubes with a foam height is 1cm (16).

Characterization of reducing compounds. In a beaker, 3g of plant material was added to 20 ml of 50% ethanol, and then the mixture was heated for 15 minutes. The

sample was filtered and the filtrate was tested next: 3 ml of the ethanoic extract was treated with 5 ml of distilled water and a few drops of Fehling's solution. After heating, a positive test was revealed by the formation of a brick-red precipitate (17).

Tannins test (Ferric chloride test). Two milliliters (2 ml) of the aqueous solution of the GSEs were added to a few drops of 10% Ferric chloride solution (light yellow). The occurrence of the blackish blue color showed the presence of gallic tannins and a green-blackish color indicated the presence of catechol tannins (13-18).

Liebermann–Burchard test for sterols and triterpenes. 0.5 of vegetable powder was agitated with 10 ml of ethyl ether for 24 hours. The mixture was then filtered and adjusted to 10 ml. A mixture of 0.1 ml of acetic anhydride and 0.1 ml of chloroform was added to the residue obtained by steaming 1 ml of the ether solution. 0.1 ml of concentrated H_2SO_4 was added to the previous solution. Blue indicates the presence of sterols, whereas red indicates the presence of triterpenes (12, 19).

Total phenolics in GSEs

The quantity of total soluble polyphenols in GSE was quantified by spectrophotometry according to the Folin-Ciocalteau method (21-22). Gallic acid was used as a calibration standard and the results were presented as gallic acid equivalents (GAE) in milligrams per 1 gram of dry seed extract. All analyses were performed in triplicate and the results averaged (22).

Antioxidant assay: DPPH radical scavenging

The antiradical activity of plant extracts was determined by the DPPH radical scavenging assay according to the method adopted by Orphanides et al (23). A volume of 3.9 ml of DPPH$^\bullet$ solution (0.04 mM) was mixed with 100 μl of plant extract prepared at different concentrations (10, 9, 8, 7, 6, 5, 4, 3, 2 and 1 μg ml^{-1}) and incubated for 30 min at room temperature. The absorbances were then measured by a spectrophotometer (Jenway 6315-United Kingdom) set to 517 nm. Butylated hydroxytoluene (BHT) and Ascorbic Acid (AA) were used as a standard antioxidant. The capability to scavenge the DPPH radicals was calculated using the following equation (24):

$$A_{DPPH^\bullet} (\%) = 100 \times (A_{Control} - A_{Sample})/A_{Control}$$

Where $A_{Control}$ is the absorbance of the control reaction (containing all reagents except for the extract) and A_{Sample} is the absorbance in the presence of the GSEs. The values of antioxidant activity were investigated for the various concentrations of the GSEs (24, 23).

Microorganisms' preparation

Microorganisms were obtained from the culture collections of the Department of Microbiology at the *Pasteur Institute of Algeria.* The strains were as follows: four Gram-negative bacteria *Escherichia coli* ATCC *25922, Pseudomonas aeruginosa* ATCC 27853*, Pasteurella* sp.*, Salmonella sp.,* three Gram-positive bacteria *Staphylococcus aureus*

Original scientific paper

ATCC 25923, Enterococcus (or *Streptococcus) faecalis* ATCC 29212, *Clostridium* sp.*,* and the yeast *Candida albicans.*

Antimicrobial activity studies

Antimicrobial activity was determined by the Agar disk diffusion test. The strains were grown on Mueller-Hinton (bacteria) or Sabouraud Dextrose slants (yeasts) 24 h at 37 °C. After incubation, the strains were suspended in a sterile physiological solution. Inocula were prepared by diluting cultures to 0.5 McFarland standards turbidity. The grape seed extracts were dissolved in a 50% (V/V) aqueous solution of dimethylsulfoxide (DMSO) to obtain the concentrations listed in Table 2 (c_1= 0.4 mg/ disk to c_5 =12.8 mg/disk).

Statistic analysis

All measurements in this study were carried out in triplicate (n=3), and were presented as means ± SD. Values were calculated using Microsoft Office Excel 2010.

RESULTS AND DISCUSSION
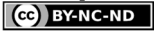
Phytochemical analysis

The phytochemical analysis is a crucial preliminary step since it reveals the presence of constituents known by their physiological activities and possessing medicinal virtues. The phytochemical screening of Algerian GSEs is shown in Table 1. The results revealed the presence of important secondary metabolites which are tannins (gallic), flavonoids, coumarins, reducing substances, cardenolides, anthracene derivatives, and saponosides. Whereas, the alkaloids were absent in GSEs.

Table 1. Summary table of detection of secondary metabolites in Algerian GSEs

Secondary metabolites	GSEs (*Red globe* and *Valenci varieties*)
Flavonoids (flavon)	+++
Tannins (galliques)	+++
Coumarins	++
Anthracene derivatives	+++
Alkaloids	-
Saponosides	++
Cardenolides	++
Reducing compounds	++
Triterpenes	+

(+++), (++), (+) and (-) refer to, high, moderate ,low and absent amount, respectively

The results are somewhat similar to those obtained from the literature, the differences are in coumarins, alkaloids and saponosides metabolites. According to Buvaneswari et al**.** (25), Hanaa et al**.** (26), and Hassan et al**.** (27), saponosides are absent in Indian and Egyp-

tian varieties, while they are present in those of Algeria. Moreover, the researches of Hanaa et al. and Buvaneswari et al. confirmed the presence of alkaloids in Egyptian and Indian grape seeds. On the *contrary, our results show* that Algerian grape seeds are free of alkaloids. Furthermore, Hassan et al proved the absence of coumarins, whereas they are present in Algerian varieties.

Quantitative analysis of total phenolic components

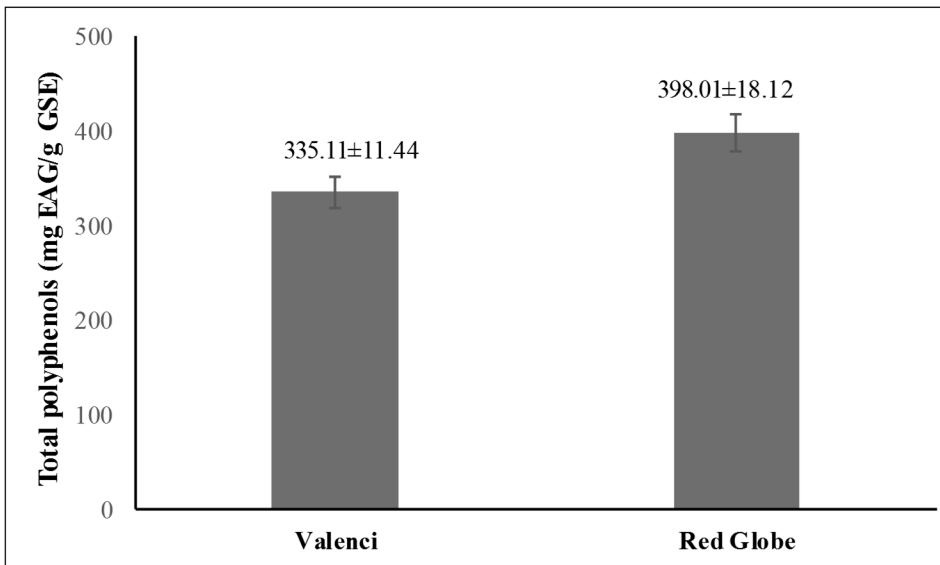The results of the spectrophotometric analysis of polyphenolic components are shown in Figure 1.

Figure 1. Total polyphenols in two varieties of Algerian *Vitis vinifera L.*

The *Red globe* variety has the highest polyphenol content (398.01 ± 18.12 mg EAG/g of GSE), followed by the *Valenci* one (335.11 ± 11.44 mg EAG/ g of GSE). Hanaa et al (25) reported similar results in the methanolic extract of grape seed in the order of 372.5 ±5.00 mg EAG/g GSE for Egyptian varieties. More significant content has been recorded in the Turkish GSEs, the results ranged between 506.60 ± 19.78 mg EAG/g GSE and 589.09 ± 10.14 mg EAG/ g GSE using Soxhlet extraction with a ratio of 90:9.5:0.5 acetone:water:acetic acid (10).   The polyphenol content is closely linked to the extraction solvent used to extract these substances from plant material. Hanaa et al. (25) measured the content of total phenolic in grape seed extracts prepared by using different solvents: water, methanol, 70% acetone and 70% ethanol, a significant difference between the results was found with the lowest recorded for the aqueous extract (186±8,485 mg EAG/g GSE) and the highest for the hydroacetone extract (528±16.97 mg EAG/g GSE).

Antioxidant activity of GSEs

The antioxidant activity of GSEs was determined in vitro by the DPPH method. The percentages of inhibited DPPH versus extract, AA, and BHT concentrations were plotted to obtain the IC_{50} index. This latter is defined as the necessary antioxidant concentration to decrease 50% of the initial DPPH˙ concentration. The values of the IC_{50} are recorded in Figure 2.
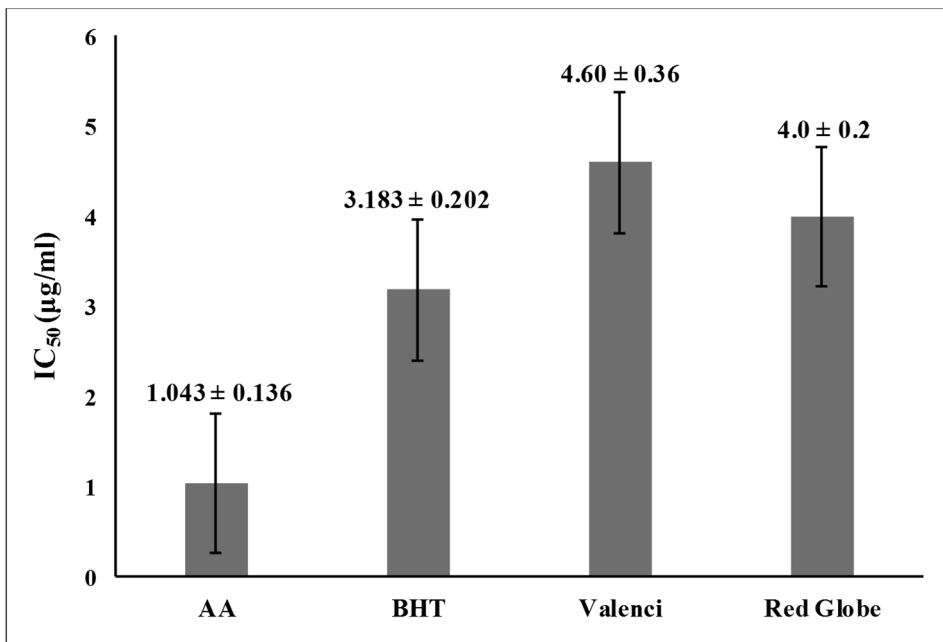

Figure 2. Comparison of the two Algerian varieties of *Vitis vinifera L* and reference products according to the IC_{50} value

According to the results reported in figure 2, the highest antioxidant effect is found in GSE of the *Red globe* with an $IC_{50} = 4 \pm 0.2$ µg/ml, followed by the extract of the *Valenci*, which yielded an IC_{50} of 4.6 ± 0.36 µg/ml. The two GSEs of *Red globe* and *Valenci* varieties have excellent antioxidant power and this in comparison with the reference products, AA ($IC_{50} = 1.043 \pm 0.136$ µg/ml) and BHT ($IC_{50} = 3.183 \pm 0.202$ µg/ml). These results are in accordance with the phenolic contents in both plant varieties. In fact, polyphenols are known for their high capacity to scavenge DPPH˙ radicals. Comparing with the study of Hanaa et al (26), it is noted that among the different solvents used, grape seed acetone extract was the most antioxidant compared to methanolic extract. Thus, Bagchi et al. (28) reported the superior antioxidant effect of GSE compared to other known antioxidants, including vitamin C, vitamin E, and β-carotene (28, 29).
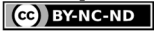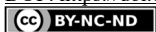
Antimicrobial activity

The results of the antimicrobial activity of two grape seed extracts from *Red globe* and *Valenci* varieties are presented in Table 2.

Table 2. Antimicrobial activity of the GSEs of *Red globe* and *Valenci* varieties from Algerian *Vitis vinifera L*

		C1= 0.4	C2=0.8	C3=1.6	C4=3.2	C5=6.4	C6=12.8
		mg/disk					
E.Coli	Valenci	12± 0.5	13.2± 0.61	13.68± 0.32	14.83± 0.28	15.2± 0.35	15.83± 0.29
	Red globe	11.66±0.57	13.83±0.763	14.83±0.76	17.16±0.29	18.5±0.5	19.17±0.29
S.aureus	Valenci	Ø	10.33±0.57	11.9±0.36	12.36±0.32	13.33±0.29	13.33±0.288
	Red globe	12.66±1.60	13±0.86	13.83±0.29	14.66±0.29	16.35±0.13	17.16±0.29
E. faecalis	Valenci	Ø	9.33±0.57	11±0.5	12.16±0.58	13.25±0.5	13.83±0.58
	Red globe	12.83±0.28	13.33±0.14	14.23±0.25	15.05±0.18	16.18±0.16	18.16±0.29
P.aeruginosa	Valenci	8.5±0.5	9.5±0.5	11.6±0.61	11.98±0.03	12.95±0.09	13.67±0.29
	Red globe	11.816±0.16	12.33±0.57	14.4±0.17	13.86±0.32	14.2±0.61	15.08±0.38
C. albicans	Valenci	10.85±0.304	12.58±0.38	13.03±0.057	15.33±0.76	16.93±0.12	17±0.5
	Red globe	10.01±0.011	10.88±0.34	12.9±0.79	14.6±0.36	16.23±0.25	16.33±0.289
Pasteurella. sp.	Valenci	12.05±0.08	13.416±0.52	16.05±0.08	17.03±0.05	18.01±0.029	17.93±0.81
	Red globe	11.5±0.86	13.16±0.14	15.66±0.57	14.83±0.29	14.67±0.28	15.83±0.28
Salmonella sp.	Valenci	Ø	Ø	Ø	12.16±0.28	12.33±0.58	12.08±0.14
	Red globe	Ø	Ø	Ø	11.33±0.58	13.42±0.52	14.08±0.38
Clostridium sp.	Valenci	Ø	Ø	Ø	Ø	11.67±0.29	12.08±0.14
	Red globe	Ø	Ø	Ø	Ø	13.75±0.25	14.16±0.14

Ø – no activity (growth around disk)

In this study, the results are expressed by the diameter of the inhibition zone (mm) around each disk. The GSEs proved to be effective on the different tested strains. The results indicate that for the strains: *Escherichia coli* ATCC 25922, *Staphylococcus aureus* ATCC 25923, *Streptococcus faecalis* ATCC 29212, *Pseudomonas aeruginosa* ATCC 27853, *Salmonella* sp. and *Clostridium* sp. the *Red globe* variety has a higher antimicrobial potential than the *Valenci* one. This latter, on the other hand, generates greater antimicrobial activity against the *Candida albicans* and *Pasteurella* sp. strains. The best results were recorded for *Escherichia coli* and *Streptococcus faecalis* with an inhibition diameter of 19.166±0.288 mm and 18.166±0.288 mm respectively, for the highest concentration of the *Red globe* variety. This shows high sensitivity (very sensitive if the inhibition diameter is between 15 and 19 mm). The inhibition zone was directly proportional to the concentration of GSEs. Therefore, the highest concentration (C6 = 12.8 mg/disk) always provides the best antimicrobial effects. Comparing with the results of Bayader et al. (10), the Turkish GSEs gave higher inhibition zones than those illustrated by our extracts because of the difference in polyphenol content. From the registered results, it is clear that each variety has significant antimicrobial activity against certain microbial strains. Hence, antimicrobial activity depends on the quality as well as the quantity of the active biomolecules present in the plant material. In this context, previous research con-

ducted by Avato et al (30), De Souza et al (31), Abbassy et al (32) and Akhtar et al (33) have shown that saponosids, coumarins and cardenolides could be responsible for the antimicrobial effect.

CONCLUSION

The present study falls within the valorization of Algerian medicinal plants. The phytochemical analysis of the GSEs of *Red globe* and *Valenci* varieties from Algerian *Vitis vinifera L.* revealed the presence of important secondary metabolites such as tannins (gallic), flavonoids, coumarins, reducing substances, cardenolides, anthracene derivatives, and saponosides. This group of metabolites offers an interest in the therapeutic investigation in grape seeds. Oppositely, the same test proved the absence of alkaloids. The obtained results indicate that the GSEs of both varieties are a rich source of polyphenol with significant antioxidant activity. The *Red globe* variety registered a high amount of polyphenol to that of the *Valenci* one. The calculated IC_{50} values confirmed an excellent DPPH scavenging activity of the extracts. The highest antioxidant effect is reported for the *Red Globe* GSE, followed by the *Valenci GSE*. Concerning the antimicrobial activity, the obtained results show that the two Algerian varieties have a significant antimicrobial potency against the eight microbial studied strains. Both varieties inhibited microbial growth with different diameters of inhibition that depends on the concentration of the extracts. Based on these comparisons, we conclude that each variety has significant antimicrobial activity against certain microbial strains. Thus, this activity depends on the quality and quantity of the active substances of each variety. The results of this study could be exploited in many fields: in pharmaceuticals, for example, to fight against oxidative stress and/or infectious diseases caused by pathogenic germs. Also, in the food industry, grape seed extracts could be used in the preservation of food and drinks as a food additive.

Acknowledgements

REFERENCES

1. Winkler, A. J.; Cook, J. A.; Kliewer, W. M.; Lider, L. A. General viticulture. Berkeley and Los Angeles: University of California Press. **1997**.
2. Delgado Adámez, J.; Gamero Samino, E.; Valdés Sánchez, E.; González-Gómez, D. In Vitro Estimation of the Antibacterial Activity and Antioxidant Capacity of Aqueous Extracts from Grape-Seeds (Vitis Vinifera L.). *Food Control.* **2012**, *24* (1–2), 136–141.

Original scientific paper

3. Monagas, M.; Gómez-Cordovés, C.; Bartolomé, B.; Laureano, O.; Ricardo Da Silva, J. M. Monomeric, Oligomeric, and Polymeric Flavan-3-Ol Composition of Wines and Grapes from Vitis Vinifera L. Cv. Graciano, Tempranillo, and Cabernet Sauvignon. *J. Agric. Food Chem.* **2003**, *51* (22), 6475–6481.

4. Maier, T.; Schieber, A.; Kammerer, D. R.; Carle, R. Residues of Grape (Vitis Vinifera L.) Seed Oil Production as a Valuable Source of Phenolic Antioxidants. *Food Chem.* **2009**, *112* (3), 551–559.

5. Fernandes, L.; Casal, S.; Cruz, R.; Pereira, J. A.; Ramalhosa, E. Seed Oils of Ten Traditional Portuguese Grape Varieties with Interesting Chemical and Antioxidant Properties. *Food Res. Int.* **2013**, *50* (1), 161–166.

6. Zhao, X.; Chen, L.; Zhao, L.; He, Y.; Yang, H. Antimicrobial Kinetics of Nisin and Grape Seed Extract against Inoculated Listeria Monocytogenes on Cooked Shrimps: Survival and Residual Effects. *Food Control* **2020**, *115* (March), 107278.

7. Chen, L.; Zhou, Y.; He, Z.; Liu, Q.; Lai, S.; Yang, H. Effect of Exogenous ATP on the Postharvest Properties and Pectin Degradation of Mung Bean Sprouts (Vigna Radiata). *Food Chem.* **2018**, *251* (April 2017), 9–17.

8. Haskaraca, G.; Juneja, V. K.; Mukhopadhyay, S.; Kolsarici, N. The Effects of Grapefruit Seed Extract on the Thermal Inactivation of Listeria Monocytogenes in Sous-Vide Processed Döner Kebabs. *Food Control* **2019**, *95*, 71–76.

9. Jayaprakasha, G. K.; Selvi, T.; Sakariah, K. K. Antibacterial and Antioxidant Activities of Grape (Vitis Vinifera) Seed Extracts. *Food Res. Int.* **2003**, *36* (2), 117–122.

10. Baydar, N. G.; Sagdic, O.; Ozkan, G.; Cetin, S. Determination of Antibacterial Effects and Total Phenolic Contents of Grape (Vitis Vinifera L.) Seed Extracts. *Int. J. Food Sci. Technol.* **2006**, *41* (7), 799–804.

11. Tabasco, R.; Sánchez-Patán, F.; Monagas, M.; Bartolomé, B.; Victoria Moreno-Arribas, M.; Peláez, C.; Requena, T. Effect of Grape Polyphenols on Lactic Acid Bacteria and Bifido-bacteria Growth: Resistance and Metabolism. *Food Microbiol.* **2011**, *28* (7), 1345–1352.

12. **B**edou, F. Etude phytochimique et activités biologiques de deux plantes médicinales sahariennes Rumex vesicarius L. et Anvillea radiata Coss. & Dur. Ph.D Thesis. Université Abou Bekr Belkaid , Tlemcen Algérie. 2015.

13. Gacem, M. A.; Telli, A.; Gacem, H.; Ould-El-Hadj-Khelil, A. Phytochemical Screening, Antifungal and Antioxidant Activities of Three Medicinal Plants from Algerian Steppe and Sahara (Preliminary Screening Studies). *SN Appl. Sci.* **2019**, *1* (12), 1–13.

14. Trease, G. E.; Evans, W. C. A Textbook of Pharmacognosy, Bailliere Tinall Ltd, London, 1989.

15. Fasina, K. A.; Adesetan, T. O.; Oseghale, F.; Egberongbe, H. O.; Aghughu, O. O.; Akpobome, F. A. Bacteriological and Phytochemical Assessment of Ficus Asperifolia Linn. Infusion. *Biomed Res. Int.* **2020**, *2020*.

16. Saihi , R. Etude phytochimique, Extraction des produits actifs de la plante Artemisia campestris de la région de Djelfa. Mise en évidence de l'activité biologique. Mémoire pour l'obtention de magister en chimie organique. Université d'Oran, Algérie. 2011.

17. Berreghioua, A. Investigation phytochimique sur des extraits bioactifs de deux Brassicaceae E medicinales du sud algérien :*Moricandia arvensis et Zilla macroptera*, Ph.D Thesis. Université Abou Bekr Belkaid , Tlemcen Algérie. 2016.

18. Auwal, M. S.; Saka, S.; Mairiga, I. A.; Sanda, K. A.; Shuaibu, A.; Ibrahim, A. Preliminary Phytochemical and Elemental Analysis of Aqueous and Fractionated Pod Extracts of Acacia Nilotica (Thorn Mimosa). *Vet. Res. forum an Int. Q. J.* **2014**, *5* (2), 95–100.

19. Dhayalan, A.*; Gracilla, D.E.; Peña Jr, R.A.D.; Malison, M.T.; Pangilinan, C.R* . Phytochemical constituents and antimicrobial activity of the ethanol and chloroform crude leaf extracts of *Spathiphyllum cannifolium* (Dryand. ex Sims) Schott. J Pharm Bioall Sci . **2018,** 10(1), 15–20.

20. Da Porto, C.; Porretto, E.; Decorti, D. Comparison of Ultrasound-Assisted Extraction with Conventional Extraction Methods of Oil and Polyphenols from Grape (*Vitis Vinifera* L.) Seeds. *Ultrason. Sonochem.* **2013**, *20* (4), 1076–1080.

21. Singleton , V. L.; R, Orthofer.; R. M, Lamuela-Raventós. Analysis of Total Phenols and Other Oxidation Substrates and Antioxidants by Means of Folin-Ciocalteu Reagent. *Meth Enz.* *1*999, *299* (1974), 152-178.

22. Mandic, A.; Djilas, S.; Canadanovic-Brunet, J.; Cetkovic, G.; Vulic, J. Antioxidant Activity of White Grape Seed Extracts on DPPH Radicals. *Acta Period. Technol.* **2009**, *220* (40), 53–61.

23. Orphanides, A.; Goulas, V.; Gekas, V. Effect of Drying Method on the Phenolic Content and Antioxidant Capacity of Spearmint. *Czech J. Food Sci.* **2013**, *31* (5), 509–513.

24. Vulić, J. J.; Tumbas, V. T.; Savatović, S. M.; Dilas, S. M.; Ćetković, G. S.; Čanadanović-Brunet, J. M. Polyphenolic Content and Antioxidant Activity of the Four Berry Fruits Pomace Extracts. *Acta Period. Technol.* **2011**, *42*, 271–279.

25. Buvaneswari, K. M.; Sumayaa, S. Qualitative Phytochemical Analysis of Grape Seed. *Int. J. Reserch Anal. Rev.* **2020**, *6* (2), 0–4.

26. Hanaa, M. A.; Elshafie, M. A.; Ismail, H. A.; Mahmoud, M. E.; Ibrahim H.M. Chemical Studies and Phytochemical Screening of Grape Seeds (*Vitis vinifera* L .). *Minia J. Agric. Res. Dev.* **2015**, *35* (2), 313–325.

27. Hassan, E. M.; Shalaby, E.; Abou Baker, D.H. Phytochemical Investigation and Radical Scavenging Activity of Wastes of Some Grape Varieties Grown in Egypt. *Glob. J. Pharmacol.* **2013**, *7* (4), 465–473.

28. Bagchi, D.; Sen, C. K.; Ray, S. D.; Das, D. K.; Bagchi, M.; Preuss, H. G.; Vinson, J. A. Molecular Mechanisms of Cardioprotection by a Novel Grape Seed Proanthocyanidin Extract. *Mutat. Res. - Fundam. Mol. Mech. Mutagen.* **2003**, *523–524*, 87–97.

29. Dasgupta, A.; Klein, K. Herbal and Other Dietary Supplements That Are Antioxidants. *Antioxidants Food, Vitam. Suppl.* **2014**, 295–315

30. Avato, P.; Bucci, R.; Tava, A.; Vitali, C.; Rosato, A.; Bialy, Z.; Jurzysta, M. Antimicrobial Activity of Saponins from Medicago Sp.: Structure-Activity Relationship. *Phyther. Res.* **2006**, *20* (6), 454–457.

31. De Souza, S. M.; Delle Monache, F.; Smânia, A. Antibacterial Activity of Coumarins. *Zeitschrift fur Naturforsch. - Sect. C J. Biosci.* **2005**, *60* (9–10), 693–700.

32. Abbassy, M. A.; Kadous, E. A.; Marei, G. I. K. Isolation and Identification of Cardenolide Compounds of Gomphocarpus Sinaicus and Their Fungicidal Activity Against Soil Borne and Post Harvest Fungi. *J. Life Sci.* **2012**, *6*, 985–994.

33. Akhtar, N.; Malik, A.; Noor Ali, S.; Kazim, S. U. Proceragenin, an Antibacterial Cardenolide from Calotropisprocera. *Phytochemistry.* **1992**, *31* (8), 2821–2824.
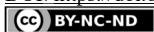
ENCAPSULATION OF CAROTENOIDS EXTRACTED FROM TOMATO WASTE

Slađana M. Stajčić, Gordana S. Ćetković, Jasna M. Čanadanović-Brunet,
Vesna T. Tumbas Šaponjac, Jelena J. Vulić, Vanja N. Šeregelj*

University of Novi Sad, Faculty of Technology Novi Sad, Bulevar Cara Lazara 1, 21000 Novi Sad

Utilization of carotenoids as a nutraceutical ingredients or natural colorants within foods is currently limited due to their instability. Encapsulation is one of the prominent means used to improve carotenoid stability. In this study the content of bioactive compounds (lycopene, β-carotene and phenolics) and antioxidant activity (DPPH, ABTS, superoxide anion and reducing power test) were investigated in the tomato waste extract. Based on the obtained results, tomato waste showed high contents of lycopene (13.72 mg/100 g DW), β-carotene (12.36 mg/100 g DW) and phenolic compounds (203.33 mg/100 g DW). Also, high values of antioxidant activity were determined in all applied tests. To protect extracted sensitive carotenoid compounds (lycopene and β-carotene) tomato waste extract was encapsulated with various encapsulating materials (soy protein, pea protein, inulin and gum arabica) by freeze drying method. The influence of applying different encapsulating materials on the encapsulation efficiency of carotenoids (lycopene and β-carotene) was studied. Also, obtained encapsulates were characterized in terms of water activity, moisture content, hygroscopicity, flowability, density ratios and particles size. Encapsulate on the basis of gum arabic showed highest encapsulation efficiency of β-carotene (53.47%), while encapsulate prepared with soy protein as encapsulating material showed highest encapsulation efficiency of lycopene (51.44%). The results of this study support the need for preparation of encapsulates with different encapsulating material and evaluation of their characteristics with the aim of development powder forms suitable for supplementation and food fortification.

Keywords: tomato waste, bioactive compounds, lycopene, β-carotene, encapsulation

INTRODUCTION

Tomatoes (*Lycopersicum esculentum*) are considered richer sources of several bioactive antioxidants, such as lycopene, β-carotene, flavonoids, phenolic acids, ascorbic acid, in addition to basic nutritional compounds (1, 2). The evidences suggest that health benefits of tomato have been principally ascribed to its phenolics (flavonoids, phenolic acids, etc.), vitamin C content and carotenoid constituents (particularly lycopene and β-carotene) (3).

As one of the most popular vegetables in the world, tomato is used both in fresh as well as in processed forms in food preparations (4, 5). Although tomatoes are commonly consumed fresh, over 80% of the tomato consumption comes from processed tomato pro-

---

* Corresponding author: Slađana M. Stajčić, University of Novi Sad, Faculty of Technology Novi Sad, Bulevar Cara Lazara 1, 21000 Novi Sad, Serbia, e-mail: sladja@uns.ac.rs

ducts such as tomato juice, paste, puree, ketchup and sauce (6). During commercial processing of tomato a large quantity of waste at different stages is generated. The major part of the tomato waste is the tomato pomace that comes from the pulper (5). The wet pomace contains 33% seed, 27% skin and 40% pulp, while the dried pomace contains 44% seed and 56% pulp and skin (7). On average, tomato pomace accounts for approximately 3-5% (w/w) of the raw material applied for processing (8).

Generally, agro-industrial by-products are a valuable resource for bioactive compounds such as polyphenols, carotenoids, dietary fibers and others (9). Tomato processing wastes contain high quantities of the above mentioned bioactive compounds (8). Due to the increasing demand for natural additives in food production the valorization of bioactive compounds from tomato wastes gained substantial interest (9). Incorporation of β-carotene and lycopene in various food systems is limited by their instability in presence of light, heat, and oxygen (10, 11). Among several strategies to protect carotenoids, encapsulation is one that has been often applied and was found to enhance the stability of carotenoids (12). The protective mechanism of encapsulation is to form a membrane (wall system) to enclose the droplets or particles of the encapsulated material (core) (13).

For the encapsulation of bioactive compounds different techniques and wall materials have been used (14). Among different encapsulation techniques, lyophilisation is one of the most suitable for heat sensitive samples (15). In addition to selection of encapsulation technique, the correct choice of the wall material is also very important for encapsulation process, because it influences the encapsulation efficiency and stability of the microcapsule (16). The criteria for selecting a wall material are mainly based on its physicochemical properties (such as solubility, emulsifying, drying properties, etc.), nature of the core material, process of encapsulation, economics and requirements for a certain application (17). For encapsulation of bioactive substances carbohydrate polymers and proteins are most broadly used encapsulant materials (14).

The aim of our study was to determine lycopene, β-carotene and phenolic content, as well as antioxidant activity of tomato waste. For the protection of extracted sensitive bioactive compounds (lycopene and β-carotene) tomato waste was encapsulated with various encapsulating materials by freeze drying method. Another major objective of this study was to investigate the influence of different encapsulating materials on the encapsulation efficiency and other physicochemical properties of obtained encapsulates.

EXPERIMENTAL

Chemicals and instruments

Folin-Ciocalteau reagent, 2,2-diphenyl-1-picrylhydrazyl radical (DPPH·), 2,2′-azino-bis-3-ethylbenzothiazoline-6-sulphonic acid (ABTS·+), Trolox and trichloroacetic acid were purchased from Sigma Chemical Co. (St Louis, MO, USA), ferric chloride was obtained from J.T. Baker (Deventer, Holland). Soy protein isolate were purchased from Olimp Laboratories (Debica, Poland), Gum arabica from Carlo Erba (Val de Reuil, France), pea protein from Beyond d.o.o. (Niš, Serbia) and inulin from Elephant Co. (Belgrade, Serbia). Other chemicals and solvents were of the highest analytical grade. Spectropho-

Original scientific paper

tometric measurements were done with a MultiskanGO microplate reader (Thermo Fisher Scientific Inc., Waltham, MA, USA). Freeze dryer, model Christ Alpha 2-4 LSC, was from Martin Christ (Osterode am Harz, Germany).

Plant material and dried tomato waste preparation

Fresh tomato waste material obtained after pressing the pulp as by-product from the fruit and vegetable processing industry (Zdravo Organic d.o.o., Selenca, Serbia). Tomato waste was dried in freeze dryer at -40 °C for 48h. Dried tomato waste material was ground, packed in vacuumed plastic bags and stored at -20 °C until further analysis. Weight of fresh tomato waste before and after drying was 155.86 g and 24.37 g, respectively.

Extraction procedure

Dried waste was extracted using acetone:ethanol mixture (36:64 v/v) in solid to solvent ratio 1:20 w/v for 10 min using a laboratory shaker (Unimax 1010, Heidolph Instruments GmbH, Kelheim, Germany) at 300 rpm, under light protection, at room temperature. The extraction was performed three times with the same volume of solvents. The obtained three extracts were filtered (Whatman paper No.1), combined, and stored in dark bottles at -20 °C till further analysis.

Determination of bioactive compounds content in tomato waste extract

Total β-carotene and lycopene content. Total content of β-carotene and lycopene in tomato waste extract was analyzed spectrophotometrically by the method of Nagata and Yamashita (18) adapted for 96 well microplate. The total β-carotene and lycopene content was expressed as mg of β-carotene or lycopene per 100 g sample (DW).

Total phenolic content. The total content of phenolics (TP) in waste extract was determined spectrophotometrically by Folin-Ciocalteau method adapted for 96 well microplate (19). Results were expressed as gallic acid equivalents (GAE) per 100 g sample (DW).

Determination of tomato waste extract bioactivity

DPPH assay. Antioxidant activity on DPPH radicals (AA_{DPPH}) was performed spectrophotometrically in a 96-well microplate reader, according to Girones-Vilaplana et al. (20). The calibration curve was made with Trolox and results were expressed as mg TE per 100 g of sample (DW).

Reducing power assay. Reducing power (RP) was determined by the method of Oyaizu (21) adapted for 96 well microplate. The calibration curve was made with Trolox and results were expressed as mg TE per 100 g of sample (DW).

ABTS assay. Antioxidant activity on $ABTS^+$ radicals (AA_{ABTS}), i.e. the ability of samples to scavenge $ABTS^{+\bullet}$ was evaluated employing modified method according to Tumbas Šaponjac et al. (22). Results were expressed as mg TE per 100 g of sample (DW).

Original scientific paper

Superoxide anion assay. Antioxidant activity on superoxide anion radicals ($AA_{O2}•-$), i.e. the ability of samples to scavenge superoxide anion radicals was evaluated employing method of Nishikimi et al. (23) adapted for 96 well microplate. Results were expressed as mg TE per 100 g of sample (DW).

Encapsulation process

Freeze dried encapsulates were prepared according to the method developed by Indrawati et al. (24) with some modifications. Wall material (28 g) was dissolved in 42 ml of water at 60 °C and kept under stirring until the temperature reached 30 °C. Separately, 160 ml of tomato waste extract was combined with sunflower oil (6 ml), concentrated under reduced pressure on a rotary evaporator set at 40 °C to remove the organic solvent, and immediately mixed with 0.1 g of Tween 80 and with previously prepared carrier solution. The mixtures were homogenized (Heidolph DIAX 900, Heidolph Instruments GmbH, Kelheim, Germany) at 11000 rpm for 5 min at room temperature and subjected to drying. The previously prepared mixture was frozen overnight at -70 °C and then freeze dried at -40 °C and 0.01 mbar for 72 h to ensure complete drying. Collected freeze dried encapsulate was stored at -20 °C until further use.

Determination of the physicochemical properties of the encapsulates

Water activity, moisture content, hygroscopicity, solubilty, bulk density (Db), tapped density (Dt), Carr's Index (CI), Hausner ratio (HR) and particle size was determined as reported previously (25).

Determination of encapsulation efficiency

Encapsulation efficiency of carotenoids (β-carotene and lycopene), total and surface carotenoids in encapsulate were determined by following a modified method of Barbosa et al. (26). For total β-carotene (TC) and total lycopene (TL) determination, 0.125 g of sample was vortexed with 2.5 ml of 0.2 M PBS (pH 7) for 1 min to break the capsules, extracted with 1 ml of acetone and 1.5 ml of diethyl ether on a vortex, and then subjected to ultrasound for 5 min, centrifuged for 10 min at 4000 rpm, and the supernatant was separated. Surface β-carotene (SC) and surface lycopene (SL) were determined by direct extraction of encapsulate (0.1 g) with 1 ml acetone on a vortex for 20 s, followed by centrifugation at 3000 rpm (10 min) and supernatant separation. The supernatants obtained after separations were filtered (0.45 μm, PTFE) and β-carotene and lycopene quantification was carried out according to the previously described protocol of Nagata and Yamashita (18). The results were expressed as mg of β-carotene or lycopene per 100 g encapsulate (mg/100 g encapsulate). The encapsulation efficiency of β-carotene ($EE_{β-Carotene}$) and lycopene ($EE_{Lycopene}$) was calculated by using the equations:

$$EE_{β-Carotene} (\%) = ((TC-SC)/TC) \times 100;$$
$$EE_{Lycopene} (\%) = ((TL-SL)/TL) \times 100;$$

where TC and TL are the total β-carotene and lycopene, while SC and SL are the surface β-carotene and lycopene in the encapsulate. Simultaneously, the control samples, i.e. the wall materials without extract, were prepared in the same way, for the correction of interfering substances originating from the wall materials.

Statistical analysis

All experiments were run in triplicate and results were represented as means ± standard deviation. Statistical analyses were carried out using Origin 7.0 software package and Microsoft Office Excel 2010.
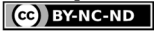
RESULTS AND DISCUSSION

In order to investigate tomato processing waste as a source of natural bioactive molecules, tomato waste was subjected to evaluation of antioxidant contents and activity. Results of the determination of β-carotene, lycopene and phenolic contents in the tomato waste are shown in table 1.

Table 1. Content of β-carotene, lycopene and phenolics in the tomato waste

Bioactive compounds	Content (mg/100 g DW)
β-Carotene	12.36 ± 0.06
Lycopene	13.72 ± 0.12
Phenolics	203.33 ± 4.74

The content of lycopene (13.72 mg/100 g DW) and β-carotene (12.36 mg/100 g DW) revealed in this study were in accordance with the previous research findings (9, 27, 28, 29). In the study of Stajčić et al. (29) the lycopene and β-carotene content determined in waste of different tomato genotypes ranged from 13.40 to 81.54 mg/100 g DW and from 8.64 to 50.14 mg/100 g DW, respectively. The results of research conducted on tomato waste by Szabo et al. (9) indicated that lycopene content in tomato waste depending on genotype varied from 14.9 to 28.8 mg/100 g DW, while the content of β-carotene was in range from 2.9 to 4.8 mg/100 g DW. Knoblich et al. (27) found that amounts of lycopene and β-carotene in tomato skin were 73.4 and 2.93 mg/100 g, while lycopene and β-carotene in tomato seed were 13.0 and 1.44 mg/100 g of dry by-product, respectively. In the study of Kalogeropoulos et al. (28), lycopene and β-carotene content of tomato waste was 413.7 mg/kg and 149.8 mg/kg, respectively.

The phenolic cotent in tomato waste (203.33 mg/100 g DW) determined in this study was consistent with phenolic contents (111.9 - 407.7 mg/100 g DW) in waste of different tomato genotypes determined using HPLC in the study of Szabo et al. (9). The results of phenolic contents (423.43 - 719.73 mg/100 DW) determined spectrophotometrically in tomato wastes obtained from different genotypes where higher than the phenolic contents (69.83 - 177.94 mg/100 g DW) determined using HPLC method (30). It is known that interfering substances (particularly sugars, aromatic amines, ascorbic acid, etc.) present in

Original scientific paper

extracts could be responsible for higher obtained results by Folin-Ciocalteu method (31).
The differences in the reported results of bioactive compound contents could be due to
the period of harvesting, cultivar, maturation stage, geography and climate (32).

   Based on the obtained results, it can be concluded that the tomato waste showed high
values of antioxidant activity in all applied tests (table 2).

Table 2. Antioxidant activity of tomato waste measured by different assays

Antioxidant assay	Antioxidant activity (mg TE/100 g DW)
DPPH	356.32 ± 9.62
ABTS	181.66 ± 5.82
Reducing power	277.54 ± 12.08
Superoxide anion	785.64 ± 36.35

   The variation it the results of antioxidant activity determined by different assays can
be explained by the fact that antioxidant activity of antioxidants could be attributed to
different mechanism (33). Antioxidant activity determined on DPPH radicals (356.32 mg
TE/100 g DW, or 1423.63 μmol/100 g DW) is in the range of antioxidant activities (199 -
404 mg TE/100 g DW; 794 - 1614 μmol/100 g DW) which were determined for the waste
of different tomato genotypes in the study of Savatović et al. (34), and is higher than the
antioxidant activities (~ 420 - 574 μmol TE/100 g DW) which were determined for the
waste of 10 tomato genotypes in the study of Szabo et al. (19). The differences between
the reported antioxidant activities may be caused by the above mentioned reasons for the
variation in the content of bioactive compounds (32).

   In the study of Stajčić (30), a significant correlation was found between the reducing
power of ethanolic tomato waste extracts and flavonoid content. Also, higher correlation
between the results of ABTS test and lycopene content in tomatoes of different genotypes
than the correlation of the results of ABTS test and polyphenolic content compounds was
established in the study of Ilahy et al. (35). In the study of Belović (36), it was shown that
carotenoids present in tomato waste extract and tomato juice are stronger antiradical
agents determined according to the superoxide anion radical test than polyphenolic com-
pounds. Also, it was found that synergistic and/or antagonistic effects between the pre-
sent antioxidants, as well as their interaction with other constituents determine the anti-
oxidant activity of tomato extracts (35).

   For improvement of the stability of lycopene and β-carotene present in tomato waste
extract encapsulation method was employed with the aim for the development of lycope-
ne and β-carotene forms suitable for incorporation in food products. Tomato waste ex-
tract encapsulates were prepared using different wall materials (soy protein, pea protein,
inulin and gum arabica). Obtained encapsulates were characterised in terms of physico-
chemical properties and encapsulation efficiency.

   The physicochemical characteristics i.e., water activity, moisture content and hygro-
scopicity are essential for powder products stability and storage, while solubility is cor-
related with ability of powders for reconstitution (37). Flowability and density ratios are
of importance for packing granular materials and their industrial applications (38). Physi-
cochemical characteristics of tomato waste extract encapsulates are shown in table 3.

Table 3. Characterisation of tomato waste extract encapsulates

Physicochemical properties	EPS*	EPP*	EIN*	EGA*
Water activity (a$_w$)	0.036 ± 0.001	0.017 ± 0.000	0.020 ± 0.000	0.656 ± 0.020
Moisture content (%)	3.73 ± 0.11	2.49 ± 0.04	2.21 ± 0.06	22.54 ± 0.45
Hygroscopicity (%)	12.81 ± 0.38	12.75 ± 0.25	14.67 ± 0.29	3.55 ± 0.07
Bulk density (Db; g/ml)	0.17 ± 0.00	0.16 ± 0.00	0.23 ± 0.00	0.24 ± 0.00
Tapped density (Dt; g/ml)	0.25 ± 0.01	0.25 ± 0.01	0.30 ± 0.01	0.29 ± 0.01
Carr index (CI)	31.76 ± 0.98	35.14 ± 0.47	24.08 ± 0.45	16.00 ± 0.32
Hausner ratio (HR)	1.47 ± 0.02	1.54 ± 0.01	1.32 ± 0.01	1.19 ± 0.00
Flowability	Very poor	Very poor	Passable	Fair
Solubility (%)	18.5 ± 0.5	7.3 ± 0.1	46.4 ± 0.92	54.4 ± 1.63
Average diameter of particles (μm)	92.88	98.33	62.29	206.89

*EPS, EPP, EIN and EGA - encapsulates of the tomato waste extracts on the basis of soy protein, pea protein, inulin and gum arabica, respectively.

Water activity (a$_w$) represents the availability of free water in a food system which is responsible for biochemical reactions (39). Therefore, water activity has long been considered as one of the most important quality factors for dried products especially for long term storage (32). Basically, product with a$_w$ less than 0.6 is microbiologically stable and when the water activity level drops below 0.4 the most of the unfavorable changes in food during storage such as lipid oxidation, enzymatic reactions and non-enzymatic browning are almost completely hindered (40, 41). Water activity of EPS, EPP and EIN encapsulates insured their stability. Higher a$_w$ value, about 0.66, found for the EGA encapsulate in comparison to other encapsulates indicating that probably longer drying time could be required for EGA encapsulate to reach lower a$_w$ value, and therefore to improve its stability. Similarly, higher moisture content was determined in the EGA encapsulate than in other investigated encapsulates.

For determination of flowability of encapsulates Carr index (CI) and Hausner ratio (HR) were used. Encapsulates prepared with carbohydrates as wall materials (EIN and EAG) showed higher flowability than encapsulates on the basis of protein wall materials (EPS and EPP).

The aqueous solubility is one of the main powder quality indicators (42). For aqueous solubility of encapsulates the selection of wall material is very important, not only to the solubility itself but also to the crystalline state that is conferred to the dried powder (43).

In this study, the higher solubility may be related to the high solubility of the encapsulating agents used (gum arabic and inulin).

The hygroscopicity values varied from 3.55% to 14.67% (table 3), indicating relatively low hygroscopicity of powders, thus facilitating its conservation and the preservation of color and bioactive compounds (44). The lower hygroscopicity values found for EGA powder can be related to its larger particle size when compared to the ESP, EPP and EIN powders, since larger the particle size, lower is the exposed surface area and consequently lower is the water absorption (44).

The total and surface content, and therefore encapsulation efficiency of encapsulated compounds are the most important parameters for evaluating the properties of microcapsules. The contents and encapsulation efficiency of β-carotene and lycopene in encapsulates are shown in the table 4 and table 5.
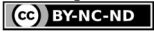
Original scientific paper

Table 4. Total and surface content, and encapsulation efficiency of β-carotene in encapsulates

Encapsulates*	TB (mg/100 g DW)**	SB (mg/100 g DW)**	EE$_{β-Carotene}$ (%)**
EPS	1.11 ± 0.05	0.73 ± 0.02	34.48
EPP	1.04 ± 0.03	0.61 ± 0.02	41.33
EIN	1.16 ± 0.03	0.72 ± 0.01	37.39
EGA	1.83 ± 0.06	0.85 ± 0.03	53.47

*EPS, EPP, EIN and EGA - encapsulates of the tomato waste extracts on the basis of soy protein, pea protein, inulin and gum arabica, respectively; **TB - total β-carotene content; SB - surface β-carotene content; EE$_{β-Carotene}$ - encapsulation efficiency of β-carotene.

Table 5. Total and surface content, and encapsulation efficiency of lycopene in encapsulates

Encapsulates*	TL (mg/100 g DW)**	SL (mg/100 g DW)**	EE$_{Lycopene}$ (%)**
EPS	1.56 ± 0.07	0.76 ± 0.03	51.44
EPP	1.56 ± 0.04	0.94 ± 0.05	39.74
EIN	1.79 ± 0.05	0.95 ± 0.04	46.86
EGA	2.05 ± 0.08	1.16 ± 0.01	43.44

*EPS, EPP, EIN and EGA - encapsulates of the tomato waste extracts on the basis of soy protein, pea protein, inulin and gum arabica, respectively; **TL - total lycopene content; SL - surface lycopene content; EE$_{Lycopene}$ - encapsulation efficiency of lycopene.

Highest total β-carotene and lycopene contents were determined in encapsulate on the basis of gum arabic as wall material (EGA) (table 4; table 5). Highest encapsulation efficiency of β-carotene was obtained with gum arabic (EGA) (table 4), while highest encapsulation efficiency of lycopene was obtained with soy protein (ESP) as encapsulating material (table 5). Numerous techniques and different carriers were employed to achieve greater encapsulation efficiency and better preservation of carotenoids. In the study of Nogueira et al. (45), carotenoids were encapsulated by lyophilization technique with soy protein as a carrier, and their encapsulation efficiency was about 65%. Singh et al. (46) studied β-carotene encapsulation on poly(ethylene glycols) based functionalized amphiphilic copolymers by the lyophilization technique, and for different encapsulation formulations the encapsulation efficiency ranged from 22.60% to 28.08%. Mulyadi et al. (47) examined encapsulation efficiencies depending on the different concentration of encapsulated carotenoids from kabocha pumpkin into coating agents chitosan-sodium alginate-sodium tripolyphosphate by freeze-drying technique. The content of total carotenoids at a concentration of 0.5% was 117.98 mg/100 g, and the encapsulation efficiency was 90.86%, while at a concentration increase of 3% the carotenoid content was 318.29 mg/100 g, and the encapsulation efficiency was significantly reduced to 54.72%; therefore the application of higher carotenoid concentration did not contribute to the increase in encapsulation efficiency probably due to over loading of carotenoids used (47). Also, Thamaket and Raviy (48) concluded that the loading carotenoids with high concentration did not provide better encapsulation efficiency. With the aim to minimize lycopene instability, Rocha et al. (49) encapsulated the lycopene by spray drying, using a modified

starch as an encapsulating agent. In their study encapsulation efficiency, calculated as the quantity of lycopene present in the capsules compared to the lycopene initially used to produce them, ranged between 21.01 and 29.73%. Shu et al. (50) encapsulated lycopene in gelatin and sucrose by atomization in a spray dryer and verified that the greater the quantity of core, the encapsulation was less efficient. Varying parameters such as the wall:core ratio, the gelatin mass:sucrose mass ratio, lycopene purity, homogenization pressure, inlet temperature and feed temperature in the spray dryer, they observed an encapsulation efficiency varied between 12.1 and 82.2% (50). Rodrigues-Huezo et al. (51) reported values for encapsulation efficiency between 25.6 and 87.5% for encapsulates obtained by spray drying of emulsions containing carotenoids using gum arabic, gellan gum and maltodextrin as encapsulation materials (49). In the study of Ranveer et al. (52) the effect of different process parameters, core to wall ratio, sucrose to gelatin and inlet temperature on encapsulation yield and encapsulation efficiency of lycopene in encapsulates obtained by spray-drying technique were investigated. Highest encapsulation efficiency (92.6 %) and encapsulation yield (82.2%) was observed when the core to wall ratio was 1:4, sucrose to gelatin ratio was 7:3 and inlet temperature was 180 °C (52). Guo et al. (53) presented a new way of preparation of lycopene microcapsules with ultrasonic emulsification and after optimization of the process parameters the encapsulation efficiency had increased to 64.4%. In the study of Nunes and Mercadante (54), lycopene was encapsulated using the mixture of gum arabic and sucrose (8:2) as wall materials by spray-drying technique, and encapsulation efficiency ranged from 94 to 96%. Encapsulation efficiency of β-carotene and lycopene determined in our study were in range of previously reported results.

CONCLUSIONS

In the present study, due to the increasing demand for natural additives in food production, tomato processing waste was subjected to investigation as a source of bioactive compounds. Based on the results, tomato waste showed high content of bioactive compounds (lycopene, β-carotene and phenolics) and antioxidant activity in all applied tests. In order to overcome the problem of carotenoids (lycopene and β-carotene) instability the encapsulation of tomato waste extract was employed. Producing encapsulates using different wall materials resulted in different encapsulation efficiency of carotenoids (lycopene and β-carotene), and physicochemical properties such as water activity, moisture contents, hygroscopicity, flowability, density ratios and particles size, depending on the characteristics of each wall material. Encapsulate on the basis of gum arabic showed highest encapsulation efficiency of β-carotene, while encapsulate prepared with soy protein as encapsulating material showed highest encapsulation efficiency of lycopene. Our results suggest that tomato processing waste represent a reliable source of natural bioactive molecules with high antioxidant activity. Also, overall results support the need for preparation of encapsulates with different encapsulating material and evaluation of their encapsulation efficiency and other physicochemical characteristics with the aim of development functional ingredients in new food formulations.

Acknowledgements

REFERENCES

1. Demiray, E.; Tulek, Y.; Yilmaz Y. Degradation kinetics of lycopene, β-carotene and ascorbic acid in tomatoes during hot air drying. *LWT - Food Science and Technology*. **2013,** *50*, 172-176.

2. Gheonea (Dima), I.; Aprodu, I.; Cîrciumaru, A.; Râpeanu, G.; Bahrim, G.E.; Stănciuc N. Microencapsulation of lycopene from tomatoes peels by complex coacervation and freeze-drying: Evidences on phytochemical profile, stability and food applications. *J. Food Eng.* **2020**, *288*, 110166.

3. Siddiqui, M.W.; Chakraborty, I.; Homa, F.; Dhua, R.S. Bioactive compounds and antioxidant capacity in dark green, old gold crimson, ripening inhibitor, and normal tomatoes. *Int. J. of Food Prop.* **2016,** *19*, 688-699.

4. Pandya, D.; Akbari, S.; Bhatt, H.; Joshi, D.C. Standardization of solvent extraction process for lycopene extraction from tomato pomace. *J. Appl. Biotechnol. Bioeng.* **2017,** *2* (1), 12-16.

5. Kaur, D.; Wani, A.A.; Oberoi, D.P.S.; Sogi, D.S. Effect of extraction conditions on lycopene extractions from tomato processing waste skin using response surface methodology. *Food Chem.* **2008,** *108*, 711-718.

6. Rao, V.S.; Waseem, Z.; Aggarwal, S. Lycopene content of tomatoes and tomato products and their contribution to dietary lycopene. *Food Res. Int.* **1998**, *31*, 737-741.

7. Sogi, D.S.; Bawa, A.S. Studies on dehydration of tomato processing waste. *Indian Food Packer*. **1998,** *52* (2), 26-29.

8. Lu, Z.; Wang, J.; Gao, R.; Ye, F.; Zhao G. Sustainable valorisation of tomato pomace: A comprehensive review. *Trends in Food Sci. Technol.* **2019,** *86*, 172-187.

9. Szabo, K.; Dulf, F.V.; Diaconeasa, Z.; Vodnar, D.C. Antimicrobial and antioxidant properties of tomato processing byproducts and their correlation with the biochemical composition. *LWT - Food Science and Technology*. **2019,** *116*, 108558.

10. Gul, K.; Tak, A.; Singh, A.K.; Singh, P.; Yousuf, B.; Wani, A.A. Chemistry, encapsulation, and health benefits of β-carotene - A review. *Cogent Food & Agric.* **2015**, *1*, 1018696.

11. Shi, J.; Qu, Q.; Kauda, Y.; Yeung D.; Jiang, Y. Stability and synergistic effect of antioxidative properties of lycopene and other active components. *Crit. Rev. Food Sci. Nutr.* **2004,** *44*, 559-573.

12. Rascón, M.P.; Beristain, C.I.; Garcia, H.S.; Salgado, M.A. Carotenoid retention and storage stability of spray-dried encapsulated paprika oleoresin using gum arabic and soy protein isolate as wall materials. *LWT - Food Science and Technology*. **2011,** *44*, 549-557.

13. Ranveer, R.C.; Gatade, A.A.; Kamble, H.A.; Sahoo, A.K. Microencapsulation and storage stability of lycopene extracted from tomato processing waste. *Braz. Arch. Biol. Technol*. **2015**, *58* (6), 953-960.

14. Labuschagne, P.; Impact of wall material physicochemical characteristics on the stability of encapsulated phytochemicals: A review. *Food Res. Int.* **2018,** *107*, 227-247.

15. Morais, A.R.V.; Alencar, É.N.; Júnior, F.H.X.; Oliveira, C.M.; Marcelino, H.R.; Barratt, G.; Fessid, H., Egito; E.S.T.; Elaissari, A. Freeze-drying of emulsified systems: A review. *Int. J. Pharm*. **2016,** *503*, 102-114.

16. da Silva, P.T.; Fries, L.L.M.; C.R. de Menezes; Holkem, A.T.; Schwan, C.L.; Wigmann, É.F.; Bastos, J.de O.; da Silva C. de B. Microencapsulation: concepts, mechanisms, methods and some applications in food technology. *Ciência Rural, Santa Maria*. **2014,** *44* (7), 1304-1311.

17. Chranioti, C.; Tzia, C. Binary mixtures of modified starch, maltodextrin and chitosan as efficient encapsulating agents of fennel oleoresin. *Food Bioprocess. Technol.* **2013,** *6*, 3238-3246.

18. Nagata, M.; Yamashita, I. Simple method for simultaneous dermination of chlorophyll and carotenoids in tomato fruit. *J. Jap. Soci. Food Sci. Tehnol.* **1992,** *39*, 925-928.

19. Singleton, V.L.; Rossi, J.A. Colorimetry of total phenolics with phosphomolybdicphosphotungstic acid reagents. *Am. J. Enol.Viticult.* **1965,** *16*, 144158.

20. Girones-Vilaplana, A.; Mena, P.; Moreno, D.A.; Garcia-Viguera, C. Evaluation of sensorial, phytochemicaland biological properties of new isotonic beverages enriched with lemon and berries during shelf life. *J. Sci. Food Agric.* **2014,** *94*, 1090-1100.

21. Oyaizu, M. Studies on product of browning reaction prepared from glucose amine. *Japanese Journal of Nutrition.* **1986,** *44*, 307-315.

22. Tumbas Šaponjac, V.; Girones-Vilaplana, A.; Djilas, S.; Mena, P.; Ćetković, G.; Moreno, D.A.; Čanadanović-Brunet, J.; Vulić, J.; Stajčić, S.; Krunić, M. Anthocyanin profiles and biological properties of caneberry (*Rubus* spp.) press residues. *J. Sci. Food Agric.* **2014,** *94,* 2393-2400.

23. Nishikimi, M.; Rao, N.A.; Yagi, K. The occurrence of superoxide anion in the reaction of reduced phenazine methosulfate and molecular oxygen. *Biochem. Biophys Res. Co.* **1972**, *46*, 849-854.

24. Indrawati, R.; Sukowijoyo H.; Dumilah esti Wjayantu, R.; Limantara, L. Encapsulation of brown seaweed pigment by freeze drying: characterization and its stability during storage. *Procedia Chem.* **2015,** *14*, 353-360.

25. Šeregelj, V.; Tumbas Šaponjac, V.; Lević, S.; Kalušević, A.; Ćetković, G.; Čanadanović-Brunet, J.; Nedović, V.; Stajčić, S.; Vulić, J.; Vidaković, A. Application of encapsulated natural bioactive compounds from red pepper waste in yogurt. *J. Microencapsul.* **2019**, *36* (8), 704-714.

26. Barbosa, M.I.M.J.; Borsarelli, C.D., Mercadante, A.Z. Light stability of spraydried bixin encapsulated with different edible polysaccharide preparations. *Food Research Int.* **2005,** *38*, 989-994.

27. Knoblich, M.; Anderson, B.; Latshaw, D. Analyses of tomato peel and seed by products and their use as a source of carotenoids. *J. Sci. Food Agr.*, **2005,** *85*, 1166-1170.

28. Kalogeropoulos, N.; Chiou, A.; Pyriochou, V.; Peristeraki, A.; Karathanos, V.T. Bioactive phytochemicals in industrial tomatoes and their processing byproducts. *LWT – Food Science and Technology*. **2012,** *49*, 213-216.

29. Stajčić, S.; Ćetković, G., Čanadanović-Brunet, J.; Djilas, S.; Mandić, A.; Četojević-Simin, D. Tomato waste: Carotenoids content, antioxidant and cell growth activities. *Food Chem.* **2015,** *172*, 225-232.

30. Stajčić, S. High-valuable functional compounds from tomato by-products. Ph.D.Thesis, University of Novi Sad, November 2012.

31. Prior, R.L.; Wu, X.; Schaich, K. Standardized methods for the determination of antioxidant capacity and phenolics in foods and dietary supplements. *J. Agric. Food Chem*. **2005,** *53*, 4290-4302.

32. Caliskan, G.; Dirim, S.N. Drying characteristics of pumpkin (*Cucurbita moschata*) slices in convective and freeze dryer. *Heat Mass Transfer.* **2017,** *53*, 2129-2141.

33. Roshanak, S.; Rahimmalek, M.; Goli, S.A.H. Evaluation of seven different drying treatments in respect to total flavonoid, phenolic, vitamin C content, chlorophyll, antioxidant activity

and color of green tea (*Camellia sinensis* or *C. assamica*) leaves. *J. Food Sci. Technol*. **2016,** *53* (1), 721-729.

34. Savatović, S.; Ćetković, G.; Ćanadanović-Brunet, J.; Djilas, S. Tomato waste: A potential source of hydrophilic antioxidants. *Int. J. Food Sci. Nutr.* **2012,** *63* (2), 129-137.

35. Ilahy, R.; Hdider, C.; Lenucci, M.S.; Tlili, I.; Dalessandro, G. Phytochemical composition and antioxidant activity of high-lycopene tomato (*Solanum lycopersicum* L.) cultivars grown in Southern Italy. *Sci. Hortic.* **2011,** *127*, 255-261.

36. Belović, M. Utilization of tomato processing byproduct as raw material for value-added food products. Ph.D.Thesis, University of Novi Sad, 2016.

37. Tonon, R.V.; Brabet, C.; Hubinger, M.D. Influence of process conditions on the physico-chemical properties of açai (*Euterpe oleraceae* Mart.) powder produced by spray drying. *J. Food Eng.* **2008,** *88* (3), 411-418.

38. Santomaso, A.; Lazzaro, P.; Canu, P. Powder flowability and density ratios: the impact of granules packing. *Chem. Eng. Sci.* **2003,** *58*, 2857-2874.

39. Papoutsis, K.; Golding, J.B.; Vuong, Q.; Pristijono, P.; Stathopoulos, C.E.; Scarlett, C.J.; Bowyer, M. Encapsulation of citrus by-product extracts by spray-drying and freeze-drying usingcombinations of maltodextrin with soybean protein and ι-carrageenan. *Foods*, **2018,** *7*, 115.

40. Nawi, N.M.; Muhamad, I.I.; Marsin A.M. The physicochemical properties of microwave-assisted encapsulated anthocyanins from Ipomoea batatas as affected by different wall materials. *Food Science & Nutrition*. **2014,** doi: 10.1002/fsn3.132

41. Roongruangsri, W.; Bronlund, J.E. Effect of air-drying temperature on physico-chemical, powder properties and sorption characteristics of pumpkin powders. *Int. Food Res. J.* **2016,** *23* (3), 962-972.

42. Oliveira, A.R.; Ribeiro, A.E.C.; Oliveira, É.R.; Garcia, M.C.; Soares Júnior, M.S., Caliari, M. Structural and physicochemical properties of freeze-dried açaí pulp (*Euterpe oleracea* Mart.). *Food Sci. Technol., Campinas*, **2020,** *40* (2), 282-289.

43. Cortês-Rojas, D.F.; Souza, C.R.F.; Oliveira, W.P. Optimization of spray drying conditions for production of *Bidens pilosa* L. dried extract. *Chem. Eng. Res. Des*., **2015,** *93*, 366-376.

44. Rezende, Y.R.R.S.; Nogueira, J.P.; Narain, N. Microencapsulation of extracts of bioactive compounds obtained from acerola (*Malpighia emarginata* DC) pulp and residue by spray and freeze drying: Chemical, morphological and chemometric characterization. *Food Chem.* **2018,** *254*, 281-291.

45. Nogueira, M.B.; Prestes, C.F.; Burkert J.F.M. Microencapsulation by lyophilization of carotenoids produced by *Phaffia rhodozyma* with soy protein as the encapsulating agent. *Food Sci. Technol.*, Campinas, **2017,** 37(Special issue), 1-4.

46. Singh, B.B.; Shakil, N.A.; Kumar J.; Walia S.; Kar A. Development of slow release formulations of β-carotene employing amphiphilic polymers and their release kinetics study in water and different pH conditions. *J. Food Sci. Technol.* **2015,** *52* (12), 8068-8076.

47. Mulyadi, N.M.; Widyaningsih, T.D.; Wijayanti, N.; Indrawati, R.; Heriyanto, H.; Limantara L. Microencapsulation of kabocha pumpkin carotenoids. *Int. J. Chem. Eng. Appl.* **2017,** *8* (6), 381-386.

48. Thamaket, P.; Raviyan, P. Preparation and physical properties of carotenoids encapsulated in chitosan cross-linked tripolyphosphate nanoparticles. *Food and Applied Bioscience Journal.* **2015,** *3* (1), 69-84.

49. Rocha, G.A.; Fávaro-Trindade, C.S.; Grosso, C.R.F. Microencapsulation of lycopene by spray drying: Characterization, stability and application of microcapsules. *Food and Bioprod. Process.* **2012,** *90,* 37-42.

50. Shu, B.; Yu, W.; Zhao, Y.; Liu X. Study on microencapsulation of lycopene by spray-drying. *J. Food Eng.* **2006,** *76*, 664-669.

51. Rodríguez-Huezo, M.E.; Pedroza-Islas, R.; Prado-Barragán, L.A.; Beristain, C.I.; Vernon-Carter, E.J. Microencapsulation by spray drying of multiple emulsions containing carotenoids. *J. Food Sci.* **2004,** *69* (7), E351-E359.

52. Ranveer, R.C.; Gatade, A.A.; Kamble, H.A.; Sahoo, A.K. Microencapsulation and storage stability of lycopene extracted from tomato processing waste. *Braz. Arch. Biol. Technol.* **2015,** *58* (6), 953-960.

53. Guo, H.; Huang, Y.; Qian, J.-Q.; Gong, Q.-Y.; Tang, Y. Optimization of technological parameters for preparation of lycopene microcapsules. *J. Food Sci. Technol.* **2014,** 51 (7), 1318-1325.

54. Nunes, I.L.; Mercadante, A.Z. Encapsulation of lycopene using spray-drying and molecular inclusion processes. *Braz. Arch. Biol. Techn.* **2007,** *50* (5), 893-900.

INFLUENCE OF CALCINED SNAIL SHELL PARTICULATES ON MECHANICAL PROPERTIES OF RECYCLED ALUMINIUM ALLOY FOR AUTOMOTIVE APPLICATION

M.Y. Kolawole[1]*, J.O. Aweda[2], S. AbdulKareem[2], S.A. Bello[3], A. Ali[4], F. Iqbal[4]

[1] Department of Mechanical Engineering, Faaculty of Engineering and Technology,
Kwara State University Malete, Nigeria
[2] Department of Mechanical Engineering, Faaculty of Engineering and Technology,
University of Ilorin, Ilorin, Nigeria
[3] Department of Materials Science and Engineering, Faaculty of Engineering and Technology,
Kwara State University Malete, Nigeria
[4] Interdisciplinary Research Centre on Biomedical Materials,
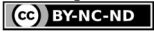COMSATS University Islamabad, Lahore Campus, Pakistan

Nowadays, low-cost particulate reinforced metal matrix composites with improve mechanical properties are highly sought in various industrial and critical engineering applications including automotive and aerospace sectors. Meanwhile, increasing consumption rate of African giant land snail (Archachatina marginata) had been posing disposal challenges of its shells. Therefore, this paper tends to investigates the influence of waste snail shells particulates on the physical and mechanical properties of recycled aluminum-silicon alloy matrix. Different weight proportions i.e. (0 – 7.5) wt% of calcined snail shell particles at an interval of 1.5 wt% were successfully incorporated into Al-Si alloy matrix melted at 750 °C using stir-casting route. The microstructure, physical and mechanical properties of the resulting composites were examined and presented. Microstructural examination shows fairly uniform dispersion of snail shell particles in the aluminium alloy matrix intermingled with aluminium-silicon dendrites. Mechanical properties such as hardness, impact, compressive and tensile strengths increased with increasing addition of calcined snail shell particulate up to 6 wt% while density and elongation decreases. The total equivalent density reduction of 5.4% in composites compared to unreinforced alloy was obtained at 7.5 wt% snail shell addition. The maximum hardness, impact, compressive and tensile strengths obtained are 118±4 HV, 88 J, 552±20 MPa and 211 ± 4.8 MPa equivalent to 21, 25, 19 and 36 percent increase respectively relative to un-reinforced aluminium-silicon alloy. Hence, mechanical and physical properties of Al-Si alloy can be enhanced using calcined snail shell particulates which can widen its application in automotive industries.

Keywords: metal marix composite, low-cost reinforcement, mechanical properties, stir-casting, automotive and aluminium alloy

INTRODUCTION

The demand for light weight and cost-effective engineering materials with higher strength especially in automotive, aerospace and structural applications for enhance performance are on the increase (1, 2). Interestingly, aluminium and its alloys with matching
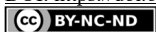
---

* Corresponding author: M.Y. Kolawole, Department of Mechanical Engineering, Faaculty of Engineering and Technology, Kwara State University Malete, Nigeria, e-mail: maruf.kolawole@kwasu.edu.ng

characteristics of light weight, low cost, good thermal and electrical properties desirable in various engineering applications had stimulated research interest. These overwhelming properties as well as the recyclability of aluminium had made it a promising candidate material of the present century in engineering applications. Moreover, good resistance to corrosion has further preserved the integrity of aluminium and its alloys' properties for improved performance in many environments. Barely all sectors of human endeavour today including and not limited to cooking utensils, household furniture, electrical industries, aerospace, automobile and structural applications are making use of aluminium either in their pure or and alloyed forms. However, global increasing demand for lightweight material with enhance mechanical properties over the conventional alloys in the emerging industrial applications and requirements has recently fuelled the curiosity of researchers on advanced engineering materials (metal matrix composites) developments (3, 4). Reinforcing a metal matrix phase resulted in metal matrix composite with processing techniques serving as major hub for tailoring the resulting properties into desired application. By literature search (5), research birth in metal matrix composites (MMCs) was dated back to about two decades ago. Interestingly, this has transpired into modern days advanced materials finding application in structural, aerospace, automotive, marine, electronic, wear and thermal applications. This was due to improved physical, mechanical properties and weight savings advantage associated with metal matrix composite compared to unreinforced alloys (6, 7).

Reinforcement materials can simply be regarded as strength enhancer or load carrying member in MMCs. It is usually a non-metallic in nature including ceramics, agro and bioshell wastes. It can also be classified according to its geometry into, continuous and discontinuous fibre, wiskers or particulate reinforcement materials (8). Literature has shown (9) that the mechanical properties of MMCs with continuous fibre has superior strength compered to whisker or particulate reinforced composites. However, particulate metal matrix composites (PMMCs) are easier to process, cost-effective with good isotropic properties advantages which could be automated (4, 10). In addition, properties of PMMCs can easily be processed for desirable applications by modifying the parameters thereof such as the particle size, volume fraction, stirring speed and time, melt temperature and solidification rate. As a result, synthetic reinforcement particles such as silicon carbide (SiC), alumina (Al_2O_3) are the earlier and mostly investigated in MMCs. However, their use in industrial production of MMCs had greatly been hindered by the scarce and increasing cost of synthetic reinforcement materials like alumina, silica oxide and silica carbide. As a result, modern day researches on material development are now exploring the use of industrial and agro allied waste products as a cost-effective and potential source of reinforcement materials in MMCs production (4, 6, 11). Various viable industrial and agro-wastes that had been investigated in aluminium alloy matrix include agricultural (rice husk, bamboo leaves, coconut shells and fibers, maize corb and husk, egg shells) wastes and industrial (fly ash, red mud) wastes materials (5, 12-19). Their findings revealed that agro and industrial wastes can be use as aluminium matrix reinforcement materials due to their promising properties enhancement.

African giant land snail shells (*Archachatina marginata*) is a bio-waste material readily available in Nigeria and other tropical regions of the world. However, their increasing consumption of its flesh due to medicinal benefit especially in Nigeria has been re-

sulting into indiscriminate disposal with associated environmental threats (4, 20, 21). But a recent study (4) of this species of snail shell confirmed the presence of ceramics phases with promising potentials to be use as low-cost metal matrix reinforcement material. Various available processing routes for processing of MMCs include squeeze casting, infiltration, powder metallurgy and stir casting techniques. However, stir casting process has widely been reported to be the most viable and economical route for particle reinforced metal matrix composites (PMMCs) processing and production (22). Moreover, its simplicity, cheap and applicability for large scale industrial production has made it to surpassed other fabrication routes (23, 24). Hence in this paper, Physical and mechanical properties of *Archchatina marginata* snail shell particulate reinforced aluminium-silicon alloy are presented.

MATERIALS AND METHODS

Materials used in this work are piston scraps made of aluminium-silicon alloy as matrix material and discarded African giant land snail shells as reinforcement materials.

Processing of matrix materials

The scraps of aluminium piston sourced from Ipata-Oloje mechanic market in Ilorin, Kwara State, Nigeria was used in this study. The collected piston scraps were washed with detergents and warm water to obtain a clean and oily free aluminium scrap. It was then sun dried for three days before melted in pit furnace and de-slagged three times to eliminate the impurities. The chemical composition of processed aluminium scrap used in this study as examined with SEM/EDX analysis is presented in Table 1.

Table 1: Elemental composition of Al-Si alloy

Elements	Al	Si	C	O	Na	Br	Sr
Wt% Composition	87.10 ± 1.500	7.70 ± 0.950	0.03 ± 0.001	4.95 ± 0.250	0.01 ± 0.005	0.18 ± 0.002	0.03 ± 0.001

Reinforcement materials preparation and characterization

Figures 1 (a & b) shows the photograph of the *Archachatina Marginata* snail shells (SnS_p) and its powder form as used in this study. The elemental composition (by weight) of snail shell had previously been reported to contains 81% calcium carbonate in addition to other elements like silicon, aluminium, Sulphur, bromine, tin and potassium (4). The cleaned and dried snail shells were crushed into powder via a disc mill and subjected to calcination at 900 °C for 3 hours to obtain a thermally stable reinforcement material. The resulting powder obtained from calcination was followed by sieving analysis using BS1377:1990 standard procedure. The sieve sizes were arranged in descending order of fineness (250, 200, 150 and 100 µm). The powder retained at 100 µm sieve size was used in this work. The functional group analysis of both calcined and un-calcined S_nS_p inspected using Thermo-Nicolet 6700P FTIR Spectrometer (USA) in the range of 4000 cm⁻¹ to 500 cm⁻¹ using Attenuated Total Reflectance (Smart iTR) mode. Determination of SnS_p

(calcined and un-calcined) phase analysis was investigated using Cu-Kα (1.54 Å) radiations using PANalytical X'Pert Powder X-ray diffractometer from Philips, Netherlands. The diffractograms selected span through the range of 20 and 80° with step size of 0.02° and count time of 1 s per step. In addition, the morphology and particle size of the selected calcined snail shell powder (100 μm) was determined using SEM image supported with Microsoft word and Gwyddion 2.31. Resolution of SEM image as determined by Microsoft word is 0.91inches which is equivalent to 1 μm in the image. This scale was then used to determine the width (5.50 μm) and height (5.51 μm) of the SEM image which were used as impute data for width and height in the Gwyddion software for determining the particle sizes.
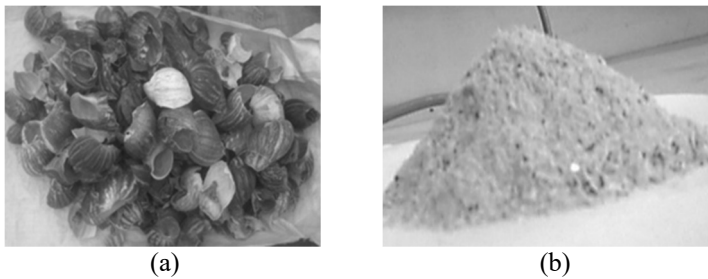

(a) (b)

Figure 1. Pictures of (a) Snail shell and (b) Snail shell powder.

Aluminium-silicon alloy/SnS$_p$ composite production

Figure 2 shows the illustrative sketch of the stir-casting process used for the production of Al-Si alloy/xSnS$_p$ matrix composite. Required amount of Al-Si alloy was kept in crucible which was first preheated to a red-hot condition in Thermo Scientific^{TM} FD1340M electric muffle furnace before subsequently raising the temperature to 750 °C at 10 °C/min heating rate. Thereafter, 0.1 wt% of magnesium ribbon was added to the molten aluminum to enhance wettability (12, 25). 1.5 wt% 100 μm of calcined snail shell powders were preheated at 400 °C to increase its wettability and prevent hydrogen gas inclusion in the melt through absorption of moisture (OH$^-$) (26). The liquid Al-Si alloy at 750 °C was poured into a preheated graphite crucible and incorporate the preheated calcined snail shell particulates into the melt followed by manual stirring for 5 minutes. The slurry mixture was then placed in locally fabricated electric stirrer set-up with attached heat source and type K- thermocouple for temperature monitoring (Figure 2). The molten composite slurry at 750±10 °C was then stirred at 400 rpm for 120 s and finally poured into ϕ20 mm cavity of 150 mm height steel die. The same procedure was followed for 3, 4.5, 6 and 7.5 wt% of SnS$_p$ additions in aluminium-silicon alloy matrix. The solidified Al-Si/xSnS$_p$ composites were then subjected to mechanical properties test.
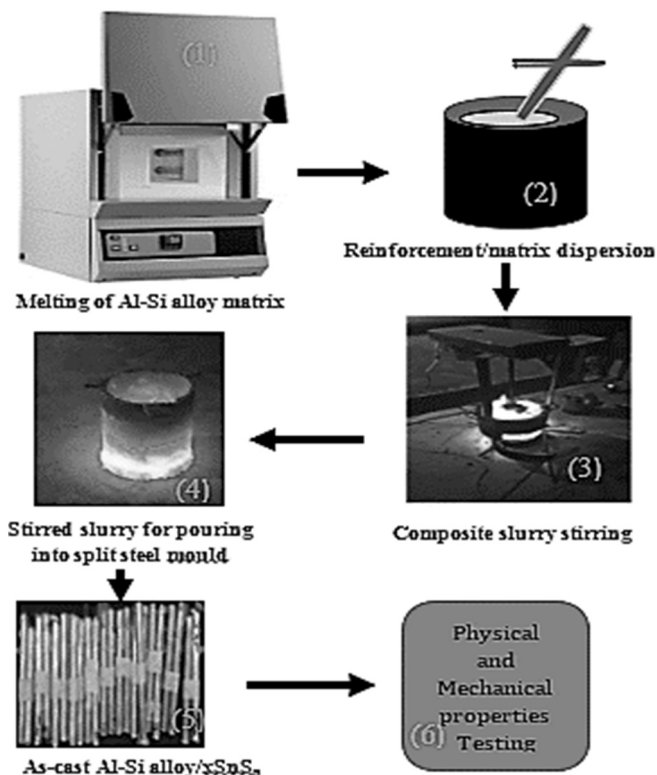
Figure 2. Illustrative pictures of Al-composite production process using stir-casting technique.

Physical, mechanical and morphology properties characterization

The Al-Si/xSn$_p$ composite obtained from stir-casting were evaluated by carry out physical, mechanical and morphological characterization.

Microstructural investigation of Al-Si/xSnS$_p$ composites

The surface microstructural analysis of Al-Si alloy matrix and reinforced composite specimens were examined using Scanning Electron Microscope (SEM) Vega LMU from TESCAN Brno, Czech Republic incorporated with X-Act Energy Dispersive Spectroscopy (EDS) detector from Oxford Instruments, Oxford UK operated at 20kV accelerated voltage. Samples for SEM observation were prepared by cutting and machined down to ϕ8 mm by 4 mm height dimension and grinded up to 2000 grit size SiC paper in a sequence of 400, 800, 1200 and 2000 grits to produce a smooth shiny surface. The ground surface was then etched in 5 % nital solution before finally mounted on a SEM sample holder for morphological examination.

Density determination

Archimedes' principle as reported in the work of Usman et al., (12) was adopted to evaluate the density of Al-Si/xSnS$_p$ composite and aluminium-silicon alloy. The weight of Al-Si/xSnS$_p$ composite was firstly carried out in air as (w_a) on a digital electronic weighing (Kern;D-72336 Balingen, Germany) balance with serial number W1500761 and then immersed in graduated measuring cylinder to obtain the corresponding weight in water (w_l) equivalent to rise in volume. The weight in water was then taken and recorded to obtain the density of Al-Si/xSnS$_p$ composite according to Equation 1.

$$\rho = \frac{w_a}{w_a - w_l} \qquad [1]$$

Where ρ = density (g/cm^3), w_a = weight in air and w_l = weight in water

Micro-hardness measurement

The hardness of the samples ground up to 1200 grit size at 400, 800 and 1200 grit size order for smoothness and flatness was measured as per ASTM E384 – 17 using a micro-Vickers hardness tester under an applied load of 4.9 N for 10 s. A minimum of five readings were taken at different points on each sample and the averaged of the readings were recorded as the hardness value for the Al-Si/xSnS$_p$ composite samples.

Evaluation of tensile and compressive strengths of Al-Si alloy/xSnS$_p$ composite

The tensile test of both unreinforced and Al alloy/SnS$_p$ composites specimen (Figure 3a) were carried out using computerized Testometric Universal UTM (TUE-C-500) model tensile machine (Figure 3b) by subjecting the specimen into a gradual applied tensile force at 10^{-3} s^{-1} until fracture occurred. The specimens were prepared as per ASTM E-8 standard strain rate (27, 28). The compressive strengths of Al-Si/xSnS$_p$ composite samples were also examined in accordance with ASTM E9-09 standard procedure under 10^{-3} s^{-1} strain rate and specimen dimension kept constant at 2.0 length to diameter ratio.

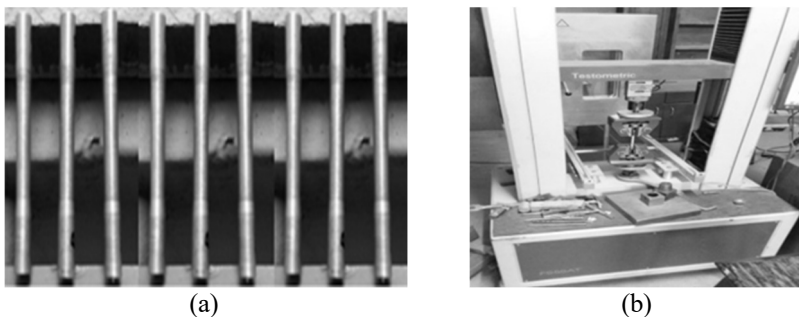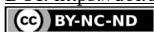(a)   (b)

Figure 3. Mechanical testing: (a) tensile samples and (b) tensile testing process

Impact strength determination

The impact strength of the Al-Si/xSnS$_p$ composite was performed following ASTMD 256-93 standard using Avery Dension Universal Izod Impact – Testing machine, model number 6705U/33122 (18). The prepared samples (75×10×10 mm) of both un-reinforced and reinforced alloy samples was conducted on notched samples at depth of 2 mm in the middle and a notch tip radius of 0.25 mm at an angle of 45°. The striking hammer was raised to the maximum height and release freely to fall from gravity on the already clamped specimen and the readings of absorbed energy to fracture the samples were taken.

RESULTS AND DISCUSSION

Fourier Transform Infrared (TIR) analysis of reinforcement material

The Fourier Transform Infrared (FTIR) patterns of both calcined and uncalcined *Archachatina marginata* snail shell powders were as illustrated in Figure 4. This test was carried out to identify the functional group and phase composition of both the calcined and un-calcined SnS$_p$ samples. The FTIR of un-calcined SnS$_p$ contains mainly aragonite, calcite (CaCO$_3$), carbonate (CO$_3^-$) group with characteristic intensity peaks at 1452, 849.802 and 1799 (cm^{-1}) wavelengths respectively. A small peak of Ca(OH)$_2$ absorption functional group was also observed at 667 cm^{-1} (29). On the other hands, the calcined SnS$_p$ depicts the characteristics IR bands at 1416 and 866 cm^{-1} intensity. These peaks correspond to CaO formation which is in line with the work of Loy et al. (29). In addition, a sharp peak of Ca(OH)$_2$ absorption was noticed with calcined SnS$_p$ sample at 3644.26 cm^{-1} (29, 39). This may be attributed to high reactivity and affinity for moisture of CaO as a result of its hygroscopic nature when exposed at the time of characterization (30). Figure 5 was a plot of intensity against angle (2theta) for the XRD analysis of calcined and un-calcined SnS$_p$. The Figure shows uncalcined snail shell powders were characterized with many peaks unlike the calcined form which shows a well crystalized and scanty peaks. This implies that, uncalcined SnS$_p$ has more phases than the calcined form with mono detectable phase. The main phase identified in un-calcined SnS$_p$ sample occurs at diffraction peaks (26.27, 36.20, 37.9, 38.56, 45.91, 48.48, 50.2, 52.4)° corresponding to aragonite according to JCPDS 00-041-1475 reference code. Meanwhile, the main phase of calcined SnS$_p$ sample occurs at diffraction peaks (32.43, 37.49, 53.89 and 67.73) corresponding to calcia (CaO) according to JCPDS 00-037-1497 reference code. The result implies that untreated snail shell powder mainly contains calcium carbonate and its calcination yielded mainly calcium oxide as the resulting product of calcination process of SnS$_p$ due to loss of volatile phases. The high proportion of CaO ceramic phase in calcined shell suggests African giant land snail shell as a potential alternative inexpensive source of reinforcement material in metal matrix composites. These results are in good agreement with FTIR results (Figure 4) which also confirmed the liberation of carbonate group for the formation of CaO.
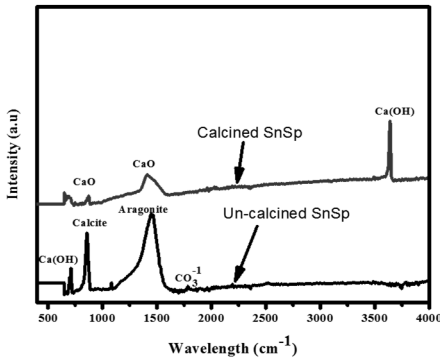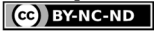
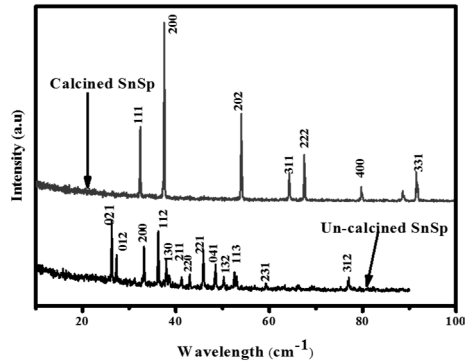**Figure 4.** FTIR of calcined and un-calcined snail shell

Figure 5. XRD graph of calcined and un-calcined snail shell

The morphology and particle size examination of calcined snail shell particulates used as reinforcement was as presented in Figure 6. It was observed that the calcined SnS particulates consist of particles of different sizes and shapes as a result of thermal necking and agitation of the calcination process. The minimum and maximum particle sizes as revealed by Gwyddion analysis were 0.219 µm and 2.009 µm respectively. The particles tend to disintegrate from larger particle size into smaller size through the process of diffusion into spheroid, oval, irregular quadrilateral shaped particles in fused form. Differences in colour of particles as depicted in the morphology were indication of heating effect of calcination process without any change in the compositional phases as indicated by XRD results.
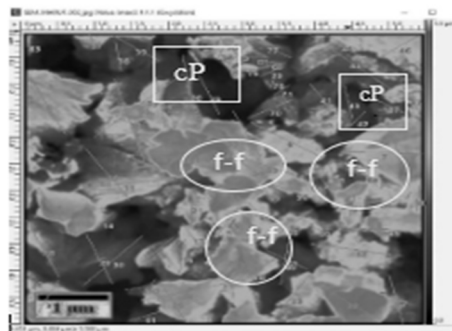
Figure 6. SEM morphology of calcined SnS powder

Density of aluminium-silicon/xSnS$_p$ composites

Figure 7 is a graph of density variation of aluminium-silicon matrix reinforced with varying weight additions of calcined SnS$_p$ and equivalent percentage density reduction in the composite produced. The graph shows decreasing trends in density of aluminium-silicon/SnS$_p$ composite produced with increasing weight addition of SnS$_p$. The density of
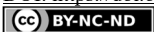
unreinforced sample as presented in Figure 7 was 2.757gcm^{-3} and decreases with increasing addition of snail shell addition to 2.609 gcm^{-3} at 7.5 wt%. Quantitatively the addition of 7.5 wt% of SnS$_p$ in aluminum-silicon alloy resulted in 5.37% density reduction in reinforced aluminium-silicon/SnS$_p$ composite. The reduction in weight of composite produced could be attributed to the addition of light weight calcined snail shell powder as reported in our previous study which replaced the higher dense soft matrix phase alloy. Hence, addition of less dense and hard SnS$_p$ can enhance the production of light weight composite material for improve performance. This result is in line with earlier reported works on metal matrix composites (31-35). Prasad *et al.* obtained a 2.4 % decrease in density with 8 wt% of rice husks while Shanmughasundaram *et al.* (32), reported 6.6 wt% density using flyash as reinforcement in aluminium composite and Usman *et al.* (12) recorded 19.9 % declined in density of bagasse reinforced aluminium matrix composite using double stir casting technique.
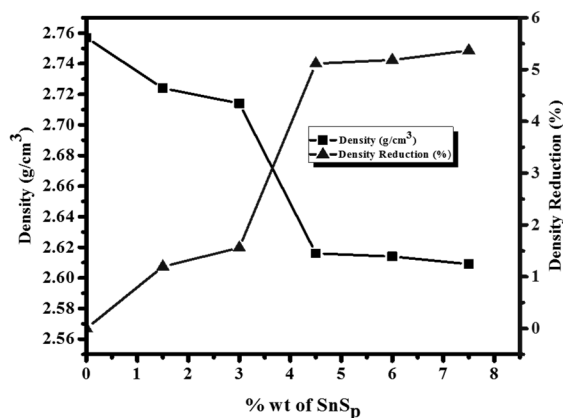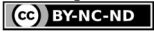

Figure 7. Density of Al-alloy/xSnS$_p$ composite with wt% of SnS$_p$ reinforcement.

Microstructure and chemical composition of Al-Si alloy/SnS$_p$ composites

Figure 8 shows the microstructure and corresponding EDS analysis of SnS$_p$ reinforced Al-Si alloy composites as obtained from scanning electron microscopy (SEM/EDS). The unreinforced aluminium alloy only shows a single phase with traces of silicon dendrites as discernible in the EDS micrograph. With 0.5 wt% SnS$_p$ addition in Al-Si matrix, the calcium peak as shown in respective EDS result and as displayed in the microstructure appeared as separate phases (Figure 8b). This observation was similar to all microstructures obtained with varying weight addition of SnS$_p$ (Figures 8c-f) in Al-matrix even though particle size of the matrix-reinforcement phases are becoming bigger given rise to spatial agglomeration and porosity inclusion within the Al-Si alloy matrix at 6 and 7.5 wt% of SnS$_p$ addition. This could be due to high reactivity of calcium oxide and it's affinity for silicon at high temperature and as well as difficulty in stirring at high speed in such a condition. The addition of SnS$_p$ is presumed to have enrich the dendritic strands of aluminium-silicon alloy in the unreinforced matrtix to forming calcium trioxo-silicate dendrite phase and aluminium-calcium phase particles which can act dislocation locker

for improve mechanical properties as evidenced in tensile, compressive and impact strengths of the composite produced. However, the open porosity as observed in in Figure 8e-f can be attributed to gradual drop in strengths of the composites. The EDS analysis of the respective alloy and composites as illustrated in Figure 8 and also provided in Table 2 as an attached file.
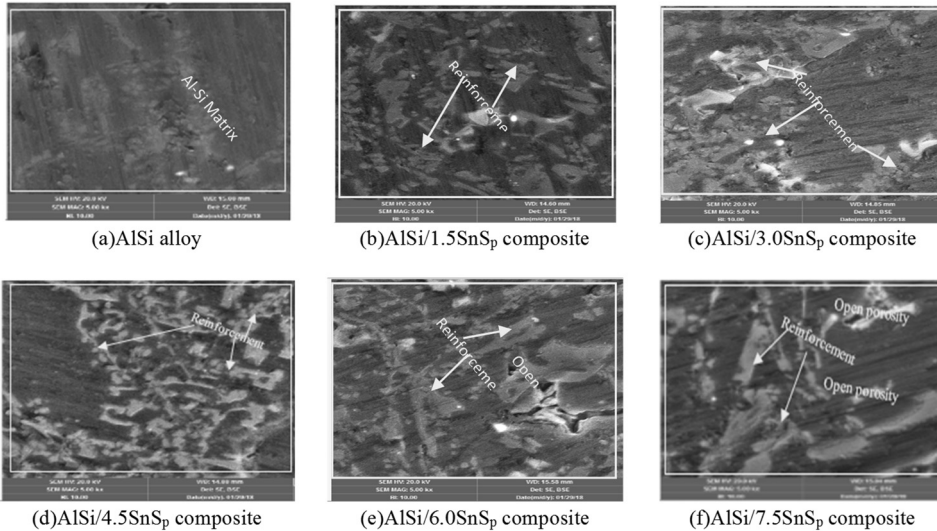

(a)AlSi alloy

(b)AlSi/1.5SnS$_p$ composite

(c)AlSi/3.0SnS$_p$ composite

(d)AlSi/4.5SnS$_p$ composite

(e)AlSi/6.0SnS$_p$ composite

(f)AlSi/7.5SnS$_p$ composite

Figure 8. Microstructure of calcined snail shell at 0 – 7.5%wt
(a-f) reinforced aluminium silicon alloys composites

Only aluminium, silicon and oxygen with no peaks of calcium or carbon was obtained in Figure 8a and Table 2. Addition of 1.5 wt% of SnS$_p$ resulted in 0.6 wt% of calcium and as well as Al and Si as the main element in AlSi/1.5 SnS$_p$ composite (see Table 2).

Table 2. EDS compsition of AlSi alloy and AlSi/xSnS$_p$ composites

Composites	Al (wt%)	Std	Si (wt%)	Std	Ca (wt%)	Std	O (wt%)	Std	Od (wt%)	Std
Ao	87.15	0.85	7.70	0.01	0.00	0.00	4.85	0.50	0.30	0.00
A1	87.30	0.15	7.69	0.13	0.61	0.48	4.25	0.22	0.15	0.02
A2	87.05	1.25	7.65	0.63	1.20	0.48	3.88	0.2	0.22	0.00
A3	86.04	0.77	7.60	0.55	1.90	0.51	4.41	0.25	0.05	0.01
A4	87.90	0.50	7.30	1.02	1.80	0.46	2.36	0.18	0.64	0.01
A5	89.40	0.85	5.59	0.98	1.59	0.35	2.76	0.35	0.66	0.08

Od - other elements (C, Fe, Br, Na); Ao - AlSi alloy; A1 - AlSi/1.5SnS$_p$; A2 - AlSi/3.0SnS$_p$; A3 - AlSi/4.5SnS$_p$; A4 – AlSi/6.0 SnS$_p$ and A5 – AlSi/7.5SnS$_p$

Further addition of SnS$_p$ increase the peaks of calcium content in addition to Al, Si O$_2$ and other trace elements including carbon, iron, sodium and bromine of the resulting composites up to 4.5 wt% of SnS$_p$. However, above 4.5 wt% addition of SnS$_p$, a rapid fall
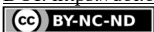
in calcium, silicon and oxygen peaks was observed in 6 and 7.5 wt% of SnS_p reinforced composites with the calcium peaks decreases to 1.80 and 1.59 wt% respectively in the resulting composites as discernible in Table 2. The presence of calcium peak (s) in the composites is an indication of presence of calcined snail shell particles in the aluminium matrix compared to un-reinforced alloy. The decrease in silicon, oxygen and calcium especially at higher calcined SnS_p addition, can be attributed to slag formation noticed at higher weight addition of SnS_p which may possibly coagulate out some of these elements along with the slag due to high reactivity. This factor might have been responsible for some decreases noticed in strength at higher percentage addition of SnS_p in Al-Si matrix composites.

Tensile fracture surface characteristics

Figure 9 shows SEM morphologies of the tensile fractured surfaces of unreinforced Al-Si alloy (Figure 9a) and reinforced Al-Si/$xSnS_p$ composites samples (Figures 9b-f) respectively. The Figure shows a characteristic feature of cup and cone (cc), goose and dimples (gd) and as well as fibrous (F) morphologies in both the unreinforced and reinforced composites though with slight differences.

a – Al-Si

b – Al-Si/1.5SnS

c – Al-Si/3SnS

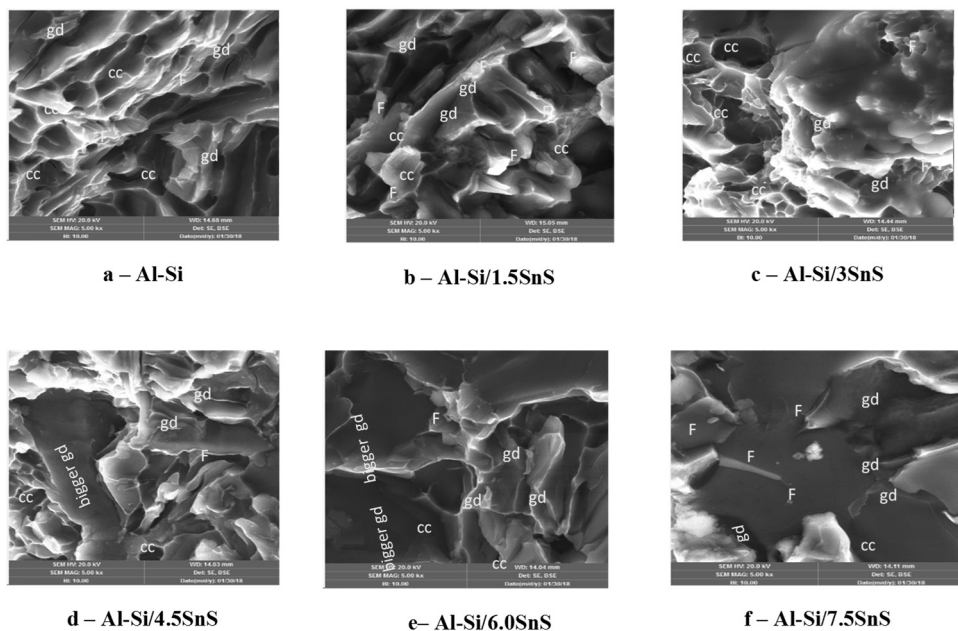d – Al-Si/4.5SnS

e– Al-Si/6.0SnS

f – Al-Si/7.5SnS

Figure 9. SEM of Al-Si composites' tensile fracture surfaces

These characteristic features imply a ductile failure mode in both un-reinforced and reinforced composites in which more energy can be absorbed before failure. However, increasing wt% addition of calcined SnS_p has no significant influence on the morpho-

logies but only results in gradual disappearance of the cone and cup structure into a large goose and dimple structure. This metamorphosis of structure with poor resistance to crack initiation tends to reduce the resilience of material to plastic deformation to pave way for sudden failure of the material. Hence gradual reduction in ductility of the composite may resulted with increasing addition of calcined SnS_p and as evidenced in percentage strain results in Figure 12.

Micro-hardness measurement

The hardness variation of control and Al-Si/xSnS_p composite produced with increasing weight percent addition of calcined snail shell was depicted in Figure 10. It was observed that the hardness increases with increasing weight percent of SnS_p for all reinforced Al-Si alloy. For instance, the hardness value of Al-Si alloy was 97.844 HV at 0 wt% and steadily increased to 118.02 HV at 6 wt% of SnS_p and then decreased to 108.36 HV at 7 wt% SnS_p addition. The increments in hardness results can be arrogated to an increase in weight percentage of hard ceramic phases of calcined SnS_p in aluminium alloy matrix. The calcined SnS_p contains phases like CaO, Fe_2O_3, Cr_2O_3 and remnant carbon of calcination process as revealed by XRD result (Figure 5). These phases are ceramics materials which are hard and rigid. Their presence in the Al-Si alloy matrix enhances composite phase hardness. Thus, resulting in strong bond interface between the matrix and reinforcement for increased hardness values in the produced composites (17, 33, 34). This is in accordance with the works of earlier authors (3, 12) and increase in composites hardness was linked to addition of hard ceramic reinforcement phase in the matrix. However, the slight decrement in hardness at 7.5 wt% could be as a result of removal of some hard phases (calcium) in form of slag due to high reactivity as noticed in SEM/EDS results.
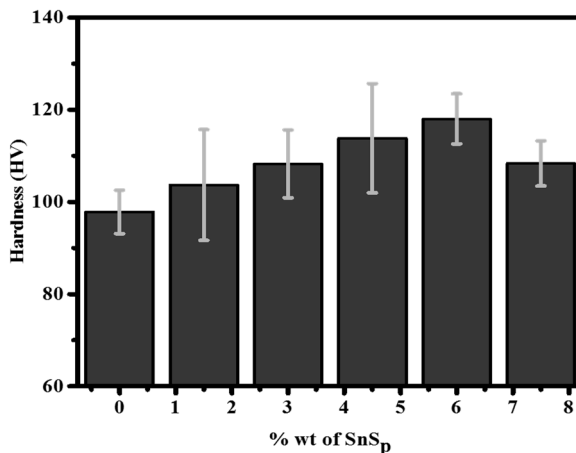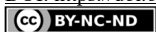

Figure 10. Influence of SnS_p wt% on hardness of Al-Si alloy/xSnS_p composite

Tensile and compressive strengths behaviour of Al-Si alloy/xSnS$_p$ composites

The tensile and compressive strengths of Al-Si alloy/xSnS$_p$ composites produced by stir-casting technique are presented in Figures 11 and 12, respectively. Both strengths increase with increasing weight percent of SnS$_p$. For instance, the average tensile strength increases from 155 ±5 MPa at 0 wt% to 211± 4.8 MPa when 4.5 wt% of SnS$_p$ was incorporated into Al-Si matrix. Addition of SnS$_p$ beyond this range does not further increase tensile strength but only resulted in slight decrement by 5 MPa. This implies that a maximum of 36% tensile strength increment at 4.5 wt% SnS$_p$ addition in Al-Si alloy was achieved. Also, it is worthy of noting that, 6 and 7.5 wt% addition of SnS$_p$ yielded 32 and 28% in tensile enhancement respectively compared to unreinforced Al-Si alloy.

Similarly, the compressive strength (Figure 12) of the same Al-Si/SnS$_p$ composites depicted similar pattern of the tensile strength behaviour. The compressive strength increased with increasing addition of SnS$_p$ from 462 ± 22.30 MPa SnS$_p$ with Al-Si alloy matrix up to a maximum strength of 551.748 ± 19.56 MPa at 6 wt% of SnS$_p$ addition though with slight reduction in percentage elongation. Beyond this limit of addition, only resulted in compressive strength decrement. The equivalent compressive strength increment at 6 wt% of SnS$_p$ was 19% relative to unreinforced Al-Si alloy. The increase in both tensile and compressive strength as noticed in Al-Si/SnS$_p$ composites was attributed to addition of hard ceramic phase of snail shell particles in Al-Si alloy with no signs of agglomeration as illustrated Figure 8. The presence of this SnS$_p$ in Al-Si matrix restricts the displacement of silicon in aluminium matrix phase. Thus, resulted in high dislocation density which in turn requires higher force for plastic deformation. Moreover, the improvement in both strengths can be attributed to strain hardening effect as a result of localized stress action of SnS$_p$ particles at different points within the matrix coupled with good wettability of SnS$_p$ preheated at 400 °C prior the addition into the Al-Si alloy. These results corroborate with the works of Hassan and Aigbodion, Dwivedi *et al.*, Aigbodion and Hassan, Prasad and Ramma (3, 19, 33, 35), where the strength improvement of reinforced matrix was attributed to the presence of hard particles and higher dislocation density along the grains of the matrix alloy. However, beyond 4.5 and 6 wt% of SnSp inclusion in matrix, the tensile and compressive strengths decrease marginally as depicted in Figures 11 & 12 respectively. This was due to addition of calcined snail shell in Al-Si alloy phase exceeding the saturation limit thus resulting in mis-matching of reinforcement-matrix interface giving rise to reduced dislocation density. Hence, reduction in strength of the composite set-in as noticed in both tensile and compressive strengths (Figures 11 & 12). Similar results were obtained by earlier researchers where decrease in strength was attributed to poor uniform distribution of harder phase in matrix at higher content (19). Moreover, the magnitude of compressive strength presented in Figure 10 was found to be higher than that of the tensile strength (Figure 11) of the same Al-Si/SnS$_p$ composites. This can be attributed to presence of some defects such as micropore, gas inclusion in which the tensile strengths are more sensitive to compared to compressive strength action as experienced during testing. This is because the opposite applied loads coming towards each other during compressive action of the testing tends to entangle the interatomic interface which will initially increase the dislocation density and must be overcome before deformation commences. Thus, higher compressive strength compared to tensile strength.

Original scientific paper
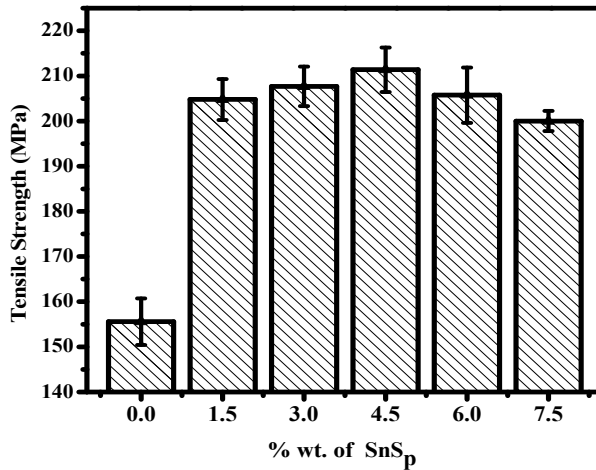
Figure 11. Influence of SnS$_p$ wt% on tensile strength of Al-alloy/xSnS$_p$ composite
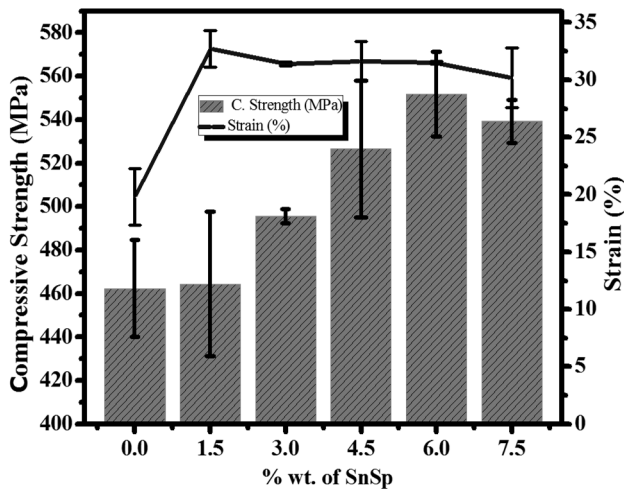
Figure 12. Influence of SnS$_p$ wt% on compressive strength and strain of Al-alloy/xSnS$_p$ composite

Influence of SnS$_p$ addition on impact energy of Al-Si alloy

Figure 13 shows the impact energy of Al-Si alloy/xSnS$_p$ composites. With increase in wt% of SnS$_p$ addition in Al-Si matrix, the impact strength increases. As illustrated from Figure 13, the impact energy increased from 72.5 Joules at 0 wt% to 90.5 Joules when 7.5 wt% of SnS$_p$ was dispersed in to the Al-Si alloy phase. The increment in impact strength obtained in Al-Si/7.0%SnS$_p$ composite is equivalent to 25% when compare to un-reinforced Al-Si alloy. It was noticed that, this result looks contrary to some earlier reported
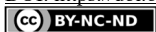
work in that, increasing addition of hard brittle reinforcement in metal matrix resulted into corresponding decrease in impact strength due to loss of ductility (3, 36). However, it will be noticed from the present work that, with addition of 1.5 wt% of calcined snail shell in the matrix, the percentage strain of the composite increases from 20% for the control sample to 30% plus which with further addition of reinforcement particles only result in slight reduction in strain. Therefore, the increase in impact energy as obtained in the study can be linked to good percentage strain property which damped the loading constraint and the rigidity of the calcined SnS_p second phase particles to hinder the composite impact deformation. This result was and follow the pattern reported in the work of Bello *et al*. and Abdullahi *et al*. (37, 38), where they reported increase in impact energy with increase in reinforcement addition in the matrix.
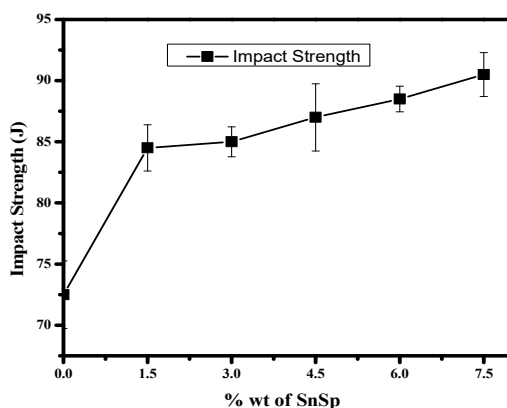
Figure13. Effect of SnS_p on impact strengths of Al- alloy/$xSnS_p$ composite

CONCLUSIONS

From the results and discussion in this research work, the following conclusions are hereby submitted:

1. Calcined giant land snail shells particles were successfully incorporated as reinforcement material in aluminium-silicon scrap via stir casting technique.
2. Microstructural examination of the produced composites revealed a fair dispersion of SnS_p with high desolution in aluminum-silicon matrix with discernible aluminu-calcium-silicon dendrites, a major factor causing improvement in mechanical properties of Al-alloy/$xSnS_p$ composites synthesized.
3. The dispersion of calcined SnS_p in Al-Si alloy matrix yielded a lighter and high impact energy in Al-Si/$xSnS_p$ composite by 5.4 and 25 % respectively at 7.5 wt%. This implies that the developed composite can absorbed more energy before failure compared to un-reinforced Al-Si alloy.
4. The maximum tensile and compressive strengths obtained in as-cast Al-Si/$xSnS_p$ composites were 211 ± 4.8 MPa and 552 ± 19.56 MPa at 4.5 wt% and 6.0 wt% SnS_p addition equivalent to 36 and 19% respectively relative to un-reinforced Al-Si8 alloy.

The study concluded that calcined African giant land snail shell particulate can serves as an alternative low-cost reinforcement material in Al-Si alloy matrix for the production of lightweight with enhanced mechanical properties. The Al-Si/SnS$_p$ composites can find application in the production of automotive components such as piston, connecting rods and cylinder lining.

Acknowledgements

REFERENCES

1. Lancaster, L.; Lung, M.H.; Sujan, D. Utilization of Agro-industrial wastes in metal matrix composites: Towards sustainability. *Waset 2013,* **2013,** 1136-1144.
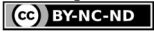2. Silva, M.J.; Kardoso, K.R.; Travessa, D.N. Production of NbC reinforced aluminium matrix composites by mechanical alloying. 21° CBECIMAT - Congresso Brasileiro de Engenharia e Ciência dos Materiais 09 a 13 de Novembro de 2014, Cuiabá, MT, Brasil, **2014,** *5738*(1), 2665–72.
3. Hassan, S.B.; Aigbodion, V.S. Effects of eggshell on the microstructures and properties of Al–Cu–Mg/eggshell particulate composites. *J King Saud Univ - Eng Sci.* **2015**, *27*(1), 49–56.
4. Kolawole1, M.Y.; Aweda, J.O.; AbdulKareem S. Archachatina marginata bio-shells as reinforcement material in metal matrix composites. *Int J Automot Mech Eng.* **2017,** *14*(1), 4068–79.
5. Oghenevweta, J.E.; Aigbodion, V.S.; Nyiorm G.B.; Asuke F. Mechanical properties and microstructural analysis of Al–Si–Mg/carbonized maize stalk waste particulate composites. *J King Saud Univ - Eng Sci.* **2016**, *28*(2), 222–9.
6. Madakson, P.B.; Yawas, D.S.; Apasi A. Characterization of coconut shell ash for potential utilization in metal matrix composites for automotive applications. *Int J Eng Sci Technol.* **2012**, *4*(3), 1190–8.
7. Aigbodion, V.S.; Hassan, S.B. Effects of silicon carbide reinforcement on microstructure and properties of cast Al-Si-Fe/SiC particulate composites. *Mater Sci Eng A.* **2007**, *447*(1–2), 355–60.
8. Bodunrin, M.O.; Alaneme, K.K. Aluminium matrix hybrid composites: a review of reinforcement philosophies; mechanical, corrosion and tribological characteristics. *J Mater Res Technol.* **2015**, *4*(4), 434–45.
9. Kumar, G.B.V.; Rao, C.S.P; Selvaraj, N. Mechanical and tribological behavior of particulate reinforced aluminum metal matrix composites – a review. *J Miner Mater Charact Eng.* **2011,** *10*(01), 59–91.

10. Miyajima, T.; Iwai, Y. Effects of reinforcements on sliding wear behavior of aluminum matrix composites. *Wear,* **2003,** *255*(1–6), 606–16.

11. Fatile, O.B.; Akinruli, I J. F.; Amori, A.A. Microstructure and mechanical behaviour of stir-cast al-mg-sl alloy matrix hybrid composite reinforced with corn cob ash and silicon carbide. *Int J Eng Technol Innov.* **2014**, *4*(4), 251–9.

12. Usman, A.M.; Raji, A.; Hassan, M. A.; Waziri, N.H. A comparative study on the properties of al-7 % si-rice husk ash and al-7 % si-bagasse ash composites produced by stir casting. *Int J Eng Sci.* **2014**, *3*(8), 1–7.

13. Khan, M.Z.; Anas, M.; Hussain, A.; Irshadul Haque, M.; Rasheed, K. Effect on mechanical properties of aluminium alloy composites on adding ash as reinforcement material. *J Met Mater Miner.* **2015**, *25*(2), 1–7.

14. Saravanan, S.D.; Kumar, M.S.; Effect of mechanical properties on rice husk ash reinforced aluminum alloy (AlSi10Mg) matrix composites. *Procedia Eng.* **2013**, *64*, 1505–13.

15. Alaneme, K.K.; Fatile, B.O.; Borode, J.O. Mechanical and corrosion behaviour of Zn-27Al based composites reinforced with groundnut shell ash and silicon carbide. *Tribol Ind.* **2014**, *36*(2), 195–203.

16. Singh, J.; Suri, N.M; Verma A. Affect of mechanical properties on groundnut shell ash reinforced Al6063. *Int J Technol Res Eng.* **2015,** *2*(11), 2347–4718.

17. Aku, S.Y.; Yawas, D.S.; Apasi, A. Evaluation of cast Al-Si-Fe alloy/coconut shell ash particulate composites. *Gazi Univ J Sci.* **2013**, *26*(3), 449–57.

18. Agunsoye, J.O.; Talabi, S.I.; Bello, S.A.; Awe, I.O. The effects of Cocos nucifera (coconut shell) on the mechanical and tribological properties of recycled waste aluminium can composites. *Tribol Ind.* **2014**, *36*(2), 155–62.

19. Dwivedi, S.P.; Sharma, S.; Mishra, R.K. Characterization of waste eggshells and $CaCO_3$ reinforced AA2014 green metal matrix composites: A green approach in the synthesis of composites. *Int J Precis Eng Manuf.* **2016**, *17*(10), 1383–93.

20. Jatto, E.O.; Asia, I.O.; Egbon, E.E; Otutu, J.O.; Chukwuedo, M.E; Ewansiha, C.J. Treatment of waste water from food industry using snail shell. *Acaedmia Arena.* **2010,** *2*(1), 32–6.

21. Aluko, F.A.; Adisa, A.A.; Taiwo, B.B.A.; Ogungbesan, A.M.; Awojobi, H.A. Quantitative measurements of two breeds of snail. *American Journal of Research Communication,* **2014**, *2*(5), 175–82.

22. Kant, S.; Singh, V. A. Stir casting process in particulate aluminium metal matrix composite: A review. I*nt J Mech Solids.* **2017**, *9*(1), 973–1881.

23. Babalola, P.O.; Bolu, C.A.; Inegbenebor, A.O.; Odunfa, K.M. Development of aluminium matrix composites: A review. *Online International Journal of Engineering and Technology Research,* **2014**, *2*, 1–11.

24. Sijo, M.T.; Jayadevan, K.R. Analysis of stir cast aluminium silicon carbide metal matrix composite: A comprehensive review. *Procedia Technol.* **2016**, *24*, 379–85.

25. Prasad, K.N.P.; Ramachandra, M. Effect of squeeze pressure on the hardness and wear resistance of Aluminium flyash composite manufactured by stir-squeeze casting. *Int J Eng Invent.* **2013**, *3*(4), 2278–7461.

26. Bhandare, R.G.; Sonawane, P.M. Preparation of aluminium matrix composite by using stir casting method. *Int J Eng Adv Technol.* **2013**, *3(*2), 61–5.

Original scientific paper

27. Paul, K. K.; Sijo, M.T. Effect of stirrer parameter of stir casting on mechanical properties of aluminium silicon carbide composite. *Int. J. of Modern Eng. Res.* **2015**, *5*(August), 43–9.

28. Jain, S.; Rana, R.S.; Jain P. Study of microstructure and mechanical properties of Al- Cu metal matrix reinforced with b 4 c particles composite. *Int Res J Eng Technol.* **2016**;*3*(1):499–504.

29. Loy, C.W.; Matori, K.A.; Lim, W.F.; Schmid, S.; Zainuddin, N.; Wahab, Z.A. Effects of Calcination on the crystallography and nonbiogenic aragonite formation of Ark clam shell under ambient condition. *Adv Mater Sci Eng.* **2016**, *2016*, 1-8

30. Galván-Ruiz, M.; Hernández, J.; Baños, L.; Noriega-Montes, J.; Rodríguez-García, M.E.; Characterization of calcium carbonate, calcium oxide, and calcium hydroxide as starting point to the improvement of lime for their use in construction. *J Mater Civ Eng.* **2009**, *21*(11), 694–8.

31. Krishna, M.V.; Xavior, A.M. An investigation on the mechanical properties of hybrid metal matrix composites. *Procedia Eng.* **2014**, *97*, 918–24.

32. Shanmughasundaram, P.; Subramanian, R.; Prabhu, G. Some studies on aluminium - Fly ash composites fabricated by two step stir casting method. *Eur J Sci Res.* **2011**, *63*(2), 204–18.

33. Aigbodion, V.S.; Hassan, S.B. Experimental correlations between wear rate and wear parameter of Al-Cu-Mg/bagasse ash particulate composite. *Mater Des.* **2010**, *31*(4), 2177–80.

34. Rajan, T.P.D.; Pillai, R.M.; Pai, B.C.; Satyanarayana, K.G.; Rohatgi, P.K. Fabrication and characterisation of Al-7Si-0.35Mg/fly ash metal matrix composites processed by different stir casting routes. *Compos Sci Technol.* **2007,** *67*(15–16), 3369–77.

35. Prasad, D.S.; Krishna, A.R. Production and mechanical properties of A356.2/RHA composites. *Int J Adv Sci Technol.* **2011**, *33*, 51–8.

36. Alaneme, K.K.; Adama, S.I.; Oke, S.R. Mechanical properties and corrosion behaviour of ZN-27AL based composites reinforced with silicon carbide and bamboo leaf ash. *Leonardo Electron J Pract Technol.* **2014**, *13*(25), 58–71.

37. Bello S.A.; Agunsoye J.O.; Adebisi J.A.; Hassan S.B. Effect of aluminium particles on mechanical and morphological properties of epoxy nanocomposites. *Acta Period Technol.* **2017**, *48*, 25–38.

38. Abdullah, S.I.; Ansari, M.N.M. Mechanical properties of graphene oxide (GO)/ epoxy composites. *HBRC J.* **2015**, *11*(2), 151–6.
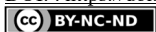
SELECTION OF ANTAGONISTS FOR BIOCONTROL OF
Xanthomonas euvesicatoria

Ivana S. Pajčin[1]*, Vanja R. Vlajkov[1], Dragoljub D. Cvetković[1], Maja V. Ignjatov[2],
Mila S. Grahovac[3], Damjan G. Vučurović[1], Jovana A. Grahovac[1]

[1] University of Novi Sad, Faculty of Technology Novi Sad, Bulevar cara Lazara 1, 21000 Novi Sad, Serbia
[2] Institute of Field and Vegetable Crops, Maksima Gorkog 30, 21000 Novi Sad, Serbia
[3] University of Novi Sad, Faculty of Agriculture, Trg Dositeja Obradovića 8, 21000 Novi Sad, Serbia

Xanthomonas euvesicatoria is a worldwide causer of pepper bacterial spot, a bacterial plant disease responsible for massive losses of fresh pepper fruits. Considering the current problems in management of bacterial plant diseases, biological control using antagonistic microbial strains with high potential for plant pathogens suppression emerges as a possible solution. The aim of this study was to select suitable antagonists for suppression of X. euvesicatoria among the bacteria, yeast and fungi from the genera Pseudomonas, Lactobacillus, Saccharomyces and Trichoderma, based on in vitro antimicrobial activity testing using the diffusion disc method. The results of this study have revealed that cultivation broth samples of the antagonists Lactobacillus MK3 and Trichoderma reseii QM 9414, as well as supernatant samples of the antagonist Pseudomonas aeruginosa I128, have showed significant potential to be applied in biological control of X. euvesicatoria. Further research would be required to formulate suitable cultivation medium and optimize bioprocess conditions for production of the proposed pepper bacterial spot biocontrol agents.

Keywords: *Pseudomonas* spp., *Lactobacillus* spp., *Saccharomyces cerevisiae*, *Trichoderma reseii*, antimicrobial activity

INTRODUCTION

Bacterial plant diseases represent a worldwide problem for sustainable food production due to difficulties and insufficient efficacy of existing agricultural practices in plant disease management. Furthermore, the lack of efficient disease suppression agents and heavy usage of copper-based chemicals and antibiotics have led to emergence of resistant bacterial pathogenic strains (1). Bacteria of the genus *Xanthomonas* are among the important plant pathogens, having a wide spectrum of plant hosts (2). The species *Xanthomonas euvesicatoria* is a causer of tomato and pepper bacterial spot, a plant disease responsible for massive fresh fruit losses, resulting in their degraded quality, lower market value and insufficient amount for industrial processing (3). Since usual bacterial spot disease management practices, such as crop rotation, usage of healthy planting material and copper bactericides (2) haven't given satisfying results in previous decades, biological control using microbial biocontrol agents emerges as a possible solution.

Bacteria of the genus *Pseudomonas* have been largely employed as biocontrol agents due to their several beneficial abilities: to colonize and multiply in the rhizosphere, to

---

colonize plants endophytically, to aggressively compete with other microorganisms and to adapt to environmental stress (4). Furthermore, these bacteria produce wide range of different biocontrol metabolites: antibiotics, siderophores, volatiles and plant growth promoters (5). Biocontrol traits of *Lactobacillus* spp. rely on production of bioactive metabolites such as organic acids and bacteriocins (6). An additional advantage for their application as biocontrol agents is GRAS (Generally Regarded As Safe) and QPS (Qualified Presumption of Safety) status of several *Lactobacillus* strains (7). *Saccharomyces cerevisiae* is also a promising biocontrol agent with several biocontrol traits: competition and production of hydrolytic enzymes and volatiles (8). *Trichoderma* spp. are well-known as biocontrol agents exhibiting several indirect or direct biocontrol mechanisms, including competition for nutrients and space, modifying the environmental conditions, plant growth promotion, antibiosis, mycoparasitism and activation of plant defense mechanisms (9). Fungi of the genus *Trichoderma* produce wide range of compounds inducing localized or systemic resistance responses, and also contribute to substantial changes to plant proteome and metabolism, simultaneously promoting root growth and development, uptake and use of nutrients and crop productivity (10). Some of these compounds include plant growth factors, antibiotics, siderophores and enzymes (9).

The aim of this study was to select suitable antagonists for suppression of *X. euvesicatoria* pathogenic strains, isolated from pepper plants with symptoms of bacterial spot, among the isolates from the genera *Pseudomonas, Lactobacillus, Saccharomyces* and *Trichoderma*. The main indicator of antagonistic activity was inhibition zone diameter, obtained as a result of antimicrobial activity testing using the diffusion disc method.

EXPERIMENTAL

Antagonists and pathogens

In this study several antagonists were investigated: *Pseudomonas aeruginosa* ATCC 27853 (A1), *Pseudomonas aeruginosa* I128 (A2) isolated from water, *Pseudomonas putida* I315 (A3) isolated from water, three *Lactobacillus* strains isolated from cheese – *Lactobacillus* I14 (A4), *Lactobacillus* I19 (A5) and *Lactobacillus* MK3 (A6), *Saccharomyces cerevisiae* P31 (A7) and *Trichoderma reseii* QM 9414 (A8). Three phytopathogenic *Xanthomonas euvesicatoria* strains (X1, X2 and X3) were isolated from leaves of pepper plants with symptoms of bacterial spot in 2015 at the cadastral municipality Pivnice, Serbia.

Cultivation of antagonists

Inocula of the antagonistic strains were prepared using the following media: nutrient broth (HiMedia, India) for *Pseudomonas* spp. (A1, A2, A3), MHB (Mueller-Hinton broth – HiMedia, India) for *Lactobacillus* spp. (A4, A5, A6), SMB (Sabouraud maltose broth – HiMedia, India) for *Trichoderma reseii* QM 9414 (A8) and semi-synthetic medium for *Saccharomyces cerevisiae* P31 (A7) (11). Inocula were prepared on a laboratory shaker at 30 °C, with mixing (150 rpm) and spontaneous aeration during 48 h. Cultivation of antagonists was performed using the similar media as for the inocula preparation, under the similar conditions, except bioprocess duration was 96 h.
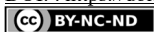
Testing of antimicrobial activity

Three suspensions of pathogenic *X. euvesicatoria* strains (X1, X2 and X3) were pre-
pared using a sterile saline to achieve 10^8 CFU/mL. These suspensions were used to ino-
culate the melted and tempered (50±1°C) test media – YMA (yeast maltose agar) (12).
Samples for antimicrobial activity testing were cultivation broth samples, obtained after
the end of the cultivation of selected antagonists, as well as their supernatants obtained by
centrifugation of cultivation broth samples at 13000 g for 10 min (Rotina 380R, Hettich,
Germany) which were afterwards filtrated through nylon syringe filters (0.22 µm pore
diameter, Agilent Technologies, Germany) to completely remove biomass of antagonists.
Commercial streptomycin disks containing 30 µg of streptomycin (Torlak, Serbia) were
used as positive control, while sterile distilled water was used as negative control. Anti-
microbial activity testing was performed in triplicates using the diffusion disc method
(13) with 10 µL of sample per each disk. After incubation at 26 °C for 72 h, inhibition
zone diameters were measured.

Experimental data analysis

The obtained data regarding inhibition zone diameters were processed using several
statistical methods (Levene's test, ANOVA – analysis of variance, Duncan's multiple
range test) using the software Statistica 13.5 (Tibco Software Inc., USA). All statistical
analyses were performed at significance level of 95%. Mean values and standard devia-
tions of inhibition zone diameters were calculated using Microsoft® Excel 2010 software
(Microsoft Corporation, USA).

RESULTS AND DISCUSSION

After cultivation of eight selected antagonists, cultivation broth samples and biomass-
free supernatants were tested for antimicrobial activity against three *X. euvesicatoria*
phytopathogenic strains in order to select the most suitable antagonist and also to deter-
mine a suitable biocontrol agent (cultivation broth containing biomass of antagonists, or
extracellular metabolites produced by the antagonists contained in biomass-free superna-
tants). The experimental data regarding the obtained inhibition zone diameters were
hence analyzed separately for cultivation broth and supernatant samples. Levene's test
was performed for both datasets and it confirmed hypothesis of variance homogeneity in
both cases. Furthermore, one-way ANOVA was applied to determine statistical signifi-
cance of the antagonists' and pathogens' effect to inhibition zone diameter. Finally, Dun-
can's multiple range test was performed to establish homogenous groups of antagonists
and pathogens with the same level of statistical significance when it comes to their effect
on antimicrobial activity of the tested cultivation broth and supernatant samples against
X. euvesicatoria.

The results of one-way ANOVA for antimicrobial activity of cultivation broth samp-
les of the selected antagonists against *X. euvesicatoria* are given in Table 1. As it could
be observed, these results have revealed statistically significant effect of the tested anta-
gonistic strains to the obtained inhibition zone diameters at the significance level of 99%,
since the obtained *p*-value is less than 0.0001.

Original scientific paper

Table 1. One-way ANOVA of inhibition zone diameters obtained as a result of antimicrobial activity testing of cultivation broth samples of the selected antagonists against *X. euvesicatoria*

Effect	SS	MS	DF	F-value	*p*-value
Intercept	41525.38	41525.38	1	32795.18	**<0.0001**
Antagonist	3843.95	480.49	8	379.48	**<0.0001**
Error	91.17	1.27	72	-	-

SS – sum of squares, MS – mean squares, DF –degree of freedom

Furthermore, homogenous groups of antagonists established by the Duncan's multiple range test when it comes to testing of antimicrobial activity of the cultivation broth samples are given in Table 2.

Table 2. Results of Duncan's multiple range test for inhibition zone diameters (mean values, standard deviations and significance levels) obtained as a result of antimicrobial activity testing of cultivation broth samples of the selected antagonists against *X. euvesicatoria*

Antagonist	Inhibition zone diameter (mm)
A7	15.72±0.97[a]
A1	16.83±1.41[b]
A5	17.28±0.83[b]
A3	17.89±1.05[b]
A2	20.00±0.87[c]
A4	23.89±1.05[d]
A8	26.50±1.12[e]
A6	27.22±1.39[e]
S	38.44±1.26[f]

A1 - *Pseudomonas aeruginosa* ATCC 27853, A2 – *Pseudomonas aeruginosa* I128, A3 – *Pseudomonas putida* I315, A4 - *Lactobacillus* I14, A5 - *Lactobacillus* I19, A6 - *Lactobacillus* MK3, A7 – *Saccharomyces cerevisiae* P31, A8 – *Trichoderma reseii* QM 9414, S – streptomycin

The lowest values of inhibition zone diameters were obtained using the cultivation broth sample of the antagonist A7 (*S. cerevisiae* P31), while the highest values of inhibition zone diameters in range 25.5-28.5 mm were obtained by the cultivation broth samples of *Lactobacillus* I14 (A4) and *T. reseii* QM 9414 (A8). These two antagonists are also at the same level of statistical significance, indicating that each of them could be successfully applied for suppression of *X. euvesicatoria*. In the study published by Daranas et al. (7) *Lactobacillus* spp. were successfully applied as biocontrol agents for suppression of *Xanthomonas* spp., where the most dominant *in vitro* inhibitory effect was lowering of the pH value due to production of lactic acid. Shrestha et al. (14) have also observed significant potential of *Lactobacillus* spp. to be used as biocontrol agents of pepper bacterial
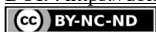
spot. *Trichoderma* spp. have provided systemic protection against *X. euvesicatoria* in the range 24.13-95.94% (15). *Trichoderma* strains in mixed culture with other antagonistic microorganisms, such as *Bacillus* strains, could also provide satisfying plant protection from bacterial spot (16).

When it comes to testing of antimicrobial activity of biomass-free supernatants obtained by centrifugation of cultivation broth samples of the selected antagonists, one-way ANOVA results (Table 3) have revealed statistically significant effect of the antagonists to inhibition zone diameters against *X. euvesicatoria* at the significance level of 99%.

Table 3. One-way ANOVA of inhibition zone diameters obtained as a result of antimicrobial activity testing of supernatant samples of the selected antagonists against *X. euvesicatoria*

Effect	SS	MS	DF	F-value	*p*-value
Intercept	13046.72	13046.72	1	22395.42	<0.0001
Antagonist	11327.34	1415.92	8	2430.50	<0.0001
Error	41.94	0.58	72	-	-

SS – sum of squares, MS – mean squares, DF –degree of freedom

The results of the Duncan's multiple range test have showed that biomass-free supernatant samples of three tested antagonists (A1 – *P. aeruginosa* ATCC 27853, A5 – *Lactobacillus* I19 and A7 – *S. cerevisiae* P31) hadn't showed any antimicrobial activity against *X. euvesicatoria* phytopathogenic strains, indicating that these antagonist don't have an ability to synthesize antimicrobial compounds in the form of extracellular metabolites effective against the tested bacterial phytopathogens. Each other antagonist has showed an ability to suppress growth of *X. euvesicatoria* by the mechanism of antimicrobial activity which includes synthesis of extracellular antibacterial compounds. The highest level of *X. euvesicatoria* suppression was achieved by the extracellular antibacterial compounds produced by *P. aeruginosa* I128 (A2), an antagonistic strain isolated from water. Since isolate from water has showed stronger antimicrobial activity against *X. euvesicatoria* in both cases of cultivation broth and biomass-free supernatant testing compared to referent strain A1 (*P. aeruginosa* ATCC 27853), these results have also confirmed the thesis that wild strains isolated from the environment usually express higher level of antimicrobial activity compared to referent strains, due to their better adaptation abilities in various ecosystems (17). Similarly, Spago et al. (18) have showed the ability of *P. aeruginosa* strain to produce secondary metabolites which have biological activity against different plant pathogenic *Xanthomonas* species. Production of extracellular compounds with antibiotic activities against *Xanthomonas* strains by *Pseudomonas* sp. has also been reported by Oliveira et al. (19). *Pseudomonas* spp. have also been successfully applied as a foliar treatment in biological control of bacterial spot (20). Bacteriocins, as the secondary metabolites produced by *Pseudomonas* spp., have also been investigated for suppression of *X. euvesicatoria* (21).

Table 4. Results of Duncan's multiple range test for inhibition zone diameters (mean values, standard deviations and significance levels) obtained as a result of antimicrobial activity testing of supernatant samples of the selected antagonists against *X. euvesicatoria*

Antagonist	Inhibition zone diameter (mm)
A1	0.00 ± 0.00^a
A5	0.00 ± 0.00^a
A7	0.00 ± 0.00^a
A4	9.78 ± 0.71^b
A6	13.61 ± 1.11^c
A8	14.11 ± 0.78^c
A3	16.17 ± 0.79^d
A2	22.11 ± 0.82^e
S	38.44 ± 1.26^f

A1 - *Pseudomonas aeruginosa* ATCC 27853, A2 – *Pseudomonas aeruginosa* I128, A3 – *Pseudomonas putida* I315, A4 - *Lactobacillus* I14, A5 - *Lactobacillus* I19, A6 - *Lactobacillus* MK3, A7 – *Saccharomyces cerevisiae* P31, A8 – *Trichoderma reseii* QM 9414, S – streptomycin

Furthermore, one-way ANOVA was performed in order to estimate statistical significance of the tested *X. euvesicatoria* pathogenic strains to the obtained inhibition zone diameter during antimicrobial activity testing (Table 5). As it could be seen, the effect of pathogens to inhibition zone diameter wasn't statistically significant at the significance level of 95%, both in cases of cultivation broth and supernatant samples.

The fact that the effect of pathogens isn't statistically significant has further been confirmed by the Duncan's multiple range test (Table 6), which was performed in order to establish homogenous groups of pathogens according to their sensitivity towards the tested cultivation broth and supernatant samples of the selected antagonists.

Table 5. One-way ANOVA of inhibition zone diameters obtained as a result of antimicrobial activity testing against different *X. euvesicatoria* strains

Effect	SS	MS	DF	F-value	*p*-value
Intercept	41525.38^{CB} 13046.72^S	41525.38^{CB} 13046.72^S	1^{CB} 1^S	824.65^{CB} 89.53^S	$<0.0001^{CB}$ $<0.0001^S$
Pathogen	7.41^{CB} 2.82^S	3.71^{CB} 1.41^S	2^{CB} 2^S	0.07^{CB} 0.01^S	0.9291^{CB} 0.9904^S
Error	3927.70^{CB} 11366.46^S	50.36^{CB} 145.72^S	78^{CB} 78^S	-	-

SS – sum of squares, MS – mean squares, DF –degree of freedom
^{CB} – samples of cultivation broth, ^{S} – samples of supernatant

The results given in Table 6 show that all pathogenic isolates (X1, X2 and X3) were at the same level of statistical significance, both in cases of antimicrobial activity testing using cultivation broth and supernatant samples. These results indicate that there are no statistically significant differences between the tested pathogenic strains, i.e. all of them

are equally sensitive to antimicrobial action of the tested cultivation broth and supernatant samples of the selected antagonists, meaning that the selected antagonistic strains could be equally successfully applied against all tested phytopathogens.

Table 6. Results of Duncan's multiple range test for inhibition zone diameters (mean values, standard deviations and significance levels) obtained as a result of antimicrobial activity testing against different *X. euvesicatoria* strains

Pathogen	Inhibition zone diameter – samples of cultivation broth (mm)	Inhibition zone diameter – samples of supernatant (mm)
X1	22.28±6.86[a]	12.50±11.77[a]
X3	22.63±6.84[a]	12.63±11.96[a]
X2	23.02±7.57[a]	12.94±12.74[a]

CONCLUSION

The results of this study have revealed significant *in vitro* potential of cultivation broths containing biomass of the antagonists *Lactobacillus* MK3 and *T. reseii* QM 9414, as well as antibacterial compounds produced by the antagonist *P. aeruginosa* I128, to be successfully applied as biocontrol agents against *X. euvesicatoria*, causing pepper bacterial spot, which was also confirmed by the similar sensitivity of the tested pathogenic strains towards the investigated biocontrol agents. Identification and characterization of extracellular antibacterial compounds produced by the antagonist *P. aeruginosa* I128 would make a significant step towards the understanding of the mechanisms involved in biological control of *X. euvesicatoria*. Further research in this field should include optimization of bioprocess parameters, as well as cultivation medium, to produce sufficient amount of highly-efficient biocontrol agents through a cost-effective biotechnological process.

Acknowledgements

REFERENCES

1. Sundin, G.W.; Castiblanco, L.F.; Yuan, X.; Zeng, Q.; Yang, C.-H. Bacterial Disease Management: Challenges, Experience, Innovation and Future Prospects. *Mol. Plant Pathol.* **2016**, *17*, 1506-1518.
2. An, S.-Q.; Potnis, N.; Dow, M.; Vorhölter, F.-J.; He, Y.-Q.; Becker, A.; Teper, D.; Li, Y.; Wang, N.; Bleris, L.; Tang, J.-L. Mechanistic Insights into Host Adaptation, Virulence and Epidemiology of the Phytopathogen *Xanthomonas*. *FEMS Microbiol. Rev.* **2020**, *44*, 1-32.

Original scientific paper

3. Marin, V.R.; Ferrarezi, J.H.; Vieira, G.; Sass, D.C. Recent Advances in the Biocontrol of *Xanthomonas* spp. *World J. Microbiol. Biotechnol.* **2019**, *35*, 72.

4. Weller, D.M. *Pseudomonas* Biocontrol Agents of Soilborne Pathogens: Looking Back Over 30 Years. Phytopathology **2007**, *97* (2), 250-256.

5. Mercado-Blanco, J. *Pseudomonas* Strains that Exert Biocontrol of Plant Pathogens. In *Pseudomonas*; Ramos, J.L., Goldberg, J.B., Filloux, A., Eds.; Springer Science+Business Media Dordrecht: Berlin, Germany, 2015; pp 121-172.

6. Reis, J.A.; Paula, A.T.; Casarotti, S.N.; Penna, A.L.B. Lactic Acid Bacteria Antimicrobial Compounds: Characteristics and Applications. *Food Eng. Rev.* **2012**, *4*, 124-140.

7. Daranas, N.; Roselló, G.; Cabrefiga, J.; Donati, I.; Francés, J.; Badosa, E.; Spinelli, F.; Montesinos, E.; Bonaterra, A. Biological Control of Bacterial Plant Diseases with *Lactobacillus plantarum* Strains Selected for Their Broad-Spectrum Activity. Ann. Appl. Biol. **2019**, *174*, 92-105.

8. Freimoser, F.M.; Rueda-Meija, M.P.; Tilocca, B.; Migheli, Q. Biocontrol Yeasts: Mechanisms and Applications. *World J. Microbiol. Biotechnol.* **2019**, *35*, 154.

9. Benítez, T.; Rincón, A.M.; Limón, M.C.; Codón, A.C. Biocontrol Mechanisms of *Trichoderma* Strains. *Int. Microbiol.* **2004**, *7* (4), 249-260.

10. Harman, G.E.; Howell, C.R.; Viterbo, A.; Chet, I.; Lorito, M. *Trichoderma* Species - Opportunistic, Avirulent Plant Symbionts. *Nat. Rev. Microbiol.* **2004**, *2* (1), 43-56.

11. Grahovac, J.; Pajčin, I.; Vlajkov, V.; Rončević, Z.; Dodić, J.; Cvetković, D.; Jokić, A. *Xanthomonas campestris* Biocontrol Agent: Selection, Medium Formulation and Bioprocess Kinetic Analysis. Papper accepted for publication in *Chem. Ind. Chem. Eng. Q.* 2020.

12. Pajčin, I.; Rončević, Z.; Dodić, J.; Dodić, S.; Jokić, A.; Grahovac, J. Production of biocontrol agents using *Bacillus* sp. in a laboratory scale bioreactor. *Journal on Processing and Energy in Agriculture* **2018**, *22*, 138-142.

13. Bauer, A.W.; Kirby, W.M.M; Sherris, J.C.; Turck, M. Antibiotic Susceptibility Testing by a Standardized Single Disk Method. *Am. J. Clin. Pathol.* **1966**, *36*, 493-496.

14. Shrestha, A.; Kim, B.S.; Park, D.H. Biological Control of Bacterial Spot Disease and Plant Growth-Promoting Effects of Lactic Acid Bacteria on Pepper. *Biocontrol Sci. Technol.* **2014**, *24* (7), 763-779.

15. Fontenelle, A.D.B.; Guzzo, S.D.; Lucon, C.M.M.; Harakava, R. Growth Promotion and Induction of Resistance in Tomato Plant Against *Xanthomonas euvesicatoria* and *Alternaria solani* by *Trichoderma* spp. *Crop Prot.* **2011**, *30* (11), 1492-1500.

16. Chien, Y.-C.; Huang, C.-H. Biocontrol of Bacterial Spot on Tomato by Foliar Spray and Growth Medium Application of *Bacillus amyloliquefaciens* and *Trichoderma asperellum*. *Eur. J. Plant Pathol.* **2020**, *156*, 995-1003.

17. Botelho, G.R; Mendonça-Hagler, L.C. Fluorescent *Pseudomonads* Associated with the Rhizosphere of Crops - an Overview. *Braz. J. Microbiol.* **2006**, *37* (4), 401-416.

18. Spago, F.R.; Ishii Mauro, C.R.; Oliveira, A.G.; Beranger, J.P.O.; Cely, M.V.T.; Stanganelli, M.M.; Simionato, A.S.; San Martin, J.A.B.; Andrade, C.G.T.J.; Mello, J.C.P.; Andrade, G. *Pseudomonas aeruginosa* Produces Secondary Metabolites That Have Biological Activity Against Plant Pathogenic *Xanthomonas* Species. *Crop Prot.* **2014**, *62*, 46-54.

19. Oliveira, A.G.; Murate, L.S.; Spago, F.R.; Lopes, L.P.; Beranger, J.P.O.; San Martin, J.A.B.; Nogueira, M.A.; Mello, J.C.P.; Andrade. C.G.T.J.; Andrade, G. Evaluation of the Antibiotic Activity of Extracellular Compounds Produced by the *Pseudomonas* Strain Against the *Xanthomonas citri* pv. *citri* 306 Strain. *Biol. Control* **2011**, *56* (2), 125-131.

20. Ji, P.; Campbell, H.L.; Kloepper, J.W.; Jones, J.B.; Suslow, T.V.; Wilson, M. Integrated Biological Control of Bacterial Speck and Spot of Tomato Under Field Conditions Using Foliar Biological Control Agents and Plant Growth-Promoting Rhizobacteria. *Biol. Control* **2006**, *36* (3), 358-367.

Original scientific paper

21. Príncipe, A.; Fernandez, M.; Torasso, M.; Godino, A.; Fischer, S. Effectiveness of Tailocins Produced by *Pseudomonas fluorescens* SF4c in Controlling the Bacterial-Spot Disease in Tomatoes Caused by *Xanthomonas vesicatoria. Microbiol. Res.* **2018**, *212-213*, 94-102.

SUBCRITICAL WATER EXTRACTION OF POLYPHENOLS FROM ENDEMIC ALGERIAN PLANTS WITH MEDICINAL PROPERTIES

Abdelmoumen Benmerzoug[1,2,3], Jaroslava Švarc-Gajić[1]*, Nataša Nastić[1], Sofiane Guettaf[2], Daoud Harzallah[2]

[1] Faculty of Technology; Department for Applied and Engineering Chemistry; University of Novi Sad, Bulevar cara Lazara 1, 21 000 Novi Sad, Serbia.
[2] Laboratory of Applied Microbiology, Faculty of Nature and Life Sciences, University of Ferhat Abbas Sétif 1, Algeria.
[3] Department of Nature and Life Sciences, Ecole Normale Superieure Ouargla, Ouargla, Algeria

Ephedra alata, Ononis angustissima, and Genista saharae are endemic Algerian plants with pharmacological potential, used for centuries in traditional medicine. Herein the efficiency of subcritical water extraction (SWE) of phenols and flavonoids from these plants was evaluated by spectrophotometric assays. The most important operational parameters of the technique (temperature, pressure, time) were optimized for each plant based on phenols yield. At defined optimal extraction conditions (140 °C for E. alata, 155 °C for O. angustissima and G. saharae, 50 bars, 15min), maximum contents of phenols in the extracts were 16.13, 18.33, and 21.12 mg GAE/g dry weight, for E. alata, O. angustissima, and G. saharae, respectively. Considering the safety of the used solvent, excellent yields of phenols and short extraction time, subcritical water extraction can efficiently be used in exploitation of pharmacological potentials of the studied plants.

Keywords: *Ephedra alata, Ononis angustissima, Genista saharae,* subcritical water extraction, phenols, flavonoids.

INTRODUCTION

Medicinal plants have been used in Algeria for centuries for their valuable bioactive compounds to treat different ailments (1). Besides its desertic and semi-desertic areas, Algeria is characterized by large pool of plants with high pharmacological potential (1, 2). Many of plant sources still haven`t been sufficiently explored. *Ephedra alata*, *Ononis angustissima* and *Genista saharae* are promising Saharan endemic medicinal plants used to treat many diseases by the local population.

Ephedra is a genus of non-flowering seed plants belonging to the Ephedraceae family (3), which includes approximately 67 species, growing mainly in the desert areas of Asia, America, Europe and North Africa (4). Among these species, *Ephedra alata* Decne (Alanda, Arabic) is particularly interesting for its ephedrine alkaloids (5), which acts on the sympathetic nervous system as a sympathomimetics (6). Ephedrine, the major *E.alata* alkaloid is widely used pharmaceutical for prevention of arterial hypotension during spinal anesthesia. It is commonly used as nasal decongestant and appetite-suppressant (7).

Besides alkaloids, the plant represents good source of polyphenolic compounds (8). The decoction of *E. alata* stems have been used in folk medicine as a stimulant, deob-

---

* Corresponding author: Jaroslava Švarc-Gajić, University of Novi Sad, Faculty of Technology Novi Sad, Bulevar cara Lazara 1, 21000 Novi Sad, Serbia, e-mail: jaroslava@tf.uns.ac.rs
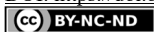
struent, to treat different disorders (kidney, bronchi, circular system, digestive system), to relieve asthma attack and as antifungal agent (9). Traditionally, the plant stems are chewed to treat bacterial and fungal infections (10). Previous *in vitro* studies have shown that its aqueous extracts exhibit anticancer activities, inducing apoptosis, inhibiting proliferation, inducing cell cycle arrest, and supressing tumorangiogenesis (11, 12). Furthermore, extracts show strong antimicrobial effects (13, 14).

The genus Ononis, belongs to the Fabaceae family and comprises 75 species that grow in Europe, Asia and the Mediterranean region (15). In Algeria more than 34 species have been identified (16). Members of the genus have been shown to exhibit antipyretic, antibiotic, analgesic, anti-inflammatory, cytotoxic, and antidiabetic activities (17, 18, 19). In traditional Turkish medicine, Ononis species were used for many centuries for their antiseptic, antimicrobial and diuretic properties (17, 18, 19). Ononis decoctions are reported to be useful in the treatment of rheumatic and skin diseases (18). *Ononis angustissi*ma Lam. is endemic plant of the North of Algerian Sahara (Guardaia, Bechar, Biskra, Boussaada and Beni Abbas) (20). The decoction of its aerial parts is used in traditional medicine for its hemostatic properties (21). Literature search indicate that *O. angustissima* hasn't been sufficiently studied and data on its chemical profile are scarce. However, it has been reported that its aerial parts are a good source of antioxidant polyphenols and flavonoids (22, 24, 20).

The Genista genus, from the family of Fabaceae, consists of 87 species, mainly represented in the Mediterranean area. Among them, 11 species are endemic in Algeria (25). Genista species have various uses throughout Mediterranean area. Different plant parts are used as dietary sources, animal feed, or in medicinal applications. Antioxidant properties of crude extracts of *G. tenera, G. sessifolia* and *G. tinctoria, G. cadasonenesis, G. Sandrasica* and *G. vuralii* have been reported in the literature (26, 27, 28, 29). *Genista saharae Coss. & Dur. Section Spartidium Spach.* (formerly *Spartidium saharae Coss. & Dur*) is a Saharian endemic shrub that grows in North Africa (Algeria, Libya, Morocco, Tunisia, and Egypt) (25, 30). According to ethnobotanical reports, aerial parts of *G. Saharae* were traditionally used for treating respiratory diseases and for its diuretic properties. Published studies also indicate that *G. sahara* aerial parts have strong antibacterial (31, 32) and antioxidant (23) properties. Some previous studies have focused on the chemical composition of this species revealing that the plant is a good source of antioxidant phenolic compounds such as O- and C-glycosylflavonoids and isoflavonoids (33, 34, 35).

Phenolic compounds are synthesyzed by plants as secondary metabolites necessary for their growth and physiology (36). These chemicals are continuously in the focus of scientific research because of their potent effects and because they represent the most abundant phytochemicals in human diets. These phytochemicals exhibit array of biological effects important for health protection, disease prevention and overall wellbeing (37). Phenolic compounds have protective role in diseases caused by oxidative damage (coronary and heart disease, stroke and cancers) (38, 39, 40). These molecules act against free radicals through antioxidant, redox and metal chelation capacity, acting as reducing agents, hydrogen donors or singlet oxygen quenchers (38).

Phenolic compounds have been extracted from plants sources by using various conventional extraction techniques such as maceration or Soxhlet extraction (41, 42, 43). However, these methods have a number of obvious disadvantages, such as long duration,

consumption of organic solvents and limited efficiency towards different classes of phenolics (44). A variety of innovative extraction techniques have been developed for the extraction of bioactive compounds from natural sources, including subcritical water extraction (SWE) (45, 46, 47, 48, 49), supercritical fluid extraction (SFE) (50), ultrasound-assisted extraction (UAE) (51), microwave-assisted extraction (MAE) (52), ultrahigh pressure-assisted extraction (UPE) (43) and pulsed electric field extraction (PEF) (53). In the recovery of bioactive compounds from plant sources SWE captures more and more attention due to its safety, superior efficiency, selectivity and environment-friendly nature. As a solvent, subcritical water has the advantages of high diffusivity, low viscosity, and low surface tension, making the extraction process more efficient due to more intimate contact with sample matrix, improved solubility, and enhanced desorption kinetics (47, 61). Literature search reports subcritical water extraction of different bioactive ingredients such as polysaccharides, proteins, antioxidants, and polyphenols from plant sources (54, 55, 56). As an environmentally-friendly and efficient extraction technique, SWE shows great potential for application in different fields considering the safety of obtained extracts, superior chemical composition and compatibility of the extracts with food, pharmaceutical and cosmetic products (44).

According to available literature, there are no reports on the use of subcritical water for the recovery of polyphenols from *Ephedra alata*, *Ononis angustissima,* and *Genista saharae*. Thus, the aim of this study was to evaluate the efficiency of SWE for obtaining *E. alata*, *O. angustissima,* and *G. saharae* extracts with high content of polyphenols. The influence of the extraction temperature, pressure and time on the extraction yield has been investigated. Total content of phenolic compounds (TPC) was determined by Folin-Ciocalteau method. For every plant species, the most important operational parameters were optimized for the highest content of polyphenols.

MATERIALS AND METHODS

Chemicals and reagents

Folin Ciocalteau's phenol reagent and rutin were purchased from Sigma-Aldrich (St. Louis, Missouri, USA). Aluminium chloride hexahydrate and sodium carbonate were purchased from Merck (Darmstadt, Germany). Gallic acid monohydrate (GA; *purum*), was acquired from Sigma-Aldrich (Steinheim, Germany). Nitrogen was of 99.999% purity (Messer, Germany). All other chemical and reagents were of analytical reagent grade**.**

Plant material

Genista saharae was harvested in Maiter Oued in the region of Bou Saada, South of M'sila, and *Ononis angustissima* was harvested in the region of Hadjeb, west of Biskra.

Both of plant samples were collected during flowering stage in April of 2019. However *Ephedra alata* was harvested in the region of El Hadjira, North of Ouargla. The identification of collected plant samples was carried out by the Laboratory of development of natural biological resources (LVRBN) at the University of Setif. The aerial parts

of each plant sample were dried, grounded in a blender, and stored in dark at ambient temperature until use.

Subcritical water extraction

SWE was performed in a house-made subcritical water extractor. Extraction procedure and apparatus were described previously (48). Total capacity of high-pressure stainless-steel vessel was 1.7 L. Pressurization of the extraction vessel was performed with 99.999% nitrogen (Messer, Germany). In all experimental runs, sample to distilled water ratio was 1:20 w/w. Extraction temperature (110–185 °C), extraction pressure (10-90 bar), and extraction time (15-60 min) were investigated as independent variables, while agitation rate (3 Hz) was held constant. After the extraction, the process vessel was immediately cooled in flow-through water-bath at 20 °C. Depressurization was done by valve opening and purging nitrogen through a valve. Obtained extracts were filtrated and stored in the refrigerator at 4 °C until analysis.

Determination of extraction yield

In order to determine extraction yield (EY), 2 ml of the total extracts volume obtained after the extraction was dried at 60 °C until a constant mass, weigted and used to calculate the total extraction yield. Further calculation was done according to the procedure described in Pharmacopoeia (57).

Determination of total phenolic content

Total phenolic content was measured by the Folin– Ciocalteu method (58). The reaction mixture consisted of 400 µl of the sample or standard solution and 2 ml of 1:10 v/v diluted Folin–Ciocalteu reagent. After 4 minutes, 1.6 ml of Na_2CO_3 7.5% (w/v) was added. After 90 min of incubation at room temperature, the absorbance was measured at 765 nm. The blank was prepared by replacing the extract with distilled water. Gallic acid (0–200 mg/l) was used for the standard calibration curve. The results were expressed as mg of gallic acid equivalent per g of dry plant material (mg GAE/g), and calculated as mean value ± SD (n = 3).

Determination of total flavonoid content

Flavonoids content in the extracts was determined by colorimetric assay with $AlCl_3$ according to the method described by Bahorun et al. (59). Briefly, 2 ml of 2 % $AlCl_3$, was added to 2 ml of the extract or standard solution. After 10 minutes, the absorbance was measured at 430 nm. Rutin (0–125 mg/l) dissolved in distilled water, was used as a standard. Results were expressed as mg of rutin equivalent per g of dry weight of plant (mg RE/g), and calculated as mean value ± SD (n = 3).

Optimisation of the extraction parameters

The influence of the extraction temperature

The aim of the present study was to define optimal conditions for SWE of phenolic compounds from *E. alata*, *O. angustissima* and *G. saharae*. According to available literature, subcritical water extraction hasn`t been previously applied in the extraction of these plant matrices.

Temperature is the most important factor in the SWE process, influencing extraction efficiency and selectivity (47, 49, 48, 60). As a solvent, subcritical water has the advantages of high diffusivity, low viscosity and low surface tension, making the extraction process more efficient due to more intimate contact with sample matrix, improved solubility and enhanced desorption kinetics (47, 61).

The influence of the extraction temperature on the extraction efficiency was investigated at six different temperatures (110-185 °C), applying the extraction time of 30 min, agitation frequency of 3 Hz, and pressure of 20 bar. The temperature influence was observed by measuring yields of total phenols (expressed as mg of gallic acid equivalent per g of dry plant material (mg GAE/g)) and flavonoids (expressed as mg of rutin equivalent per g of dry weight of plant (mg RE/g)) (Table1).

Table 1. The influence of the extraction temperature on the yields of total phenols and flavonoids

Temperature (°C)	*E. alata*		*O. angustissima*		*G. saharae*	
	TPC[a] (mg GAE/g)	TFC[b] (mg RE/g)	TPC (mg GAE/g)	TFC (mg RE/g)	TPC (mg GAE/g)	TFC (mg RE/g)
110	11.75 ±0.12[c]	5.62 ±0.19	11.30 ±0.34	9.13 ±0.14	18.03 ±0.24	8.68 ±0.18
125	15.12 ±0.18	5.28 ±0.06	11.55 ±0.3	7.81 ±0.2	19.93 ±0.19	7.59 ±0.09
140	15.58 ±0.17	4.22 ±0.12	11.67 ±0.32	8.29 ±0.2	20.90 ±0.29	7.73 ±0.15
155	14.53 ±0.09	3.74 ±0.06	16.19 ±0.12	6.99 ±0.13	24.80 ±0.43	7.04 ±0.15
170	13.90 ±0.99	3.33 ±0.05	15.34 ±0.36	6.19 ±0.13	21.82 ±0.19	6.33 ±0.07
185	14.94 ±0.19	2.76 ±0.05	13.88 ±0.4	5.11 ±0.16	18.58 ±0.31	4.79 ±0.11

[a] mean total phenols content (GAE: gallic acid equivalents).
[b] mean total flavonoids content (RE: rutin equivalents).
[c] mean± SD

Total phenols content increased with the extraction temperature from 110 to 155 °C for *O. angustissima* and *G. saharae*, and from 110 to 140 °C for *E. alata*, With further temperature increase, a drop in phenolic content was observed probably due to their degradation. The highest concentration of total phenols for *O. angustissima* (16.19 mg GAE/g) and *G. saharae* (24.80 mg GAE/g) was achieved at the temperature of 155 °C whereas the temperature of 140 °C was the optimal for *E. alata* (15.58 mg GAE/g) (Table 1).

The highest concentration of total flavonoids was observed at the lowest tested temperature (110 °C) for all three plants, *O. angustissima* (9.13 mg RE/g), *G. saharae* (8.68 mg RE/g) and *E. alata* (5.62 mg RE/g). With further temperature increase there was a slight decrease in flavonoids content for all three plant sampels (Table 1).

The increase in phenolic content with the temperature could be explained by enhancement of the diffusion coefficients, and solubility of the target compounds with temperature increase. Decreased viscosity and surface tension of the solvent are allowing better contact with porous solid samples (62, 47, 63). The most pronounced temperature influence however, is on the polarity, by varying the extraction temperature, the dielectric constant of water can be modulated affecting it`s selectivity. Consequently, the polarity of water at elevated temperatures becomes equivalent to that of common organic solvents, targeting specific chemical class. This implies that more polar solutes soluble in ambient water are extracted efficiently at lower temperatures, whereas moderately polar and non-polar compounds require less polar solvent and higher temperatures (64, 48). It was therefore shown that major phenolics classes in analyzed plant samples are such that they are the best solubilized with water at 155 °C (*O. angustissima* and *G. saharae*) and 140 °C (*E. alata*).

The temperature affects physicochemical properties of water, but also causes degradation of the thermally labile analytes (65). Thus at higher temperatures, it can be assumed that a part of phenols and flavonoids was degraded due to high water reactivity and strong hydrolytic potential of superheated water (49), causing the drop in the extraction yields of phenols above 155 °C for *O. angustissima* and *G. saharae*, and 140 °C for *E. alata*, and also the steadily decreasing the flavonoids content above 110 °C.

Several previous studies of SWE conducted with other plant samples (66, 67, 49, 63, 68) have reported similar fashion of the decrease in phenols content with the temperature increase. The reported optimal temperatures for total phenols in SWE of *Teucrium montanum*, *Chamomilla matricaria*, *Matricaria recutita*, (*Prunus avium*, *Prunus cerasus*), and *Allium ursinum L.* were 160 °C, 130 °C, 160 °C, 150 °C, and 179 °C respectivelly.

The influence of the extraction pressure

The principal operational parameter in SWE is the temperature owing to effects described earlier. In SWE applied pressure mostly serves to maintain water in its liquid state, even though slight efects on water polarity with pressure increase have been reported. Namely, water polarity negligibly increases with pressure, not favoring the process of the extraction of less polar solutes, and making the process operationally less convenient (47). Elevated pressures, however, allow better solvent penetration into the pores of extracted medium making the solvent/solute contact more intimate and accelerating the process. Unlike temperature, the pressure has no significant effect on the extraction efficiency by subcritical water (67, 68). Previous studies have also shown that elevated pressures didn't improve the recovery of compounds from natural sources by SWE (71, 72, 73). However high pressures applied during the extraction help to control problems related to the formation of air bubbles within the matrix, which hinder solvent contact with the matrix (47, 62). In order to determine the influence of pressure on the recovery of phenols from studied plant materials, investigation was carried out at previously defined optimal temperatures of 155 °C for *O. angustissima* and *G. saharae*, and 140 °C for

Original scientific paper

E. alata, applying agitation rate of 3 Hz, and extraction time of 30 min. The influence of this operational parameter was observed at four different pressures (10, 30, 50, and 70 bar). Table 2 shows extraction yields of phenols and flavonoids obtained by SWE at different pressures.

Table 2. The influence of the extraction pressure on the yields of phenols and flavonoids.

Pressure (bar)	*E. alata*		*O. angustissima*		*G. saharae*	
	TPC (mg GAE/g)	TFC (mg RE/g)	TPC (mg GAE/g)	TFC (mg RE/g)	TPC (mg GAE/g)	TFC (mg RE/g)
10	14.13 ±0.6 [a]	4.05 ±0.09	17.21 ±0.1	7.63 ±0.06	19.47 ±0.07	6.61 ±0.12
30	14.78 ±0.82	4.06 ±0.05	17.70 ±0.06	6.98 ±0.12	21.24 ±0.1	8.15 ±0.18
50	17.15 ±0.52	4.36 ±0.04	18.61 ±0.11	6.15 ±0.05	23.59 ±0.25	8.30 ±0.04
70	14.99 ±0.05	4.63 ±0.02	18.29 ±0.14	5.48 ±0.05	23.44 ±0.13	7.37 ±0.11

[a] ±SD

Investigation of the pressure influence revealed complex and diverse effects for different plant matrices and different chemical classes. In all cases studied here, the pressure did slightly affect flavonoid content. The calculated differences between minimal and maximal calculated contents for total phenols and flavonoids at different investigated pressures is shown in Tables 3 and 4.

The pressure of 50 bars showed to be the optimal for extracting phenols from all studied plant samples, and flavonoids from *G. saharae* (Table 2). This was in slight collision with other previously reported studies, in which, for most of plant samples optimal pressure in SWE was 20 bar (68) and 30 bar (67, 49). Švarc-Gajić, J et al. (68) extracted phenols from *Prunus avium* and *Prunus cerasus* stems reaching highest values at 20 bar, whereas Cvetanović, A et al. (67) and Švarc-Gajić et al. (49) reported the optimal pressure of 30 bar for phenols extraction from *Chamomilla matricaria* and *Matricaria recutita*.

Suprisingly, the highest flavonoids content for *E. alat*a (4.63 mg RE/g) was achieved at 70 bars, which was quite high pressure in comparisson to other studied plant matrices. Previous studies reported that the optimal pressures for flavonoids extraction from *Matricaria recutita* (49) and *Chamomilla matricaria* (67) were 30 and 45 bar, respectively.

Table 3. Minimum and maximuma extraction efficiencies of phenols at different pressures.

	Pression (bar)	E. alata	*O. angustissima*	*G. saharae*
Min TPC[a] (mg GAE/g)	10	14.13	17.21	19.47
Max TPC[b] (mg GAE/g)	50	17.15	18.61	23.59
Relative TPC change (%)		21.37	8.13	21.16

Min TPC[a]: Minimum TPC.
Max TPC[b]: Maximum TPC.

Original scientific paper

Table 4. Minimum and maximuma extraction efficiencies of flavonoids
at different pressures

	Min TFCa (mg RE/g)	Max TFCb (mg RE/g)	Relative TFC change (%)
E. alata	4.05 (10 bar)	4.63 (70 bar)	14.32
O. angustissima	5.48 (70 bar)	7.63 (10 bar)	39.23
G. saharae	6.61 (10 bar)	8.30 (50 bar)	25.57

Min TFCa: Minimum TFC.
Max TFCb: Maximum TFC.

For *O. angustissima* the lowest pressure of 10 bar provided the highest flavonoids content (7,63 mg RE/g) making elucidation of the pressure influence complex. It is obvious from our results that plant matrix has pronounced effect on the interaction of subcritical water at different pressure, stressing the necessity to carefully optimize this operational parameter for every plant matrix.

Defined optimal pressure for SWE of phenols from *O. angustissima*, *G. saharae*, *E. alata* was 50 bars, and kept constant in the following experiments.

The influence of the extraction time

Defining the optimal extraction time is important since prolonged extraction can induce degradation of the target compounds (68). In order to determine the influence of time on the recovery of phenols from studied plant materials, investigation was carried out at previously defined optimal temperatures of 155 °C for *O. angustissima* and *G. Saharae*, and 140 °C for *E. alata*, and optimal pressure of 50 bars, applying agitation rate of 3 Hz. Figures 1 and 2 summarize extraction yields of phenols and flavonoids obtained by SWE at different times.

The highest concentration of total phenols and flavonoids was observed at the lowest extraction time (15 min) for all three plants. Further prolongation of the extraction led to a slight decrease in phenols and flavonoids contents (Figures 1, 2).

The decrease in phenolic and flavonoids content with time could be explained by analyte degradation with longer extraction times. In fact, many previous studies confirm that longer extraction causes analyte degradation (63, 66, 67, 68). The reported optimal times for phenols in SWE of *Prunus avium*, *Prunus cerasus, Chamomilla matricaria*, *Teucrium montanum,* and *Allium ursinum L* were 30 min for *Prunus avium*, *Prunus cerasus, Chamomilla matricaria*, *Teucrium montanum* and 10 min for *Allium ursinum L*. According to these results, extraction time of 15 min was sufficient for the recovery of phenols and flavonoids by SWE and was adopted as optimal. Relatively short extraction times with good yields of the target compounds represent one more advantage of subcritical water extraction (68), making this technology efficient, time and energy saving.
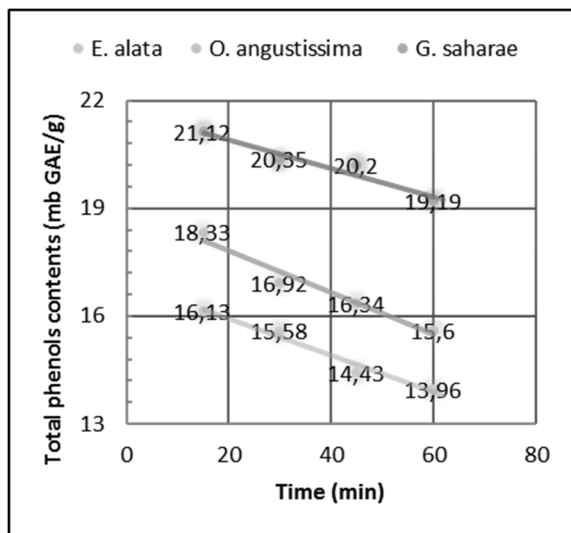
Figure 1. The influence of the extraction time on the yields of phenols
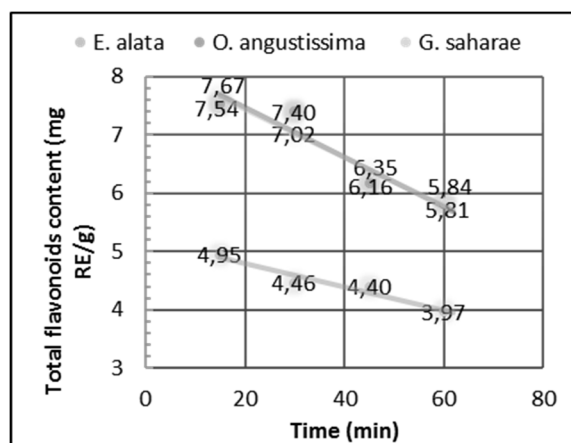
Figure 2. The influence of the extraction time on the yields of flavonoids

This idea may be implemented in the exploitation of medicinal plants at semi- and industrial level bringing the idea of flow-through technology since short extraction times are required.

Table 5 summerises maximal observed contents of total phenols and flavonoids for all three plant samples, and operational parameters at which those were achieved.

Original scientific paper

Table 5. The maximum total phenols and flavonoids contents of *E. alata*,
O. angustissima and *G. saharae* extracts.

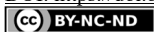|	E. alata	O. angustissima	G. saharae
TPC (mg GAE/g dry weight)	16.13 ±0.3	18.33 ±0.32	21.12 ±0.48
TPC (mg GAE/g extract)	95.46 ±1.75	109.02 ±1.88	111.88 ±2.52
TFC (mg RE/g)	4.95 ±0.06	7.54 ±0.06	7.67 ±0.15
Optimal temperature (°C)	140	155	
Optimal pressure (bar)	50		
Optimal time (min)	15		

In ethanolic extract of Palestinian *E.alata,* determined total phenolic content was 9.18 mg GAE/g of extract whereas in methanolic extract the content was significantly higher (47.62 mg GAE/g of extract) (10). The contents determined in this study applying SWE were much higher, being more than two fold greater in comparison to methanolic extract. Total phenols in infusions, decoctions, and EtOH/H$_2$O extracts of Algerian *E. alata* harvested in the region of Tebessa determined by LC-DAD-ESI/MS were 294 mg/g extract, 380 mg/g, and 240 mg/g, respectively (27). Danciu et al. (74) determined total phenols content (156.23 mg GAE/g extract) in hydroalcoholic extracts of Tunisian *E. alata*, which was higher than the total phenols extracted by SCW in our study. The content of plants secondary metabolites in addition to being dependent on the applied extraction technique depends also on other factors, such as plant variety, geographical region, climate, soil composition, etc.

For *O. angustissima*, the total phenols obtained in our study for subcritical water extracts (109.02 mg GAE/g extract) were comparable to those obtained in aqueous extracts (118.55 mg GAE/g extract) (22), but higher (18.33 mg GAE/g dry weight) in comparison to methanolic extracts (12.03 mg GAE/g dry weight) (24) obtained after 48 hour of maceration in 80% methanol.

The content of total phenols in methanolic extracts of *G. saharae* growing in Oued Souf region (Algerian desert) (1.33 GAE/g extract) was significantly lower in comparison to contents determined in this study (111.88 mg GAE/g extract) (75). The authors applied 72 hour of maceration in methanol. The contents determined in this work were also higher than that found by Meriane et al. (33) in the MeOH extract of different parts of *G. saharae* from the region of Oued El-Maadher, Boussaâda, Wilaya of M'Sila, Algeria. In roots the authors determined 93.3 mg pyrogallol equivalent/g extract, whereas in flowers they calculated the content of 90.67 pyrogallol equivalent/g extract. The contents of total phenols determined by Guettaf et al. (23) in aqueous (130.44 mg GAE/g extract) and

ethyl acetate (459.28 mg/g extract) extracts of the same plant, and that grown in Ghardaya-Algeria, respectively, were higher of those found in this study (31).

CONCLUSION

In this study, the efficiency of subcritical water extraction of phenols and flavonoids from three endemic Algerian plants (*E. alata, O. angustissima, and G. saharae*) with medicinal properties was evaluated. The most important extraction parameters of the technique (temperature, pressure, time) were optimized for each plant. Optimal temperature for SWE of *E. alata* was 140 °C, whereas maximum yield of phenols and flavonoids in extracts of *O. angustissima* and *G. saharae* were achieved applying extraction temperature of 155 °C. For all studied plant samples, maximum yields of phenols were achieved at relatively short extraction time of 15 min at the pressing of 50 bars. At defined optimal extraction parameters, maximum contents of phenols in the extracts of *E. alata, O. angustissima, and G. saharae* were 16.13, 18.33, and 21.12 mg GAE/g dry weight, respectively.

Owing to the safety of the used solvent and excellent yields of bioactive compounds from medicinal plants, the extracts may have good potential to be used in pharmaceutical industry. Presented study, thus, represents the first step to more throughout chemical and biological study of these extracts.

Acknowledgements

REFERENCES

1. Ziani, B.E.C.; Heleno, S.A.; Bachari, K.; Dias, M.I.; Ferreira, I.C.F. Phenolic compounds characterization by LC-DAD-ESI/MSn and bioactive properties of Thymus algeriensis Boiss. & Reut. and Ephedra alata Decne. *Food Research International.* **2019**, *116,* 312-319.
2. Benarba, B. Medicinal plants used by traditional healers from South-West Algeria: An ethnobotanical study. J. Intercult. *Ethnopharmacol.* **2016**, *5*(4), 320–330.
3. D'Auria, M.; Emanuele, L.; Racioppi, R. Natural product research: Formerly natural product letters FT-ICR-MS analysis of lignin FT-ICR-MS analysis of lignin [J]. *Nat Prod Res.* **2012,** *26*(15), 1368-1374.
4. Zhang, BM.; Wang, ZB.; Xin, P.; Wang, QH.; Bu, H.; Kuang, HX. Phytochemistry and pharmacology of genus Ephedra. *Chin. J. Nat. Med.* **2018,** *16*, 811–828.
5. Danciu, C.; Muntean, D.; Alexa, E.; Farcas, C.; Oprean, C.; Zupko, I.;Hancianu, M. Phytochemical characterization and evaluation of the antimicrobial, antiproliferative and pro-apoptotic potential of Ephedra alata Decne. Hydroalcoholic extract against the MCF-7 breast cancer cell line. *Molecules.***2019**, *24*(1), 13.
6. Ibragic, S.; Sofi´c, E. Chemical composition of various Ephedra species. *Bosn. J. Basic Med. Sci.* **2015**, *15*, 21–27.

7. Magalhães, E.; Govêia, C.S.; Ladeira, L.C.d.A.; Nascimento, B.G.; Kluthcouski, S.M.C.
    Ephedrine versus phenylephrine: Prevention of hypotension during spinal block for cesarean
    section and effects on the fetus. *Braz. J. Anesthesiol*. **2009**, *59*, 11–20.

8. Cocan, I.; Alexa, E.; Danciu, C.; Radulov, I.; Galuscan, A.; Obistioiu, D.; Morvay, A.A.; Su-
    malan, R.M.; Poiana, M.A.; Pop, G.; et al. Phytochemical screening and biological activity of
    Lamiaceae family plant extracts. *Exp. Ther. Med*. **2018**, *15*(2), 1863-1870.

9. Al-Qarawi, A. A.; Abd Allah, E. F.; & Abeer, H. Effect of Ephedra alata on nucleic acids and
    nitrogen metabolism of seedborne Aspergillus flavus. *Pakistan Journal of Botany*. **2012**, *44*(1),
    425–428.

10. Jaradat, N.; Hussen, F. ;Al Ali, A. Preliminary phytochemical screening, quantitative estima-
    tion of total flavonoids, total phenols and antioxidant activity of Ephedra alata. *Journal of
    Materials Environmental Science*. **2015**, *6*(6), 1771–1778.

11. Shukla, S.;Mehta, A. Anticancer potential of medicinal plants and their phytochemicals: A
    review. *Brazilian Journal of Botany*. **2015**, *38*, 1–12.

12. Sioud, F.; Amor, S.; Toumia, I. B.; Lahmar, A.; Aires, V.; Chekir-Ghedira, L.; Delmas, D. A
    new highlight of ephedra alata decne properties as potential adjuvant in combination with
    cisplatin to induce cell death of 4T1 breast cancer cells in vitro and in vivo. *Cells*.**2020**, *9*(2),
    362.

13. Ghanem, S.; El-Magly, U. I. A. Antimicrobial activity and tentative identification of active
    compounds from the medicinal Ephedra alata male plant. *Journal of Taibah University Medical
    Sciences*. **2008**, *3*(1), 7–15.

14. Parsaeimehr, A.; Sargsyan, E., & Javidnia, K. A comparative study of the antibacterial, anti-
    fungal and antioxidant activity and total content of phenolic compounds of cell cultures and
    wild plants of three endemic species of Ephedra. *Molecules*. **2010**, *15*, 1668–1678.

15. Wollenweber, E.; Dörr, M.; Rivera, D.; Roitman, JN. Externally accumulated flavonoids in
    three Mediterranean Ononis species. *Zeitschrift fuer Naturforschung C*. **2003**, *58*(11-12), 771-
    775.

16. Quezel, P. ; Santa, S. Nouvelle flore de l'Algérie et des régions désertiques méridionales.
    Editions du C.N.R.S, Paris. **1962**, Tome I. 470-471.

17. Kozan, E.; Çankaya, IT.; Kahraman, C.; Akko, EK.; Akdemir, Z. The in vivo anthelmintic
    efficacy of some Verbascum species growing in Turkey. *Experimental parasitology*. **2011**, *129*
    (2), 211-214.

18. Liebezeit, G. Ethnobotany and phytochemistry of plants dominant in salt marshes of the Lower
    Saxonian Wadden Sea, southern North Sea. *Senckenbergiana maritime*. **2008**, *38*(1), 1-30.

19. Honda, G.; Sakakibara, F.; Yazaki, K.; Tabata, M. Isolation of deoxyshikonin, an antiderma-
    tophytic principle from Lithospermum erythrorhizon cell cultures. *Journal of natural products*.
    1988, *51*(1), 152-154.

20. Bouheroum, M.; Zaiter, L.; Benayache, S.; Benayache, F.; Bermejo, JB.; Leon, F.; Garcia, V.
    Four flavonoids from the aerial part of Ononis angustissima species. *Chemistry of natural
    compounds*. **2009**, *45*(6), 874-875.

21. Chehma, A. ; Djebar, MR. Les espèces médicinales spontanées du sahara septentrional Al-
    gérien: distribution spatio-temporelle et étude ethnobotanique. Synthèse. *Revue des Sciences et
    de la Technologie*, **2015**, *17*, 36-45.

22. Guettaf, S.; Abidli, N.; Kariche, S.; Bellebcir, L.; Bouriche, H. Evaluation of antioxidant
    potential and phytochemical studies of ononis Angustissima L. (Fabaceae). *World Journal of
    Pharmaceutical Research*. **2016**, *5* (3), 1793-1815.

23. Guettaf, S.; Abidli, N.; Kariche, S.; Bellebcir, L.; Bouriche, H. Phytochemical screening and
    antioxidant activity of aqueous extract of Genista Saharae (Coss. &Dur.). *Der Pharmacia
    Lettre*.**2016**, *8*(1), 50-60.

24. Djeridane, A. ; Yousfi, M. ; Brunel, JM. ; Stocker,P. Isolation and characterization of a new steroid derivative as a powerful antioxidant from Cleome arabica in screening the in vitro antioxidant capacity of 18 Algerian medicinal plants. *Food and Chemical Toxicology*. **2010**, *48*(10), 2599-2606.

25. Quézel, P.; Santa, S. Nouvelle flore d'algérie et des régions désertiques méridionales. *Editions du Centre National de la Recherche Scientifique: Paris, France*. **1963**, Volume 1–2.

26. Serrilli, A.M.; Graziosi, V.; Ballero, M.; Foddis, C.; Serafini, M.; Poli, F.; Scartezzini, P.; Bianco, A. Endemic sardinian plants: The case of Genista cadasonensis valsecchi. *Nat. Prod. Res*. **2010**, *24*, 942–947.

27. Orhan, I.E.; Tosun, F.; Tamer, U.; Duran, A.; Alan, B.; Kok, A.F. Quantification of genistein and daidzein in two endemic genista species and their antioxidant activity. *J. Serb. Chem. Soc*. **2011**, *76*, 35–42.

28. Rigano, D.; Cardile, V.; Formisano, C.; Maldini, M.T.; Piacente, S.; Bevilacqua, J.; Russo, A.; Senatore, F. Genista sessilifolia DC. and Genista tinctoria l. Inhibit UV light and nitric oxide-induced DNA damage and human melanoma cell growth. *Chem. Biol. Interact*. **2009**, *180*, 211–219.

29. Rauter, A.P.; Martins, A.; Lopes, R.; Ferreira, J.; Serralheiro, L.M.; Araújo, M.-E.; Borges, C.; Justino, J.; Silva, F.V.; Goulart, M.; et al. Bioactivity studies and chemical profile of the antidiabetic plant Genista tenera. *J. Ethnoph*. **2009**, *122*, 384–393.

30. Maire, R. Flore de l'afrique du nord. *Éditions Paul Lechevalier: Paris, France.* **1967**, Volume 13.

31. Bouchouka, E.; Djilani, A.; Bekkouche, A. Antibacterial and antioxidant activities of three endemic plants from Algerian Sahara. *Acta Scientiarum Polonorum Technologia Alimentaria.* **2012**, *11*(1), 61-65.

32. Barek, S.; Rahmoun, N. M.; Aissaoui, M. ; El Haci, I. A. ; Bensouici, C. ; Choukchou-Braham, E. N. Phenolic Contents, Antioxidant, and Antibacterial Activities of the Algerian Genista saharae Solvent Extracts. *Journal of Herbs, Spices & Medicinal Plants*. **2020,** *26*(1), 1-13.

33. Meriane, D. ; Genta-Jouve, G. ; Kaabeche, M. ; Michel, S. ; Boutefnouchet, S. Rapid identification of antioxidant compounds of Genista saharae Coss. & Dur. by combination of DPPH scavenging assay and HPTLC-MS. *Molecules*. **2014**, *19*(4), 4369-4379.

34. Mekiou, R.; Touahr, H.; Dijoux-Franca, M.G.; Mariotte, A.M.; Benayache, S.; Benayache, F. A new isoflavone from Genista saharae. *Biochem. Syst. Ecol*. **2005**, *33*, 635-638.

35. Lograda, T.; Chaker, A.N.; Charlard, P.;Ramdani, M.; Chalchat, J.C.; Silini, H.;Figueredo, G.Chemical composition and antimicrobial activity of essential oil of Genista numidica Spach. and G. saharae Coss et Dur. *Assian J. Plant Sci*. **2009**, *8* (7), 495-499.

36. Duthie, G.G.; Peter T. G.; Kyle, J. AM. "Plant polyphenols: are they the new magic bullet?." *Proceedings of the Nutrition Society*. **2003**, *62*(3), 599-603.

37. Ozcan, T.; Akpinar-Bayizit, A.; Yilmaz-Ersan, L.; Delikanli, B. Phenolics in human health. *International Journal of Chemical Engineering and Applications*. **2014**, *5*(5), 393–396.

38. Carocho, M.;Ferreira, I. C. F. R. A review on antioxidants, prooxidants and related controversy: Natural and synthetic compounds, screening and analysis methodologies and future perspectives. *Food and Chemical Toxicology*. **2013**, *51*, 15–25.

39. Guimarães, R.; Barros, L.; Calhelha, R. C.; Carvalho, A. M.; Queiroz, M. J. R. P.; Ferreira, I. C. F. R. Bioactivity of different enriched phenolic extracts of wild fruits from Northeastern Portugal: A comparative study. *Plant Foods for Human Nutrition*. **2014**, *69*, 37–42.

40. Shahidi, F.;Ambigaipalan, P. Phenolics and polyphenolics in foods, beverages and spices: Antioxidant activity and health effects: A review. *Journal of Functional Foods*. **2015**, *18*, 820-897.

41. Kimbaris, A. C. ;Siatis, N. G. ; Daferera, D. J. ; Tarantilis, P. A. ; Pappas, C. S. ; Polissiou, M. G. Comparison of distillation and ultrasound-assisted extraction methods for the isolation of

Original scientific paper

sensitive aroma compounds from garlic (Allium sativum). *Ultrasonics Sonochemistry*. **2016**, *13*, 54–60.

42. Trochimczuk, A.; Kabay, N.; Arda, M.; Streat, M. Stabilization of solvent impregnated resins (SIRs) by coating with water soluble polymers and chemical crosslinking. *Reactive and Functional Polymers*. **2004**, *59*, 1–7.

43. Zhao, M. ;Prasad, K. N. ; Yang, B. ; Shi, J. ; Yu, C. ; Xue, S. Enhanced antioxidant and antityrosinase activities of longan fruit pericarp by ultra-high-pressureassisted extraction. *Journal of Pharmaceutical and Biomedical Analysis*. **2010**, *51*, 471–477.

44. ZHANG, J.; WEN, C.; ZHANG, H. Recent advances in the extraction of bioactive compounds with subcritical water: A review. *Trends in Food Science & Technology*. **2020**, *95*,183-195

45. Zhang, J. ; Wen, C. ; Chen, M. ; Gu, J. ; Zhou, J. ; Duan, Y. ; ZHANG, H. ; MA, H. . Antioxidant activities of Sagittaria sagittifolia L. polysaccharides with subcritical water extraction. *International Journal of Biological Macromolecules*. **2019**, *134*, 172–179.

46. Zhang, J.; Wen, C.; Gu, J.; Ji, C.; Duan, Y.; Zhang, H. Effects of subcritical water extraction microenvironment on the structure and biological activities of polysaccharides from Lentinus edodes. *International Journal of Biological Macromolecules*. **2019**, *123*, 1002–1011.

47. Švarc-Gajić, J. Sampling and sample preparation in analytical chemistry. *Nova Science Publishers*. **2012**.

48. Švarc-Gajić, J.; Cvetanović, A.; Segura-Carretero, A.; Linares, I.B.; Mašković, P. Characterisation of ginger extracts obtained by subcritical water. *J. Supercrit. Fluids*. **2017**, *123*, 92-100.

49. Švarc-Gajić, J., and A. Cvetanović. "The influence of temperature on apigenin extraction from chamomile (Matricaria recutita) by superheated water." *Int. J. Chem. Mol. Eng.* **2014**, *1*, 578.

50. McHugh, M.; Krukonis, V. Supercritical fluid extraction: Principles and practice. *Elsevier.* **2013**.

51. Wen, C. ; Zhang, J. ; Yao, H. ; Zhou, J. ; Duan, Y. ; Zhang, H. Advances in renewable plant-derived protein source: The structure, physicochemical properties affected by ultrasonication. *Ultrasonics Sonochemistry*. **2018**, *53*, 83–98.

52. Kaufmann, B.;Christen, P. Recent extraction techniques for natural products: Microwave-assisted extraction and pressurised solvent extraction. Phytochemical Analysis. *International Journal of Plant Chemical and Biochemical Techniques*. **2002**, *13*, 105–113.

53. Corrales, M.; Toepfl, S.; Butz, P.; Knorr, D.;Tauscher, B. Extraction of anthocyanins from grape by-products assisted by ultrasonics, high hydrostatic pressure or pulsed electric fields: A comparison. *Innovative Food Science & Emerging Technologies*. **2008**, *9*, 85–91.

54. Herrero, M.; Cifuentes, A.; Ibañez, E. Sub-and supercritical fluid extraction of functional ingredients from different natural sources: Plants, food-by-products, algae and microalgae: A review. *Food Chemistry*. **2006**, *98*, 136–148.

55. Zakaria, S. M.; Kamal, S. M. M. Subcritical water extraction of bioactive compounds from plants and algae: Applications in pharmaceutical and food ingredients. *Food Engineering Reviews*. **2016**, *8*, 23–34.

56. Getachew, A. T.; Chun, B. S. Molecular modification of native coffee polysaccharide using subcritical water treatment: Structural characterization, antioxidant, and DNA protecting activities. *International Journal of Biological Macromolecules*. **2017**, *99*, 555–562.

57. Anekpankul, T.; Goto, M.; Sasaki, M.; Pavasant, P.; Shotipruk, A. Extraction of anti-cancer damnacanthal from roots of Morinda citrifolia by subcritical water. *Sep. Purif. Technol*. **2007**, *55* , 343-349.

58. Li, H.; Cheng, K.;Wong, C.; Fan, K.; Chen, F.; Jiang, Y. Evaluation of antioxidant capacity and total phenolic content of different fractions of selected microalgae. *Food chemistry*. **2007**, *102*(3), 771-776.

59. Bahorun, T.;Gressier, B.; Trotin, F.; Brunet, C.; Dine, T.; Luyckx, M.; Pinkas, M. Oxygen species scavenging activity of phenolic extracts from hawthorn fresh plant organs and pharmaceutical preparations. *Arzneimittel-forschung*. **1996**, *46(*11), 1086-1089.

60. Hawthorne, S. B.; Grabanski, C. B.; Martin, E.; Miller, D. J. Comparisons of Soxhlet extraction, pressurized liquid extraction, supercritical fluid extraction and subcritical water extraction for environmental solids: Recovery, selectivity and effects on sample matrix. *Journal of Chromatography A*. **2000**, *892*, 421–433.

61. Smith, R. M. Extractions with superheated water. *Journal of Chromatography A*. **2002**, *975*, 31–46.

62. Mustafa, A.;Turner C. Pressurized liquid extraction as a green approach in food and herbal plants extraction: a review, Anal. *Chim. Acta*. **2011**, *703,* 8–18.

63. Tomšik, Alena, et al. Subcritical water extraction of wild garlic (Allium ursinum L.) and process optimization by response surface methodology. *The Journal of Supercritical Fluids.* **2017**, *128,* 79-88.

64. Smith, R.M. Superheated water: the ultimate green solvent for separation science, *Anal. Bioanal. Chem*. **2006**, *385,*419–421.

65. Kronholm, J.; Hartonen, K.; Riekkola, M.-L. Analytical extractions with water at elevated temperatures and pressures. *TRAC Trends in Analytical Chemistry*. **2007**, *26*, 396–412.

66. Nastić, N.; Švarc-Gajić, J.; Delerue-Matos, C.; Morais, S.;Barroso, M. F.; Moreira, M. M. Subcritical water extraction of antioxidants from mountain germander (Teucrium montanum L.). *The Journal of Supercritical Fluids*. **2018**, *138*, 200-206.

67. Cvetanović, A.; Švarc-Gajić, J.; Gašić, U.; Tešić, Ž.; Zengin, G.; Zeković, Z.; Đurović, S. Isolation of apigenin from subcritical water extracts: optimization of the process. *The Journal of Supercritical Fluids*. **2017**, *120*, 32-42.

68. Švarc-Gajić, J.; Cerdà, V.; Clavijo, S.; Suárez, R.; Mašković, P.; Cvetanović, A.; Delerue-Matos, C.; Carvalhod, A.; Novakova V. Bioactive compounds of sweet and sour cherry stems obtained by subcritical water extraction. *Journal of Chemical Technology & Biotechnology*. **2018**, *93* (6), 1627-1635.

69. Krieger, M. S;Wynn, J. L.; Yoder, R. N. Extraction of cloransulam methyl from soil with subcritical water and supercritical CO2. *Journal of Chromatography A*. **2000**, *897*, 405–413.

70. Kronholm, J.; Revilla-Ruiz, P.; Porras, S. P.; Hartonen, K.; Carabias-Martınez, R.;Riekkola, M.-L. Comparison of gas chromatography-mass spectrometry and capillary electrophoresis in analysis of phenolic compounds extracted from solid matrices with pressurized hot water. *Journal of Chromatography A*. **2004**, *1022*, 9–16.

71. Deng, C.; Li, N.; Zhang, X. Rapid determination of essential oil in Acorus tatarinowii Schott. By pressurized hot water extraction followed by solid-phase microextraction and gas chromatography-mass spectrometry. *Journal of Chromatography A*. **2004**, *1059*, 149–155.

72. Deng, C.;Yao, N.; Wang, A.; Zhang, X. Determination of essential oil in a traditional Chinese medicine, Fructus amomi by pressurized hot water extraction followed by liquid-phase microextraction and gas chromatography-mass spectrometry. *Analytica Chimica Acta*. **2005**, *536*, 237–244.

73. Kim, W.; Kim, J.; Veriansyah, B.; Kim, J.; Lee, Y.; Oh, S.; Extraction of bioactive components from Centella asiatica using subcritical water. *The Journal of Supercritical Fluids*. **2009**, *48*, 211–216.

74. Corina, D.; Delia, M.; Ersilia, A.; Claudia, F.; Camelia, O.; Istvan, Z.; Andrea, B.; Daliana, M.; Maria, P.; Valentina, B.; Monica, H.; Oana, C.; Codruta, S.; Sofia, P.; Cristina, AD. Phytochemical characterization and evaluation of the antimicrobial, antiproliferative and pro-apoptotic potential of Ephedra alata Decne. hydroalcoholic extract against the MCF-7 breast cancer cell line. *Molecules*. **2019**, *24* (1), 13.

Original scientific paper

75. Chouikh, A.; Alia, F.; Neffar, S.; Rebiai, A.; Adjal, E. H.;Chefrour, A. Evaluation of phenolic contents (quantitative and qualitative) and antioxidant activities in different physiological phases of Genista saharae COSS. & DUR. Growing in the Sahara of Algeria. *Analele Universitatii din Oradea, Fascicula Biologie*. **2018**, *25*(2).

EDITORIAL POLICY

The journal *Acta Periodica Technologica* (formerly *Proceedings of Faculty of Technology*) publishes reviews and original scientific papers covering from all branches of technology (food, chemical, biochemical, and pharmaceutical), process engineering and related scientific fields.

Acta Periodica Technologica is an Open Access journal.

Contributions to journal shall be submitted in English, with summaries in English and Serbian which is closely defined with Instruction for manuscript preparation.

The Journal is issued once a year.

The journal is indexed in Chemical Abstracts, Columbus, Ohio, Referativnyi zhurnal - Khimija, VINITI, Moscow, Ulrich's International Periodical Directory, and Elsevier Bibliographic databases - SCOPUS.

Editorial responsibilities

The Editorial Board is responsible for deciding which articles submitted to *Acta Periodica Technologica* will be published. The Editorial Board is guided by the Editorial Policy and constrained by legal requirements in force regarding libel, copyright infringement and plagiarism.

The Editor-in-Chief reserves the right to decide not to publish submitted manuscripts in case it is found that they do not meet relevant standards concerning the content and formal aspects. The Editorial Staff will inform the authors whether the manuscript is accepted for publication within 60-90 days from the date of the manuscript submission.

Editor-in-Chief must hold no conflict of interest with regard to the articles they consider for publication. If an Editor feels that there is likely to be a perception of a conflict of interest in relation to their handling of a submission, the selection of reviewers and all decisions on the paper shall be made by the Editorial Board.

Editor-in-Chief and Editorial Board shall evaluate manuscripts for their intellectual content free from any racial, gender, sexual, religious, ethnic, or political bias.

The Editor and the Editorial Staff must not use unpublished materials disclosed in submitted manuscripts without the express written consent of the authors. The information and ideas presented in submitted manuscripts shall be kept confidential and must not be used for personal gain.

Editors and the Editorial Staff shall take all reasonable measures to ensure that the reviewers remain anonymous to the authors before, during and after the evaluation process.

Authors' responsibilities

Authors warrant that their manuscript is their original work, that it has not been published before and are not under consideration for publication elsewhere. Parallel submission of the same paper to another journal constitutes a misconduct and eliminates the manuscript from consideration by *Acta Periodica Technologica.*

The Authors also warrant that the manuscript is not and will not be published elsewhere after the publication in *Acta Periodica Technologica* in any language without the consent of the Publisher.

In case a submitted manuscript is a result of a research project, or its previous version has been presented at a conference in the form of an oral presentation (under the same or similar title), detailed information about the project, the conference, etc. shall be provided in *Acknowledgement* at the end of paper, and before List of references. A paper that has already been published in another journal cannot be reprinted in *Acta Periodica Technologica.*

It is the responsibility of each author to ensure that papers submitted to *Acta Periodica Technologica* are written with ethical standards in mind. Authors affirm that the article contains no unfounded or unlawful statements and does not violate the rights of third parties. The Publisher will not be held legally responsible should there be any claims for compensation.

Reporting standards. A submitted manuscript should contain sufficient detail and references to permit reviewers and, subsequently, readers to verify the claims presented in it. The deliberate presentation of false claims is a violation of ethical standards.

Authors are exclusively responsible for the contents of their submissions and must make sure that they have permission from all involved parties to make the data public.

Authors wishing to include figures, tables or other materials that have already been published elsewhere are required to obtain permission from the copyright holder(s). Any material received without such evidence will be assumed to originate from the authors.

Authorship. Authors must make sure that all only contributors who have significantly contributed to the submission are listed as authors and, conversely, that all contributors who have significantly contributed to the submission are listed as authors. If persons other than authors were involved in important aspects of the research project and the preparation of the manuscript, their contribution should be acknowledged in a Acknowledgements section.

Acknowledgment of Sources. Authors are required to properly cite sources that have significantly influenced their research and their manuscript. Information received in a private conversation or correspondence with third parties, in reviewing project applications, manuscripts and similar materials, must not be used without the express written consent of the information source.

Plagiarism. Plagiarism, where someone assumes another's ideas, words, or other creative expression as one's own, is a clear violation of scientific ethics. Plagiarism may also involve a violation of copyright law, punishable by legal action.

Plagiarism includes the following:

- Word for word, or almost word for word copying, or purposely paraphrasing portions of another author's work without clearly indicating the source or marking the copied fragment (for example, using quotation marks);
- Copying equations, figures or tables from someone else's paper without properly citing the source and/or without permission from the original author or the copyright holder.

Please note that all submissions are thoroughly checked for plagiarism.

Any paper which shows obvious signs of plagiarism will be automatically rejected and authors will be temporarily forbidden to publish in the journal.

In case plagiarism is discovered in a paper that has already been published by the journal, it will be retracted in accordance with the procedure described below under Retraction policy, and authors will be temporarily forbidden to publish in the journal.

Conflict of interest. Authors should disclose in their manuscript any financial or other substantive conflict of interest that might have influenced the presented results or their interprettation.

Fundamental errors in published works. When an author discovers a significant error or inaccuracy in his/her own published work, it is the author's obligation to promptly notify the journal Editor or publisher and cooperate with the Editor to retract or correct the paper.

By submitting a manuscript the authors agree to abide by the Acta Periodica Technologica's Editorial Policies.

Reviewers' responsibilities

Reviewers are required to provide written, competent and unbiased feedback in a timely manner on the scholarly merits and the scientific value of the manuscript.

The reviewers assess manuscript for the compliance with the profile of the journal, the relevance of the investigated topic and applied methods, the originality and scientific relevance of information presented in the manuscript, the presentation style and scholarly apparatus.

Reviewers should alert the Editor to any well-founded suspicions or the knowledge of possible violations of ethical standards by the authors. Reviewers should recognize relevant published works that have not been cited by the authors and alert the Editor to substantial similarities between a reviewed manuscript and any manuscript published or under consideration for publication elsewhere, in the event they are aware of such. Reviewers should also alert the Editor to a parallel submission of the same paper to another journal, in the event they are aware of such.

Reviewers must not have conflict of interest with respect to the research, the authors and/or the funding sources for the research. If such conflicts exist, the reviewers must report them to the Editor without delay.

Any selected referee who feels unqualified to review the research reported in a manuscript or knows that its prompt review will be impossible should notify the Editor without delay.

Reviews must be conducted objectively. Personal criticism of the author is inappropriate. Reviewers should express their views clearly with supporting arguments.

Any manuscripts received for review must be treated as confidential documents. Reviewers must not use unpublished materials disclosed in submitted manuscripts without the express written consent of the authors. The information and ideas presented in submitted manuscripts shall be kept confidential and must not be used for personal gain.

Peer review

The submitted manuscripts are subject to a peer review process. The purpose of peer review is to assists the Editor-in-Chief and Editorial Board in making editorial decisions and through the editorial communications with the author it may also assist the author in improving the paper.

All papers submitted to the journal will be reviewed by at least two independent referees who will be asked to complete the refereeing job within 2-4 weeks. Final decision on publication will be made by the Editorial Board.

The choice of reviewers is at the Editors' discretion. The reviewers must be knowledgeable about the subject area of the manuscript; they must not be from the authors' own institution and they should not have recent joint publications with any of the authors.

In a main phase of peer review process, the reviewers must fill reviewer's form which indicates which aspects to be covered in order to make decision about manuscript publication. In the final part of the form, reviewers must submit their observations and suggestions on how to submitted manuscript improve.

All of the reviewers of a paper act independently and they are not aware of each other's identities. If the decisions of the two reviewers are not the same (accept/reject), the Editor may assign additional reviewers.

During the review process Editor may require authors to provide additional information (including raw data) if they are necessary for the evaluation of the scholarly merit of the manuscript. These materials shall be kept confidential and must not be used for personal gain.

The Editorial team shall ensure reasonable quality control for the reviews. With respect to reviewers whose reviews are convincingly questioned by authors, special attention will be paid to ensure that the reviews are objective and high in academic standard. When there is any doubt with regard to the objectivity of the reviews or quality of the review, additional reviewers will be assigned.

Procedures for dealing with unethical behaviour

Anyone may inform the editors and/or Editorial Board at any time of suspected unethical behaviour or any type of misconduct by giving the necessary information/evidence to start an investigation.

Investigation. Editor-in-Chief will consult with the Editorial Board on decisions regarding the initiation of an investigation.

During an investigation, any evidence should be treated as strictly confidential and only made available to those strictly involved in investigating.

The accused will always be given the chance to respond to any charges made against them.

If it is judged at the end of the investigation that misconduct has occurred, then it will be classified as either minor or serious.

Minor misconduct. Minor misconduct will be dealt directly with those involved without involving any other parties, e.g.:
- Communicating to authors/reviewers whenever a minor issue involving misunderstanding or misapplication of academic standards has occurred.
- A warning letter to an author or reviewer regarding fairly minor misconduct.

Major misconduct. The Editor-in-Chief, in consultation with the Editorial Board, and, when appropriate, further consultation with a small group of experts should make any decision regarding the course of action to be taken using the evidence available. The possible outcomes are as follows (these can be used separately or jointly):
- Publication of a formal announcement or editorial describing the misconduct.
- Informing the author's (or reviewer's) head of department or employer of any misconduct by means of a formal letter.
- The formal, announced retraction of publications from the journal in accordance with the Retraction Policy (see below).
- A ban on submissions from an individual for a defined period.

- Referring a case to a professional organization or legal authority for further investigation and action.

When dealing with unethical behaviour, the Editorial Board will rely on the guidelines and recommendations provided by the Committee on Publication Ethics (COPE): http://publicationethics.org/resources/.

Retraction policy

Legal limitations of the publisher, copyright holder or author(s), infringements of professional ethical codes, such as multiple submissions, bogus claims of authorship, plagiarism, fraudulent use of data or any major misconduct require retraction of an article. Occasionally a retraction can be used to correct errors in submission or publication. The main reason for withdrawal or retraction is to correct the mistake while preserving the integrity of science; it is not to punish the author.

Standards for dealing with retractions have been developed by a number of library and scholarly bodies, and this practice has been adopted for article retraction by *Acta Periodica Technologica*: in the electronic version of the retraction note, a link is made to the original article. In the electronic version of the original article, a link is made to the retraction note where it is clearly stated that the article has been retracted. The original article is retained unchanged, save for a watermark on the PDF indicating on each page that it is "retracted."

Open access policy

Acta Periodica Technologica is an Open Access Journal. All articles can be downloaded free of charge from:

http://www.doiserbia.nb.rs/journal.aspx?issn=1450-7188 or

http://www.tf.uns.ac.rs/site/index.php/sr-lat/delatnost/publikacije and used with terms defined with Creative Commons licence (http://creativecommons.org/licenses/by-nc-nd/3.0/rs).

The journal does not charge any fees at submission, reviewing, and production stages.

Self-archiving Policy

The journal *Acta Periodica Technologica* allows authors to deposit Publisher's version/PDF in an institutional repository and non-commercial subject-based repositories, such as PubMed Central, Europe PMC or arXiv, or to publish it on Author's personal website (including social networking sites, such as ResearchGate, Academia.edu, etc.) and/or departmental website, at any time after publication. Full bibliographic information (authors, article title, journal title, volume, issue, pages) about the original publication must be provided and a link must be made to the article's DOI.

Copyright

Once the manuscript is accepted for publication, authors shall transfer the copyright to the Publisher. If the submitted manuscript is not accepted for publication by the journal, all rights shall be retained by the author(s).

Authors grant to the Publisher the following rights to the manuscript, including any supplemental material, and any parts, extracts or elements thereof:

- the right to reproduce and distribute the Manuscript in printed form, including print-on-demand;
- the right to produce prepublications, reprints, and special editions of the Manuscript;
- the right to translate the Manuscript into other languages;
- the right to reproduce the Manuscript using photomechanical or similar means including, but not limited to photocopy, and the right to distribute these reproductions;
- the right to reproduce and distribute the Manuscript electronically or optically on any and all data carriers or storage media - especially in machine readable/digitalized form on data carriers such as hard drive, CD-Rom, DVD, Blu-ray Disc (BD), Mini-Disk, data tape - and the right to reproduce and distribute the Article via these data carriers;
- the right to store the Manuscript in databases, including online databases, and the right of transmission of the Manuscript in all technical systems and modes;
- the right to make the Manuscript available to the public or to closed user groups on individual demand, for use on monitors or other readers (including e-books), and in printable form for the user, either via the internet, other online services, or via internal or external networks.

The authors and third parties who wish use the article in a way not covered by the Creative Common licence (http://creativecommons.org/licenses/by-nc-nd/3.0/rs) must obtain a written consent of the publisher. Contact e-mail for written consent is: apteff@tf.uns.ac.rs.

Authors grant to the publisher the right to publish the article, to be cited as its original publisher in case of reuse, and to distribute it in all forms and media.

Disclaimer

The views expressed in the published works do not express the views of the Editor-in-Chief and Editorial Board. The authors take legal and moral responsibility for the ideas expressed in the articles. Publisher shall have no liability in the event of issuance of any claims for damages. The Publisher will not be held legally responsible should there be any claims for compensation.

Acta Periodica Technologica publishes reviews and scientific papers covering all branches of food, chemical, biochemical, and pharmaceutical technologies, as well as process engineering and related scientific fields.

Acta Periodica Technologica is published in English. The journal may include supplements from congresses, meetings or symposiums.

SUBMISSION OF PAPERS

All correspondence, including submission of the manuscript, notification of the Editor's decision and requests for revision, takes place by e-mail apteff@tf.uns.ac.rs or apteff.tf.uns@gmail.com.

Authors are expected to propose the category of manuscript (review or original scientific paper) and three potential reviewers. Reviewers should be experts in the field of the paper, and not associated with the institution with which the authors are affiliated. The final choice of referees will remain entirely with the Editor. Also, optionally, the authors should state any person that is not desired as a reviewer.

Submission of paper implies that:
- it is prepared according to this Instructions,
- it has not been published previously (except in the form of an abstract or as a whole in the proceedings of papers of a scientific meeting, or as part of a published lecture or academic thesis),
- it is not under consideration for publication elsewhere, and
- it will not be published elsewhere in the same form, in English or any other language, without the written consent of the publisher.

PREPARATION OF MANUSCRIPT

Language: Manuscript should be written in English.

Typing: Manuscript must be written in Word with a font size 10 pt, 1.5 lines spaced, with 2.5 cm margins, on A4 pages (maximum 15 pages for scientific papers and 25 pages for review papers). All lines of the manuscript should be numbered restarting on each page. Also, all pages must be numbered. Import tables and figures into the text. Abbreviations and symbols-notation should be explained at first appearing, or on a separate list at the end of the manuscript.

General format. The manuscript should contain the following in this order: Title page, ABSTRACT and KEYWORDS, INTRODUCTION, EXPERIMENTAL, RESULTS and DISCUSSION, CONCLUSIONS, ACKNOWLEDGEMENTS and REFERENCES.

Title page: On the first page should be the title without symbols, formulae or abbreviations (capital bold letters). The title should be concise and explanatory of the content of the paper. Full name (name, initial and surname) of authors (without degrees, professional or official titles) should be given under the title, written in italic. Clearly indicate

(with an asterisk) who is responsible for correspondence at all stages of refereeing and publication. Ensure that e-mail address and the full postal address are provided. Affiliation of authors should be given after the author's name. Indicate all affiliations with the superscript number immediately after authors name and in front of the appropriate address. If the paper was given, wholly or in part, at a scientific meeting, this should be stated in a footnote on the title page.

Abstract of the paper (100-250 words, written in italic) should be given under the title and authors. Abstracts should contain the aim of investigated work, methods, results and conclusion.

Keywords (normal letters, max. 5 keywords) should be listed afterward.

Introduction should state previous relevant work with appropriate references, the problem investigated and the aim of work.

Experimental. The materials and methods used should be stated clearly in sufficient detail to permit the work to be repeated by others. Only new techniques should be described in detail; known methods must have adequate references.

Results and Discussion. Results should be presented concisely, with tables or illustrations for clarity. The significance of the findings should be discussed without repetition of the material in the Introduction. The adequate number of illustrations, graphs and chemical formulae used must be kept on a minimum.

Conclusions. This section should present the main conclusions of the study. Also, conclusions should indicate the significance of contribution and application possibilities of the obtained results.

Acknowledgements: These should be kept to a minimum.

References cited should be indicated in the text using Arabic numerals in round brackets ( ), in the order of appearing. All publications cited in the text should be presented in a list of references given on a separate page. Abbreviations of journal titles should be given according to the Chemical Abstracts Service (CASSI Search Tool; http://cassi.cas.org). The list of references should be presented according to the *ACS citation style* and their appearance in the text. Give names of all authors (do not use „et.al.“), with their initials after respective surnames. Include article titles in journals. The abbreviated titles should be followed by the year (**bold**), volume (*italic*), number (in brackets if exists), and first and last page numbers.

Examples:

Journals: Pascual, E.C.; Goodman, B.A; Yeretzian, C. Characterisation of Free Radicals in Solubile Coffee by Electron Paramagnetic Resonance Spectroscopy. *J. Agric. Food Chem.* **2002,** *50* (21), 6114-6122.

Books: Morris, R. *The Last Sorcerers: The Path from Alchemy to the Periodic Table;* Joseph Henry Press: Washington, DC, 2003; pp 145-158.

Book with more chapters: Puls, J.; Saake, B. Industrially Isolated Hemicelluloses. In *Hemicelluloses: Science and Technology;* Gatenholm, P., Tenkanen, M., Eds.; ACS Symposium Series 864; American Chemical Society: Washington, DC, 2004; pp 24-37.

Book of Abstracts: Noe, W.; Howaldt, M.; Ulber, R.; Scheper, T. Immunobase elution assay for process control, 8th European Congress on Biotechnology, Budapest, 17-21 August 1997, Book of Abstracts WE 163, p. 246.

Thesis: Linstead, J.B.: Linstead, J.B. Effects of adding natural antioxidants on colour stability of paprika. Ph.D. (or M.S.) Thesis, University of Glasgow, November 2006.

Patent: Lenssen, K. C.; Jantscheff, P.; Kiedrowski, G.; Massing, U. Cationic Lipids with Serine Backbone for Transfecting Biological Molecules. Eur. Pat. Appl. 1457483, 2004.

Unpublished data: Should be cited with one of the following comments: *in press*, *unpublished work* or *personal communication*.

Online citations: Should include the author, title, website and date of access.
Example: Wright, N.A. The Standing of UK Histopathology Research 1997-2002. http://pathsoc.org.uk (accessed 7 October 2004).

Chemical nomenclature and units. Authors are requested to use SI units and chemical nomenclature following the rules of Chemical Abstracts whenever possible.

Tables. Each Table is numbered with an Arabic numeral, followed by the title (**Table 1.** The result...). The table width must be 12.5 cm max.

Figures. Each drawing or figure should also be numbered with Arabic numerals followed by the title (**Figure 1.** Chromatogram of...). Graphs and charts must be prepared by Microsoft Excel or Origin. Schemes must be prepared by Microsoft Visio or Corel Draw. *It is necessary to submit them as separate files in the original extension* (xls, xlsx, vdr, cdr). Scanned black & white schemes should be submitted in tiff, wmf, or bmp form. Photographs should be submitted in jpg form.

Formulae and Equations. Type formulas and mathematical equations clearly, accurately placing superscripts and subscripts. Equations should be indicated in the text using Arabic numerals in square brackets [ ].

Review process. All papers submitted to the journal will be reviewed by at least two independent referees who will be asked to complete the refereeing job within 2-4 weeks. The final decision on publication will be made by the Editorial Board. Manuscripts may be sent back to authors for revision if necessary. Revised manuscript submissions should be made as soon as possible (within 2 weeks) after the receipt of the referees' comments.

Proofs. One set of page proofs will be sent by e-mail to the corresponding author. Please use this proof only for checking the typesetting, editing, completeness and correctness of the manuscript. The author may list the corrections and return to the journal in an e-mail within 48 hours of receipt.

Author service. For inquiries relating to the submission of the manuscript, please send an e-mail to the Editor's office (apteff@tf.uns.ac.rs or apteff.tf.uns@gmail.com). Postal address: *Acta Periodica Technologica*, Editorial Board, Bulevar cara Lazara 1, 21000 Novi Sad, Serbia.

THIS ISSUE OF ACTA PERIODICA TECHNOLOGICA
IS FINANCIALLY SUPPORTED BY:

FORMER EDITORS-IN-CHIEF

Prof. Dr. Adalbert Šenborn (1967-1970)
Prof. Dr. Radivoj Žakula (1972-1975)
Prof. Dr. Miroslava Todorović (1976-1994)
Prof. Dr. Biljana Škrbić (1995-1998)
Prof. Dr. Sonja Đilas (1999-2016)

Editorial:

University of Novi Sad, Faculty of Technology Novi Sad,
Bulevar Cara Lazara 1, 21000 Novi Sad, Serbia

Phone: +381 21 485 3693
Fax:+381 21 450 413
e-mail: apteff@tf.uns.ac.rs, apteff.tf.uns@gmail.com

Prepress: Branislav S. Bastaja